UNIVERSITY OF ALBERTA

FOAMY OIL FLOW IN POROUS MEDIA

by

James Jiaping Sheng ©

A thesis submitted to the Faculty of Graduate Studies and Research in partial fulfillment of the requirements for the degree of

Doctor of Philosophy
in
Petroleum Engineering

Department of Civil and Environmental Engineering

Edmonton, Alberta

Spring 1997

National Library
of Canada

Acquisitions and
Bibliographic Services

395 Wellington Street
Ottawa ON K1A 0N4
Canada

Bibliothèque nationale
du Canada

Acquisitions et
services bibliographiques

395, rue Wellington
Ottawa ON K1A 0N4
Canada

Your file Votre référence

Our file Notre référence

The author has granted a non-exclusive licence allowing the National Library of Canada to reproduce, loan, distribute or sell copies of his/her thesis by any means and in any form or format, making this thesis available to interested persons.

The author retains ownership of the copyright in his/her thesis. Neither the thesis nor substantial extracts from it may be printed or otherwise reproduced with the author's permission.

L'auteur a accordé une licence non exclusive permettant à la Bibliothèque nationale du Canada de reproduire, prêter, distribuer ou vendre des copies de sa thèse de quelque manière et sous quelque forme que ce soit pour mettre des exemplaires de cette thèse à la disposition des personnes intéressées.

L'auteur conserve la propriété du droit d'auteur qui protège sa thèse. Ni la thèse ni des extraits substantiels de celle-ci ne doivent être imprimés ou autrement reproduits sans son autorisation.

0-612-21633-0

Canada

UNIVERSITY OF ALBERTA

LIBRARY RELEASE FORM

Name of Author: **James Jiaping Sheng**

Title of Thesis: **Foamy Oil Flow in Porous Media**

Degree: **Doctor of Philosophy**

Year This Degree Granted: **Spring 1997**

Permission is hereby granted to the University of Alberta Library to reproduce single copies of this thesis and to lend or sell such copies for private, scholarly, or scientific research purposes only.

The author reserves all other publication and other rights in association with the copyright in the thesis, and except as hereinbefore provided, neither the thesis nor any substantial portion thereof may be printed or otherwise reproduced in any material form whatever without the author's prior written permission.

Permanent Address:

SHENGJIA VILLAGE
DAOSHI TOWN, DANYANG
JIANGSU PROVINCE
P.R. CHINA

Dated: November 4, 1996

UNIVERSITY OF ALBERTA

FACULTY OF GRADUATE STUDIES AND RESEARCH

The undersigned certify that they have read, and recommend to the Faculty of Graduate Studies and Research for acceptance, a thesis entitled **Foamy Oil Flow in Porous Media** in partial fulfilment of the requirements for the degree of **Doctor of Philosophy** in **Petroleum Engineering**.

Dr. R.E. Hayes, *Supervisor*

Dr. B.B. Maini, *Co-Supervisor*

Dr. S.M. Farouq Ali

Dr. R.G. Bentsen

M. Williams
Dr. M. Williams

Dr. R.C.K. Wong, *External Examiner*

November 1, 1996

To My Father

Abstract

A number of heavy oil reservoirs under solution gas drive show anomalously good primary performance. Foamy oil behaviour is believed to be one of the reasons. This dissertation presents an improved understanding of foamy oil flow in porous media.

It was found experimentally that the volume fraction of dispersed gas in foamy oil was very low ($< 20\%$), and that the time the dispersed gas remained in the oil was short, e.g., half-life times were of the order of tens of minutes. It was also found that foamy oil stability increased with higher oil viscosity, higher oil column, higher dissolved gas content and higher pressure decline rate. Asphaltene content was not observed to increase foamy oil stability significantly.

Three models were proposed to describe the dynamic processes of bubble nucleation, bubble growth and bubble disengagement from the liquid oil. In these models, bubble nucleation was assumed to be instantaneous; the rate of bubble growth was described by a power-law function of time in Model 1 and Model 2 and by an exponential function of time in Model 3; the disengagement of dispersed bubbles from the oil was proposed to be an exponential decay in the three models. Model 1 is theoretically sound because it considers the effect of bubble age. Model 2 and Model 3 can not consider the effect of bubble age, but they can be implemented easily into a

numerical flow model. Model 3 was used in the flow model proposed in this dissertation because the results from it were less sensitive to the time step size than those from Model 2.

A mathematical model to simulate foamy oil flow in porous media was proposed which includes the dynamic processes. The proposed model satisfactorily matched primary depletion tests in a laboratory scale sand pack. The simulation results show that, although the lifetimes of supersaturation and dispersed gas bubbles are short, it is still possible that supersaturation exists, and that gas bubbles are dispersed in the oil during the whole period of production, if the system pressure continuously declines. It was demonstrated also that it is important to include the dynamic processes for a reliable prediction of production performance; and the flow behaviour mainly depends on how much gas remains dispersed in the oil.

A discussion of published models suggests that the mechanisms of oil mobility enhancement or oil viscosity reduction proposed in these models may not be plausible. One obviously important mechanism involved in solution gas drive foamy oil reservoirs is the more effective utilization of expansion energy from the foamy oil system, probably because of low gas relative permeability and/or viscous coupling effects.

Acknowledgements

I have gone a long way in this Ph.D. program. Along this way, I have received much guidance and support from many of those to whom I wish to express my sincere gratitude and appreciation.

Dr. Robert E. Hayes, Supervisor, Professor in Chemical Engineering, encouraged me to come back to school from the oil industry to pursue a Ph.D. degree. In addition to his guidance in this study and his financial support, his encouragement and understanding are particularly appreciated.

Dr. Brij B. Maini, one of my co-supervisors, has provided direct guidance and supervision throughout this study, for which I am greatly appreciative. In addition, I gladly acknowledge that I have benefitted from his understanding of this thesis topic and from the many stimulating discussions which made my years during this study productive.

Dr. W. Simon Tortike, one of my co-supervisors, worked in Australia during this study. His guidance by means of electronic mail and facsimile, at the cost of more time spent, are much appreciated. Particularly, I am grateful to his steady encouragement and his understanding of the difficulties I met during this program. Appreciation is also extended for his financial support during the early stages of the program.

The great interests and critical comments about this study from Dr. Syed M. Farouq Ali and Dr. Ramon G. Bentsen are much appreciated. The financial support from Dr. S.M. Farouq Ali in the early stages of this program is appreciated. I also appreciate that Dr. Bentsen corrected the grammar of the thesis draft.

This study was conducted at the Petroleum Recovery Institute (PRI). The financial support and the permission to use its equipment and laboratory test data are greatly appreciated. I wish to thank Mr. Fausto (Nick) Nicola, Mr. Clive Jackson and Mr. Paul Stanislav for their help in the experiments. I wish to thank Ms. Wendy Faid and Mrs. Irene Comer who hunted and delivered even more references than were used. I would also like to thank my colleagues, fellow students and friends at PRI for their discussions and help.

I would like to thank Dr. S.M. Farouq Ali for serving on my supervisory committee, my candidacy examination committee and my final examination committee, Dr. R.G. Bentsen for serving on my candidacy examination committee and my final examination committee, Dr. Frederick D. Otto for serving on my candidacy examination committee, Dr. Ron C.K. Wong and Dr. M. Williams for serving on my final examination committee.

I would like to thank my friend Xuelong Zhou who provided the convenience of my life and work at Calgary. Thanks are extended to Dr. Xuehai Li and Dr. Chonghui

Shen for useful discussions.

Financial support from Imperial Oil Resources Limited is greatly appreciated. Additional financial support from the Natural Science and Engineering Research Council of Canada (NSERC) is appreciated. I wish to acknowledge the Petroleum Society Fellowship Award of the Canadian Institute of Mining, Metallurgy and Petroleum (CIM).

I would like to thank my family for their love, encouragement and support during my graduate studies. I am most grateful to my father who has given me wonderful love, selfless support and steady encouragement throughout my life. Without him I would not have pursued a Ph.D. degree. It is to him that I dedicate this dissertation.

Table of Contents

Abstract v

Acknowledgements vii

Table of Contents x

List of Tables xv

List of Figures xvi

Nomenclature xviii

Chapter 1 Introduction

1.1 Background of the Study and Terminology in the Dissertation 1

1.2 Objectives of the Study 3

1.3 Scope and Layout of the Study 4

1.4 References 7

Chapter 2 Introduction and Overall Discussion of Foamy Oil Flow

2.1 Introduction 8

2.2 Definition and Characteristics of Foamy Oil 9

  2.2.1 Definitions of Foamy Oil and Foamy Oil Flow 9

  2.2.2 Properties of Foamy Oils 11

2.3 Issues of Solution Gas Drive Related to Foamy Oil Flow 19

  2.3.1 Critical Gas Saturation 20

  2.3.2 Slip Velocity 23

  2.3.3 Flow pattern 24

  2.3.4 Effects on Oil Recovery 26

  2.3.5 Internal versus External Gas Drive 30

2.4 Discussion of the Unusually High Production Performance 32
  2.4.1 Field Observations 32
  2.4.2 Possible Causes of High Performance 34
  2.4.3 Justification of Foamy Oil Contribution 36
2.5 Mechanisms Involved in Solution-Gas-Drive Foamy Oil Reservoirs . 39
2.6 Solution Gas Drive Models Related to Foamy Oil Flow 42
2.7 Summary 44
2.8 References 45

Chapter 3 Discussion of Foamy Oil Viscosity

3.1 Introduction 52
3.2 Literature Information of the Viscosity of Gas-Oil Mixture 52
  3.2.1 Gas-Oil Viscosity in Pipe Flow 53
  3.2.2 Dispersion Viscosity 54
3.3 Discussion of Reduced Oil Viscosity Models 56
  3.3.1 Analogous to Pipe Flow 56
  3.3.2 Dilatant Effect 58
  3.3.3 Asphaltene Adsorption Effect 60
  3.3.4 Lubrication Effect 61
3.4 Derivation of Foamy Oil Viscosity 66
3.5 Conclusions 68
3.6 References 69

Chapter 4 Experimental Study of Foamy Oil Stability

4.1 Introduction 72
4.2 Literature Review of Gas-Liquid Dispersion Stability 73
  4.2.1 Mechanisms of Bubble Decay 73
  4.2.2 Effect of Liquid Phase Viscosity 74
  4.2.3 Effect of Water Content 76
  4.2.4 Effect of Irrigation 76
  4.2.5 Effect of Solid Particles 76

4.2.6 Effect of Porous Media 77
4.2.7 Effect of Heavy Oil System 79
4.3 Experimental 80
4.3.1 Apparatus 80
4.3.2 Measurement of Foamy Oil Stability 82
4.4 Results and Discussion 83
4.4.1 Effect of Viscosity 86
4.4.2 Effect of Asphaltene 86
4.4.3 Effect of the Height of the Oil Column 88
4.4.4 Effect of Dissolved Gas Content 90
4.4.5 Effect of Pressure Decline Rate 92
4.4.6 Effect of Porous Media 92
4.4.7 Further Discussion 93
4.5 Conclusions 94
4.6 References 95

Chapter 5 Proposed Models to Describe Foamy Oil Dynamic Processes

5.1 Introduction 98
5.2 Dynamic Processes Involved in Foamy Oils 99
5.2.1 Bubble Nucleation 101
5.2.2 Bubble Growth 110
5.2.3 Bubble Disengagement 114
5.3 The Basic Model (Model 1) 116
5.3.1 Assumptions 119
5.3.2 Modification of *K* Value 120
5.3.3 Estimation of the Moles of Evolved Gas 121
5.3.4 Estimation of the Moles of Dispersed Gas 123
5.3.5 Estimation of the Moles of Other Components and the Mole Fractions of Foamy Oil Phase 127
5.3.6 Formulation of the Model by Volumetric Quantities 128
5.4 Verification of the Basic Model 132

5.4.1 Justification of Power-Law Bubble Growth 132
5.4.2 Justification of Exponential Decay 135
5.4.3 Matching the Experimental Results 137
5.5 Calculation Results and Sensitivity Study 139
5.6 Other Models 143
5.6.1 Power-Law Bubble Growth (Model 2) 144
5.6.2 Exponential Bubble Growth (Model 3) 145
5.6.3 Justification of Model 2 and Model 3 146
5.6.4 Discussion of the Models 148
5.7 Concluding Remarks 151
5.8 References 152

Chapter 6 Simulation Study of Foamy Oil Flow in Porous Media

6.1 Introduction 158
6.2 Discussion of Published Models 159
6.2.1 Conventional Models 159
6.2.2 Pseudo-Bubblepoint Model 160
6.2.3 Modified Fraction Flow Model 160
6.2.4 Reduced Oil Viscosity Model 162
6.3 Description of the Proposed Flow Model 162
6.3.1 Model Assumptions 163
6.3.2 Mathematical Equations 164
6.3.3 Method of Solution 168
6.3.4 Grid System and Time Step Size 169
6.3.5 Estimation of the Rates of Mass Transfer 170
6.3.6 Fluid Properties 173
6.4 Validation of Model 176
6.5 Simulation of Primary Depletion Tests 179
6.5.1 Description of the Experiment 179
6.5.2 Simulation of the Depletion Tests with Boscan Oil 181
6.5.3 Discussion of λ_s and λ_{sc} 186

6.6 Discussion of the Proposed Model 192
6.7 Discussion of Simulation Results 195
6.8 Conclusions 199
6.9 References 200

Chapter 7 Conclusions and Recommendations

7.1 Conclusions 202
  7.1.1 Definition of Foamy Oil 202
  7.1.2 Foamy Oil Stability 203
  7.1.3 Foamy Oil Properties 203
  7.1.4 Description of Dynamic Processes 204
  7.1.5 Dynamic Flow Model 206
  7.1.6 Recovery Mechanisms Involved in Foamy Oil Reservoirs . 206
  7.1.7 Effects of Pressure Decline Rate 207
7.2 Recommendations for Future Work 208
7.3 References 210

Appendix A Mathematical Formulation of the Numerical Flow Model

A.1 Basic Finite-Difference Formulation 212
A.2 Implicit Treatment of Production Rates 223
A.3 Calculation of Mass Transfer Rates 227

Appendix B Calculation of Supersaturation 233

List of Tables

Table 2.1 Range of critical gas saturation values reported in the literature . . . 22
Table 4.1 Oil properties, test conditions and results 85
Table 5.1 Range of supersaturation values reported in the literature 103
Table 5.2 Data used in matching experimental data 139
Table 6.1 Properties of the sand pack and fluids used in the tests 182
Table 6.2 Halflives of the decays of supersaturation and dispersed gas 196

List of Figures

Figure 1.1 An organizational map depicting the scope of this study 5
Figure 2.1 Calculated foamy oil compressibility 16
Figure 2.2 Schematic diagram of a bubble penetrating a pore constriction 28
Figure 3.1 Comparison of pressure distributions 64
Figure 3.2 Velocity distribution in a capillary 67
Figure 4.1 Schematic of foamy oil stability test 81
Figure 4.2 Height of dispersed gas vs. time 84
Figure 4.3 Effect of gas-free oil viscosity 87
Figure 4.4 Lifetimes of different foamy oils 87
Figure 4.5 Effect of the height of the oil column 90
Figure 4.6 Effect of dissolved gas content 91
Figure 4.7 Effect of pressure decline rate 93
Figure 5.1 Dynamic processes of foamy oils 100
Figure 5.2 Schematic description of Model 1 118
Figure 5.3 Measured non-equilibrium gas saturation 135
Figure 5.4 Lab data for the volume of dispersed bubbles 137
Figure 5.5 Matching foamy oil volume change 140
Figure 5.6 Mole fraction changes with time 140
Figure 5.7 Effect of equilibrium time 142
Figure 5.8 Effect of bubble growth index 142
Figure 5.9 Effect of decay coefficient 143
Figure 5.10 Comparing the matching results from three models 149
Figure 5.11 Effect of time step size in Model 1 149

Figure 5.12 Effect of time step size in Model 2 150
Figure 5.13 Effect of time step size in Model 3 150
Figure 6.1 Comparison of results from STARS model and the present model . 177
Figure 6.2 Effect of grid block size 178
Figure 6.3 Effect of time step size 178
Figure 6.4 Schematic diagram of primary depletion tests 180
Figure 6.5 Average pressure vs. cumulative oil for Boscan 1 184
Figure 6.6 Average pressure vs. cumulative oil for Boscan 2 185
Figure 6.7 Average pressure vs. cumulative oil for Boscan 3 185
Figure 6.8 Cumulative gas for Boscan 3 187
Figure 6.9 Mid-point pressure for Boscan 3 187
Figure 6.10 Effect of the supersaturation decay coefficient for a fast depletion test 189
Figure 6.11 Effect of the dispersed gas decay coefficient for a fast depletion test 189
Figure 6.12 Effect of the dispersed gas decay coefficient for a slow depletion test 191
Figure 6.13 Effect of the supersaturation decay coefficient for a slow depletion test 191
Figure 6.14 Effect of pressure decline rate 192
Figure 6.15 Comparison of the results from the dynamic model and the equilibrium model 194
Figure 6.16 An attempt to match Boscan 3 by adjusting k using the equilibrium model 194
Figure 6.17 Supersaturation in the sand pack 197
Figure 6.18 Volumetric fraction of dispersed gas in the sand pack 198

Nomenclature

a = coefficient of the power function, Eq. 5-61, m^3/s^b
a' = coefficient of the power function, Eq. 5-62, fraction
A = area, m^2
A_1 = kinetic parameter in Eq. 5-2, $m^{-3}s^{-1}$
A_2 = thermodynamic parameter in Eq. 5-2, Pa^2
b = bubble growth index, dimensionless
B = volume factor, m^3/m^3
c = compressibility, Pa^{-1}
C = solute concentration, $kmole/m^3$
C_{Ki} = coefficients in the expression of K value, $i = 1,\ldots,4$
ΔC_s = supersaturation in concentration difference, $kmole/m^3$
D = diffusion coefficient, m^2/s
f = volumetric fraction in foamy oil phase, fraction
F = correction factor in Eq. 5-27
F_1 = nucleation site wettability-geometry function in Eq. 5-3
g = gravitational acceleration, m/s^2
G = rate of bubble growth, m/s
h = height, m
h_{max} = maximum height of dispersed bubbles, m
$h_o(0)$ = height of initial live oil, m
J = rate of bubble nucleation, $m^{-3}s^{-1}$
k = permeability, m^2
K = gas/oil thermodynamic equilibrium ratio (K value), fraction

K' = modified K value, fraction

k_{hn} = kinetic constant in Eq. 5-3, $m^{-3}s^{-1}$

K_H = solubility constant, $Pa \cdot m^3/kmole$

k_r = relative permeability, fraction

k_{rg} = gas phase relative permeability, fraction

k_{ro} = oil phase relative permeability, fraction

L = length of a capillary or the sand pack, m

M = molecular weight, kg/kmole

n = moles of matter, kmoles

Δn_{eq} = moles of evolved gas according to thermodynamic equilibrium, kmole

Δn_s = supersaturation expressed in moles of gas, kmole

p = pressure, Pa

Δp = pressure difference, Pa

Δp_s = supersaturation expressed in pressure, Pa

q = production rate, kmole/s

q_{fgv} = volumetric production rate of foamy oil, m^3/s

q_{fov} = volumetric production or flow rate of free gas, m^3/s

r = radius, m

r_c = radius of a capillary, m

R = universal gas constant, 8314 $Pa \cdot m^3(kmole)^{-1}K^{-1}$

$R_{dg \to fg}$ = rate of transfer from dispersed gas to free gas, kmole/s

$R_{eg \to dg}$ = rate of transfer from evolved gas to dispersed gas, kmole/s

$R_{eg \to fg}$ = rate of transfer from evolved gas to free gas, kmole/s

$R_{sg \to eg}$ = rate of transfer from solution gas to evolved gas, kmole/s

R_s = solution gas/oil ratio, m^3/m^3

R_s' = modified solution gas/oil ratio, m^3/m^3

S = saturation, fraction

S_{gc} = critical gas saturation, fraction

S_{or} = residual oil saturation, fraction

S_{wi} = interstitial water saturation, fraction

S^* = normalized saturation, fraction
t = time, s
t_l = lifetime, s
$t_{1/2}$ = half-life, s
t^* = time for foam to collapse completely, s
t_{dg} = age of a dispersed gas bubble, s
t_{eg} = effective time for bubble growth or age of an evolved gas bubble, s
t_{eq} = time to reach thermodynamic equilibrium, s
t_o = time for bubbles to separate from oil almost completely, s
Δt = time step size, s
T = transmissibility; or temperature, K
u = unknown variable or parameter, unit depending on the variable or parameter
v = velocity vector, m/s
V = volume (of one block, Chapter 6), m^3
V_{eq} = volume of evolved gas according to thermodynamic equilibrium, m^3
W = crevice mouth size, m
x = mole fraction in liquid phase, fraction
ΔX = block size, m
z = gas compressibility factor, fraction
Z = vertical position, m

Greek Symbols

α = index, dimensionless
α_{dg} = fraction of initial dispersed gas, fraction
α_{eg} = fraction of evolved gas, fraction
β = isobaric thermal cubic expansion coefficient, $°C^{-1}$
δ = time difference operator
κ = constant coefficient, dimensionless

λ = decay coefficient, s^{-1}
λ_{dg} = decay coefficient of dispersed gas at p, s^{-1}
λ_s = "lambdas", decay coefficient of supersaturation, s^{-1}
λ_{sc} = "lambdasc", decay coefficient of dispersed gas at p_{sc}, s^{-1}
λ_c = a constant decay coefficient of dispersed gas, s^{-1}
μ = viscosity, Pa·s
ρ = molar density, kmole/m^3
σ = interfacial tension, N/m
ϕ = porosity, fraction
υ = molar specific volume, m^3/kmole
ε = tolerance for convergence, unit depending on the variable
Φ = potential, Pa

Operators

∇ = "del" or "nabla" operator
Δ = difference operator

Subscripts

a = apparent
b = bubble or bubble point
d = downstream block in Chapter 6, or dispersed matter in Chapter 3
dg = dispersed gas in oil phase
do = dead oil in oil phase
e = effective
eg = evolved gas
eq = thermodynamic equilibrium
f = formation or fluid
fg = free gas
fo = foamy oil (phase)

g = gas (phase)
i = block in Chapter 6, or location of site in Chapter 5
j = location of site
in = flowing-in
l = liquid
m = mixture
n = nucleation
o = oil
out = outlet (production port) of the sand pack or flowing-out
s = supersaturation or saturation
sc = standard conditions: 101 kPa and 15.6 °C
sg = solution gas
st = stationary
u = upstream block

Superscripts

0 = initial
i = time step i
j = time step j
l = latest iteration
$l+1$ = present iteration
n = previous (latest) time step
$n+1$ = present time step (of interest)
T = matrix or vector transpose

Chapter 1

Introduction

1.1 Background of the Study and Terminology in the Dissertation

An oil reservoir is a solution-gas-drive reservoir if it undergoes primary depletion with the main reservoir energy supplied by the release of gas from the oil and the expansion of the in-place fluids as the reservoir pressure drops. A solution gas drive is also called a dispersed gas drive or an internal gas drive. Solution-gas-drive reservoir performance is characterized by (1) relatively rapid pressure decline (faster than with fluid injection); (2) low initial producing gas/oil ratio (GOR) rising to a much higher GOR; (3) declining oil production rate; (4) relatively low oil recovery - 5% to 30% (Steffensen, 1987). The fraction of the original oil in place that can be recovered by a solution gas drive declines with increasing oil viscosity. For heavy oil reservoirs, the expected solution gas drive recovery factor is typically lower than 5% (Sheng and Maini, 1996). However, a number of heavy oil reservoirs under solution gas drive show anomalously good primary performance: high oil production rates, low production GOR and high oil recovery. The oil samples at the wellhead produced from these reservoirs are in the form of an oil-continuous foam which has the appearance of chocolate mousse and contains a certain volume fraction of gas (Maini *et al.*, 1993). People have often used the term "foamy oil" to describe such oils. Since the flow behaviour of such oils is very complex, and it is believed to be one of the reasons causing the unusually high performance, oil operators, especially in Alberta, have stimulated research on foamy oil flow behaviour. However, the flow behaviour remains controversial and poorly understood. The purpose of this study is to develop an improved understanding of the flow behaviour of foamy oils in porous media.

Foamy oil is not a firmly established topic. The definition and the existence in reservoirs remain controversial. As will be discussed in Section 2.2.1, the term "foamy oil" may not be an appropriate one to describe such a dispersion of gas bubbles in the liquid oil. However, because this term is widely used in the recent petroleum literature and in the oil industry, it is also used in this dissertation.

In conventional oils, when the pressure of a saturated oil is reduced, solution gas (dissolved gas) evolves very rapidly. This gas evolution process is assumed to occur instantaneously. The gas is called evolved gas. Since the evolved gas disengages (separates) from the oil very rapidly, this process of gas disengagement is also assumed to occur instantaneously, and the evolved gas is also called free gas or simply gas. However, in some heavy oils the processes for solution gas to evolve and for the evolved gas to become free gas take time, and these processes are believed to be important. When the pressure is reduced, gas embryos at some nucleation sites will be activated. This process is called bubble nucleation or simply nucleation. The gas embryos grow gradually. This process is called bubble growth. The gas that comes out of solution is called evolved gas. Unlike conventional oils, this evolved gas initially remains dispersed in the oil, gradually disengaging from the oil. The evolved gas which remains dispersed is called dispersed gas; and the evolved gas which has disengaged from the oil is called free gas. The amount of evolved gas is always equal to the sum of the dispersed gas and the free gas. Since the process of gas bubbles becoming disengaged from the oil occurs simultaneously with the coalescence of bubbles and the decrease of foamy oil volume or the decrease of dispersed gas volume, the terms "bubble disengagement", "bubble decay" and "bubble coalescence" are used to describe such unstable process of gas/oil dispersion.

1.2 Objectives of the Study

The overall objectives of this study were to develop an improved understanding of foamy oil flow in porous media. The specific objectives were:

1. To study foamy oil stability.
2. To develop a model to describe the dynamic processes of bubble nucleation, bubble growth and bubble disengagement which can be implemented easily in a flow model.
3. To develop a model for the simulation of foamy oil flow in porous media.
4. To explore the recovery mechanisms in solution-gas-drive foamy oil reservoirs.

1.3 Scope and Layout of the Study

To reach the objectives of this study, the following work has been done:

1. A coherent and comprehensive review and discussion of the issues related to foamy oil flow has been provided.
2. An experimental study of foamy oil stability has been designed and conducted.
3. A methodology to describe the dynamic processes of bubble nucleation, bubble growth and bubble disengagement has been developed.
4. A dynamic model to simulate foamy oil flow in porous media has been developed.

The primary depletion tests used in Chapter 6 were designed and conducted by the Petroleum Recovery Institute. The scope of the study is shown in Figure 1.1. In detail, the dissertation is organized as follows:

Chapter 2 introduces foamy oil flow and its roles in heavy oil reservoirs. The unusually high performance in heavy oil reservoirs is reviewed. The relevant issues and the mechanisms involved in solution-gas-drive foamy oil reservoirs are discussed. Several published models related to foamy oil flow are also discussed.

Chapter 3 presents a literature review of the viscosity of gas-oil mixtures and a discussion of several reduced oil viscosity models. A simple derivation of an equation for foamy oil viscosity in a capillary is presented. Since oil viscosity is an important issue of foamy oil flow, the objective of this chapter was to provide a basis for under-

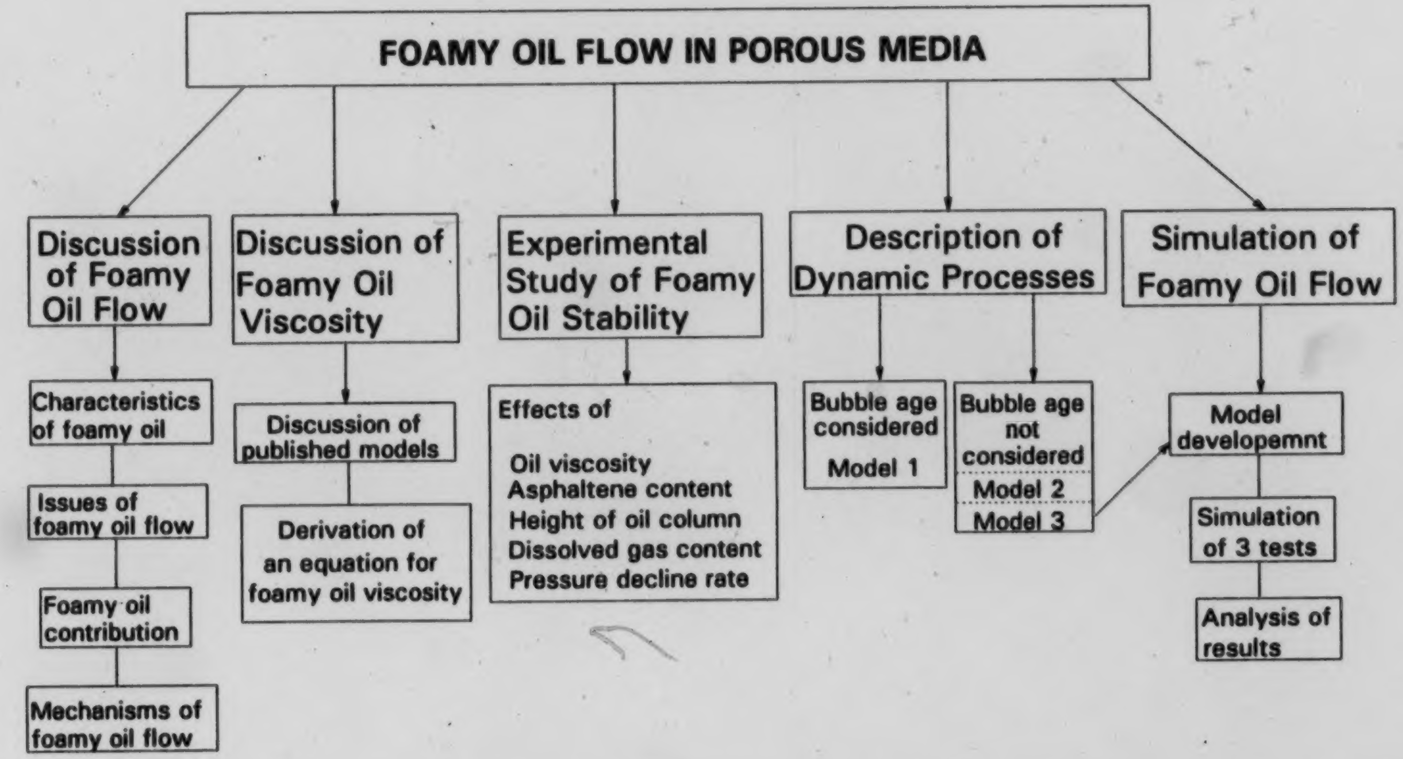
FOAMY OIL FLOW IN POROUS MEDIA
Discussion of Foamy Oil Flow
Characteristics of foamy oil
Issues of foamy oil flow
Foamy oil contribution
Mechanisms of foamy oil flow
Discussion of Foamy Oil Viscosity
Discussion of published models
Derivation of an equation for foamy oil viscosity
Experimental Study of Foamy Oil Stability
Effects of
Oil viscosity
Asphaltene content
Height of oil column
Dissolved gas content
Pressure decline rate
Description of Dynamic Processes
Bubble age considered
Model 1
Bubble age not considered
Model 2
Model 3
Simulation of Foamy Oil Flow
Model developemnt
Simulation of 3 tests
Analysis of results

Fig. 1.1 - An organizational map depicting the scope of the study.

standing recovery mechanisms in foamy oil reservoirs.

Chapter 4 describes the experimental procedures used to study foamy oil stability. The effects of oil viscosity, height of oil column, asphaltene content, dissolved gas content and pressure decline rate on foamy oil stability are investigated.

Chapter 5 presents the development of models to describe the dynamic processes: bubble nucleation, bubble growth and bubble disengagement from the liquid oil. The relevant literature for these dynamic processes is reviewed and discussed in this chapter to provide a theoretical background for the proposed models. The dynamic processes described in this chapter are included in the flow model in Chapter 6.

Chapter 6 presents the development of a dynamic model for the simulation of foamy oil flow in porous media based on the information presented in the preceding chapters, with a detailed formulation given in Appendix A. The proposed model is used to match primary depletion tests in a laboratory-scale sand pack. The simulation results for the non-equilibrium phenomenon of gas evolution and the unstable phenomenon of dispersed gas bubbles are discussed.

Finally, Chapter 7 summarizes the conclusions reached in this study and proposes recommendations for future work.

1.4 References

Maini, B.B., Sarma, H.K. and George, A.E.: "Significance of Foamy-Oil Behaviour in Primary Production of Heavy Oils," *The Journal of Canadian Petroleum Technology (JCPT)* (Nov. 1993) **32**, No. 9, 50-54.

Sheng, J.J. and Maini, B.B.: *Foamy Oil Flow in Primary Production of Foamy Oil - A literature Review*, the Petroleum Recovery Institute Report 1995/96-7 (Feb. 1996) 10.

Steffensen, R.J.: "Solution-Gas-Drive Reservoirs," *Petroleum Engineering Handbook*, Society of Petroleum Engineers, Richardson TX (1987) 37-1 to 37-27.

Chapter 2

Introduction and Overall Discussion of Foamy Oil Flow

2.1 Introduction

The term "foamy oil" is used to describe certain heavy oils produced by solution gas drive which display obvious foaminess in wellhead samples. Reservoirs that produce foamy oils exhibit anomalously high oil production, in terms of both the production rate and the primary recovery factor. Smith (1988) appears to have been the first to publish a detailed analysis of such unusual production behaviour, although such a phenomenon was noticed much earlier (at least as early as the late sixties). Since then, the flow behaviour of such gas/oil dispersions has become a subject of several experimental and theoretical investigations. The importance of foamy oil flow behaviour has been recognized by many heavy oil producers, especially in Alberta and Saskatchewan.

This chapter introduces foamy oil flow including the definitions of foamy oil and foamy oil flow, and the properties of foamy oil. The unusually high primary production in heavy oil reservoirs is reviewed. The mechanisms involved in solution gas drive in foamy oil reservoirs are briefly discussed. The issues of solution gas drive related to foamy oil flow are discussed which include critical gas saturation, slip velocity, flow pattern and internal versus external gas drive. Several published models related to foamy oil flow are also discussed.

The objectives of this chapter are: (1) to introduce foamy oil and its flow; (2) to provide the current understanding of foamy oil flow and its related issues; and (3) to provide justification for the assumptions in the dynamic models proposed in Chapters 5 and 6.

2.2 Definition and Characteristics of Foamy Oil

2.2.1 Definitions of Foamy Oil and Foamy Oil Flow

In solution gas drive reservoirs, solution gas is evolved due to a decline in reservoir pressure. Generally, the evolved gas initially remains dispersed in the oil phase. The dispersed gas eventually separates from the oil phase to form a free gas phase, but this separation takes time to occur. In some heavy oil reservoirs, since the oil samples at the wellhead display obvious foaminess, the term "foamy oil" has been used to describe such oils. This term was first used by Sarma and Maini (1992), and it was defined as a viscous (heavy) oil containing dispersed gas bubbles (Sheng *et al.*, 1994). Claridge and Prats (1995) used the terms "foamy heavy oil" and "foamy crude". Other names have appeared in the literature. Smith (1988) used "oil/gas combination" and "mixed fluid" to describe the mixture of oil and gas which is entrained in heavy oil as very tiny bubbles. Baibakov and Garushev (1989) used the term "viscous-elastic systems" to describe such highly viscous oil with very fine bubbles present in it. There appears to be no clear definition of foamy oil.

In the context of a solution gas drive, foamy oil is characterized by: (1) dispersed gas bubbles flowing with the oil; (2) a foam in which the continuous phase is oil; (3) or any other form which causes trapping of a large volume of gas within the porous medium (Maini, 1994). Morphologically, two limiting cases can be visualized: (1) a dispersion of very small gas bubbles in the oil which can be compared to an emulsion; and (2) an oil continuous foam in which oil lamellae keep relatively large gas bubbles separated. It is likely that both forms occur in the field at different stages of primary depletion (Sheng and Maini, 1996).

Although foamy oils bear some resemblance to conventional foams, there are also important differences. One difference is that the volume fraction of gas bubbles in a foamy oil (foam quality) is much lower than that of conventional foams (Sheng *et al.*, Oct. 1995; see also Section 4.4.7). Consequently, "foamy oil" may not be an appropriate name. Instead, "bubbly oil" or "gas/oil dispersion" may be a better one. Generally, foamy oil may be defined as a gas/oil dispersion with gas bubbles entrained in the liquid oil. In this dissertation, the name foamy oil is used, because it has been used publically.

"Foamy oil flow" is treated as a pseudo-single-phase flow of a heavy oil containing dispersed gas bubbles in this dissertation. Maini (April 1994) defined it as an unusual form of two phase (oil-gas) flow which can be invoked to explain the high solution gas drive recovery in certain heavy oil reservoirs. In such two-phase oil-gas flow, the rate processes associated with the formation, growth and eventual disengagement of gas bubbles from the liquid exert a significant influence on the flow behaviour.

2.2.2 Properties of Foamy Oils

In order to study foamy oil flow, it is important to be able to calculate foamy oil properties properly. Since bubble nucleation, bubble growth and the disengagement of gas bubbles from the liquid oil phase are dynamic processes, foamy oil properties are not only pressure-dependent, but also time-dependent. Several previous investigators have attempted to describe foamy oil properties. However, their approaches do not account for the time (or rate) dependent changes in foamy oil characteristics. This section discusses the status of research in this area. A method used to calculate foamy oil compressibility, as the reservoir pressure declines with time, is presented. Methods used to calculate other properties such as viscosity are not presented because of a lack of information. Considerable future research is needed in this area.

2.2.2.1 Compressibility

The compressibility of a foamy oil containing dispersed gas bubbles is higher than that of the same oil containing only dissolved gas. Since gas compressibility is much higher than liquid compressibility, the total compressibility of the dispersion is dominated by gas, once a significant volume fraction of gas has evolved and dispersed in the oil. Since the ideal gas compressibility varies inversely with pressure, the compressibility of a foamy oil is approximately equal to the volume fraction of gas divided by the absolute pressure. Smith (1988) proposed that the compressibility of foamy oil, c_{fo}, can be estimated as

$$c_{fo} = \frac{\kappa}{p}, \tag{2-1}$$

where p is the system pressure and κ is a constant coefficient. For a Lloydminster oil, κ is about 0.25 to 0.4, so the oil/gas combination is about one-fourth as compressible as an ideal gas. The compressibility of a dispersion of gas bubbles in liquid can be calculated from a knowledge of the volume fraction of gas present and the compressibilities of the liquid and the gas. Secondary effects, such as the difference in pressure between the gas and the oil due to capillarity and the change in gas solubility with pressure should also be accounted for in computations of the foamy oil compressibility. This requires a knowledge of the equilibrium PVT behaviour and the interfacial tension behaviour. Finally, some deviations from the equilibrium behaviour may also be important. Obviously, these features are not included in Eq. 2-1. A serious fault of Eq. 2-1 is that it assumes that a fraction, or even all, of the evolved gas is dispersed in the oil phase, depending on the value of κ. The foamy oil stability tests presented in Chapter 4 show that the dispersed gas can finally separate from the oil. At that time, the foamy oil volume is almost the same as the live oil volume; the compressibility is close to the single-phase oil compressibility, rather than the value given by Eq. 2-1.

In experiments using binary mixtures of C_1/n-C_{10} with a constant rate of expansion, Firoozabadi *et al.* (1992) observed that, immediately below the bubblepoint pressure of 1,071 psia (7486 kpa) and above the nucleation threshold pressure, the measured PVT data showed the same behaviour as in the undersaturated region. This behaviour implies that the fluid in the porous medium has the same compressibility as the liquid when the pressure is above the nucleation pressure. Only at the minimum pressure of 1,013 psia (7086 kPa) did the pressure begin to rise because of gas bubble formation. But unlike supersaturation in open space where a sharp rise in pressure occurs, there was a gradual pressure increase in the porous medium.

Since the dispersed gas will gradually disengage from the liquid oil phase, the volume of foamy oil is not only pressure-dependent, but also time-dependent. Islam and Chakma (1990) measured the volume changes of a high-pressure saturated oil sample after its pressure was suddenly reduced to atmospheric pressure. The produced volumes of oil with dispersed gas first reached a maximum value, then decreased with time due to the release of gas. They observed that the rate of release was much lower for crude oil compared to other oils without asphaltene. However, the results of the stability tests presented later in Section 4.4.2 do not show that asphaltene improves the foamy oil stability significantly. McCaffrey and Bowman (1991) presented similar experimental data for volume changes with time.

Sheng *et al.* (May 1995, June 1995) proposed a model (Model 1 in Chapter 5) to describe foamy oil dynamic processes, which provides a methodology to estimate how the amount of each component changes with time and pressure. Based on this model, the foamy oil properties may be estimated as follows.

The isothermal compressibility, c_f, at a constant temperature, T, is defined as

$$c_f(p,\ T,\ t) = -\frac{1}{V_f}\left[\frac{\partial V_f}{\partial p}\right], \qquad (2\text{-}2)$$

where V_f is the fluid volume with the subscript f representing fluids. The parameter f

could be *fo*, *sg*, *dg*, or *do* standing for foamy oil, solution gas, dispersed gas and dead oil, respectively.

If one assumes that

$$V_{fo} = V_{do} + V_{sg} + V_{dg}, \tag{2-3}$$

then

$$c_{fo} = -\frac{1}{V_{fo}}\left[\left(\frac{\partial V_{do}}{\partial p}\right)\left(\frac{V_{do}}{V_{do}}\right) + \left(\frac{\partial V_{sg}}{\partial p}\right)\left(\frac{V_{sg}}{V_{sg}}\right) + \left(\frac{\partial V_{dg}}{\partial p}\right)\left(\frac{V_{dg}}{V_{dg}}\right)\right], \tag{2-4}$$

that is,

$$c_{fo} = \frac{1}{V_{fo}}\left(V_{do}c_{do} + V_{sg}c_{sg} + V_{dg}c_{dg}\right). \tag{2-5}$$

Since

$$V_f = n_f v_f\,, \tag{2-6}$$

where n_f and v_f are the number of moles and the molar specific volume of a fluid, respectively, one has

$$c_{fo} = \frac{1}{v_{fo}}\left[c_{do}v_{do}\left(\frac{n_{do}}{n_{fo}}\right) + c_{sg}v_{sg}\left(\frac{n_{sg}}{n_{fo}}\right) + c_{dg}v_{dg}\left(\frac{n_{dg}}{n_{fo}}\right)\right], \tag{2-7}$$

that is

$$c_{fo} = \frac{1}{v_{fo}}\left(c_{do}v_{do}x_{do} + c_{sg}v_{sg}x_{sg} + c_{dg}v_{dg}x_{dg}\right), \tag{2-8}$$

where

$$v_{fo} = x_{do}v_{do} + x_{sg}v_{sg} + x_{dg}v_{dg}. \tag{2-9}$$

The molar specific volumes of the components in the foamy oil phase are calculated as

$$v_{do}(p,\ T) = v_{do,sc}\,[1 - c_{do}(p-p_{sc})]\ [1 + \beta_{do}(T-T_{sc})], \tag{2-10}$$

$$v_{sg}(p,\ T) = v_{sg,sc}\,[1 - c_{sg}(p-p_{sc})]\ [1 + \beta_{sg}(T-T_{sc})], \tag{2-11}$$

$$v_{dg}(p,\ T) = \frac{zRT}{p}, \tag{2-12}$$

where β denotes the thermal expansion coefficient, z is the gas compressibility factor, and R is the universal gas constant. If the dispersed gas is assumed to be an ideal gas, under isothermal conditions, its compressibility is

$$c_{dg} = c_g = \frac{1}{p}. \tag{2-13}$$

Figure 2.1 is an example of the calculated foamy oil compressibility. The parameters, x_{do}, x_{sg} and x_{dg}, were calculated using Model 1 to be proposed in Chapter 5. It shows how the foamy oil compressibility varies with time. In this example, the pressure was reduced linearly from 700 psig (4927 kPa) to 350 psig (2515 kPa) in 16 min (960 s), and this lower pressure was maintained afterwards. The data used are shown in Table 5.2 of Chapter 5. Although the pressure was maintained at 350 psig after 16 min, the compressibility changes significantly with time, which clearly demonstrates that the time-dependent effect is very important to foamy oil properties. For comparison, the mole fraction of dispersed gas is also shown in the same figure. Figure 2.1 shows that the changes of compressibility keep pace with those of the dispersed gas mole fraction.

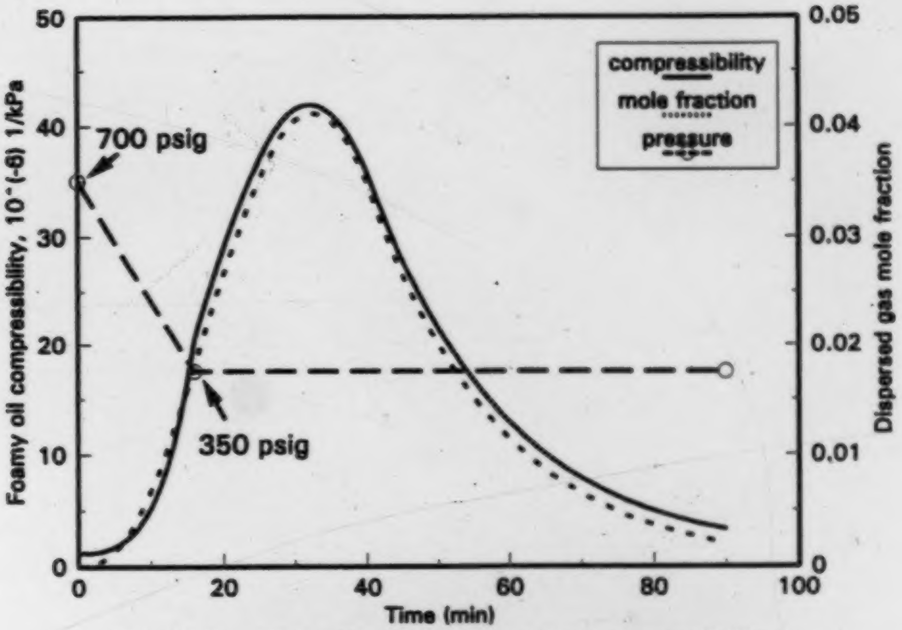

Fig. 2.1 - Calculated foamy oil compressibility.

Therefore, the foamy oil compressibility is mainly dependent upon the amount of dispersed gas. Figure 2.1 also shows that the foamy oil compressibility could be higher than that of the single-phase oil by one order of magnitude.

2.2.2.2 *Viscosity*

Several investigators have proposed foamy oil viscosity models which show that microbubbles dispersed in the oil phase would reduce the oil viscosity. They attributed the viscosity reduction to flow in porous media analogous to pipe flow (Smith, 1988), to the dilatant effect of non-Newtonian foamy oils (Poon and Kisman, 1992), to asphaltene adsorption on the bubble surfaces (Claridge and Prats, 1995) and to the lubrication effect of microbubbles on the pore walls (Shen and Batycky, 1996). There is no experimental verification for any of these models. Since foamy oil viscosity is an important parameter, these models will be discussed in detail in the next chapter.

There has been no verified method to measure foamy oil viscosity in porous media. Bora *et al.* (1995) measured foamy oil viscosity in a bulk vessel using a rotatory viscometer. Their data suggest that foamy oil viscosity is a little higher or close to the live oil viscosity. In their experiments, the volume fraction of the dispersed gas bubbles in the foamy oils was low. It seems that their data are consistent with the theory of dispersion viscosity.

2.2.2.3 Oil/Gas Relative Permeabilities

The oil/gas relative permeability characteristics of foamy oil systems present several challenges. Except for the unique effect of microbubbles in a foamy oil system, there are two fundamental issues about relative permeabilities: (1) Are the two-phase oil-gas relative permeabilities in a solution gas drive (internal gas drive) different from those in an external gas drive? (2) Are the relative permeability relationships for foamy oil systems likely to change with the operating variables, such as the flow rate, pressure decline rate and oil viscosity?

Stewart *et al.* (1953, 1954) studied solution gas drive in limestones. They found that for limestone cores having sandstone-type porosity, the production characteristics for solution and external gas drives were similar. For cores whose pore spaces were microscopically heterogeneous (i.e., consisting of combinations of solution cavities, matrices, and fissures), the production characteristics for solution and external gas drives varied widely. They concluded that limestones may show very great differences in oil/gas relative permeability relationships between solution gas drive and external gas drive. They found that, for non-uniform porosity limestones, the laboratory solution-gas-drive relative permeability characteristics are affected by: (1) rate of pressure decline, (2) original bubble point pressure of the gas-oil solution, (3) oil viscosity and (4) gas solubility characteristics.

Chatenever *et al.* (1959) observed that saturation distributions in solution gas drives were similar to those found in external gas drives. This suggests that the customary procedure of calculating solution gas drive behaviour from external gas drive relative permeability data may be satisfactory.

Smith (1988) stated that the rationale that the permeability is independent of fluid viscosity is true for single-phase absolute permeability and also may be true for some simple two-phase situations. It is not true in the phase-transition fluid system unless other parameters already explicitly remove the effects of changes in viscosity and flow regime caused by the two-phase interaction.

In order to history match the primary performance of a high rate Celtic well, Loughead and Saltuklaroglu (1992) had to use such relative permeability curves that the oil relative permeability, k_{ro}, was reduced less than 5% when the oil saturation was reduced 35%.

The relative permeability of a porous medium to a given phase in multiphase flow is usually considered to be dependent only upon the saturation and generally independent of the properties of the fluids involved. However, Yuster (1951) made a theoretical analysis of relative permeability in idealized capillary systems and found that the relative permeability to oil is not a single valued function of the saturation but also depends on the viscosity ratio. He hypothesized that multiphase flow occurs coaxially. His theoretical results also indicate that the relative permeability to the oil phase may be greater than one. However, he did not show any experimental data to support his hypothesis. Physically, he attributed the higher relative permeability to "vortex ring motion" or "ball bearing" action which means the spinning in place of an apparently immobile phase. Odeh (1959) supported this phenomenon using both theoretical considerations and experimental results. From their experimental results, Downie and Crane (1961) also concluded that oil viscosity can influence the effective oil permeability of some natural rocks.

These papers discussing the effect of viscosity all considered a water/oil system in which water is the wetting phase and oil is the non-wetting phase. A question is: what is the effect of viscosity in an oil/gas system in which the oil is the wetting phase and the gas is the non-wetting phase?

There is not much work published on the relative permeabilities in solution gas drive reservoirs and the effects of operating conditions. It is apparent that the oil-gas relative permeabilities in foamy oil reservoirs could be different from the normal two-phase relative permeabilities.

2.3 Issues of Solution Gas Drive Related to Foamy Oil Flow

The disengagement of dispersed gas bubbles from the liquid oil is a very complex process. The literature on this process is quite sparse. Since this process is similar to the process of forming a continuous flowing gas phase in conventional solution gas drive reservoirs, the information on the critical gas saturation will be useful in the understanding of foamy oil flow. Also, the slip velocity of gas bubbles and the flow pattern are closely related to the process of bubble coalescence. Therefore, the characteristics of the critical gas saturation, slip velocity and flow pattern are discussed in this section. The effects on oil recovery are reviewed. The internal gas drive is compared with the external gas drive.

2.3.1 Critical Gas Saturation

The critical gas saturation, S_{gc}, is an important parameter in the solution gas drive process. However, ambiguity still exists in both the concept and the reported values in porous media. A commonly used definition is the maximum gas saturation at which the gas relative permeability remains zero. Previous investigators defined different critical gas saturations, depending on different experimental techniques and data interpretation. Moulu and Longeron (1989) defined S_{gc} as the maximum gas saturation before any flow of gas may occur. Kortekaas and van Poelgeest (1991) defined S_{gc} as the gas saturation at which gas channels have reached the top of the reservoir (for non-dispersion conditions) or interconnected gas channels (a network of gas channels) have formed (for dispersion conditions) and gas can flow freely to the top of the reservoir. Li and Yortsos (1991) defined S_{gc} as the gas saturation at which the gas phase first reaches the production outlet. Firoozabadi *et al.* (1992) defined the critical gas saturation as the minimum gas saturation at which gas-phase flow can occur. Kamath and Boyer (1993) defined S_{gc} as the saturation when the measured GOR increased from the dissolved GOR. Li and Yortsos (1993) pointed out that a more robust definition of S_{gc} should involve the formation of a sample-spanning cluster, which indicates the appearance of a sample-conducting and free-flowing gas. In the context of foamy oil flow, the use of an appropriate definition of critical gas saturation is very important. Since the gas released from solution can flow in the form of dispersed gas bubbles, a definition based on the formation of a sample-spanning cluster of gas appears to be the most appropriate.

The critical gas saturation is usually obtained by two different approaches: estimation from field production data or measurement in the laboratory. On a field production scale, production data can be used to estimate the critical gas saturation by a material balance method (Platt and Lewis, 1969; de Swaan, 1981). The critical gas saturation estimated by this approach usually represents the performance of the whole reservoir, but the drawback is that its estimation cannot be done until oil production data are available, which requires time. Because of this, a more popular approach is to use core samples to measure the critical gas saturation in the laboratory. Traditionally, the value of the critical gas saturation is often established by extrapolating the gas relative permeability curve for an external gas drive process. Another approach used less frequently is the measurement of gas saturation at the point when the gas phase becomes mobile under an internal gas drive. These two methods are fundamentally different, and the critical gas saturation is different for external and internal processes (Firoozabadi *et al.*, 1992).

Since different investigators had different definitions for S_{gc}, its value could be different depending on experimental technique and data interpretation. Measured values of the critical gas saturation in the literature range from 0.5% to 38% PV as shown in Table 2.1.

Table 2.1 - Range of Critical Gas Saturation Values Reported in the Literature

Author	S_{gc} (%PV)	dp/dt (psi/day)	Effect of dp/dt on S_{gc}
Kamath & Boyer (1993)	3,10	20,100	small effect
Firoozabadi *et al.* (1992)	0.5-2	200-3000	$dp/dt \downarrow, S_{gc} \downarrow$
Kortekaas & Poelgeest (1989)	7-27	10-350	$dp/dt \downarrow, S_{gc} \downarrow$
Moulu & Longeron (1989)	6.6-12	0.435,72.5	$dp/dt \downarrow, S_{gc} \downarrow$
Danesh *et al.* (1987)	35	1440	-
Madaoui (1975)	4.4-17	3-120	non monotonic
Wit (1974)	0.6-2	13-300	non monotonic
Abgrall & Iffly (1973)	1.7-26.4	3-15	$dp/dt \downarrow, S_{gc} \downarrow$
Aldea (1970)	5-38	0.7-200	non monotonic
Platt & Lewis (1969)	21,27	-	-
Handy (1958)	4-11	4000-2(10^4)	$dp/dt \downarrow, S_{gc} \downarrow$
Stewart *et al.* (1954)	2-20	10-230	non monotonic

From Table 2.1, it can be generally accepted that S_{gc} increases with an increase in the pressure decline rate. A higher critical gas saturation may be attributed to the increase of nucleated gas bubbles when the pressure decline rate is higher (Moulu and Longeron, 1989; Kortekaas and van Poelgeest, 1991). However, this relationship may not be extrapolated to the field because of the complexity of the problem (Wall and Khurana, 1971; Wit, 1974).

Other factors may also affect the critical gas saturation. As supersaturation decreases, the critical gas saturation also decreases (Moulu and Longeron, 1989; Firoozabadi *et al.*, 1992). The amount of dissolved gas affects the rate of buildup of gas saturation, but has little effect on the critical gas saturation (Kortekaas and van Poelgeest, 1991). However, Abgrall and Iffly (1973) showed that the critical gas saturation is higher when the solution gas/oil ratio is higher. They also showed that in the case of intergranular porosity the critical gas saturation increases when the pores are more regular, when the permeability increases or when the interstitial water saturation is higher. The porous medium structure, rather than permeability, seems to be a key parameter in establishing a critical gas saturation (Kortekaas and van Poelgeest, 1991; Firoozabadi *et al.*, 1992). An increase in gas/oil interfacial tension (IFT) leads to a lower critical gas saturation, but the trend to lower critical gas saturations at higher IFT's is apparently not continued in the higher IFT range (Kortekaas and van Poelgeest, 1991).

2.3.2 Slip Velocity

In a foamy oil system, because of the high oil viscosity, small bubbles may be entrained in the oil phase. Smith (1988) stated that bubbles, once formed in the moving oil, can neither stay behind nor rush ahead, but instead must move with the oil. However, as the small bubbles grow into large bubbles due to the processes of molecular diffusion, bubble coalescence and fluid flow, these large bubbles and the liquid oil may flow at different velocities, resulting in a slip velocity (relative velocity of the phases). For bubble flow (flow of a liquid phase containing gas bubbles) in horizontal pipes, Govier and Aziz (1982, pp. 557-558) wrote

$$v_b = \alpha v_m, \qquad (2\text{-}14)$$

where $\alpha < 2$ for laminar flow of the continuous phase, and $\alpha < 1.2$ for turbulent flow of the continuous phase. The parameters v_b and v_m are the bubble velocity and the mixture velocity, respectively. For an approximate treatment, they stated that

$$v_b \approx 1.2 v_m. \qquad (2\text{-}15)$$

Islam and Chakma (1990) monitored the velocity of bubbles. Amazingly, the average velocity of the bubbles they observed was also 1.2 times higher than the liquid velocity.

Govier and Aziz (1982, p. 512) also observed that, at high liquid rates and at low gas rates, the gas bubbles are distributed more or less uniformly throughout the liquid. The concentration profile is somewhat asymmetric, peaking near the top of the tube. This is the dispersed, bubbly flow pattern. In this case, local slip is probably insignificant. The homogeneous fluid model, with an approximate allowance for holdup, is a reasonable one. This argument supports the assumption, used in Chapters 5 and 6, that the dispersed gas bubbles flow at the same velocity as the liquid oil. Baibakov and Garushev (1989) also stated that because of the high viscosity of the oil, gas cannot escape from it.

2.3.3 Flow Pattern

In laboratory studies, the flow of gas was observed to be intermittent in solution gas drives, the system exhibiting critical upper and lower limits of gas saturations between which flow occurs (Handy, 1958; Wall and Khurana, 1971, 1972; Maini *et al.*, 1993; Saidi, 1994; Firoozabadi *et al.*, 1994; Firoozabadi and Aronson, 1994). This indicates that various pores and pore throats are interconnected intermittently (Kortekaas and van Poelgeest, 1991). This phenomenon justifies that maximum and minimum dispersed gas mole fractions were included in the dynamic models in Chapters 5 and 6.

Visualization experiments using the small glass-bead pack described in Section 4.4.6 also confirmed the existence of discontinuous gas flow. However, the gas production was not observed to be obviously intermittent in the primary depletion tests in the two-metre sand pack described in Section 6.5.1. Probably, in larger systems where a number of independent gas flow paths are developed, flow at the production port will be continuous, although not all of the gas phase will be active at any given time.

Danesh *et al.* (1987) observed that, during the later stages of pressure depletion in a solution gas drive, the grown gas clusters advance by rapid jumps, promote snap-off and form smaller bubble structures, resulting in simultaneous recovery of the oil and gas phases. The pore-scale saturation patterns and flow behaviour at this stage are very similar to gas flooding conditions. They suggested that the relative permeability-saturation relationship for both operations should take similar forms. In their argument, the condition of "the later stages of pressure depletion" should be emphasized. At the later stages, enough gas clusters exist in the system. They are interconnected, possibly to form a pattern similar to that in an external gas drive. However, in the early stages, some gas clusters are isolated. Obviously, it will be much more difficult for them to flow than in the case of an external gas drive for the same gas saturation. Therefore, the flow pattern and the relative permeability-saturation relationship could be different.

Because of the resistance of very large viscous forces in foamy heavy oil, the effect of gravity on the bubble flow pattern was not observed to be significant in the visualization experiments described in Section 4.4.6. The direction of oil flow and gravity did not appear to have any effect on the patterns of growth (Danesh *et al.*, 1987). It was also observed that the oil production rates from a long sandpack were not much different along the horizontal and vertical flow directions at a given pressure drawdown (Sarma *et al.*, 1991).

2.3.4 Effects on Oil Recovery

The oil recovery in a solution gas drive is affected by many factors. Possible factors related to foamy oil reservoirs are discussed here.

2.3.4.1 Effect of Oil Viscosity

The fraction of the original oil in place that can be recovered by solution gas drive declines with increasing oil viscosity. However, experiments have shown that the viscosity of oil has little effect on the ultimate oil recovery (Baibakov and Garushev, 1989; Maini *et al.*, May 1995, Sept. 1995). Oil recovery even increased with increasing oil viscosity for a given high rate of production, as was observed by Handy (1958). Therefore, the effect of oil viscosity on heavy oils is different from that on conventional oils.

2.3.4.2 Effect of Formation Permeability

Baibakov and Garushev's (1989) experimental results show a strong effect of reservoir permeability on oil recovery. For example, the model of a petroliferous bed of microporosity type, but with a permeability of 294 Darcies, gave an oil recovery factor of 60%, whereas the same porosity-type reservoir, but with a permeability of 5.2 Darcies, yielded only 30% of the oil in place. Also, their experimental data indicate a rather high ultimate oil recovery for a fracture-type (macroporosity) reservoir. It seems that the conditions of high permeability and macroporosity needed for a high oil recovery exist in the unconsolidated foamy oil reservoirs where the macroporosity could be created by sand production.

2.3.4.3 *Effect of Pressure Decline Rate*

The displacement of oil by a solution gas drive is primarily achieved by growth of the gas nuclei. The oil recovery efficiency is believed to be reduced when the developed gas clusters become continuous. Therefore, the spacing of the nuclei, thus the pressure decline rate, may significantly affect the oil recovery.

The pressure differential, Δp, required to move a spherical bubble through a pore constriction depends on the radii of curvature, r_1 and r_2, corresponding to the trailing surface and the forward surface, respectively. The pressure differential is given by

$$\Delta p = 2\sigma\left[\frac{1}{r_1} - \frac{1}{r_2}\right], \tag{2-16}$$

where σ is the surface tension. Figure 2.2 shows a bubble penetrating a pore constriction. If the actual pressure differential across the pore is less than that predicted by Eq. 2-16, the bubble plugs the pore constriction. This describes the basis for resistance in foamy oil flow through porous media. Therefore, the pressure gradient must be high enough so

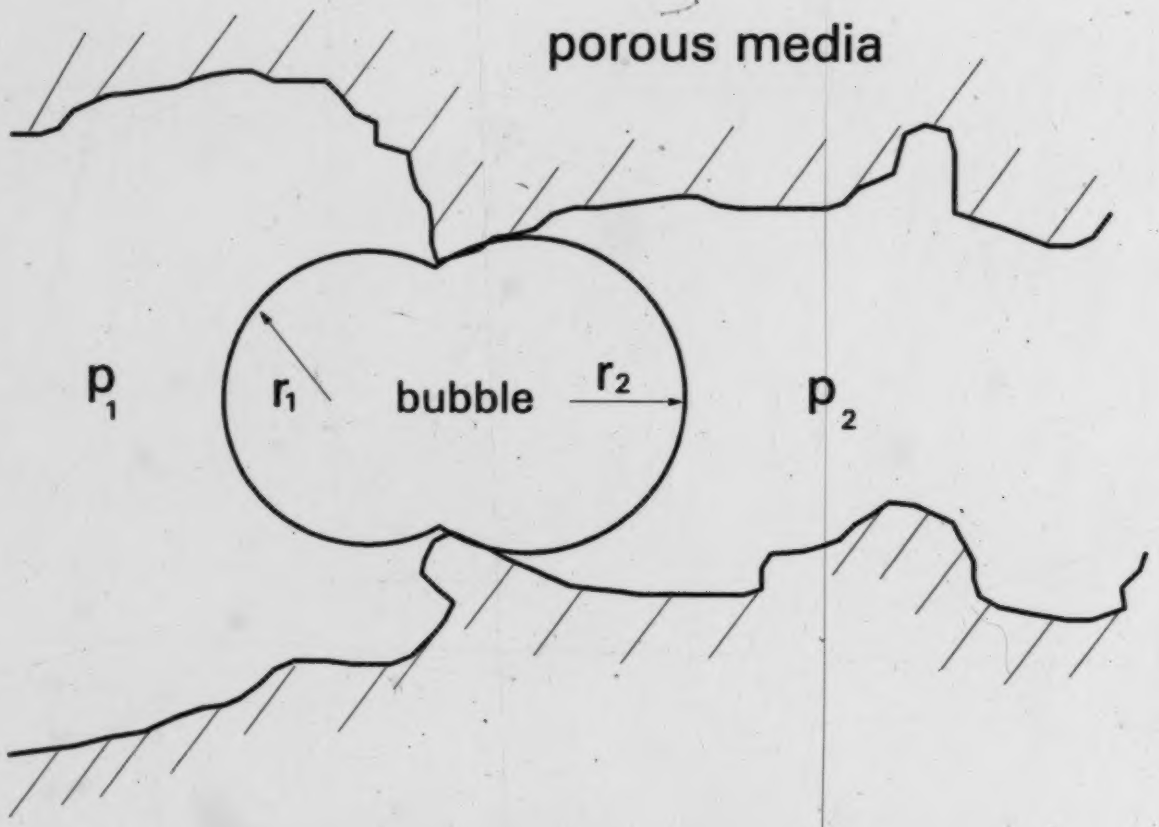
porous media
p_1
r_1
bubble
r_2
p_2

Fig. 2.2 - Schematic diagram of a bubble penetrating a pore constriction.

that the bubbles traversing such constrictions undergo a gradual deformation and the resistance to flow is overcome. A high pressure gradient occurs when the pressure decline rate is high. Obviously, when the radii of the bubbles are smaller than those of the pore constrictions, the resistance predicted by Eq. 2-16 would not occur. Also, small bubbles could be generated when the pressure decline rate is high. Therefore, when the pressure decline rate is higher, it will be easier for the oil to flow in porous media, and the oil recovery will be higher as was observed in the laboratory (Handy, 1958; Maini *et al.*, May 1995 and Sept. 1995). However, Handy (1958), Ridings *et al.* (1963) and Baibakov and Garushev (1989) observed that at low laboratory rates, recoveries were nearly independent of rate. This is because the pressure decline rate was so low that the bubbles were connected to form a continuous gas phase and the dynamic processes were not important.

If the effect of the pressure decline rate is extrapolated to the field, the field performance should be able to be predicted by conventional solution gas drive theory. However, the unusually high recovery has been observed in some solution gas drive heavy oil reservoirs. This puzzle may be explained by postulation that, although the average pressure decline rate of the whole reservoir or the whole drainage area of a well is low, the local pressure gradients could be high because of the existence of high permeability channels. These channels could be caused by sand production or naturally-existent fissures and solution cavities, etc. Reservoir heterogeneity could also be a cause for high local pressure gradients.

2.3.4.4 *Effect of GOR*

The gas content in a crude oil exerts a strong influence on the recovery factor of high viscosity oil. Baibakov and Garushev's (1989) experimental data show that oil recovery decreases as gas content decreases, especially in the case of low permeability reservoirs of the microporosity type.

2.3.5 Internal versus External Gas Drive

The growth of an initial nucleus of gas (critical nucleus) caused by diffusion and expansion, agglomeration of various nuclei and mobilization of the connected bubbles in an internal gas-expansion process is entirely different from gas-phase mobilization in external gas drive systems (Firoozabadi *et al.*, 1992). While there is some recognition of the fundamental differences between internal and external drives, surprisingly little has been published to quantify such effects (Yortsos and Parlar, 1989).

Stewart *et al.* (1953) concluded from their laboratory measurements that some limestones may show a significant difference in the oil/gas relative permeability relationship between internal and external gas drive processes. They noted that the degree of heterogeneity of the pore system should be reflected in the degree of difference between the oil/gas relative permeabilities calculated from external and solution gas drive tests. In a subsequent publication, Stewart *et al.* (1954) observed that, for non-uniform porous media, recovery of oil from the "storage" pores by an external gas drive could be accomplished only at high gas/oil ratios. However, in this type of pore, or cluster of pores, the formation of gas bubbles during a solution gas drive could result in the displacement and recovery of the oil when the system was producing at a relatively low gas/oil ratio.

Islam and Chakma (1990) carried out a series of coreflood tests to study bubble flow behaviour in the presence of heavy crude oil. They compared the effect of microbubbles with that of continuous gas/oil injection. It was observed that the pressure drop across the core in the case of continuous gas flow is twice as high as that in the presence of microbubbles, even though S_o/S_g remained the same for both cases.

Based on CT-measured gas saturation profiles, Kamath and Boyer (1993) identified the critical gas saturation value as 10% for an internal gas drive, while continuous gas flow occurred at a gas saturation of less than 1% for a capillary controlled external gas drive. They concluded that external gas drive experiments are not appropriate for determining the critical gas saturation for an internal gas drive process. However, they further pointed out that if supersaturation thresholds for nucleation are negligibly low, infinitely slow experiments on homogeneous rocks should lead to the same value of critical gas saturation in both internal and external processes. This argument may hardly stand close examination. The fundamental difference between the two processes is the difference in gas distribution. In the external process, the gas preferentially flows along more conductive channels from the higher pressure zones to lower pressure zones. In the internal process, the gas phase is formed by growth and coalescence of bubbles from randomly distributed sites. These sites could be widely distributed in the core or the reservoir. Thus it is more difficult to form a continuous gas phase, and it is easier for the gas phase to become discontinuous in the internal process, as compared to the external process.

2.4 Discussion of the Unusually High Production Performance

Unusually high performance of primary production has been observed in some heavy oil reservoirs. In this section, field observations and possible causes for this type of behaviour are reviewed. The foamy oil contribution is justified.

2.4.1 Field Observations

As mentioned earlier, the fraction of the original oil in place that can be recovered by a solution gas drive declines with increasing oil viscosity. However, some heavy oil reservoirs do not fit this expected recovery performance model and show anomalous recovery behaviour. Both the rate of production and the total recovery under solution gas drive are much higher, and the producing gas/oil ratio is much lower than what would be expected from measured reservoir parameters.

Unusually high solution gas drive recovery in a light oil fractured reservoir was reported by Platt and Lewis (1969). Anomalous recovery behaviour in heavy oil reservoirs was observed and investigated early in the late sixties. Baibakov and Garushev (1989) reported that the yield (production rate) of water-free crude and the productivity in very viscous heavy oil reservoirs did not differ from those of ordinary typical oil fields with light crudes of normal viscosity. Recently, it has been reported that a number of heavy-oil reservoirs in Canada and elsewhere in the world have been observed to exhibit similar behaviour. These reservoirs show "foamy-oil" behaviour in wellhead samples produced under solution gas drive. The oil is produced in the form of an oil-continuous foam which has the appearance of chocolate mousse and contains a high volume fraction of gas. This foam can be quite stable and may persist for several hours in open vessels. The field production data from these reservoirs suggest that the production mechanisms are complex and may be quite different from those encountered in conventional solution-gas drive reservoirs (Maini *et al.*, 1993). The wells in these reservoirs show anomalously high oil production. The rates of oil production under solution gas drive were reported to be 10 to 30 times (Poon and Kisman, 1992; McCaffrey and Bowman, 1991; Loughead and Saltuklaroglu, 1992; Lebel, 1994), or even 100 times (Yeung and Adamson, 1992) higher than what would be expected from conventional solution-gas-drive theory using the measured reservoir parameters. History matching the primary production for these wells often requires unrealistic adjustment of measured parameters, such as increasing the absolute permeability by an order of magnitude (Maini *et al.*, 1993; Claridge and Prats, 1994), or increasing the trapped gas saturation up to 35% and using unusual oil/gas relative permeabilities (Loughead and Saltuklaroglu, 1992).

McCaffrey and Bowman (1991) reported that sand production was essential for attaining high production rates in vertical wells producing from the Clear Water formation. The production rates in these wells initially increased as more sand was produced and later stabilized at a high level. Using theoretical equations and measured reservoir parameters, the estimated primary oil rates should not exceed 0.5 m^3/day. The average actual oil rate was reported to be 15 m^3/day/well. Foamy oil behaviour was believed to be one of the factors that contributed to the successes. They also reported that field and laboratory measured GOR data suggest that gas rates did not increase substantially over the production history of the well. This implies that the gas and oil are travelling to the well at the same time and this is consistent with the concept that gas breakout in viscous oils takes time and is essentially a near wellbore effect.

Poon and Kisman (1992) reported that the inflow performance of primary production heavy oil wells is also intriguing. Field experience indicated that some heavy oil wells have fluid levels of about 200 m above the perforations, which is very high considering that the nature of the process is primary recovery of viscous bitumen. When the pump rate is increased, the fluid level falls somewhat but recovers quickly to about the original level. It is not unusual to find fluid levels independent of pump rates. Furthermore, this phenomenon suggests that much higher production rates are possible if the downhole pumps could be improved. McCaffrey and Bowman (1991) also reported that even with an increase in rate, the wells still appear to maintain good fluid levels.

Another puzzle is that some wells with high primary production show very poor response to steam stimulation (Maini *et al.*, 1993). Karyampudi (1993) pointed out that the poor cyclic steam incremental oil rates and recovery (over the pre-steam cold production values) of the Cummings formation are partly due to the impairment of the primary production-enhancing mechanism by steam injection that is caused by: (a) modification of the pressure gradients established during primary production; and (b) nullification of foamy oil behaviour.

2.4.2 Possible Causes of High Performance

As discussed in the preceding section, a number of heavy oil reservoirs show anomalously high rates of production. What exactly causes the high primary production is not known, but several mechanisms for the primary production of heavy oil and bitumen have been proposed. These include i) unusual solution gas drive, or so-called foamy oil flow (Smith, 1988; Islam and Chakma, 1990; McCaffrey and Bowman, 1991; Loughead and Saltuklaroglu, 1992; Poon and Kisman, 1992; Maini *et al.*, 1993; Lebel, 1994); ii) influx of natural water from below or from the flanks providing pressure support (Smith, 1988; McCaffrey and Bowman, 1991; Poon and Kisman, 1992); iii) wormholes, fractures and other channels both naturally present and created by sand production (Poon and Kisman, 1992); and iv) sand production causing sand dilation and wormholes around the well and therefore resulting in an enhanced permeability or negative skin (Elkins, *et al.*, 1972; Smith, 1988; McCaffrey and Bowman, 1991; Loughead and Saltuklaroglu, 1992; Poon and Kisman, 1992; Lebel, 1994). Rock compaction could also be a significant factor for the primary production of heavy oils (Poon and Kisman, 1992). Sand production causes formation deformation. Probably similar to the steam injection process, deformation involves sand dilation (Dusseault and Rothernburg, 1988; Loughead and Saltuklaroglu, 1992; Beattle *et al.*, 1991) and subsequent recompaction (Beattle *et al.*, 1991). From a simulation study of reservoir drive mechanisms in the early cycles of steam stimulation at Cold Lake, formation compaction was found to be the dominant producing mechanism (about 60%); and solution-gas drive was the most important mechanism (about 20%) after formation compaction (Denbina *et al.*, 1991). Dusseault (1993) stated that a complete answer remained elusive, but the four major factors are likely enhanced drainage radius, grain movement, continuous pore deblocking and gas bubble expansion. The first three are related to sand production. The fourth is related to foamy oil flow.

It is likely that several of these mechanisms are involved in a reservoir. The relative contributions of these drive mechanisms might be evaluated using a methodology similar to Denbina *et al.*'s (1991). Denbina *et al.* developed a base model which includes all the mechanisms operative by history matching the field performance over the early cycles of steam stimulation. Then one of the mechanisms was systematically disabled and this modified simulation model was used to recalculate the production performance. By comparing the oil recovery in each case with that in the base case, the relative importance could be evaluated. If the dominant mechanism of a field is believed to be a solution gas drive, the detailed calculation results from the conventional theories based on reliable measurements of the fluid and rock properties for a field should be presented to verify the importance of the unusual solution gas drive. Unfortunately, such papers or reports have not been presented in the literature.

2.4.3 Justification of Foamy Oil Contribution

All the possible causes of anomalous productivity listed previously, except those related to sand production and foamy oil flow, are relatively well understood. Therefore, they are not expected to be the main cause for unusually high performance. It is generally believed that sand production contributes to the high production. Then a question arises: Is sand production the only factor? In other words, is there any foamy oil flow contribution in primary heavy oil production?

Sand production causes an enhanced permeability. However, laboratory studies have shown that no amount of sand remolding or fines removal would increase the permeability to the *extent* apparently observed in pressure analysis (Smith, 1988).

Loughead and Saltuklaroglu (1992) reported that the primary drive mechanism in the Celtic reservoir was believed to be solution gas drive. Rock compaction was of secondary importance overall but becomes the main drive mechanism towards the end of primary production once the gas mobilizes and is produced. Aquifer influx from below and from the reservoir flanks could not provide significant pressure support due to the highly unfavorable water/oil mobility ratio of several hundred. This could be confirmed by a material-balance calculation (Smith, 1988).

Lebel (1994) also reported that, without inclusion of foamy oil behaviour, the likelihood of achieving the recovery levels in heavy oil reservoirs is low, according to their simulation results from the reservoir models of various reservoir access geometries. In those models, the permeability enhancement due to sand production has already been included.

A simulation study of primary depletion tests showed that the predicted cumulative oil production was much less than that obtained from laboratory tests if foamy oil properties are not used (Maini, 1994). In these tests, no sand was produced.

Claridge and Prats (1995) reported that they had become aware of reservoirs with anomalous behaviour, in both North and South America, which exhibit large apparent mobilities and have produced essentially no sand. Although sand production may contribute to high production rates in some reservoirs, it is not sufficient to explain all the observed behaviour (e.g., low gas/oil ratio). High in-situ mobilities interpreted from pressure interference and pulse tests in the areas of reservoirs distant from production wells and still not very far below initial pressures strongly indicate that disturbances to unconsolidated sands (e.g., dilatation, fluidisation) do not appear to be the main cause of the apparent high mobilities.

Therefore, as Smith (1988) stated, after all the anomalous observations were considered, it was seen that alternative hypotheses were required. He suggested that the nucleation of a large number of microbubbles enhances the oil mobility. These microbubbles are entrained in the liquid oil phase and flow with it. This mixture of oil and gas bubbles was described as a non-aqueous oil-continuous foam (foamy oil) by Maini *et al.* (1993). They suggested that this foam may be a possible cause of the anomalous behaviour, since the two key factors needed for non-aqueous foam stability are present in a heavy oil system: the viscosity of the liquid phase (heavy oil) is high enough to retard drainage of liquid films by capillary forces, and plastic surface films, most likely observed in such crude oil systems. Recently, the mobility control potential of externally introduced non-aqueous foams has been recognized (Hanssen and Haugum, 1991; Irani, 1990), and the possibility of their in situ formation has been confirmed (Sarma and Maini, 1992). They further pointed out that it is well known that the flow behaviour of an aqueous foam is markedly different from that of a non-foaming water-gas mixture: the formation of a foam significantly reduces the mobility of the gas phase without appreciably changing the water mobility (Huh and Handy, 1986). By analogy, it becomes apparent that the flow in porous media of a foam-forming oil-gas mixture is likely to be very different compared to the flow of a non-foaming oil-gas mixture. If is likely that the mobility of the gas phase would be reduced significantly by foam formation while the oil mobility would not be affected.

Reilly and Scott (1995) reported that a better explanation of the Cold Lake field performance was given by a water-oil emulsion being driven by an internally expanding high (> 50%) gas saturation. This single-phase foamy emulsion concept is similar to the pseudo-single-phase foamy oil concept used to describe primary heavy oil production, which supports the existence of a foamy oil contribution. Another fact which supports the foamy oil contribution is that the anomalously high oil production usually occurs simultaneously with low production GOR.

Kraus *et al.* (1993) stated that the formation of high permeability wormholes accounts for the high initial rates delivered by wells in these types of heavy oil reservoirs; the special fluid properties of foamy oils account for the ability of these reservoirs to sustain high rates during primary depletion, unexpectedly high levels of primary recovery and low producing GOR's.

2.5 Mechanisms Involved in Solution-Gas-Drive Foamy Oil Reservoirs

A solution gas drive in a foamy oil reservoir involves many of the same mechanisms that are encountered in a conventional solution gas drive. As the reservoir pressure drops below the bubble point pressure, the oil becomes supersaturated with gas. Once the supersaturation exceeds a threshold value, the solution gas comes out of solution in the form of nucleated gas bubbles. As the pressure is reduced further, these gas bubbles grow larger in size. This growth is driven by mass transfer from the liquid phase and by volume expansion due to decreasing pressure. Small gas bubbles can flow with the oil while larger bubbles become trapped at pore throats. The trapped bubbles continue to grow and eventually become larger than the pore size and occupy several pores. The continued growth of these bubbles and the coalescence of adjoining bubbles eventually result in the formation of a continuous gas phase within the reservoir. The gas then starts to flow into the production well at an increasing rate.

Although the same processes occur in foamy oil systems and in conventional solution gas drives, their relative importance can be very different. Because of the low gas diffusivity in heavy oils, it takes more time for the dissolved gas to evolve for a given pressure drop. In other words, the non-equilibrium process of gas evolution in heavy oil reservoirs is more significant. Also, because of the effects of high oil viscosity and other factors, it takes a long time for the evolved gas bubbles to disengage from the oil phase and become free gas. It is believed that these dynamic processes play important roles in foamy oil flow.

Reported theoretical and experimental studies of the mechanisms involved in solution gas drive in foamy oil reservoirs are very limited. Smith (1988) proposed that the foamy oil contribution is due to the nucleation of a large number of microbubbles which enhances oil mobility. Claridge and Prats (1995) proposed a low-viscosity model suggesting that the adherence of asphaltenes present in the crude oil to the nucleated microbubbles reduces the oil viscosity. However, since no reliable measurements of the viscosity or mobility of foamy oils have been reported, these enhanced oil mobility and reduced oil viscosity mechanisms have not been verified.

Maini *et al.* (1993) suggested that the in-situ formation of a non-aqueous oil-continuous foam could be a possible cause of the anomalous behaviour. Because of the thermodynamic instability of gas bubbles, the fraction of the gas volume in the liquid oil phase could be low (see Section 4.4.7). Whether the behaviour of foams with high gas quality could be applied to foamy oil flow needs to be verified.

The most important mechanism involved in oil recovery may be the expansion energy from the foamy oil system. Because of the high viscosity of oil, gas cannot separate from the oil rapidly. Expanding gradually, gas provides the energy that drives the crude oil through the formation (Baibakov and Garushev, 1989). The effects observed in both field and laboratory studies of foamy oils are (1) the enhanced fluid compressibility, (2) the pressure support mechanisms, and (3) the delay of gas production (Kraus *et al.*, 1993).

It seems that the mechanisms of unusually high oil recovery in solution gas drive reservoirs is related to high permeability channels such as fractures, fissures and wormholes, etc. Early in 1969, Platt and Lewis reported the unusually high oil recovery which was predicted to exceed 50% in the Stateline field. The formation is a light tan dolomite with numerous pinpoint vugs and considerable fracturing. The viscosity of the fluid was 1.49 mPa·s at atmospheric pressure. Stewart *et al.* (1953) reported that for limestone cores having substantially sandstone type porosity, the production characteristics for solution and external gas drives are similar; for cores whose pore spaces were microscopically heterogeneous (i.e., consisted of combinations of solution cavities, matrices, and fissures), the production characteristics for solution and external gas drives vary widely. Stewart *et al.* (1954) further pointed out that since not all rocks exhibited unusual laboratory solution gas drive performance, the pore geometry probably also played an important role. In heavy oil unconsolidated reservoirs, sand production can create high permeability channels like wormholes around the wellbore. Probably, these channels provide a condition to generate high pressure gradients. As discussed in Section 2.3.4.3, the high pressure gradient enhances oil recovery.

2.6 Solution Gas Drive Models Related to Foamy Oil Flow

The fundamental difference between a conventional model and a non-conventional model is the technique used to model the evolution of solution gas as the reservoir pressure declines. In a conventional model it is assumed that the solution gas evolves from solution and becomes free gas instantaneously. In a non-conventional model, the evolution of solution gas is modelled differently in different models. Several non-conventional models to describe the solution gas drive related to foamy oil flow are reviewed in the following.

Smith (1988) appears to be the first to propose a model including the anomalous behaviour of foamy oils. He suggested that a solution gas drive in some heavy oil reservoirs may involve two-phase flow with gas in the form of tiny bubbles moving with the oil. Based on the hypothesis that the compressibility of the mixture of heavy oil and gas bubbles can be estimated by Eq. 2-1, $c_{fo} = \kappa/p$, he derived a series of equations and formulae to define the peculiar pressure-dependent multiphase flow properties, and to describe the flow of this mixture. The viscosity was estimated using the correlations for pipe flow. He argued that the theory has been used successfully to analyze the pressure and other behaviour of heavy-oil reservoirs under a solution gas drive. The predictions of the method are in agreement with the performance achieved at Lloydminster without recourse to negative skin or other permeability enhancement beyond laboratory values. According to his model, the amount of gas entrained in the oil depends on the coefficient κ and the system pressure p, being independent of time. This obviously does not conform to reality. It seems that the supersaturation (i.e., non-equilibrium) was not considered. The treatment of the viscosity needs experimental verification.

Poon and Kisman (1992) proposed that the dilatant (shear thickening) effects of non-Newtonian fluids can provide an explanation for low apparent viscosities at a distance from the wellbore where shear rates are low and for the high production performance. This model can not stand close examination as will be discussed in Section 3.3.2.

Several researchers (Yortsos and Parlar, 1989; Li and Yortsos, 1991, 1993; Kashchiev and Firoozabadi, 1993) investigated bubble nucleation and growth in porous media. The two main issues in the solution gas drive process, supersaturation and critical gas saturation, were examined. Most of their studies focused on the effect of the pressure decline rate. Yortsos and Parlar (1989) used the percolation approach at low super-saturation (low decline rate) to estimate the critical gas saturation and relative permeability from nucleation and pore structure characteristics. Li and Yortsos (1991, 1993) developed a theoretical analysis and a pore network simulation to investigate the bubble growth pattern. The critical gas saturation value depends on the underlying growth pattern. Based on some simplified assumptions, Firoozabadi and Kashchiev (1993) formulated the volume increase of the gas phase in the cases of constant system volume expansion rate and constant system pressure decline rate. A common weakness of these models is that the dynamic process of bubble disengagement from the liquid oil phase was not included. As was discussed in Section 2.2.2.1 and will be discussed in Sections 5.5 and 6.5.3., this process is very important, since it can affect significantly the foamy oil properties and the ultimate recovery of a solution gas drive.

Several other models including a pseudo-bubblepoint model, a modified fractional flow model and a reduced viscosity model have been published. As will be discussed in Chapter 3, these models were based on empirical adjustments or modification of fluid properties, rather than having a solid theoretical basis. These models were validated by history matching the field performance. This kind of model validation may not be persuasive because of inadequate and/or inaccurate data. For example, the properties of reservoir fluids are usually incomplete; the producing gas oil ratios from a single well are rarely recorded. A common weakness of these models is that the time-dependent effect was not properly included.

2.7 Summary

"Foamy oil" and "foamy oil flow" are not well defined. Theoretical and experimental investigations of foamy oil flow are still in their early stages. Currently, there are more questions than answers concerning various aspects of the process.

Only limited information is available on the physical properties of foamy dispersion. Obviously, foamy oil, i.e., oil containing dispersed gas bubbles, is much more compressible than conventional oil and a reasonable estimate of its compressibility can be obtained from a knowledge of the liquid and gas compressibilities, as was done in Section 2.2.2.1. However, its viscosity remains controversial. It is not even certain that the viscosity is higher or lower than that of a single oil phase. The relative permeabilities related to foamy oil flow are unexplored.

Many issues of solution gas drive related to foamy oil flow are poorly understood, e.g., critical gas saturation, gas bubble size distribution and flow pattern. All these issues vary with not only system parameters but also with the operating conditions, such as the pressure decline rate. Although it has been suggested by many that the tiny bubbles will flow with the oil, it is not known at what size and what conditions the relative phase velocity becomes non-zero.

It seems that there is a foamy oil contribution in heavy oil reservoirs. However, it is not known under what conditions this contribution is significant.

The proposed foamy oil models need to be verified theoretically and/or experimentally. The dynamic processes related to bubble nucleation, bubble growth and bubble disengagement from oil have not been considered properly in any of the published models. As a result, a lot more work is needed to explore the mechanisms involved in solution gas drive foamy oil reservoirs.

2.8 References

Abgrall, E. and Iffly, R.: "Physical Study of Flow by Expansion of Dissolved Gas," *Revue de L'Institut Français du Pétrole* (Sept. - Oct. 1973) **28**, No. 5, 667-92 (French).

Aldea, Gh.: "Mechanism of Heavy Oil Recovery by Dissolved Gas Expansion," *Revue de L'Institut Français du Pétrole* (Dec. 1970) **25**, No. 12, 1403-17 (French).

Baibakov, N.K. and Garushev, A.R.: *Thermal Methods of Petroleum Production*, Developments in Petroleum Science 25, translated by W.J. Cieslewicz, Elsevier Science Publishers B.V., Amsterdam (1989) 6-21.

Beattle, C.I., Boberg, T.C., and McNab, G.S.: "Reservoir Simulation of Cyclic Steam Stimulation in the Cold Lake Oil Sands," *SPE Reservoir Engineering* (*SPERE*) (May 1991) 200-06.

Bora, R. *et al.* "Measurements of Foamy Oil Viscosity," (1995) to be published.

Chatnever, A., Indra, M.K. and Kyte, J.R.: "Microscopic Observations of Solution Gas Drive Behaviour," *Journal of Petroleum Technology* (*JPT*) (June 1959) 13-15.

Claridge, E.L. and Prats, M.: "A Proposed Model and Mechanism for Anomalous Foamy Heavy Oil Behaviour," paper SPE 29243 presented at the International Heavy Oil Symposium, Calgary, AB, June 19-21, 1995; *Proc.*, 9-20; also the unsolicited manuscript of SPE (USMS) 29243 (1994).

Danesh, A., Peden, J.M., Krinis, D. and Henderson, G.D.: "Pore Level Visual Investigation of Oil Recovery by Solution Gas Drive and Gas Injection," paper SPE 16956 presented at the 62nd SPE Annual Technical Conference and Exhibition, Dallas, TX, Sept. 27-30, 1987.

Denbina, E.S., Boberg, T.C. and Rotter, M.B.: "Evaluation of Key Reservoir Drive Mechanisms in the Early Cycles of Steam Stimulation at Cold Lake," *SPERE* (May 1991) 207-11.

de Swaan, A.: "Development of the Critical Gas Saturation," *JPT* (May 1981) 907-08.

Downie, J. and Crane, F.E.: "Effect of Viscosity on Relative Permeability," *Society of Petroleum Engineers Journal* (*SPEJ*) (June 1961) 59-60.

Dusseault, M.B.: "Cold Production and Enhanced Oil Recovery," *JCPT* (Nov. 1993) **32**, No. 9, 16-18.

Dusseault, M.B. and Rothemburg, L.: "Shear Dilatancy and Permeability Enhancement in Oil Sands, paper No. 32 presented at the 4th UNITAR/UNDP Conference on Heavy Crude and Tar Sands, Edmonton, AB, Aug. 7-12, 1988.

Elkins, L.F., Morton, R. and Blackwell, W.A.: "Experimental Fireflood in a Very Viscous Oil-Unconsolidated Sand Reservoir, S.E. Pauls Valley Field, Oklahoma," paper SPE4086 presented at the 1972 SPE Annual Meeting, San Antonio, TX, Oct. 8-11.

Firoozabadi, A. and Aronson, A.: "Visualization and Measurement of Gas Evolution and Flow of Heavy and Light Oil in Porous Media," paper SPE 28930 (USMS) (1994) available from SPE, Richardson, TX.

Firoozabadi, A. and Kashchiev, D.: "Pressure and Volume Evolution During Gas Phase Formation in Solution Gas Drive Process," paper SPE 26286 (USMS, 1993).

Firoozabadi A., Mikkelson, M. and Ottesen, B.: "Reply to Discussion of Measurements of Supersaturation and Critical Gas Saturation," *SPE Formation Evaluation* (*SPEFE*) (June 1994) 159-60.

Firoozabadi A., Ottesen, B. and Mikkelson, M.: "Measurements of Supersaturation and Critical Gas Saturation," *SPEFE* (Dec. 1992) 337-43.

Govier, G.W. and Aziz, K.: *The Flow of Complex Mixtures in Pipes*, Robert E. Krieger Publishing Company, Inc., Florida (1982) 512, 557-558.

Handy, L.L.: "A Laboratory Study of Oil Recovery by Solution Gas Drive," *Trans.* (1958), AIME, **213**, 310-15.

Hanssen, J.E. and Haugum, P.: "Gas Blockage by Non-aqueous Foams," paper SPE 21002 presented at the International Symposium on Oilfield and Geothermal Chemistry, Anaheim, CA, Feb. 20-22, 1991.

Huh, D.G. and Handy, L.L.: "Comparison of Steady and Unsteady-State Flow of Gas and Foaming Solution in Porous Media," paper SPE 15078 presented at the 56th California Regional Meeting, Oakland, CA, April 2-4, 1986.

Irani, C.A.: "Oil Recovery Using Surfactants in Non-aqueous Drive Fluids," U.K. Patent #2,230,545 (Oct. 24, 1990).

Islam, M.R. and Chakma, A.: "Mechanics of Bubble Flow in Heavy Oil Reservoirs," paper SPE 20070 presented at the 60th California Regional Meeting, Ventura, CA, April 4-6, 1990.

Kamath, J. and Boyer, R.E.: "Critical Gas Saturation and Supersaturation in Low-Permeability rocks," paper SPE 26663 presented at the 68th Annual Technical Conference and Exhibition, Houston, TX, Oct. 3-6, 1993; also *SPEFE* (Dec. 1995) 10, No. 4, 247-53.

Karyampudi, R.S.: "Evaluation of Cyclic Steam Performance and Mechanisms in a Mobile Heavy Oil Reservoir at Elk Point Thermal Pilot," paper CIM 93-48 presented at the CIM Annual Technical Conference, Calgary, AB, May 9-12, 1993.

Kashchiev, D. and Firoozabadi, A.: "Kinetics of the Initial Stage of Isothermal Gas Phase Formation," *The Journal of Chemical Physics* (*J. Chem. Phys.*) (March 15, 1993) **98**, No. 6, 4690-99.

Kortekaas, T.F.M. and van Poelgeest, F.: "Liberation of Solution Gas During Pressure Depletion of Virgin Watered-Out Oil Reservoirs," *SPERE* (Aug. 1991) 329-35.

Kraus, W.P., McCaffrey, W.J. and Boyd, G.W.: "Pseudo-Bubble Point Model for Foamy Oils," paper CIM 93-45 presented at the 44th Annual Technical Conference of the Petroleum Society of CIM, Calgary, AB, May 9-12, 1993.

Lebel, J.P.: "Performance Implications of Various Reservoir Access Geometries," paper presented at the 11th Annual Heavy Oil & Oil Sands Technical Symposium, March 2, 1994.

Li, X. and Yortsos, Y.C.: "Visualization and Numerical Studies of Bubble Growth During Pressure Depletion," paper SPE 22589 presented at the 66th SPE Annual Technical Conference and Exhibition, Dallas, TX, Oct. 6-9, 1991.

Li, X. and Yortsos, Y.C.: "Critical Gas Saturation: Modeling and Sensitivity Studies," paper SPE 26662 presented at the 68th SPE Annual Technical Conference and Exhibition, Houston, TX, Oct. 3-6, 1993.

Loughead, D.J. and Saltuklaroglu, M.: "Lloydminster Heavy Oil Production: Why So Unusual?" paper presented at the 9th Annual Heavy Oil and Oil Sand Symposium, Calgary, AB, March. 11, 1992.

Madaoui, K.: "Critical Gas Saturation in Depletion Drive," *reports* of International Symposium on Hydrocarbon Exploration, Drilling and Production Techniques (Dec. 10-12, 1975) 203-20 (French).

Maini, B.B.: "Foamy Oil Flow," teaching notes at the workshop for the members of Petroleum Recovery Institute (PRI), April 27, 1994.

Maini, B.B., Sarma, H.K. and George, A.E.: "Significance of Foamy-Oil Behaviour in Primary Production of Heavy Oils," *JCPT* (Nov. 1993) **32**, No. 9, 50-54.

Maini, B.B., Sheng, J.J. and Nicola, F.: "Foamy Oil Flow - Improved Primary Heavy Oil Recovery," paper presented at the Annual Conference and Exhibit of the Petroleum Recovery Institute, Calgary, AB, May 25, 1995.

Maini, B.B., Sheng, J.J. and Nicola, F.: "Laboratory Investigation of Foamy Oil Flow for Improved Primary Production," Final Report to the Canada Centre for

Mineral and Energy Technology (CANMET) (Sept. 1995) 53.

McCaffrey, W.J. and Bowman, R.D.: "Recent Success in Primary Bitumen Production," paper No. 6 presented at the 8th Annual Calgary University *et al.* Heavy Oil & Oil Sands Technical Symposium, Calgary, AB, March 14, 1991.

Moulu, J.C. and Longeron, D.L.: "Solution-Gas Drive: Experiments and Simulation," *Proc.*, the 5th European Symposium on Improved Oil Recovery, Budapest, Hungary (April 1989) 145-154.

Odeh, A.S.: "Effect of Viscosity Ratio on Relative Permeability," *Trans.* (1959), AIME, **216**, 346-53.

Platt, C.R. and Lewis, W.M.: "Analysis of Unusual Performance Indicates High Solution-Gas-Drive Recovery-Stateline Ellenburger Field," *JPT* (Dec. 1969) 1507-09.

Poon, D.C. and Kisman, K.: "Non-Newtonian Effects on the Primary Production of Heavy Oil Reservoirs," *JCPT* (Sept. 1992) **31**, No.7, 55-59; also paper CIM/AOSTRA 91-33 presented at the CIM/AOSTRA Technical Conference, Banff, AB, April 21-24, 1991.

Reilly, B.T. and Scott, G.R.: "Cold Lake Project Recovery and the Role of Foamy Emulsion," paper SPE 30287 presented at the International Heavy Oil Symposium, Calgary, AB, June 19-21, 1995; *Proc.*, 403-11.

Ridings, R.L., Dalton, R.L., Greene, H.W., Kyte, J.R. and Naumann, V.O.: "Experimental and Calculated Behaviour of Dissolved-Gas-Drive Systems," *SPEJ* (March 1963) 41-48.

Saidi, A.M.: "Discussion of Measurements of Supersaturation and Critical Gas Saturation," *SPERE* (June 1994) 157-58.

Sarma, H. and Maini, B.B.: "Role of Solution Gas in Primary Production of Heavy Oils," paper SPE 23631 presented at the Second Latin American Petroleum Engineering Conference, Caracas, Venezuela, March 8-11, 1992.

Sarma, H.K., Maini, B.B., Nicola, F., and Goldman, J.: "An Experimental Study of the Gas-Nucleation Process During the Primary-Production Phase in Heavy-Oil Reservoirs Under Solution-Gas Drive," final report to CANMET (May 30, 1991).

Shen, C. and Batycky, J.P.: "Some Observations of Mobility Enhancement of Heavy Oils Flowing through Sand Pack under Solution Gas Drive," paper 96-27 presented at the 47th Annual Technical Conference of the Petroleum Society of CIM, Calgary, AB, June 10-12, 1996.

Sheng, J.J., Hayes, R.E., Maini, B.B. and Tortike, W.S.: "A Proposed Dynamic Model for Foamy Oil Properties," paper SPE 30253 presented at the International Heavy Oil Symposium, Calgary, AB, June 19-21, 1995; *Proc.*, 125-38.

Sheng, J.J. and Maini, B.B.: *Foamy Oil Flow in Primary Production of Foamy Oil - A literature Review*, the Petroleum Recovery Institute Report 1995/96-7 (Feb. 1996) 2.

Sheng, J.J., Maini, B.B., Hayes, R.E. and Tortike, W.S.: "Foamy Oil Flow - A Review," paper presented at the International Symposium on Petroleum and Petrochemical Engineering, Beijing, Sept. 14-17, 1994.

Sheng, J.J., Maini, B.B., Hayes, R.E. and Tortike, W.S.: "A Non-Equilibrium Model to Calculate Foamy Oil Properties," paper CIM 95-19 presented at the 46th Annual Technical Conference of the Petroleum Society of CIM, Banff, AB, May 14-17, 1995.

Sheng, J.J., Maini, B.B., Hayes, R.E. and Tortike, W.S.: "Experimental Study of Foamy Oil Stability," paper CIM 95-151 presented at the 6th Saskatchewan Petroleum Conference of the Petroleum Society of CIM, Regina, SK, Oct. 16-18, 1995.

Smith, G.E.: "Fluid Flow and Sand Production in Heavy Oil Reservoirs Under Solution Gas Drive," *SPE Production Engineering* (*SPEPE*) (May 1988) 169-80.

Stewart, C.R., Craig, F.F. and Morse, R.A.: "Determination of Limestone Performance Characteristics by Model Flow Tests," *Trans.* (1953), AIME, **198,** 93-102.

Stewart, C.R., Hunt, E.B., Jr., Schneider, F.N., Geffen, T.M. and Berry, V.J., Jr.: "The Role of Bubble Formation in Oil Recovery by Solution Gas Drive in Limestones," *Trans.* (1954), AIME, **201,** 294-301.

Wall, C.G. and Khurana, A.K.: "Saturation: Permeability Relationships at Low Gas Saturations," *Journal of the Institute of Petroleum* (*J. Inst. Pet.*) (Sept. 1971) **57,** No. 557, 261-69.

Wall, C.G. and Khurana, A.K.: "The Effect of Rate Pressure Decline and Liquid Viscosity on Low-Pressure Gas Saturations in Porous Media," *J. Inst. Pet.* (Nov. 1972) **58,** No. 564, 335-45.

Wit, K.: "Solution Gas Drive in Heavy Oil Reservoirs," paper presented at the Symposium on Heavy Oil recovery, Maracaibo, July 1-3, 1974.

Yeung, K.C. and Adamson, M.F.: "Burnt Lake Project - Bitumen Production from the Cold Lake Oil Sands Deposit without Steam," paper presented at the

AOSTRA/CHOA "Fueling the Future" Conference, Calgary, AB, June 10-12, 1992.

Yortsos, Y.C. and Parlar, M.: "Phase Change in Binary Systems in Porous Media: Application to Solution Gas Drive," paper SPE 19697 presented at the 64th Annual Technical Conference and Exhibition of SPE of AIME, San Antonio, TX, Oct. 8-11, 1989.

Yuster, S.T.: "Theoretical Considerations of Multiphase Flow in Idealized Capillary Systems," *Proc.*, the Third World Petroleum Congress - Section II (1951) 437-445.

Chapter 3

Discussion of Foamy Oil Viscosity

3.1 Introduction

All the papers on non-conventional heavy oil flow have assumed that, with neither theoretical nor experimental justification, microbubbles or solid fines dispersed in the oil phase reduce the oil viscosity. Such an assumption has been widely questioned. To answer this question is one of the key issues needed to understand the recovery mechanism in foamy oil reservoirs.

This chapter presents the information on the viscosity of gas-oil mixtures and discusses several reduced oil viscosity models. A simple derivation of foamy oil viscosity in a capillary is presented.

3.2 Literature Information of the Viscosity of Gas-Oil Mixture

A problem arises as how best to represent the viscosity of the gas-liquid mixture, μ_m. There are basically two sources of literature describing the viscosity of a mixture.

One is from the references that study the vertical flow of gas-oil mixtures along a wellbore where the viscosity is lower than the pure oil viscosity. Another is the references that describe dispersion viscosity where the mixture viscosity is usually higher than the dispersing phase viscosity. They are reviewed in the following.

3.2.1 Gas-Oil Viscosity in Pipe Flow

The simplest assumption would be that the viscosities of the two components should be additive:

$$\mu_m = (1-u)\mu_l + u\mu_g. \tag{3-1}$$

Here u has been expressed as a volume fraction, weight fraction, and molar fraction with no apparent justification for any of these. This assumes an ideal mixture, and no ideal mixtures have been found which follow this law no matter which way the concentration is expressed (Hagedorn and Brown, 1965). The subscripts, l and g, denote liquid and gas, respectively.

It has been noted that in real mixtures the viscosity-concentration curve is convex toward the concentration axis. This behaviour was noted also by Uren *et al.* (1930) in his work on the absolute viscosity of a gas-liquid mixture. As the gas-liquid ratio is increased, the viscosity of the mixture rapidly decreases from the viscosity of the liquid and approaches the viscosity of the gas at very high gas-liquid ratios. A similar type of curve is observed when the viscosity of an oil is plotted as a function of the gas in solution (Hagedorn and Brown, 1965). A relationship which exhibits this characteristic behaviour is an empirical equation proposed by Arrhenius (in the reference of Hatchek, 1928) which appears as follows:

$$\mu_m = \mu_l^{(1-u)} \mu_g^u, \tag{3-2}$$

where $u = f_g$, volume fraction of gas in the liquid, as modified by Hagedorn and Brown (1965). Here the logarithms of the viscosities of the components are assumed to be additive.

3.2.2 Dispersion Viscosity

As an approximation of a more complex formula, Einstein (1906, 1911) proposed on hydrodynamic and diffusion grounds for rigid (solid) uniform spheres moving without slip in a medium of equal density, at low concentrations, the well known equation:

$$\mu_m = \mu_l \, (1 + 2.5 f_d), \tag{3-3}$$

where f_d is the fraction of the total volume which is occupied by the dispersed solid particles. More generally, there are many formulae of this kind

$$\mu_m = \mu_l \, (1 + \kappa f_d), \tag{3-4}$$

where κ is a constant coefficient.

Taylor (1932) extended Einstein's work to a liquid containing small drops of another liquid in suspension. He showed that

$$\mu_m = \mu_l \left[1 + 2.5 f_d \left[\frac{\mu_d + 0.4\mu_l}{\mu_d + \mu_l} \right] \right]. \tag{3-5}$$

This expression is valid provided the surface tension is great enough to keep the drops nearly spherical. When the drops are rigid, μ_d is infinite, and this reduces to Einstein's formula. When the drops are gas bubbles, μ_d may be neglected compared with μ_l and the above expression becomes

$$\mu_m = \mu_l \, (1 + f_d), \tag{3-6}$$

a result also obtained by Eisenschitz (1933) for the case where the liquid slips freely over the surface of a rigid sphere.

There is a close similarity between the equations of elasticity and those of hydrodynamics. Mackenzie (1950) applied the theory of determining the effective elastic constant of a material containing a large number of small holes to the discussion of the effective viscosity of a liquid containing small gas bubbles. He showed that, due to the presence of the bubbles, the viscosity is reduced:

$$\mu_m = \mu_l \, (1 - \frac{5}{3} f_d). \tag{3-7}$$

This expression, in which κ is negative compared with the general equation 3-4, assumes that the bubbles deform freely during the motion so that, unless the motion is oscillatory, the bubbles will not remain spherical for long.

From the above review, it is clear that the boundary conditions assumed at the interface of the bubble play an important part in the viscosity.

3.3 Discussion of Reduced Oil Viscosity Models

The viscosity of a gas-liquid dispersion or a solid-liquid dispersion flowing as a pseudo-single phase fluid is an important parameter in modelling the flow behaviour. Because of the unstable nature of the dispersion and the possible influence of the flow geometry on apparent viscosity, it may be difficult to obtain reliable measurements. Several reduced oil viscosity models have been proposed without any experimental verification. These models attribute the viscosity reduction to different effects which are discussed in the following.

3.3.1 Analogous to Pipe Flow

Smith (1988) used a modified buildup analysis to infer apparent in-situ viscosities for foamy oil. In his analysis, it was assumed that measures of the permeability-thickness product exist; the only unknown in the kh/μ parameter is the mobile fluid viscosity, μ. A number of observations on buildup analysis were used to derive an apparent in-situ viscosity for the two-phase mixture with a combined density. He showed that the apparent viscosity derived from the buildup analysis is of the order of 100 to 500 mPa · s, whereas the range of the live single-phase crude oil viscosities as measured directly is 1700 to 3500 mPa · s. He suggested that the slug flow correlations developed for viscosity in pipe systems could be used to quantify the gas-oil mixture viscosity in porous media. He suggested that the following correlations of gas-oil mixture viscosity from pipe flow are applicable for pore flow:

$$\frac{1}{\mu_m^n} = \frac{1}{\mu_g^n} + \frac{1}{\mu_o^n}, \tag{3-8}$$

$$\mu_m = f_{dg}\mu_g + (1-f_{dg})\mu_o, \tag{3-9}$$

$$\mu_m = \mu_g^{f_{dg}}\, \mu_o^{(1-f_{dg})}. \tag{3-10}$$

For the above equations, Eq. 3-8 can be derived if a series flow of gas and oil phases (slug flow) is assumed. Eq. 3-9 can be derived for $n = 1$ if the segregated flow of gas and oil phases is assumed. As Claridge and Prats (1995) noted, Eq. 3-10 is for the pressure drop due to friction in two-phase flow up vertical tubing. It is for turbulent flow with the two phases present in large local volumes ranging from large bubbles for low gas rates, to concentric flow with gas in the middle and liquid around the perimeter of the tubing, to mist flow for very high gas rates. The mixture viscosity is used as an empirical correlation factor for calculating a mixture Reynolds number and a friction factor for the turbulent flow region. The application of this expression to foamy oil flow seems questional, unless the saturation distributions and the flow pattern are well defined. Uren *et al.* (1930) also pointed out that as oil is discharged from deep wells, after reaching the surface, there will normally be at least 60 times as much gas, by volume, as oil; and in many cases the ratio of the gas volume to that of the oil will have a value as great as 1000 or more. The character of flow through the eduction tube is doubtless turbulent, it being inconceivable that viscous flow could exist within a non-homogeneous fluid mass moving through a tube of restricted cross-section at practically high velocities.

Obviously, the applicable conditions of these viscosity correlations are not satisfied in foamy oil flow which is for microbubbles in a continuous liquid oil phase. The low viscosity derived from Smith's modified buildup analysis (Horner slope) is questionable, because the Horner slope was derived from his modified diffusivity equation which is based on the assumption (Eq. 2-1): $c_{fb} = \kappa/p$. As discussed earlier in Section 2.2.2.1, this assumption may not describe reality.

3.3.2 Dilatant Effect

The rheological behaviour of an emulsion or a dispersion can be Newtonian or non-Newtonian depending on its composition. At low to moderate values of dispersed-phase concentrations, emulsions generally exhibit Newtonian behaviour (Alvarado and Marsden, 1979). In the high-concentration range, emulsions behave as shear thinning fluids (Pal *et al.*, 1992). Also, the bitumens studied from the Athabasca and Cold Lake regions of Alberta were found to be mildly non-Newtonian. Therefore, heavy oils will very likely behave as a Newtonian fluid. However, Poon and Kisman (1992) proposed another mechanism that is related to the rheological properties of bitumen. They suggested that dilatant (shear thickening) effects provide an explanation for low apparent viscosities at a distance from the wellbore where shear rates are low. In their model, the dispersed matter is solid fines (sand). This dispersion is not a foamy oil. However, since this model was also proposed to explain the unusually high heavy oil production, it is also discussed together with the other foamy oil viscosity models.

There are several questions about their proposed mechanism. First, as they mentioned also, no laboratory measurements had been obtained which show that the mixture of heavy oil and sand at typical initial reservoir temperatures (15 °C) and at very low shear rates (less than 0.1 s^{-1}) exhibits dilatant fluid behaviour. Second, it is hard to believe that the apparent viscosity of a heavy oil and sand mixture could be lower than that of the heavy oil itself, because a dispersion should have a higher viscosity than the dispersing fluid. Third, according to the effect of a dilatant fluid, the apparent viscosity is very high around the wellbore because of the higher shear rate, which would create a resistance to fluid flow similar to well damage. They had to rely on sand production which creates a high porosity-permeability chamber around the wellbore and effectively reduce this resistance to flow. However, it was observed that some reservoirs exhibited high production and produced essentially no sand (Claridge and Prats, 1995). Also, higher recovery was obtained in the primary depletion tests in which no sand was produced (Maini *et al.*, May 1995 and Sept. 1995). Finally, their model predicted that the production rate appears to be constant for an extended production period, which is not possible in the field. One of their explanations is that their model assumes that the rheological properties are independent of shear rate; in reality, the fluid may become pseudoplastic at very low shear rates which would effectively prevent a constant production rate. If it is true, it will be difficult to justify that the shear rate is within the right range for dilatant behaviour at the early stages of production, while the shear rate will be within the pseudoplastic behaviour range at the later stages. Actually, the extended constant production rate is caused by the infinite boundary condition of the solution they used. According to their model, a higher pressure decline rate may cause a higher shear rate which would cause higher viscosity. Obviously, their proposed model could not explain the fact that the higher the pressure decline rate, the higher the oil recovery obtained.

3.3.3 Asphaltene Adsorption Effect

Claridge and Prats (1995) stated that the simple presence of microscopic gas bubbles, without a compositional change in the liquid oil phase leading to a change in that phase's viscosity, is not an adequate explanation of the difference between foamy oil production behaviour and non-foamy oil production behaviour. They postulated that the viscosity of oil decreases as the gas comes out of solution in the form of a large number of very small bubbles. They suggested that the mechanism responsible for such a reduction in viscosity is the adherence of asphaltenes present in the crude to the nucleated gas microbubbles. This adherence of asphaltenes to bubble surface stabilizes the bubbles at a small size and the bubbles can then be transported through the rock pores with the crude oil. The removal of asphaltenes as dispersed matter from the bulk oil reduces the viscosity of the oil. No experimental verification of their proposed mechanism was attempted. Their proposed mechanism could not explain the experimental observations in the foamy oil stability tests and the primary depletion tests. The results of foamy oil stability tests (Section 4.4.2) show that the system of gas and crude oil with asphaltene is more stable than that of gas and mineral oil without asphaltene. However, the difference was not observed to be significant. This implies that the effect of asphaltene might not be so significant that it would dominate foamy oil behaviour as Claridge and Prats's (1995) low viscosity model proposed. In the primary depletion tests with the mineral oil PAO-100 which did not contain asphaltene (Maini *et al.*, May and Sept., 1995), the oil recovery with the fast pressure decline rate was much higher than that with the slow pressure decline rate which implies that the so-called foamy oil behaviour was observed in the fast depletion tests even when the tested mineral oil was asphaltene-free.

3.3.4 Lubrication Effect

It is generally assumed that the rheological behaviour of the flowing fluid is independent of the geometry of the porous medium. Savins (1969) has stated that questions always arise about whether the rheological parameters determined from viscometry describe the rheological behaviour of a fluid flowing in porous media. This is a fundamental question, but the data of a few investigators show the validity of this assumption. It is found from the data (Savins, 1969; Uzoigwe, 1970; Alvarado, 1975) that the rheograms in both the viscometer and porous media are parallel but may not coincide (Abou-Kassem and Farouq Ali, 1995). In foamy oils, the dispersed gas bubbles make the effect of porous media on viscosity even more complex. Recently, Shen and Batycky (1996) proposed another foamy oil viscosity model to consider the effect of bubbles in porous media on oil viscosity. They re-interpreted the steady tests of heavy oil flow through the sand pack reported by Maini *et al.* (1993); and they believed that the foamy oil mobility was enhanced due to bubble nucleation which is not consistent with Maini *et al.*'s original conclusion. In their model, they argued that entrapment of gas bubbles in oil would reduce the oil mobility; however, the nucleation of gas bubbles at the grain surface would enhance the mobility. The mobility of heavy oil increases proportionally with the nucleation rate; but decreases with foam quality according to general dispersion viscosity models. They attributed this mobility enhancement to the so-called *lubrication* (or *slippage*) *effect*. The lubrication effect was used to explain the enhanced non-wetting (oil) phase relative permeability in two-phase coaxial flow through capillary tubes (Yuster, 1952; Odeh, 1959). In such a system, the non-wetting phase (oil) flows in the centre; and the wetting phase (water) flows or stays in the annular region between the tube wall and the non-wetting phase.

Before one discusses the lubrication effect in foamy oil flow, one has to realize that only a few papers addressed such an effect. Let's first assume that such an effect exists and has been verified in multiphase flow.

Their proposed model rests on their interpretation of Maini *et al.*'s steady tests. For a single oil rate, they used the values of parameters reported by Maini *et al.* to calculate the pressure distribution, based on the three assumptions presented in their paper. Their three assumptions are briefly: (1) single-phase flow; (2) gas bubbles can stay in the oil for an arbitrary foam quality of up to 0.3; and (3) thermodynamic equilibrium. They compared their calculated pressure gradients near the inlet region with the measured data; and they observed that the calculated pressure gradients were higher than the measured. Therefore, they deduced that the heavy oil mobility was enhanced. Such an interpretation is questionable as discussed in the following.

From the inlet to the outlet, the gas volume fraction in the oil increases from zero to a maximum. Near the inlet, the gas volume fraction is very small, 3% according to Maini's rough estimate (1994). The actual gas volume fraction would be less than that value because of supersaturation and the non-equilibrium evolution of solution gas.

Therefore, the flow near the inlet should behave like a single-phase oil flow; and the corresponding pressure distribution of the single oil phase is shown in Figure 3.1 as a dotted straight line. The pressure distribution calculated by Shen and Batycky, which is also shown in Figure 3.1, might not represent the actual one in the sand pack, because, most likely, the measured and reported values of the parameters were not accurate, and/or their assumptions were not valid. Figure 3.1 shows that the measured pressures are lower than those for the single-phase oil, rather than higher as Shen and Batycky interpreted. However, there is not enough evidence from Maini *et al.*'s experimental data to conclude that the foamy oil mobility was decreased. This is because their measurements did not provide a reliable measure of the effect of bubble nucleation on the flow of the gas-oil dispersion since the increase in the volumetric flow rate resulting from the gas nucleation was not measured. This was pointed out in the previous paper (Sheng *et al.*, 1995) and report (Sheng and Maini, 1996). Although the experimental data show that the *total* (free gas and oil with dispersed bubbles) mobility did decrease as more gas was evolved, it is not certain the foamy oil (oil with dispersed bubbles) mobility also decreased. The evolution of gas causes gas-oil two-phase flow. Therefore, the pressure distributions from the experimental data most likely reflect the total mobility of the two phases instead of the foamy oil mobility. Their tests were started at the saturation pressure. Probably, if the tests were started at a pressure higher than the saturation pressure, and a reasonably high pressure drawdown were imposed, a single liquid oil phase, a oil phase with dispersed gas bubbles (foamy oil phase) and a gas-oil two-phase mixture would exist along the sand pack. Comparing the pressure gradients along the sand pack might lead to some interesting findings. If the foamy oil mobility is

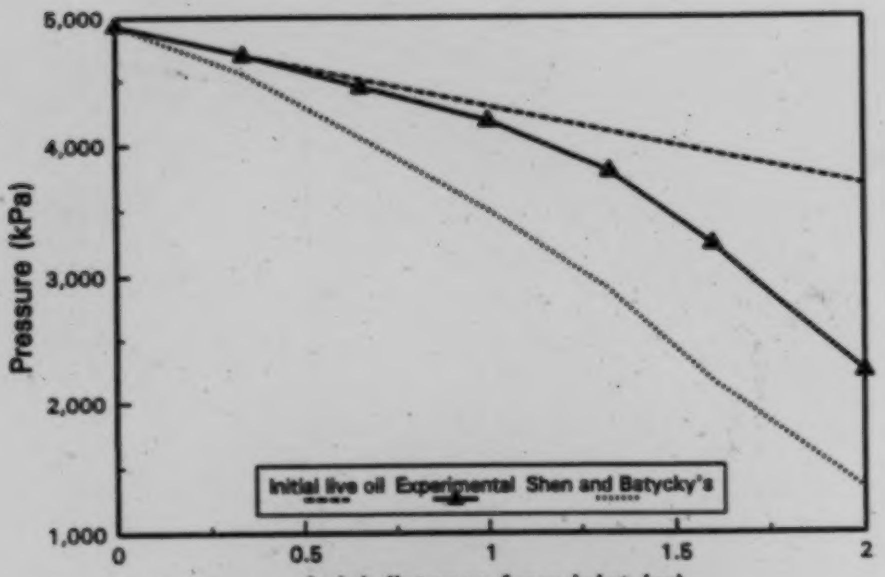

Fig. 3.1 - Comparison of pressure distributions.

higher than that of the single-phase oil, the pressure gradients within the segment of foamy oil phase should be lower than those within the segment of single oil phase. Such an experiment may be difficult, because the pressure drawdown must be carefully designed to make sure that the three phases exist along the sand pack.

There are three main assumptions for the lubrication effect: (1) the two phases flow through the same capillary tube and in the same direction; (2) the non-wetting phase flows in the cylindrical portion of the capillary and concentric with it; the wetting phase flows in the annulus between the capillary wall and the non-wetting phase or "spins" in a thin film over the wall, analogous to the action of ball bearings in the longitudinal movement of a rod in a bearing; (3) the velocity of each phase at the interface is the same. These assumptions imply that the phase next to the wall should be a continuous film which is impossible in foamy oils because of bubble coalescence.

Shen and Batycky assumed that there was fluid slip at the interface between the bulk fluid and the bubble layer *over* the mineral surface. Here they implied that the bubbles "stick" to the wall. However, observations from Li's (1993) glass micromodel experiments showed that after the initial gas bubbles nucleate on the wall, they quickly detach and migrate toward the centers of the pores.

Their proposed lubrication effect implies that gas bubbles are nucleated at the solid surfaces which is true. According to this implication, if an oil contains more solid particles, e.g., high asphaltene content, more bubbles will be formed inside the oil phase instead of on the pore walls. The lubrication effect or oil mobility enhancement will be reduced, which should not be the case according to the experimental observations of the stability study of asphaltene effect (Section 4.4.2).

They proposed that the nucleated gas bubbles on the grain surfaces provide "lubrication" to foamy heavy oil flow. Then, such a lubrication should also exist in the conventional solution gas drive, and unusual production performance should also occur in the conventional light oil reservoirs. Unfortunately, such unusual performance was not widely observed in light oil reservoirs.

From the above discussion, it may be concluded that there is *not enough* evidence to show that the presence of nucleated gas bubbles enhanced the mobility of heavy oils. Consequently, the proposed lubrication effect is unlikely to be valid.

Except for the proposed mechanisms as discussed above, no other mechanisms have been found that suggest that the foamy oil viscosity would be reduced or that the apparent mobility would be higher.

3.4 Derivation of Foamy Oil Viscosity

Because of the combination of effects of gas bubbles and pore geometry, it would be difficult to obtain a theoretical derivation of foamy oil viscosity. This section presents only an attempt to derive the foamy oil viscosity in a single capillary, which is intended to illustrate whether foamy oil viscosity is, most likely, higher or lower than the continuous oil phase viscosity.

Foamy oil was defined as a viscous heavy oil containing small dispersed gas bubbles (Sheng *et al.*, 1994). The viscosity of foamy oil derived in this section is based on that definition and the following assumptions:

1. There is no slip velocity between the gas bubbles and the liquid oil.
2. Poiseuille's law is valid in capillary flow.
3. The bubbles do not deform during flow with liquid.

According to the Poiseuille's law, for a single oil phase, the velocity distribution in a capillary cross section is

$$v_o = \frac{(r_c^2 - r^2)\Delta p}{4\mu_o L}, \tag{3-11}$$

which is shown in Figure 3.2a. Here r_c is the radius of the capillary, r is the position

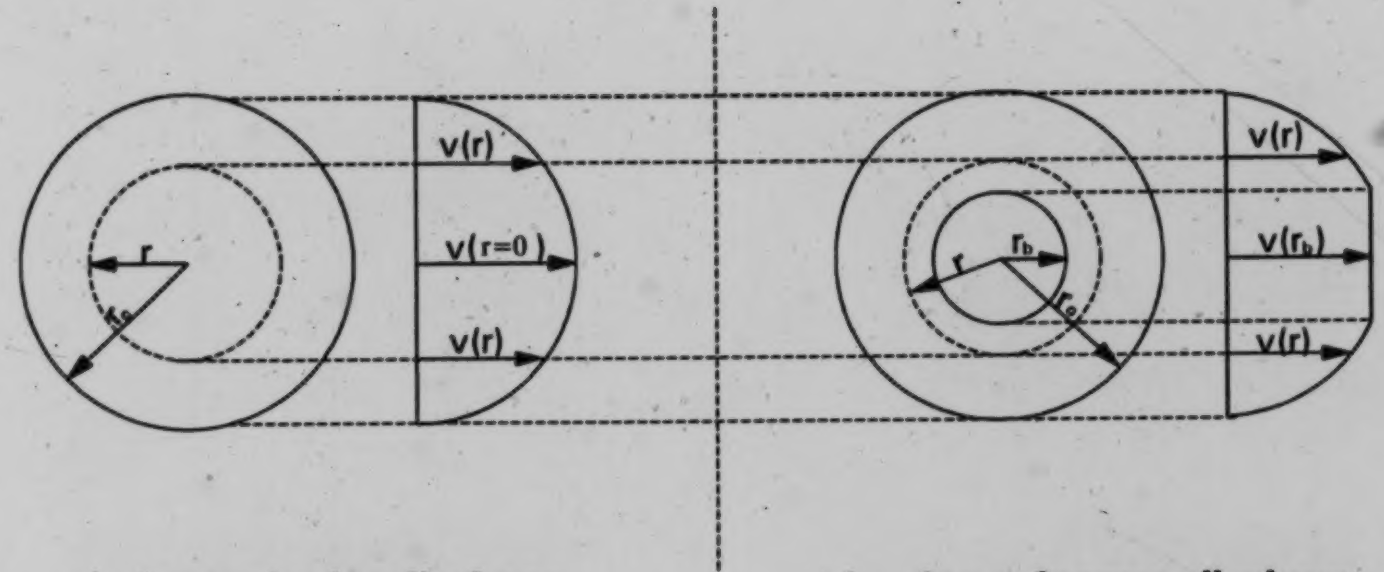
r
r_o
v(r)
v(r=0)
v(r)
r_b
r
r_o
v(r)
$v(r_b)$
v(r)

a - for a single oil phase

b - for a foamy oil phase

Fig. 3.2 - Velocity distribution in a capillary.

from the centre of the capillary, μ_o is the single oil phase viscosity, and Δp is the pressure drop along the length L of the capillary. If bubbles are dispersed in the centre of the capillary, the velocity distribution may be as shown in Figure 3-2b where the bubbles are assumed to move at the same velocity as the oil velocity at $r = r_b$. Then the volumetric flow rate of the foamy oil is

$$\begin{aligned} q_{fov} &= \int_{r_b}^{r_c} \frac{(r_c^2 - r^2)\Delta p}{4\mu_o L}(2\pi r dr) + \frac{(r_c^2 - r_b^2)\Delta p}{4\mu_o L}(\pi r_b^2) \\ &= \frac{\pi(r_c^4 - r_b^4)\Delta p}{8\mu_o L}. \end{aligned} \tag{3-12}$$

If the foamy oil is treated as a pseudo-single phase, the flow rate is

$$q_{fov} = \frac{\pi r_c^4 \Delta p}{8\mu_{fo} L}. \tag{3-13}$$

Comparing Eq. 3-13 with Eq. 3-12, one has

$$\mu_{fo} = \frac{\mu_o}{1 - (r_b/r_c)^4}, \tag{3-14}$$

which shows that the foamy oil viscosity, μ_{fo}, is increased because of bubbles dispersed in the oil phase.

3.5 Conclusions

According to the discussion and understanding presented in this chapter, the proposed models of oil viscosity reduction do not seem to be plausible. Based on the theory of dispersion viscosity and the simple derivation of the foamy oil viscosity, it is most likely that the oil viscosity would be increased if gas bubbles are dispersed in the oil phase.

3.6 References

Abou-Kassem, J.H. and Farouq Ali, S.M. : "Modelling of Emulsion Flow in Porous Media," *JCPT* (June 1995) **34**, No. 6, 30-38.

Alvarado, D.A.: *The Flow of Macroemulsions Through Porous Media*, Ph.D. dissertation, Stanford University, Stanford, CA (1975).

Alvarado, D.A. and Marsden Jr., S.S.: "Flow of Oil-in-Water Emulsions Through Tubes and Porous Media," *SPEJ* (Dec. 1979) 369-77.

Claridge, E.L. and Prats, M.: "A Proposed Model and Mechanism for Anomalous Foamy Heavy Oil Behaviour," paper SPE 29243 presented at the International Heavy Oil Symposium, Calgary, AB, June 19-21, 1995; *Proc.*, 9-20; also paper SPE 29243 (USMS, 1994).

Dealy, J.M.: "Rheological Properties of Oil Sand Bitumens," *The Canadian Journal Chemical Engineering* (*Can. J. Chem. Eng.)* (Dec. 1979) **57**, 677-83.

Einstein, A., *Annalen der Physik* (*Ann. Phys.*) (1906) **19**, 389 (Germany).

Einstein, A., *Ann. Phys.* (1911) **34**, 591 (Germany).

Eisenschitz, R., *Physikalische Zeitschrift* (*Phys. Z.*) (1933) **34**, 411 (Germany).

Hagedorn, A.R. and Brown, K.E.: "Experimental Study of Pressure Gradients Occurring During Continuous Two-Phase Flow in Small Diameter Vertical Conduits," *JPT* (April 1965) 475-84; *Trans.*, AIME, **234**.

Hatchek, E.: *The Viscosity of Liquids*, G. Bell and Sons Ltd., London (1928) 14-15.

Li, X.: *Bubble Growth During Pressure Depletion in Porous Media*, Ph.D. dissertation, University of Southern California, Los Angeles, CA (May 1993) 106.

Mackenzie, J.K.: "The Elastic Constants of a Solid Containing Spherical Holes," *Proceedings of the Physical Society of London, Section B* (*Proc. Phys. Soc. London B*) (1950) **63**, 2-11.

Maini, B.B.: "Foamy Oil Flow," teaching notes at the workshop for the members of Petroleum Recovery Institute, April 27, 1994.

Maini, B.B., Sarma, H.K. and George, A.E.: "Significance of Foamy-Oil Behaviour in Primary Production of Heavy Oils," *JCPT* (Nov. 1993) **32**, No. 9, 50-54.

Maini, B.B., Sheng, J.J. and Nicola, F.: "Foamy Oil Flow - Improved Primary Heavy Oil Recovery," paper presented at the Annual Conference and Exhibit of the Petroleum Recovery Institute, Calgary, AB, May 25, 1995.

Maini, B.B., Sheng, J.J. and Nicola, F.: "Laboratory Investigation of Foamy Oil Flow for Improved Primary Production," Final Report to the Canada Centre for Mineral and Energy Technology (CANMET) (Sept. 1995).

Odeh, A.S.: "Effect of Viscosity Ratio on Relative Permeability," *Trans.* (1959), AIME, **216**, 346-53.

Pal, R., Yan, Y and Masliyah, J.: "Rheology of Emulsions," *Emulsions, Fundamentals and Applications in the Petroleum Industry*, Schramm, L.L., Ed., *Advances in Chemistry Series* **231**, American Chemical Society, Washington, DC (1992) 139-40.

Poon, D.C. and Kisman, K.: "Non-Newtonian Effects on the Primary Production of Heavy Oil Reservoirs," *JCPT* (Sept. 1992) **31**, No.7, 55-59; also paper CIM/AOSTRA 91-33 presented at the CIM/AOSTRA Technical Conference, Banff, AB, April 21-24, 1991.

Savins, J.G.: "Non-Newtonian Flow Through Porous Media," *Industrial and Engineering Chemistry* (*Ind. Eng. Chem.)* (1969) **61**, No.10, 18-47.

Shen, C. and Batycky, J.P.: "Some Observations of Mobility Enhancement of Heavy Oils Flowing through Sand Pack under Solution Gas Drive," paper 96-27 presented at the 47th Annual Technical Conference of the Petroleum Society of CIM, Calgary, AB, June 10-12, 1996.

Sheng, J.J. and Maini, B.B.: *Foamy Oil Flow in Primary Production of Foamy Oil - A literature Review*, the Petroleum Recovery Institute Report 1995/96-7 (Feb. 1996) 3.

Sheng, J.J., Maini, B.B., Hayes, R.E. and Tortike, W.S.: "Foamy Oil Flow - A Review," paper presented at the International Symposium on Petroleum and Petrochemical Engineering, Beijing, Sept. 14-17, 1994.

Sheng, J.J., Maini, B.B., Hayes, R.E. and Tortike, W.S.: "A Non-Equilibrium Model to Calculate Foamy Oil Properties," paper CIM 95-19 presented at the 46th Annual Technical Conference of the Petroleum Society of CIM, Banff, AB, May 14-17, 1995.

Smith, G.E.: "Fluid Flow and Sand Production in Heavy Oil Reservoirs Under Solution Gas Drive," *SPEPE* (May 1988) 169-80.

Taylor, G.I.: "The Viscosity of a Fluid Containing Small Drops of Another Fluid," *Proc. Roy. Soc. London A* (1932) **138**, 41-48.

Uren, L.C., Gregory, P.P., Hancock, R.A. and Feskov, G.V.: "Flow Resistance of Gas-Oil Mixtures through Vertical Pipes," *Trans.* (1930), AIME, **86**, 209-19.

Uzoigwe, A.C.: *Emulsion Rheology and Flow Through Synthetic Porous Media*, Ph.D. dissertation, Stanford University, Stanford, CA (1970).

Yuster, S.T.: "Theoretical Considerations of Multiphase Flow in Idealized Capillary Systems," *Proc.*, the Third World Petroleum Congress - Section II (1951) 437-445.

Chapter 4

Experimental Study of Foamy Oil Stability

4.1 Introduction

A number of heavy oil reservoirs under solution gas drive show anomalously good primary performance. These reservoirs show foamy-oil behaviour in wellhead samples. The oil is produced in the form of an oil-continuous foam which contains dispersed gas bubbles. The formation of such gas-in-oil dispersions distinguishes foamy oil behaviour from conventional oil behaviour. Therefore, the important issues about foamy oils are the amount of gas dispersed in the oil and the time gas bubbles remain dispersed in the oil. It is desirable to measure the stability of such oil-gas systems in porous media. However, due to the difficulty of doing so, an easier method is to measure the stability in a bulk vessel. It has been suggested that the flow behaviour of foams in porous media can be correlated with foam stability in a bulk vessel (Maini and Ma, 1984).

This chapter presents the results of an experimental study of foamy oil stability in a bulk vessel. The effects of oil viscosity, asphaltene content, height of the oil column in the vessel, dissolved gas content and pressure decline rate were investigated. The literature on the stability of gas-liquid dispersion is also reviewed.

4.2 Literature Review of Gas-Liquid Dispersion Stability

The gas bubbles released from oil due to a pressure decline tend to remain dispersed in the oil to form an oil-continuous foam or foamy oil (Maini *et al.*, 1993). Such a foam composed of a multitude of gas/liquid interfaces forms a thermodynamically unstable system whose surface energy naturally tends to decrease. In practice this results in progressive destruction of the foam until the oil and gas are entirely separated (Minssieux, 1974; Schramm and Wassmuth, 1994). The rate of this destruction depends on foamy oil stability.

Much of the available literature on foam stability and destabilisation makes no clear distinction between aqueous and non-aqueous systems. Indeed, Ross (1967) in an article on aqueous foams stated that the same principles can be applied to non-aqueous foams (Callaghan and Neustadter, 1981). Some relevant previous work related to foamy oil stability is reviewed in the following.

4.2.1 Mechanisms of Bubble Decay

All foams are thermodynamically unstable and given sufficient time will collapse to form separate gas and liquid phases. Therefore, foam stability only describes the relative resistance of the foam to eventual phase separation. The collapse of foam is generally caused by interbubble gas diffusion and a two-stage process involving gradual thinning of liquid films followed by breakage of these films (Sheng and Maini, 1996). Callaghan *et al.* (1986) described foam collapse separately by two mechanisms:

interbubble gas diffusion and gravitational liquid drainage. Foams are collapsed by each of the mechanisms according to an exponential function of time. Their results show that the speed of foam collapse *via* interbubble gas diffusion is similar in aqueous and non-aqueous foams; and foam collapse *via* gravitational liquid drainage is more rapid in a non-aqueous foam than in an aqueous foam when the liquid viscosity was similar. Many other investigators have used exponential functions to describe the rates of decay, as will be reviewed in Section 5.2.3.

In a bulk liquid, bubble coalescence is caused by a coarsening process known as Ostwald ripening (Lifshitz and Slyozov, 1961). In porous media, a pore geometry effect is important.

In the visual micromodel experiments (Maini *et al.*, 1996), it was observed that the smaller bubbles coalesce into larger bubbles or form continuous gas clusters when the pressure decline rate is low. Larger bubbles or continuous gas clusters could be divided into smaller bubbles by the mechanisms of bubble breakup when the pressure decline rate is high. The rates of bubble coalescence and bubble breakup are affected by the local pressure gradient or fluid velocity. When the pressure decline rate is high, the fluid velocity is generally high. Therefore, in higher rate pressure depletion tests where the fluid velocity is higher, more and smaller bubbles are formed for a given pressure drop. Small bubbles can remain in the oil phase for a longer time.

4.2.2 Effect of Liquid Oil Viscosity

As in any fluid flow process, the liquid viscosity offers resistance to flow and has a direct bearing on the rate of liquid drainage. It is obvious that the rate of film thinning will decrease as the liquid viscosity increases and in the extreme case of a very high viscosity (for example, the solidified films of latex foam) the resistance to flow can make the foam very stable. The higher oil viscosity will provide higher resistance to the movement of gas bubbles in the liquid oil phase, thus making the foamy oil system more stable.

The experimental evidence of the role of liquid viscosity in determining non-aqueous foam stability has been provided by several researchers. Brady and Ross (1944) found that foam stability of refined mineral oils increased linearly with the kinematic viscosity of the oil. This dependence of stability on viscosity was confirmed by McBain and Robinson (1949) who showed that a high viscosity was often associated with high foam stability. Callaghan and Neustadter's (1981) experimental data showed that an increase in crude oil bulk viscosity leads to an almost linear increase in average foam lifetime. In their experiments, foams were formed by blowing gas (natural gas or air) into oil through fine sintered glass discs. They also observed that natural gas foams are more stable than air foams.

Govier and Aziz (1982) stated that dispersions of sufficient "fineness" (submicron particle size) may be stable, supported by Brownian movement or electrical charge even in the absence of any turbulence, or supported as a result of high or special consistency properties of the continuous phase. These may be considered pseudohomogeneous and their flow behaviour may be included with that of single-phase fluids.

4.2.3 Effect of Water Content

Callaghan and Neustadter (1981) investigated the effect of added moisture on the average lifetime of a crude oil foam. They found that the water was present as droplets and that these droplets increased in size as the added moisture content was increased. Thus, it can be hypothesized that the observed decrease in foam stability with increasing moisture content is either a reflection of the increasing ability of the water droplets to bridge the foam lamellae and cause rupture, and/or increased extraction of crude oil surfactants into the dispersed water phase.

4.2.4 Effect of Irrigation

Because of liquid drainage, the foam is "dried". Irrigation means that the liquid is added to compensate for liquid loss during liquid drainage. The great effect of irrigation on the rate of collapse would be expected to cause a marked variability of this rate. For instance, for two foam columns of equal volumes, the one of the smaller height would collapse more rapidly than the taller column (Bikerman, 1973).

4.2.5 Effect of Solid Particles

Ward and Levart (1984) indicated that very small bubbles may be present in a thermodynamically stable form in the presence of a rough surface. This surface may be either that of the boundary or that of particles suspended in the solution. Microbubbles (2 to 5 μm) formed in this way are stable, requiring a further reduction in pressure to make them grow, which reduces the possibility of growth by coalescence. Similar surface roughness may be provided by suspended asphaltene particles which are usually found in abundance in heavy oils. Initially, the bubbles are small and far from each other and coalescence is of no importance (Kashchiev and Firoozabadi, 1993). Baibakov and Garushev (1989) attributed the slow release of solution gas from high tar crude oils to adsorption of gas on the surface of tars.

4.2.6 Effect of Porous Media

Gibbs (1878) reported that a single bubble in a large volume of liquid-gas solution can have only an unstable equilibrium state. Physically this instability was thought to result from the fact that the gaseous phase inside the surface of curvature was at a higher pressure than the liquid phase; thus, it was thought that displacement from the equilibrium size resulted in either (a) the bubble dissolving away completely or (b) its continued growth leading to a transition of the system from the liquid phase to the gaseous phase. What Gibbs had shown for a single bubble in an unbounded volume of liquid-gas solution was taken , mistakenly, to be valid for a multibubble system (Ward and Levart, 1984). Ward *et al.* (1982) concluded from their experimental and theoretical study that microbubbles could be stable at some equilibrium sizes under the constraint of a closed volume and at some temperatures and pressures. Physically, the stable state of the bubble nuclei results from the competition of the bubble nuclei for the dissolved gas in the liquid phase (Ward and Levart, 1984). Ward *et al.*'s (1982) analysis indicated that it is possible to generate micro-sized bubbles in a porous medium. Because these bubbles are much smaller than the average pore throat size, gas is not restricted to flowing only as a continuous phase. These bubbles may move with or through the oil, and probably faster than it, through a common pore space (Smith, 1988).

Yortsos and Parlar (1989) stated that bubble growth is controlled by the pore wall curvature and geometry, which may stabilize otherwise unstable gas bubbles. This is what differentiates bubbles in porous media from those in a bulk vessel. Li (1993) also reported that the coarsening process which occurs in phase transition processes in the bulk did not happen in multiple bubble growth processes in his glass micromodel experiments. The main reason is that, in porous media, the concentration at the interface is not related to the bubble size, but only to the local pore curvature. This is in contrast to the case of phase transition in the bulk, where the solute concentration at the interface, directly related to its size, makes it possible for the large bubbles to grow at the expense of the smaller ones, because the bubble size and radius of curvature are directly proportional to each other. This theory is of less relevance to porous media, where cluster size and capillarity are only indirectly coupled. In porous media the competition between growing clusters is controlled by porous mediium capillary characteristics and by mass transfer, the solubility dependence on radius being insignificant (Li and Yortsos, 1993).

Kovscek and Radke (1994) also stated that bulk foams coarsen with larger bubbles growing at the expense of smaller ones that eventually disappear. However, confined foams in porous media does not coarsen in a similar fashion because bubble volume is not directly related to film curvature. Rather, lamella curvature depends on pore dimensions and on location within the pore space. Gas diffusion still proceeds from the most highly concave bubbles, forcing the lamellae to diminish their curvatures by translation toward pore-throats. In the absence of an imposed pressure gradient, it is possible for gas diffusion to drive all lamellae to pore-throats to achieve an equilibrium state of zero curvature. Coalescence occurs only when two lamellae happen to reach the same pore-throat.

The relationship between stability and mobility reduction factor observed by Maini and Ma (1984) suggests that the same types of surface forces control the rheological properties of foam in a porous medium and the foam stability characteristics outside the porous medium. They observed that in all cases investigated, the optimum surfactant concentrations for maximizing foam stability and for maximizing the mobility reduction factor were identical. It is likely that the half-life of foamy oil will be much longer in a porous medium than that measured in a bulk vessel, due to the stabilizing influence of the porous medium discussed above, however, the bulk measurements of foam stability can still provide a measure of the relative foaminess of different oils.

4.2.7 Effect of Heavy Oil System

The heavy oil foams generated by depressurization of live oils contain a number of ingredients as important factors in the stability of foams in apolar media. These include: high liquid viscosity; naturally occurring surface active chemicals; and a possibility of the formation of insoluble surface films due to precipitation of asphaltenes (Claridge and Prats, 1995). Maini *et al.* (1993) also pointed out that two key factors needed for non-aqueous foam stability are present in heavy oil systems: the viscosity of the liquid phase (heavy oil) is high enough to retard drainage of liquid films by capillary forces; and plastic surface films, most likely stabilized by high molecular weight porphyrins, have been observed in such crude oil systems.

4.3 Experimental

4.3.1 Apparatus

A diagram of the experimental apparatus is shown in Figure 4.1. An oil sample was saturated by contacting oil with methane gas at a high pressure, and then transferred to the high pressure cell equipped with a glass window and height graduations. Initially, the cell was pressurized with gas. Then the pressure was either reduced suddenly by releasing the gas in the cell, or reduced linearly using the pressure decline rate controller, to a lower pressure, and this lower pressure was maintained afterwards. Because of the pressure drop, a fraction of the dissolved gas nucleates and grows into gas bubbles. These bubbles are initially dispersed in the liquid oil phase, forming a foamy oil. The volume of the foamy oil initially increases giving a corresponding increase in liquid level. These bubbles gradually disengage from the liquid oil and become free gas, resulting in a volume reduction. By monitoring the height of the foamy oil as a function of time, the volumes of foamy oil and dispersed gas were estimated.

In this study, the initial saturation pressure was 700 psig except in Run 11 where it was 525 psig. The initial pressure was reduced to 350 psig. This intermediate pressure, rather than atmospheric pressure, was selected for measurements to avoid an

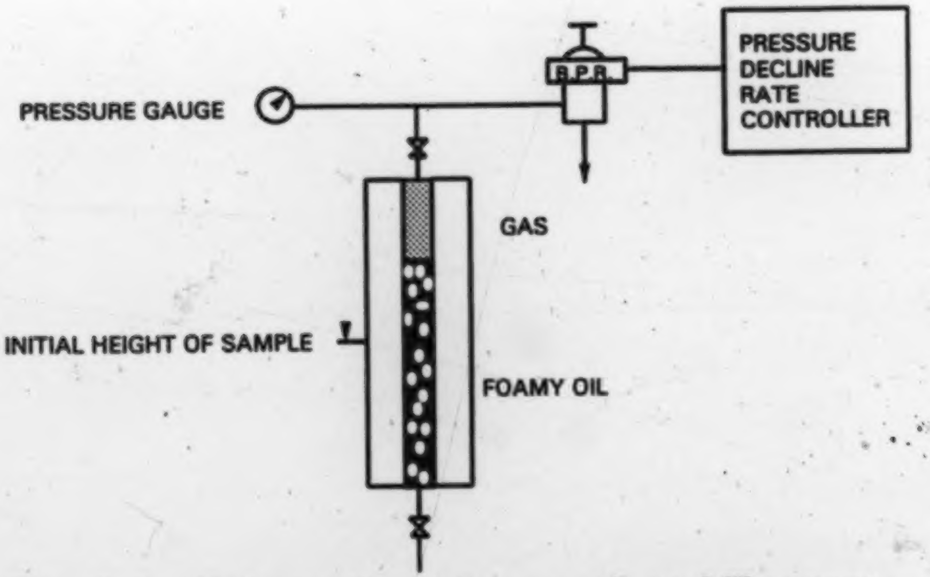
PRESSURE GAUGE
B.P.R.
PRESSURE DECLINE RATE CONTROLLER
GAS
INITIAL HEIGHT OF SAMPLE
FOAMY OIL

Fig. 4.1 - Schematic of foamy oil stability test.

experimental problem. When the pressure was suddenly reduced to atmospheric pressure, a large volume of dissolved gas was released suddenly. The height of the gas/oil mixture rose and then fell at a fast rate. In such tests, the glass window became coated with a thick layer of oil which drained down slowly. Because of the opacity of the window due to the oil coating, it was not possible to read foam heights accurately.

For all runs except Runs 9 and 10, the initial live oil volume was 20 cm^3, which is equivalent to a height of 87.5 mm in the cell. For Runs 9 and 10, the initial live oil volumes were 10 cm^3 and 30 cm^3, which are equivalent to the heights of 43.8 mm and 131.3 mm in the cell, respectively.

4.3.2 Measurement of Foamy Oil Stability

Foam stability may be measured either by monitoring the decay of a static foam or by measuring the equilibrium volume of a dynamic foam at a constant rate of foam formation. In this context, a static foam is one in which the rate of formation is zero and a dynamic foam is one that has reached a state of dynamic equilibrium between the rate of formation and the rate of decay.

Maini and Ma (1984) used the concept of half-life to describe aqueous foam stability. Callaghan and Neustadter (1981) used the foam lifetime to describe non-aqueous foam stability. Their lifetime, t_1^*, is defined as

$$t_1^* = \frac{1}{h(0)} \int_0^{t^*} h(t)dt, \qquad (4\text{-}1)$$

where $h(0)$ is the initial foam height; $h(t)$ is the foam height at time t; and t^* is the time for foam to collapse completely.

In this investigation the foam was formed by release of the solution gas. Since the release of solution gas does not occur instantaneously and continues over the entire duration of the test, the measured foam volume is a product of the balance between the rate of formation and the rate of decay. The rates of formation and decay vary during the test, as will be described in the next chapter. Therefore, the usual measures of foam stability -- the static method which requires the rate of formation to be zero and the dynamic method which requires the rate of formation to be equal to the rate of decay -- cannot be used directly.

The properties of foamy oil (e.g., compressibility) are directly related to the volume of gas dispersed in the liquid oil phase. Thus, the duration for which the dispersed gas remains in the oil should represent the nature of foamy oil. Therefore, the lifetime, t_1^*, was modified to

$$t_1 = \frac{1}{h_o(0)} \int_0^{t_o} h_{dg}(t)dt, \tag{4-2}$$

where $h_o(0)$ is the initial live oil sample height, $h_{dg}(t)$ is the height of dispersed gas bubbles at time t, and t_o is the time when the height of the total foamy oil falls back to the initial height of the live oil. The parameter, t_1, may be interpreted as "the average lifetime of dispersed gas in the foamy oil" after Bikerman (1973). Physically, t_1 represents the product of the time over which foamy oil exists and the time averaged ratio of the dispersed gas volume to the liquid phase volume. Thus it provides a combined measure of how much gas becomes dispersed and how long it remains dispersed. It is desirable that a quantity describing the foamy oil stability could relate to the oil recovery. t_1 bears such characteristics. A longer t_1 would relate to a higher oil recovery. The maximum height of the dispersed gas (h_{max}) and the half-life ($t_{1/2}$), which are defined in Figure 4.2, are also evaluated for comparison.

4.4 Results and Discussion

The properties of the tested oils, test conditions and results are shown in Table 4.1. Oils labelled PAO-100, PAO-40 and PAO-4 are mineral oils without asphaltene. The other oils are crude oils which contain asphaltene. A typical example of the height changes of dispersed bubbles is shown in Figure 4.2. For a given pressure drop, a fraction of the dissolved gas is nucleated to form microbubbles. These microbubbles grow with time. Thus the foamy oil volume increases, and the height of foamy oil will rise. The difference of the height minus that of the initial live oil is the height of dispersed gas bubbles (h_{dg}), because the reduction of oil volume due to the release of dissolved gas is relatively small. The dispersed gas height, h_{dg}, keeps rising until it reaches h_{max} when the rate of bubble formation equals the rate of bubble decay. Before this point, the rate of bubble formation is faster than that of decay. After this point, the rate of bubble decay is faster. Thus the height of dispersed bubbles will decrease with time. For a more stable foamy oil, the area encompassed by the curve of height changes and the time axis will be larger. This area divided by the initial live oil height is the lifetime, t_1. The results are discussed in the following.

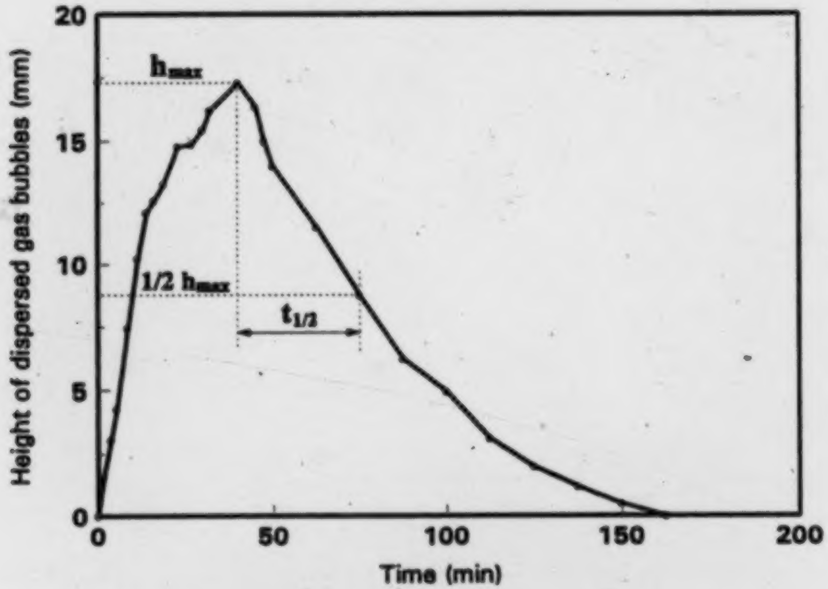

Fig. 4.2 - Height of dispersed gas vs. time.

Table 4.1 - Oil Properties, Test Conditions and Results

Run #	Oil	μ_{do} (cp)	R_s at 700 psig (m³/m³)	p^0 (psig)	$h_o(0)$ (mm)	dp/dt (psi/min)	f_{max} (%)	h_{max} (mm)	$t_{1/2}$ (min)	t_1 (min)
Run 1	Lindbergh 1	13000.0	15.5	700	87.5	Suddenly	16.67	17.5	80.0	21.43
Run 2	Lindbergh 2	9000.0	14.2	700	87.5	Suddenly	16.51	17.3	36.1	13.53
Run 3	Medicine Hat	3000.0	17.0	700	87.5	Suddenly	11.88	11.8	25.1	5.09
Run 4	Tangleflag	450.0	19.0	700	87.5	Suddenly	15.05	15.5	25.3	3.36
Run 5	Crest Hill	250.0	18.4	700	87.5	Suddenly	10.26	10.0	8.8	1.53
Run 6	PAO-100	3300.0	16.0	700	87.5	Suddenly	10.07	9.8	20.5	5.20
Run 7	PAO-40	897.0	16.0	700	87.5	Suddenly	5.81	5.4	5.5	0.62
Run 8	PAO-4	29.0	16.0	700	87.5	Suddenly	0.00	0.0	0.0	0.00
Run 9	Lindbergh 2	9000.0	14.2	700	43.8	Suddenly	15.62	8.1	23.0	8.69
Run 10	Lindbergh 2	9000.0	15.0	700	131.3	Suddenly	18.55	29.9	78.0	30.48
Run 11	Lindbergh 1	13000.0	15.5	525	87.5	Suddenly	6.82	6.4	67.5	7.37
Run 12	Lindbergh 1	13000.0	15.5	700	87.5	11.67	16.11	16.8	65.0	19.37
Run 13	Lindbergh 1	13000.0	15.5	700	87.5	6.03	6.22	5.8	50.0	6.11

4.4.1 Effect of Oil Viscosity

Runs 1 to 8 were used to investigate the effect of gas-free oil viscosity. The heights of dispersed gas bubbles as a function of time for these runs are shown in Figure 4.3.ompassed area becomes larger. This implies an increase in stability. High viscosity reduces the gas diffusion (Laidler and Meiser, 1982) which prevents microbubbles from growing rapidly, as is shown in Figure 4.3 by the slower increase of the heights of dispersed bubbles for higher viscosity oils during the early stages. High viscosity also reduces the rate of bubble disengagement from the oil phase, as is shown in Figure 4.3 by the slower decrease of the heights of dispersed bubbles at the later stages.

The lifetimes of foamy oils with different gas-free viscosities are listed in Table 4.1. Their relationship is given in Figure 4.4, which shows that the lifetime increases almost linearly with oil viscosity. Table 4.1 also shows that in the case of the lowest viscosity (29 cP) mineral oil, the foam decay was so rapid that no measurements of the height could be obtained.

These measurements suggest that the foamy oil stability increases with increasing oil viscosity.

4.4.2 Effect of Asphaltene

It was hypothesized that asphaltenes may act as dispersed nucleation sites (Smith, 1988), or stabilize the bubbles at a small size (Coskuner, 1988; Claridge and Prats, 1995). It would be desirable to compare experimentally the foam stability of an oil with asphaltene with that of the deasphalted oil. However, the viscosity of the deasphalted oil

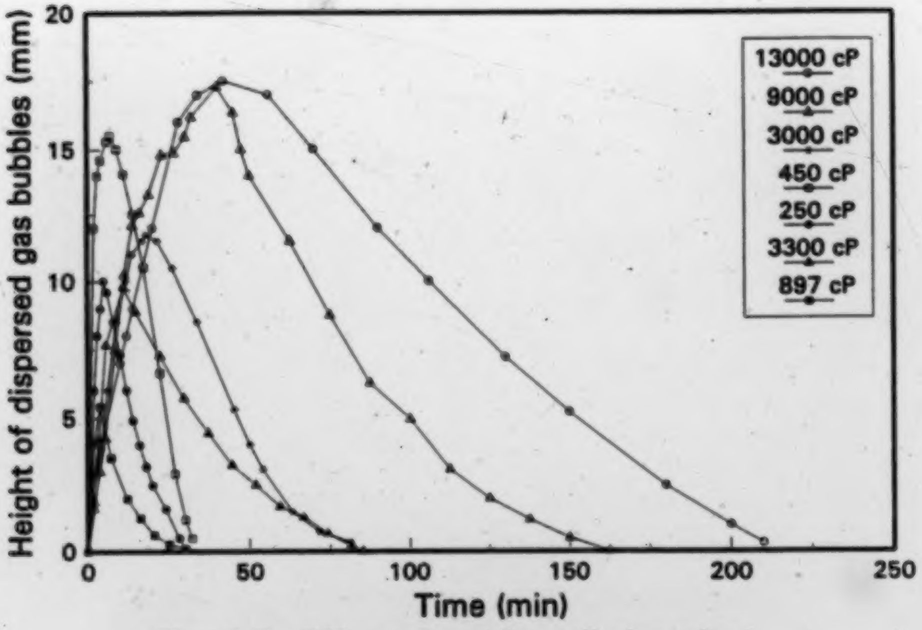

Fig. 4.3 - Effect of gas-free oil viscosity.

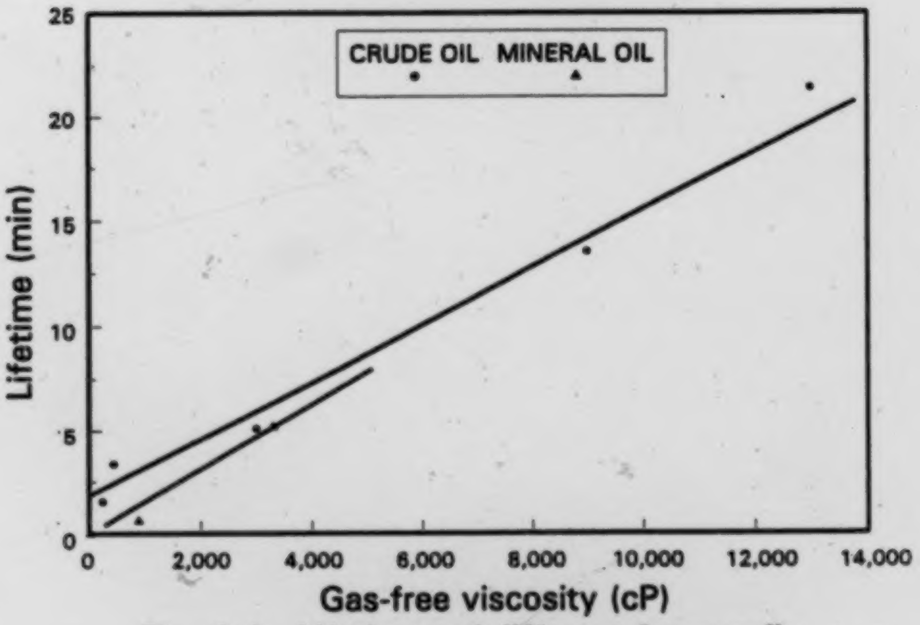

Fig. 4.4 - Lifetimes of different foamy oils.

is much lower than that of the same oil with asphaltenes. As shown earlier, viscosity plays an important role in stability. Therefore, the same oil could not be used to investigate the effect of asphaltene. Alternatively, the stability of three mineral oils with no asphaltenes (Runs 6 to 8) were compared with that of several crude oils (Runs 1 to 5). The lifetimes at different oil viscosities are shown in Figure 4.4. As mentioned in Section 4.4.1, the relationship between the lifetime and oil viscosity is almost linear. Therefore, two straight lines were drawn in Figure 4.4. One represents the relationship for the mineral oils; and the other for the crude oils. From Figure 4.4, it can be seen that the line for the mineral oils lies below that for the crude oils, which implies that the lifetime of a crude oil foam is longer than that of a mineral oil foam. Therefore, it may be inferred that the asphaltene content increases foamy oil stability. Asphaltene may provide more nucleation sites, forming more and smaller bubbles which reduces bubble coalescence. However, because of the difference in characteristics of crude oils and mineral oils, e.g., initial GOR which also affects the foamy oil stability as will be discussed later, it seems inconclusive to claim that asphaltene increases foamy oil stability. Actually, it can be seen from Figure 4.4 that the two lines are quite close to each other, which suggests that asphaltene does not increase foamy oil stability significantly.

4.4.3 Effect of Height of the Oil Column

Figure 4.3 shows that it took a maximum of 3.5 hours for the gas to completely evolve from the viscous oil. However, it was often observed that when an oil sample in a big container was exposed to atmospheric pressure, some gas bubbles remained entrained in the oil for a much longer time, sometimes several days. This inconsistency motivated an investigation of the effect of the initial live oil volume or the height of the oil column. Three runs, Runs 9, 2 and 10, were analyzed. The initial live oil volumes in Runs 9, 2, and 10 are 10 cm^3, 20 cm^3 and 30 cm^3 with corresponding heights of 43.8 mm, 87.5 mm and 131.3 mm, respectively. The oil used was Lindbergh 1. The results are shown in Figure 4.5 and Table 4.1. Figure 4.5 shows the height of dispersed gas bubbles normalized to the height of initial live oil column. If the stability is not affected by the height of the oil column, the half-lives $t_{1/2}$, lifetimes t_1, and the encompassed areas should be same for the three runs. However, from Figure 4.5 it can be seen that the areas encompassed increase as the heights of oil column increase. The estimated lifetimes are 8.69 min, 13.53 min and 30.48 min for Runs 9, 2 and 10, respectively. These lifetimes increase with the height of the oil column, even though the definition of lifetime, Eq. 4-2, and the normalized height in Figure 4.5 tend to eliminate the effect of the height of the oil column.

As the height of the oil column increases with volume, the distances travelled by the bubbles to the "exit," which was the interface between the oil phase and gas phase in the cell, also increase. Thus it will be more difficult for the bubbles to disengage from the oil phase. This phenomenon can also be explained by the effect of irrigation mentioned in Section 4.2.4. Because of the effect of irrigation, higher oil column will cause slower liquid drainage. According to the effect of the height of the oil column, it is inferred that foamy oils in reservoirs may be more stable.

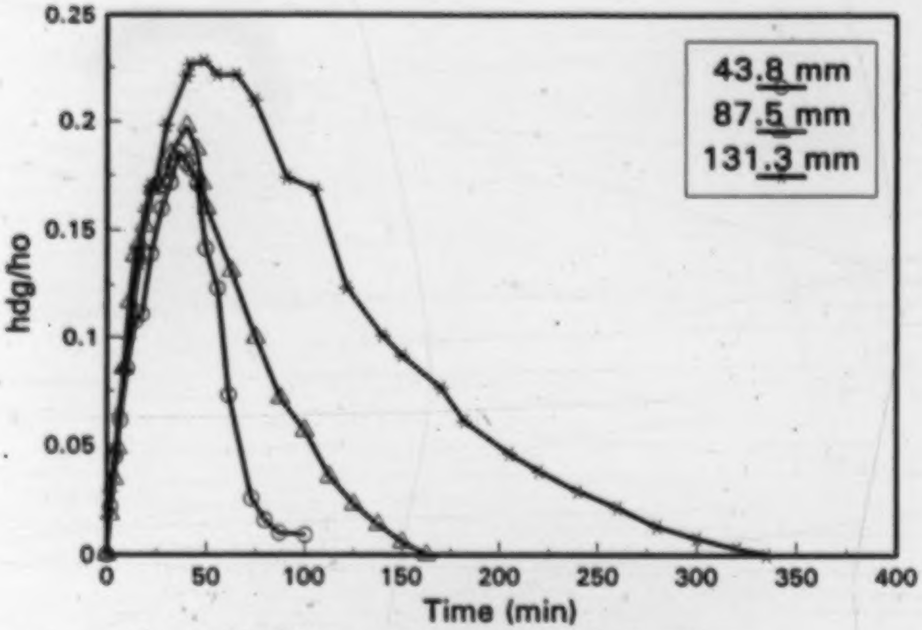

Fig. 4.5 - Effect of the height of oil column.

4.4.4 Effect of Dissolved Gas Content

The initial solution GOR determines the volume of gas that can be released from solution and this has a direct influence on the foam formation process. It may also affect foam stability via its effect on the number of bubbles nucleated and the initial bubble size distribution. To study the effect of the amount of dissolved gas, the results of two Lindbergh 1 oil samples (Runs 1 and 11) are compared in Figure 4.6. The oil sample in Run 1 was saturated at 700 psig, while the sample in Run 11 was saturated at 525 psig. Both samples were depressurized to 350 psig. Thus the pressure drop or the initial supersaturation in Run 1 is 350 psi, twice as large as that (175 psi) in Run 11. The amount of total dissolved gas released in Run 1 is about twice as large as that in Run 11.

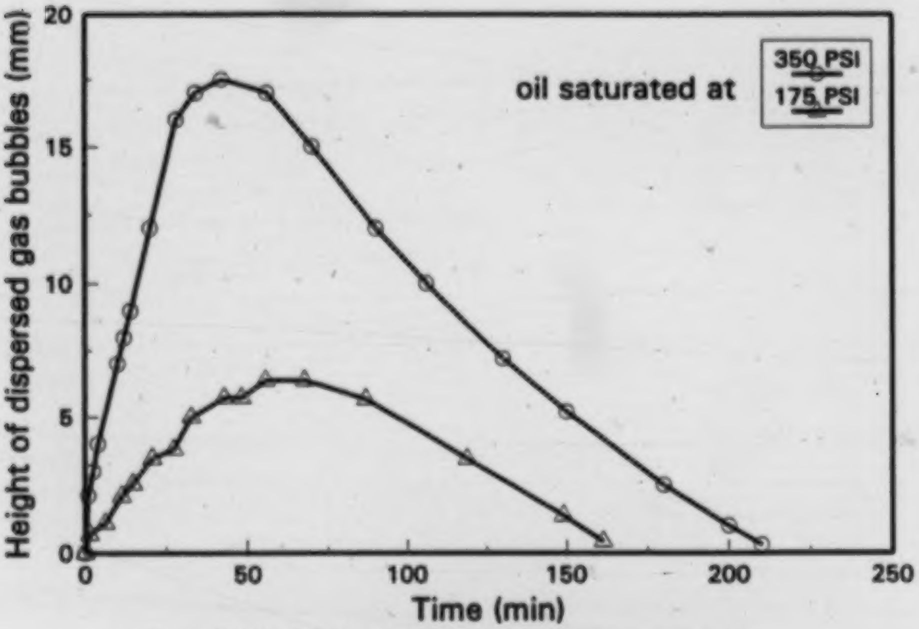

Fig. 4.6 - Effect of dissolved gas content.

Figure 4.6 shows that the encompassed area in Run 1 is more than twice as large as that in Run 11. The lifetime of the former is almost three times that of the latter (Table 4.1). The increase in stability with dissolved gas content suggests that the size distribution of bubbles may depend on the degree of supersaturation imposed on the system. With the larger supersaturation, more and smaller bubbles will be generated.

The effect of dissolved gas content on the stability observed here is consistent with the effect on oil recovery observed by Baibakov and Garushev (1989). Their experimental data show that oil recovery goes down as gas content decreases. This effect was particularly pronounced for reservoirs of low permeability. They argued that gas content in crude oil exerts a strong influence on the recovery factor of a high viscosity oil reservoir.

4.4.5 Effect of Pressure Decline Rate

The results of Runs 1, 12 and 13 are shown in Figure 4.7 and Table 4.1 which were used to investigate the effect of pressure decline rate. In Run 1, the pressure was suddenly reduced from 700 psig to 350 psig. In Runs 12 and 13, the pressure decline rates were 11.67 psi/min and 6.03 psi/min, respectively. The lifetimes of Runs 1, 12 and 13 estimated using Eq. 4-2 are 21.43 min, 19.37 min and 6.11 min, respectively. These results show that the foamy oil is more stable if the pressure decline rate is higher. As foamy oil stability depends on the competition between the rate of bubble formation and the rate of decay, the effect of the pressure decline rate was expected to be significant. If the pressure decline rate is low, the rate of bubble formation will be low and the rate of decay will be comparatively high. As a result, fewer gas bubbles will remain dispersed in the oil phase. If the pressure decline rate is high, more and smaller bubbles will be formed because of high supersaturation. Smaller bubbles can remain dispersed for a longer time.

4.4.6 Effect of Porous Media

Similar tests were also conducted in a small glass-bead-packed visual model. The apparatus for this model is similar to that shown in Figure 4.1 with the bulk vessel substituted by a small glass tube packed with glass beads. The pore volume of this glass-bead-pack is about 3 cm^3. It was observed that it took several hours for most of the gas bubbles to come out of the pack. The rest of the bubbles were observed to remain trapped inside the pack after several days. Therefore, foamy oils could be more stable

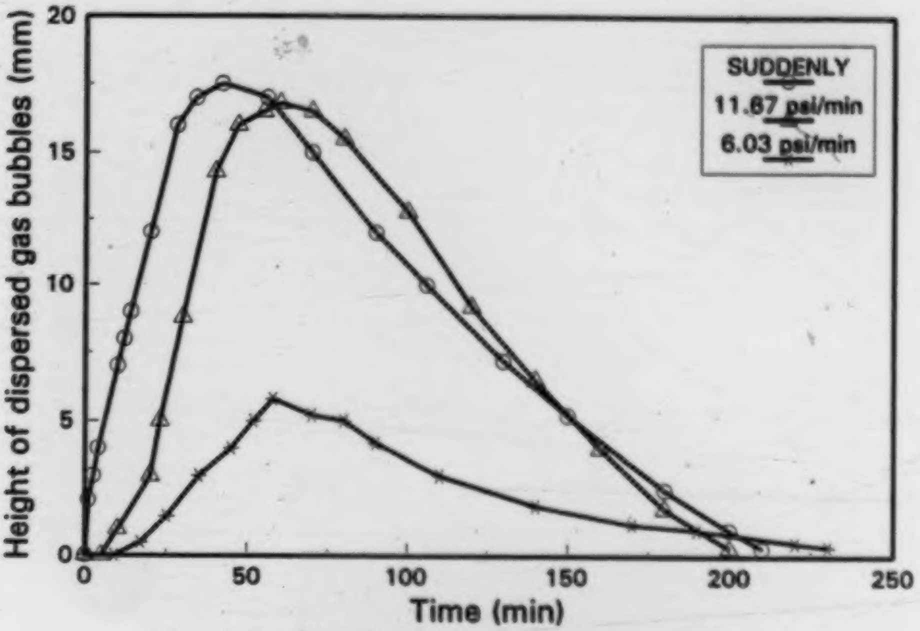

Fig. 4.7 - Effect of pressure decline rate.

in porous media than in the bulk vessel.

As it is difficult to distinguish between the bubbles dispersed in the oil and the free gas bubbles flowing or trapped in the core, the measurement defined by Eq. 4-2 can not be applied directly to describe foamy oil stability in porous media (glass-bead pack in this case). Therefore, the data for lifetimes in this glass-bead-pack are not available. The technique to investigate foamy oil stability in porous media needs to be developed further.

4.4.7 Further Discussion

In this study the measure of foamy oil stability is the lifetime. The maximum heights, h_{max}, and half-lives, $t_{1/2}$, for different runs were also shown in Table 4.1. These parameters were used to describe the foaminess and stability of conventional foams. Comparison of the data in Table 4.1 shows that the half-life $t_{1/2}$ is generally longer if the lifetime t_1 is longer; however, h_{max} does not show this trend. Since $t_{1/2}$ is consistent with t_1, $t_{1/2}$ may also be used to describe the foamy oil stability. However, it should be noted that the foam formation did not stop completely in these tests during the period over which the foamy oil volume decayed. The foam half-lives measured in these tests are likely to be larger than the true half-lives in the absence of any concurrent formation. The half-lives in the tests were found to be on the order of tens of minutes. A more accurate assessment of foam stability can be obtained by calculating the decay coefficients for foam decay using the models (preferably Model 1) to be proposed in the next chapter.

Corresponding to the maximum heights, the maximum foam qualities, f_{max}, in different tests were calculated and shown in Table 4.1. Table 4.1 shows that f_{max} never exceeds 20% in all the tests. In other words, the foam qualities of these foamy oils are low. Though a liquid foam may be properly defined morphologically as a dispersion of a gas in a liquid, such dispersions are not generally named foams unless the volume concentration of dispersed gas is very high (from 50% to > 90%) (de Vries, 1958). Therefore, the name "foamy oil" may not be the most appropriate name to describe such dispersions. Instead, "bubbly oil" may be more appropriate.

4.5 Conclusions

Based on the results and observations from the experiments conducted, the following conclusions may be drawn:

1. Foamy oil stability increases (almost linearly) with oil viscosity.
2. Asphaltene content was not observed to increase foamy oil stability significantly.
3. The height of the oil column affects foamy oil stability. With larger heights foamy oil is more stable.
4. Foamy oil stability increases with higher dissolved gas content and higher pressure decline rate, for the ranges tested in this study.
5. Foamy oil is more stable in porous media than in a bulk vessel.
6. The foam quality of foamy oil is low.

4.6 References

Baibakov, N.K. and Garushev, A.R.: *Thermal Methods of Petroleum Production*, Developments in Petroleum Science 25, translated by W.J. Cieslewicz, Elsevier Science Publishers B.V., Amsterdam (1989) 6-21.

Bikerman, J.J.: *Foams*, Springer-Verlag New York Inc., New York (1973) 89-94.

Brady, A.P. and Ross, S.: "The Measurement of Foam Stability," *Journal of American Chemical Society* (*J. Am. Chem. Soc.*) (1944) **66**, 1348-56.

Callaghan, I.C., Lawrence, F.T. and Melton, P.M.: "An Equation Describing Aqueous and Non-Aqueous Foam Collapse," *Colloid & Polymer Science* (1986) **264**, 423-34.

Callaghan, I.C. and Neustadter, E.L.: "Foaming of Crude Oils: a Study of Non-Aqueous Foam Stability," *Chemistry and Industry* (Jan. 1981) **17**, 53-57.

Claridge, E.L. and Prats, M.: "A Proposed Model and Mechanism for Anomalous Foamy Heavy Oil Behaviour," paper SPE 29243 presented at the International Heavy Oil Symposium, Calgary, AB, June 19-21, 1995; *Proc.*, 9-20; also the unsolicited manuscript of SPE (USMS) 29243 (1994).

Coskuner,G.: *Oil Field Emulsions*, the Petroleum Recovery Institute Report 1988-18 (Nov. 1988) 4-5.

de Vries, A.J.: "Foam Stability, Part I. Structure and Stability of Foams," *Recueil des Travaux Chimiques des Pays-Bas* (*Rec. Trav. Chim.*) (1958) **77,** 81-91 (English).

Gibbs, J.W.: *Trans. Conn. Acad.* (1878) **3,** 343.

Govier, G.W. and Aziz, K.: *The Flow of Complex Mixtures in Pipes*, Robert E. Krieger Publishing Company, Inc., Florida (1982) 3.

Kashchiev, D. and Firoozabadi, A.: "Kinetics of the Initial Stage of Isothermal Gas Phase Formation," *J. Chem. Phys.* (March 15, 1993) **98,** No. 6, 4690-99.

Kovscek, A.R. and Radke, C.J.: "Fundamentals of Foam Transport in Porous Media," *Foams: Fundamentals and Applications in the Petroleum Industry, Advances in Chemistry Series* **242,** Schramm, L.L., Ed., American Chemical Society, Washington, DC (1994) 137.

Laidler, K.J. and Meiser, J.H.: *Physical Chemistry*, The Benjamin/Cummings Publishing Company, Inc., California (1982) 832-34.

Li, X.: *Bubble Growth During Pressure Depletion in Porous Media*, Ph.D dissertation, University of Southern California, Los Angeles, CA (May 1993) 158.

Li, X. and Yortsos, Y.C.: "Critical Gas Saturation: Modeling and Sensitivity Studies," paper SPE 26662 presented at the 68th SPE Annual Technical Conference and Exhibition, Houston, TX, Oct. 3-6, 1993.

Lifshitz, I.M. and Slyozov, V.V.: "The Kinetics of Precipitation from Supersaturated Solid Solutions," *Journal of Physics and Chemistry of Solids* (*J. Phys. Chem. Solids*) (1961) **19,** 35-50.

Maini, B.B. and Ma, V.: "Relationship Between Foam Stability Measured in Static Tests and Flow Behaviour of Foams in Porous Media," paper SPE 13073 presented at the 59th Annual Technical Conference and Exhibition, Houston, TX, Sept. 16-19, 1984.

Maini, B.B., Sarma, H.K. and George, A.E.: "Significance of Foamy-Oil Behaviour in Primary Production of Heavy Oils," *JCPT* (Nov. 1993) **32,** No. 9, 50-54.

Maini, B.B., Sheng, J.J. and Bora, R.: "Role of Foamy Oil Flow in Heavy Oil Production," paper presented at 1996 International Energy Agency (IEA) Workshop/

Symposium on EOR, Sydney, Australia, September 29 - October 2, 1996.

McBain, J.W. and Robinson, J.V.: "Surface Properties of Oils," *National Advisory Committee for Aeronautics* (*Natl. Advis. Comm. Aeronaut.*), Technical Note No. 1844 (1949).

Minssieux, L.: "Oil Displacement by Foams in Relation to Their Physical Properties in Porous Media," *JPT* (Jan. 1974) 100-08.

Ross, S.: "Mechanisms of Foam Stabilization and Antifoaming Action," *Chemical Engineering Progress* (*Chem. Eng. Progr.*) (Sept. 1967) **63,** 41-47.

Schramm, L.L. and Wassmuth, F.: "Foams: Basic Principles," *Foams: Fundamentals and Applications in the Petroleum Industry*, Schramm, L.L., Ed., *Advances in Chemistry Series* **242**, American Chemical Society, Washington, DC (1994) 3-46.

Sheng, J.J. and Maini, B.B.: *Foamy Oil Flow in Primary Production of Foamy Oil - A literature Review*, the Petroleum Recovery Institute Report 1995/96-7 (Feb. 1996) 4.

Smith, G.E.: "Fluid Flow and Sand Production in Heavy Oil Reservoirs Under Solution Gas Drive," *SPEPE* (May 1988) 169-80.

Ward, C.A. and Levart, E.: "Conditions for Stability of Bubble Nuclei in Solid Surfaces Contacting a Liquid-Gas Solution," *Journal of Applied Physics* (*J. Appl. Phys.*) (1984) **56,** No. 2, 491-500.

Ward, C.A., Tikuisis, P. and Venter, R.D.: "Stability Analysis in a Closed Volume of Liquid of Liquid-Gas Solution," *J. Appl. Phys.* (1982) **53,** No. 9, 6076-84.

Yortsos, Y.C. and Parlar, M.: "Phase Change in Binary Systems in Porous Media: Application to Solution Gas Drive," paper SPE 19697 presented at the 64th Annual Technical Conference and Exhibition of SPE of AIME, San Antonio, TX, Oct. 8-11, 1989.

Chapter 5

Proposed Models to Describe Foamy Oil Dynamic Processes

5.1 Introduction

To estimate foamy oil properties and understand foamy oil flow behaviour, the key issues are how much gas is dissolved and how much gas remains dispersed in the liquid oil phase. Bubble nucleation, bubble growth and the disengagement of gas bubbles from the liquid oil phase are all dynamic processes. This chapter presents the development of a basic model (Model 1) to describe these dynamic processes. Bubble nucleation is implicitly assumed to be instantaneous. Simple functional relationships are proposed to describe the rate of bubble growth and the rate of bubble decay in foamy oils and validated with experimental data. Although Model 1 is theoretically sound in that it takes the bubble age into account, it is difficult to be implemented directly into a numerical flow model. Based on this model, two other models (Model 2 and Model 3) are proposed which do not consider bubble age but can be implemented easily into a numerical flow model. Since bubble nucleation, bubble growth and bubble decay are very important issues in foamy oil flow, they are reviewed and discussed in this chapter, which provides theoretical support for the proposed models.

5.2 Dynamic Processes Involved in Foamy Oils

When the pressure of a saturated live oil is reduced below the saturation pressure, some degree of supersaturation results. If the supersaturation overcomes a critical supersaturation, some fraction of the nucleation sites in the system will be activated. The microbubbles initiated from these sites will grow. Initially, these bubbles remain dispersed in the oil phase. Gradually, these bubbles will disengage from the oil phase and become free gas. Therefore, three dynamic processes will occur: (i) bubble nucleation, (ii) bubble growth and (iii) bubble disengagement. These processes are shown schematically in Figure 5.1. These processes are assumed to happen almost instantaneously in light oils. However, the dynamic behaviour of these processes is believed to be very important to viscous heavy oils.

The body of literature on nucleation and bubble growth in bulk liquids is immense. A very selective and subjective review was presented by Yortsos and Parlar (1989). In sharp contrast, the literature on phase change and bubble growth in porous media is substantially leaner. Fundamental studies on the subsequent coalescence are even fewer. In this section, the three dynamic processes are reviewed; and the premises underlying the proposed model are also discussed. The review and discussion will provide a theoretical support for the models to be proposed in later sections.

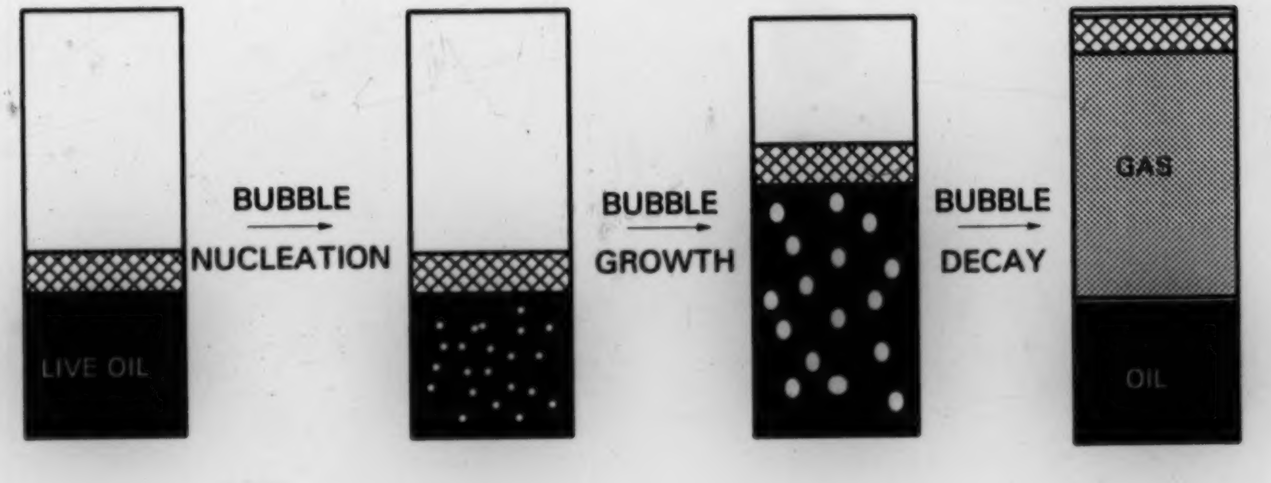
LIVE OIL
BUBBLE
NUCLEATION
BUBBLE
GROWTH
BUBBLE
DECAY
GAS
OIL

Fig. 5.1 - Dynamic processes of foamy oils.

5.2.1 Bubble Nucleation

5.2.1.1 Supersaturation

Supersaturation is an important issue to bubble nucleation. A liquid system is supersaturated with gas when the amount of gas dissolved exceeds that corresponding to equilibrium at the existing pressure and temperature. The degree of supersaturation was defined as the difference between the equilibrium pressure of a mixture and the prevailing system pressure at a given time by Firoozabadi and Kashchiev (1993), although other definitions have appeared in the literature. Supersaturation was defined by Handy (1958) as the difference between the equilibrium pressure corresponding to the observed solution GOR computed by material balance and the observed average pressure. Supersaturation was conveniently expressed as the difference between the bubble point pressure of the mixture and the prevailing pressure by Kennedy and Olson (1952). In porous media, the difference between the saturation pressure corresponding to the amount of dissolved gas and the liquid pressure consists of two components: one due to capillary forces and the other due to dynamic effects. The capillary component of supersaturation can become very significant in low permeability rocks (Kamath and Boyer, 1993). However, Firoozabadi and Kashchiev (1993) argued that the contribution of the capillary pressure was relatively small, so that the equilibrium pressure is practically the same as the pressure inside the nuclei of the bubbles.

In a foamy oil study, supersaturation may be defined as the difference between the amount of gas component present in the system and the amount of gas dissolvable assuming thermodynamic equilibrium at system conditions, because how much extra gas exists in the oil is our concern.

Supersaturation has been encountered in all laboratory solution gas drive tests (Stewart *et al.*, 1953). It prevails during the experiments and decreases with time (Dumore, 1970). At later stages, there is practically no fluid supersaturation inside the rock (Firoozabadi *et al.*, 1992). Also, there are several definitions for the critical supersaturation (Yortsos and Parlar, 1989; Kashchiev and Firoozabadi, 1993), depending on different experimental conditions and techniques. In foamy oil reservoirs, the critical supersaturation may be conveniently defined as the pressure difference between the initial saturation pressure and the pressure when a noticeable volume of gas is evolved. And this pressure is defined as the threshold nucleation pressure, p_n.

The magnitude of supersaturation would obviously depend on the characteristics of the system involved as well as on the operating conditions and the depletion level. Therefore it is not surprising that the reported laboratory values of supersaturation cover a very wide range. Some of the published results are summarized in Table 5.1.

The effect of pressure decline rate on supersaturation is the main issue. The degree of supersaturation that can develop under a low pressure decline rate will most likely differ from that developing at a high rate (Kortekaas and van Poelgeest, 1991). It has been established by laboratory tests that the degree of supersaturation decreases markedly with decreasing pressure decline rate (Stewart *et al.*, 1953, 1954; Chatenever *et al.*, 1959; Dumore, 1970; Wall and Khurana, 1971, 1972; Moulu, 1989; Firoozabadi and Kashchiev, 1993). Extrapolation of the laboratory data indicates very little supersaturation exists under most field conditions (Stewart *et al.*, 1953). However, the magnitude of the pressure-decline-rate effect on supersaturation would also depend on the system characteristics. During a 100 psi/day high pressure internal gas drive experiment in low-permeability rocks (0.04 md), Kamath and Boyer (1993) observed that the capillary component of the supersaturation was 42-66 psi whereas the dynamic component was only 6 psi. Therefore, they pointed out that the effect of the pressure decline rate might not be significant in low-permeability reservoirs. Instead, the capillary component of supersaturation could become the dominant part.

Table 5.1 - Range of Supersaturation Values Reported in the Literature

Author	Supersaturation (psi)
Firoozabadi *et al.* (1992)	10-150
Moulu (1989)	1-10
Danesh *et al.* (1987)	360
Madaoui (1975)	assumed zero
Abgrall & Iffly (1973)	assumed zero
Chatenever *et al.* (1959)	7
Handy (1958)	40-200
Wieland & Kennedy (1957)	14-25
Stewart *et al.* (1954)	20-90
Stewart *et al.* (1953)	0-72
Wood (1953)	27
Kennedy & Olson (1952)	30-770

Other factors are also important that affect supersaturation. The range of supersaturation depends on the type of rock and the fluid used (Wieland and Kennedy, 1957). Higher degrees of supersaturation could be attained in more uniform packs

(Chatenever *et al.*, 1959), and in a porous medium with smaller grains (Chatenever *et al.* 1959; Wall and Khurana, 1971). However, Firoozabadi *et al.*'s (1992) data show that pore structure could significantly affect the degree of supersaturation; the supersaturation in a porous medium with small pores was lower than in a porous medium with large pores. They drew that conclusion from the experimental results of only two samples without any explanation. The degree of supersaturation also increases with higher capillary forces (Kamath and Boyer, 1993), and higher interfacial tensions (IFT) (Wieland and Kennedy, 1957; Kortekaas and van Poelgeest, 1991; Firoozabadi and Kashchiev, 1993).

5.2.1.2 Physics of Nucleation

Classically, nucleation theories comprise homogeneous nucleation and heterogeneous nucleation. Homogeneous nucleation occurs by the spontaneous formation of bubbles in a liquid when a thermodynamic fluctuation of sufficient magnitude occurs to form a cluster of molecules bigger than a certain critical size (Wall and Khurana, 1971; Moulu, 1989; Yortsos and Parlar, 1989; El Yousfi *et al.*, 1991). It requires the absence of foreign matter in the bulk liquid, and perfectly smooth and liquid wet solid surfaces. Very high supersaturation is needed which was not observed in porous media. Therefore, such a nucleation process is discounted in porous media (Yortsos and Parlar, 1989; Kamath and Boyer, 1993). Heterogeneous nucleation takes place on foreign matter, such as walls of the container, surfaces of the particles in porous media (Kennedy and Olson, 1952; Bernath, 1952; Danesh *et al.*, 1987; Moulu, 1989; Li, 1993, p. 106; Li and Yortsos, 1993), poorly wetted cavities (Wall and Khurana, 1971; Cole, 1974;

Yortsos and Parlar, 1989; Kamath and Boyer, 1993), and pre-existent trapped gas (Fisch *et al.*, 1948; Cole, 1974; El Yousfi *et al.*, 1991; Kamath and Boyer, 1993; Li and Yortsos, 1993), etc. The crevice model, in which gas is trapped in a conical crevice in a solid inhomogeneity present in the liquid, has received considerable attention (Crum, 1982).

Li and Yortsos (1991, 1993) proposed that a nucleation site is activated, if the following condition is satisfied,

$$K_H C - p_l \geq \frac{\sigma}{W}. \tag{5-1}$$

Here K_H is the solubility constant, C is the gas concentration, p_l is the liquid pressure, σ is the interfacial tension, and W is the crevice mouth size. Although they pointed out that this nucleation condition depends only on the local variables C and p_l, and does not involve the intrinsic kinetic mechanisms of classical nucleation (whether homogeneous or heterogeneous), the above equation assumes that the impurities required by heterogeneous nucleation exist. Therefore, condition 5-1 is of the nature of heterogeneous nucleation. This condition is supported by many investigators (e.g., Ward *et al.*, 1983; Ward and Levart, 1984; Danesh *et al.*, 1987), and was reviewed extensively by Crum (1982), and also by Atchley and Prosperetti (1989).

Based on their investigation into the effects of pressure decline rate on the critical supersaturation and published experimental data reported by Kennedy and Olson (1952) and El Yousfi *et al.* (1991), Firoozabadi and Kashchiev (1993) proposed an instantaneous nucleation process (IN), in which all nucleus bubbles form at once and then they only grow. They argued that the classical nucleation theory (both homogeneous and heterogeneous) cannot describe the solution gas drive process.

El Yousfi *et al.*'s (1991) experimental data show that most of the bubbles form at the initial stage. This is because that the supersaturation in their experiments was caused by a rapid pressure drop, Δp, and the initial supersaturation was the maximum during the test, since bubble formation reduces supersaturation. According to the nucleation condition described by inequality 5-1, all the sites which could be nucleated would be nucleated at the initial stage. Afterwards, no more sites would be nucleated. Therefore, the IN process is a special case of the nucleation described by condition 5-1 when the initial supersaturation is maximum during the pressure depletion period, or when the nucleation sites are all of similar size, W. This may be a physical explanation for the IN process. Generally, maximum supersaturation will occur in the early life of the reservoir, rather than at a later date when concentration gradients have been lowered by diffusion (Kennedy and Olson, 1952).

Observations from glass micromodel experiments show that after the initial gas bubbles nucleate on the wall, they quickly detach and migrate toward the centers of the pores (Li, 1993, p. 106). Their formation appears to be distributed at random both as regards to time and to location on the solid surface (Kennedy and Olson, 1952; Hunt and Berry, 1956; Handy, 1958; Chatenever *et al.*, 1959; Li and Yortsos, 1991). This may be caused by the probability of many nucleation sites on the surfaces. However, El Yousfi *et al.* (1991) observed reproducible results. For instance, the first bubble was always observed to appear in the same pore, even for different values of the pressure drop.

The density of gas bubbles (population) could be low. This view is supported by experiments (Chatenever *et al.*, 1959; Wall and Khurana, 1971, 1972), and by calculation results. Kennedy and Olson's (1952) calculation results show that only about one pore in a million will have a bubble originating in it. Firoozabadi and Kashchiev's calculation results (1993) also show that the number of gas bubbles formed as a result of pressure decline or volume expansion rates is orders of magnitude less than the number of pores. They pointed out that due to low bubble density in comparison to the number of pores, the neglect of coalescence in the early phase of gas phase formation was justified.

Wieland and Kennedy (1957) noted that the rate of diffusion would also affect the number of bubbles formed. If the diffusion coefficient is high, the gas in solution in the oil surrounding a single bubble will tend to diffuse into the bubble rather forming other bubbles. On the other hand, the formation of more bubbles will tend to occur if the diffusion coefficient is very low.

In viscous foamy oil flow, bubble growth is restricted by the pore geometry, low diffusivity and viscous forces. Therefore, supersaturation would not be easily relieved. The higher supersaturation will cause more sites to be nucleated. Such sites required for nucleation could exist in foamy oil as suspended solids (Maini *et al.*, 1993). As a result, the bubble population in heavy oil reservoirs will be larger than that in light oil reservoirs.

5.2.1.3 Rate of Nucleation

The classical equation for the nucleation rate is (Kashchiev and Firoozabadi, 1993)

$$J = A_1 \, exp(-A_2/\Delta p_s^2), \qquad (5\text{-}2)$$

where Δp_s is the supersaturation expressed as pressure difference. The quantities A_1 and A_2 are kinetic and thermodynamic parameters, respectively, which characterize the rock-fluid system (Wit, 1974). As discussed above, this equation for classical nucleation theory should not be applied to nucleation in porous media, although Wood (1953) experimentally evaluated this relation for porous media. Hoyos *et al.* (1990) measured the nucleation rates in porous media by means of an ultrasonic technique.

Yortsos and Parlar (1989) modified the general equation to consider the effect of a porous medium as follows:

$$J = K_{het} \exp(-A_2/\Delta p_s^2 \cdot F_j), \qquad (5\text{-}3)$$

where K_{het} is a kinetic constant, and F_j is a function of site geometry and wettability.

Based on the above review and discussion of the nucleation physics and nucleation rate, it may be proposed that nucleation in porous media is instantaneous and heterogeneous (IHN), which means that the nucleation rate is so fast that it can be treated as being instantaneous in practical reservoirs; and the nucleation is heterogeneous in nature.

5.2.1.4 Effects on Nucleation

Pressure decline rate It was observed in the laboratory and/or generally believed that more bubbles were formed and they would be formed faster for higher pressure decline rates (Kennedy and Olson, 1952; Stewart *et al.*, 1954; Hunt and Berry, 1956;

Wieland and Kennedy, 1957; Aldea, 1970; Wit, 1974; Danesh *et al.*, 1987; Moulu, 1989; El Yousfi *et al.*, 1991; Kortekaas and van Poelgeest, 1991; Firoozabadi and Kashchiev, 1993). This is mainly due to the fact that a higher pressure decline rate results in greater supersaturation.

Asphaltene The role of asphaltenes in bubble nucleation during solution gas drive has not been investigated experimentally. Smith (1988) suggested that the suspended asphaltene particles could act as bubble nucleation sites. Claridge and Prats (1995) suggested that the adsorption of asphaltenes on bubble surfaces could stabilize the bubbles at a very small size. Coskuner (1988) noted that one class of emulsion stabilizing agents comprised finely divided insoluble solids which stick to the interface by reason of surface tension forces. Once situated at the interface, the solid particles make coalescence of droplets more difficult, essentially by keeping the droplets from coming into close contact. In the case of oil field emulsions these solids may be formation fines, crystalline wax or asphaltene particles. Islam and Chakma's (1990) experimental data show that the existence of asphaltene enhances gas nucleation and reduces the release of gas bubbles from the liquid phase.

Connate water Kennedy and Olson (1952) observed that the presence of water, when added to their experimental hydrocarbon mixtures, had no measurable effect on bubble frequency. However, Kamath and Boyer (1993) pointed out that oil has a lower surface energy compared to water and it is possible that there are more hydrophobic sites than oleophobic sites. Hence nucleation may be easier when cores contain connate water saturation. Danesh *et al.* (1987) suggested that the presence of a connate water might delay bubble nucleation, because diffusion of the light components of the oil into the water phase reduces the population of low density clusters in the oil and prevents the formation of bubbles. In an actual reservoir situation this would not be the case since the water will be in equilibrium with the oil.

5.2.2 Bubble Growth

5.2.2.1 Physics of Bubble Growth

After the activation of a site and the formation of a critical size nucleus which must be stable (Crum, 1982), or the release of a pre-existent or trapped microbubble (El Yousfi *et al.*, 1991), it can grow with a certain growth rate, G. In general, G is controlled by mass, momentum and/or heat transfer across the bubble-liquid interface (Theofanous *et al.*, 1969; Szekely and Martins, 1971; Szekely and Fang, 1973), and by compression or expansion (Firoozabadi and Kashchiev, 1993). Mass transfer occurs by evaporation and condensation at the interface for single component systems. Mass transfer also occurs by diffusion in the liquid phase for multicomponent systems. Momentum transfer is governed by hydrodynamic forces in connection with the capillary pressure, liquid inertia and viscosity. Heat transfer takes place by the flow of heat from the liquid towards the bubble. A change of pressure in the liquid is accompanied by expansion or resolution of gas bubbles (Firoozabadi and Kashchiev, 1993).

In the very initial stages, the growth rate is limited by factors other than diffusion, such as liquid inertia at the early stages of the process with large pressure-decline rates (Li and Yortsos, 1991), or surface tension forces, but these effects may be insignificant in many practical applications (Szekely and Martins, 1971; Szekely and Fang, 1973;

Plesset and Prosperetti, 1977). Viscous forces are unlikely to play a role in limiting bubble growth in "ordinary liquids," such as water, light oils; viscous momentum transfer may become rate limiting in highly viscous substances (Szekely and Martins, 1971; Szekely and Fang, 1973). Bubble growth in a porous medium is controlled by forces similar to those in the bulk, namely inertia, viscous forces, surface tension and pressure. Supersaturation in the liquid drives the process. The specific pore geometry of the porous medium constrains the growth pattern obtained, and stabilizes otherwise unstable gas bubbles (Yortsos and Parlar, 1989). It is believed that bubble growth in porous media at isothermal conditions is mainly controlled by diffusion (El Yousfi *et al.*, 1991; Firoozabadi and Kashchiev, 1993). Recently, Firoozabadi *et al.* (1994) emphasized that gas bubbles grow mainly by diffusion in light oils.

In foamy oil reservoirs, the effect of viscous forces is expected to be significant in controlling the bubble growth, because the expansion of the gas phase by diffusion into existing gas bubbles must be great enough to overcome the resistance caused by the surrounding viscous oil. The more viscous the oil, the lower the growth rate might be.

The competition between growing clusters in a porous medium is different than in the bulk. In the bulk, the competition is based on the solubility dependence on curvature, and the larger bubbles grow at the expense of smaller ones. In porous media, cluster size and capillarity are only indirectly coupled. The competition between growing clusters is controlled by the porous medium capillary characteristics and by mass transfer, the solubility dependence on radius being insignificant (Li and Yortsos, 1993).

It is generally accepted that bubble growth by diffusion follows a percolation pattern (El Yousfi, *et al.*, 1991) when the pressure decline rate is low (Yortsos and

Parlar, 1989; Li, 1993, p. 113). When the viscous and capillary forces are comparable, however, or when viscous forces become dominant, the bubble growth pattern will deviate from percolation (Li, 1993, p. 114). The pattern is expected to be controlled mainly by capillary and viscous forces, and to a lesser extent by mass transfer in porous media (Li and Yortsos, 1993).

The gas structures grow in a characteristic form - continuous, long and narrow. They are sometimes as narrow as one or two grains, but most often are between 5 and 10 grains (Chatenever *et al.*, 1959). They grow in a ramified fashion in a glass micromodel, rather than in the compact fashion observed in a Hele-Shaw cell (Li and Yortsos, 1991). For foamy oil flow, it was observed from the visual experiments mentioned in Section 4.4.6 that ramified and narrow gas clusters were formed along higher permeability channels to exit the pack. They could not grow spherically because of viscous resistance and pore geometry constraints.

5.2.2.2 Formulation of Bubble Growth

The general convection-diffusion equation for solute transport is (Li and Yortsos, 1993):

$$\phi\frac{\partial C}{\partial t} + \mathbf{v}\cdot\nabla C = \phi D\nabla^2 C, \tag{5-4}$$

where ϕ is the porosity of a porous medium, equal to one in a bulk vessel; D is the diffusion coefficient, and $\mathbf{v}$ is the velocity produced in the medium by bubble growth or shrinkage (Epstein and Plesset, 1950).

A more general formulation is available elsewhere (Scriven, 1959). Most investigators did not consider the convective term (Epstein and Plesset, 1950; Plesset and Prosperetti, 1977; Moulu, 1989; Yortsos and Parlar, 1989; Li and Yortsos, 1991), because the velocity of the bubble interface is low (Plesset and Prosperetti, 1977) and the effect of convection was found to be secondary (Li and Yortsos, 1991). The quasi-static approximation is widely used at low supersaturation (Yortsos and Parlar, 1989), or when enough time has elapsed for significant diffusion to take place (Epstein and Plesset, 1950). The quasi-static solution has been derived rigorously by Scriven (1959) and confirmed numerically by Szekely and Martins (1971). The effects of inertia, viscous forces and surface tension has been generally neglected in the literature.

For the rate of bubble growth, different regimes of growth result in different $r_b(t)$ dependencies. Here $r_b(t)$ is the radius of a bubble at time t. If the growth is controlled only by the liquid inertia, r_b is a linear function of t (Szekely and Fang, 1973; Kashchiev and Firoozabadi, 1993). If the growth is controlled by diffusion, r_b is proportional to the square root of t (Scriven, 1959; Szekely and Martins, 1971; Szekely and Fang, 1973; Plesset and Prosperetti, 1977; Cooper *et al.*, 1983; Moulu, 1989). These simple relationships were derived using bulk models. In general, the relationship is rather complicated either in bulk or in porous media (Scriven, 1959; Kashchiev and Firoozabadi, 1993; Li and Yortsos, 1993).

In porous media the $r_b(t)$ dependencies are expected to be more complicated. El Yousfi *et al.*'s (1991) experimental results in transparent micromodels show that the relationship between $\log(r_b)$ and $\log(t)$ is linear. This log-log relationship between r_b and t suggests that r_b could also be a power function of t. Firoozabadi and Kashchiev (1993) generalized the formula of bubble growth rate in a bulk vessel to describe the bubble growth in porous media. They used a shape factor (regarded as a constant independent of time) to account for the effects of size and geometry of the grains and the pores of the porous medium. Using scaling theory and fractal dimensions, Li and Yortsos (1993) showed that r_b is some complicated power function of t at conditions of global percolation.

Many factors control bubble growth in porous media. It would be desirable to incorporate these factors in a simple formula or in a simple model which can be implemented in a reservoir simulator. According to the above literature information, it seems that the radius of a bubble could be a power function of time as a general approximation. Since the volume or mass of gas bubbles is directly proportional to the bubble radii, it appears reasonable to suggest that the total amount of gas formed, $n_{eg}(t)$, is also proportional to some power of t:

$$n_{eg}(t) = n_{eq}\left[\frac{t}{t_{eq}}\right]^{b}. \tag{5-5}$$

Here n_{eq} is the amount of gas evolved at thermodynamic equilibrium, t_{eq} is the time required to reach the equilibrium, and b is the gas-bubble growth index. By adjusting b and t_{eq}, we can incorporate all the effects controlling bubble growth, especially the effect of the porous medium on bubble growth which has not been formulated quantitatively.

5.2.3 Bubble Disengagement

Gas bubbles released from oil due to a pressure decline tend to remain dispersed in the oil to form an oil-continuous foam. However, thermodynamically, the foam is unstable (de Vries, 1958; Schramm and Wassmuth, 1994). The dispersed gas bubbles eventually separate from the oil to form a free gas phase, but this separation takes time to occur, the time depending on the stability of the gas bubble system. The mechanisms of bubble decay are far from fully understood. A more detailed review of the effects on the stability of a liquid-gas system was presented in Section 4.2.

If the bubbles are sufficiently "small", they may be present in a stable form, and flow with or through the liquid, probably faster than it (Govier and Aziz, 1982, p. 556; Ward *et al.*, 1982; Ward and Levart, 1984; Smith, 1988). The stability is supported by Brownian movement or electrical charge even in the absence of any turbulence, or supported as a result of high or special consistency properties of the continuous phase (Govier and Aziz, 1982, p. 3). These microbubbles could be in stable equilibrium under the constraint of a closed volume and for reasonable conditions of liquid temperature and pressure (Ward *et al.*, 1982), in the presence of rough surfaces (Ward and Levart, 1984), or under the constraint of the pore wall curvature and geometry (Yortsos and Parlar, 1989). If the bubbles are small and far from each other in the early stages, the coalescence will not be significant (Kashchiev and Firoozabadi, 1993). These bubbles are so small that they may be much smaller than the average pore-throat size (Ward *et al.*, 1982; Smith, 1988), or 2 to 5 μm (Ward and Levart, 1984).

Many factors affect the foam (dispersion of bubbles) stability. It has been found in the laboratory that foam stability increases with increasing viscosity of the liquid oil (Brady and Ross, 1944; McBain and Robinson, 1949; Callaghan and Neustadter, 1981; see also Section 4.4.1).

In foam studies, many investigators have used exponential functions to describe the rate of decay. The equation to describe exponential decay has the form:

$$u(t) = u(0)\, e^{-\lambda t}, \tag{5-6}$$

or in differential form:

$$\frac{du}{dt} = -\lambda u, \tag{5-7}$$

where λ is the decay coefficient, u is a foam parameter with its value $u(0)$ at $t = 0$. The variable u has represented different parameters depending on the investigator. It could be the interfacial area of foams (Clark, 1947), the liquid volume of foams (Ross, 1969), the number of bubbles (Bikerman, 1973, p. 90), the foam volume (Bikerman, 1973, p. 90; Maini and Ma, June and Sept., 1984), or the number of flowing bubbles for the flow of aqueous foams in porous media (Ettinger and Radke, 1992; Kovscek and Radke, 1994). Bikerman (1973, p. 232) pointed out that at any rate, the velocity of liquid drainage is a poor measure of foam stability. Perhaps the gradual decay of the total area of the gas-liquid interface in foam would be a better measure of the collapse process than the diminution of the foam volume or the foam height (Bikerman, 1973, p. 94).

The above research results may be applied *mutatis mutandis* to non-aqueous foams (Ross, 1967; Callaghan and Neustadter, 1981). Therefore, it will be proposed in the following models that the amount of dispersed gas also decays according to an exponential function of time.

5.3 The Basic Model (Model 1)

The model proposed in this section is the basic model used to describe the dynamic processes involved in foamy oils. The additional two models proposed subsequently in Section 5.6 are similar to this one.

Pressure reduction below the saturation pressure creates supersaturation. For a specific reduction in pressure, Δp, a certain level of supersaturation is created, and some fraction of the total nucleation sites become active. The microbubbles originating from these sites grow in size and their number changes with time. The amount of evolved gas continues to increase until thermodynamic equilibrium is reached. It will be justified that the amount of evolved gas can be modelled as a power law function of time. The gas bubbles are initially dispersed in the liquid oil phase. They eventually disengage from the liquid oil and become free gas. The disengagement of bubbles from the liquid oil to form free gas results in a volume reduction of gas bubbles dispersed in the oil. It will also be justified that this reduction can be modelled as an exponential function of time.

The processes of nucleation, bubble growth and bubble decay occur simultaneously. In systems undergoing a gradual reduction in pressure, the total pressure drawdown can be modelled as a series of small step reductions in pressure. The dynamic processes are considered for each step change in pressure. Then the effect of the total pressure change is the sum of the effects of these small step changes. The idea is presented in Figure 5.2 in which the effect of one pressure drop is described. From time t^{i-1} to time t^i, the pressure drops from p^{i-1} to p^i. Due to this pressure drop (Δp^i), solution gas evolves and becomes evolved gas following the route A-B-C. At point B, which corresponds to

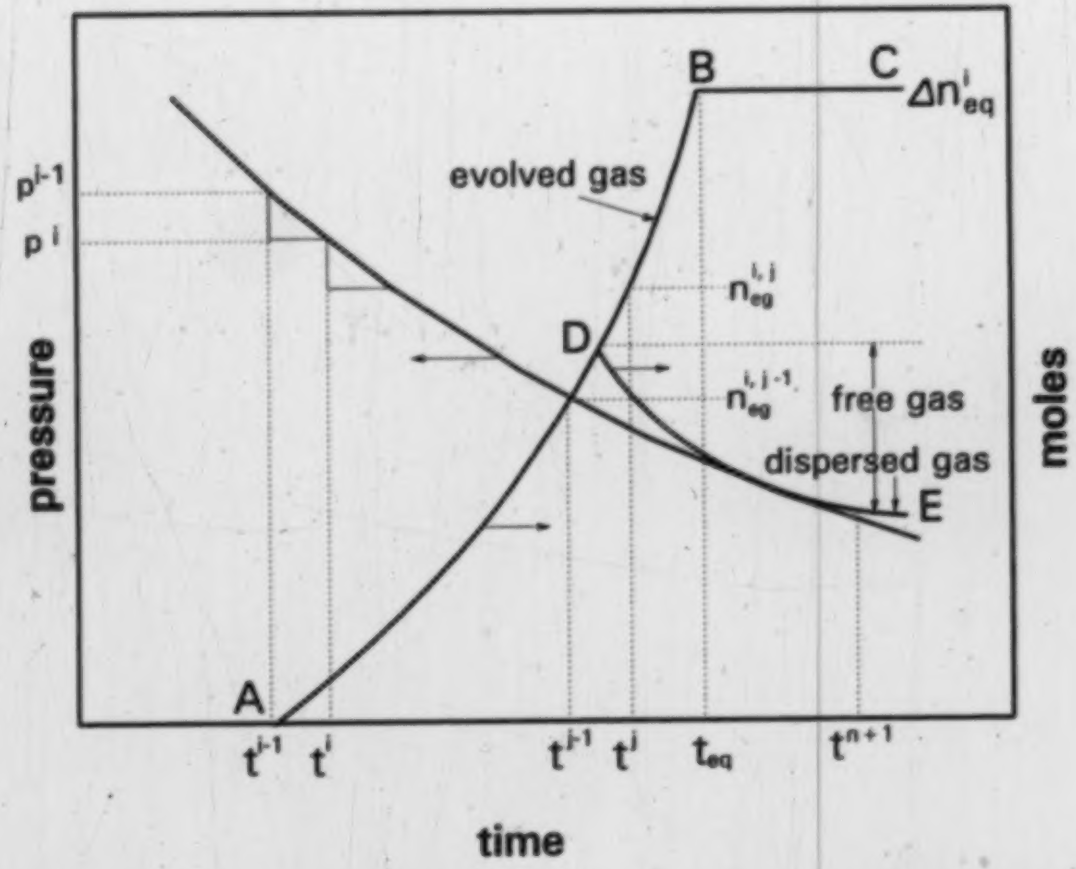

p^{i-1}
p^{i}
pressure
A
B
C
Δn_{eq}^{i}
D
E
evolved gas
$n_{eq}^{i,j}$
$n_{eq}^{i,j-1}$
free gas
dispersed gas
moles
t^{i-1}
t^{i}
t^{j-1}
t^{j}
t_{eq}
t^{n+1}
time

Fig. 5.2 - Schematic description of Model 1.

t_{eq}, the time to reach thermodynamic equilibrium, the amount of evolved gas is Δn_{eq}^{i} which can be evolved according to thermodynamic equilibrium due to this pressure drop. After B, there is no further increase in evolved gas. The evolved gas is dispersed initially in the liquid oil and gradually disengages from the oil to become free gas. The gas evolved during each time step from A to B is considered individually. Such consideration for one time step from t^{j-1} to t^{j} is shown in Figure 5.2. During this time step, the increase of evolved gas, $\Delta n_{eq}^{i,j}$, is equal to $n_{eq}^{i,j} - n_{eq}^{i,j-1}$. The amount of gas that remains dispersed in the oil due to this increase of evolved gas is shown by the curve D-E, and the rest of the evolved gas becomes free gas. Then the effect of the evolved gas due to the pressure drop Δp^{i} is the sum of the effects of these individual increases of evolved gas. The effects resulting from such small pressure drops constitute the effect of the whole pressure drop.

5.3.1 Assumptions

This model is based on the following assumptions:

1. A fraction of the evolved gas is dispersed in the form of tiny bubbles in the viscous oil when the reservoir pressure drops below the nucleation threshold pressure. Below the bubble-point pressure and above some threshold pressure, the solution gas will remain dissolved (Firoozabadi *et al.*, 1992).
2. The oil phase consists of three components: dead oil, solution gas and dispersed gas.
3. The volume of the foamy oil phase is calculated using a simple linear rule that

combines the contributions of the three components in the foamy oil phase.

4. The volume of dispersed gas is assumed to be equal to the volume that the gas would occupy in the free gas state at the same pressure and temperature.

5.3.2 Modification of *K* Value

The dissolved gas may not evolve from the liquid oil phase until the reservoir pressure declines to a nucleation threshold pressure, p_n. In other words, the liquid must be supersaturated for bubble nucleation to occur (Kortekaas and van Poelgeest, 1991; Kashchiev and Firoozabadi, 1993). Because of bubble nucleation and gas diffusion, the supersaturation will decrease with time. The actual supersaturation in a reservoir increases or decreases depending on the pressure decline rate. The supersaturation phenomenon is considered in two parts: a thermodynamic equilibrium term (pressure-dependent) and a non-equilibrium term (time-dependent), similar to Kamath and Boyer's capillary component and dynamic component of supersaturation, respectively. The time-dependent term is considered in the rate of bubble growth. The pressure-dependent term is considered by modifying the *K* value (gas/oil thermodynamic equilibrium ratio) obtained from conventional PVT data. At the nucleation threshold pressure, p_n, the modified *K* value should be equal to that measured at the bubble point pressure, p_b, in the laboratory tests; and at atmospheric pressure, p_{sc}, the modified *K* value should be equal to that measured in a standard PVT test. At atmospheric pressure, the supersaturation disappears and all dissolved gas evolves from the liquid oil phase. Between the nucleation threshold pressure and atmospheric pressure, it is assumed that the difference between the modified K value and the standard PVT value decreases linearly. Mathematically, K values are modified as follows:

$$K'(p) = K(p) + \frac{K(p_b) - K(p_n)}{p_n - p_{sc}} \cdot [p - p_{sc}] \quad (p_{sc} \le p < p_n), \tag{5-8}$$

$$K'(p) = K(p_b) \qquad (p_n \le p \le p_b), \tag{5-9}$$

$$K'(p) = K(p) \qquad (p > p_b). \tag{5-10}$$

This modification is also based on the fact that some degree of supersaturation is always observed to exist throughout the entire pressure depletion life of solution gas drive tests (Stewart *et al.*, 1954).

5.3.3 Estimation of the Moles of Evolved Gas

When the reservoir pressure declines below the nucleation threshold pressure, p_n, the solution (dissolved) gas starts to evolve from the liquid oil phase. For *one mole of live oil*, the total moles of gas, $n_{eq}(p)$, which can be flashed from p_n to p according to thermodynamic equilibrium is (Kraus *et al.*, 1993):

$$n_{eq}(p) = \frac{K'(p)/K'(p_n) - 1}{K'(p) - 1}. \tag{5-11}$$

Thus the increase in moles of flashed gas, Δn_{eq}^{j}, due to a decrease in pressure from p^{j-1} to p^{j}, at thermodynamic equilibrium, is

$$\Delta n_{eq}^{i}(p^{i}) = n_{eq}^{i}(p^{i}) - n_{eq}^{i-1}(p^{i-1}) = \frac{K'(p^{i})/K'(p_{a})-1}{K'(p^{i})-1} - \frac{K'(p^{i-1})/K'(p_{a})-1}{K'(p^{i-1})-1}. \quad (5\text{-}12)$$

However, equilibrium is not reached instantaneously; the number of moles of evolved gas increases with time. For this step change in pressure, the moles of evolved gas, $n_{eg}^{i,j}$, at the time t^{j} ($j \geq i$) is

$$n_{eg}^{i,j}(p^{i}, t^{j}) = \Delta n_{eq}^{i} \, \alpha_{eg}^{i,j}. \quad (5\text{-}13)$$

Here α_{eg} is the fraction of evolved gas defined as

$$\alpha_{eg} = \frac{\textit{Cumulative amount of gas evolved}}{\textit{Gas flashed at thermodynamical equilibrium}}. \quad (5\text{-}14)$$

From Eq. 5-5 one has

$$\alpha_{eg}^{i,j} = \left[\frac{t_{eg}^{i,j}}{t_{eq}}\right]^{b}, \quad (5\text{-}15)$$

where $t_{eg}^{i,j}$ is the bubble age or the effective time which is from the time of this step change in pressure to the time of interest. For the gas Δn_{eq}^{i} flashed from p^{i-1} to p^{i}, $t_{eg}^{i,j}$ ($j \geq i$) may be approximated as

$$t_{eg}^{i,j} = t^{j} - \frac{t^{i}+t^{i-1}}{2}, \quad (5\text{-}16)$$

and t_{eg} should satisfy the condition:

$$t_{eg} = \begin{cases} t_{eq} & \textit{if } t_{eg} \geq t_{eq} \\ t_{eg} & \textit{if } t_{eg} < t_{eq}. \end{cases} \quad (5\text{-}17)$$

From the time t^{j-1} to t^{j}, the mole increase of evolved gas is

$$\Delta n_{eg}^{i,j} = n_{eg}^{i,j} - n_{eg}^{i,j-1} = \Delta n_{eq}^{i} \left(\alpha_{eg}^{i,j} - \alpha_{eg}^{i,j-1}\right). \tag{5-18}$$

For this step pressure drop from p^{i-1} to p^{i}, the moles of evolved gas until time t^{n+1} is then

$$n_{eg}^{i,n+1} = \sum_{j=i}^{n+1} \Delta n_{eg}^{i,j}. \tag{5-19}$$

For the total pressure drop (i.e., $n+1$ step pressure drops), the total moles of evolved gas is

$$n_{eg}^{n+1} = \sum_{i=1}^{n+1} n_{eg}^{i,n+1} = \sum_{i=1}^{n+1} \sum_{j=i}^{n+1} \Delta n_{eg}^{i,j}. \tag{5-20}$$

5.3.4 Estimation of the Moles of Dispersed Gas

When the reservoir pressure declines below the nucleation threshold pressure, p_n, the solution gas starts to evolve from the liquid oil phase to become evolved gas. More generally, a fraction of the evolved gas can remain dispersed in the viscous oil phase as dispersed gas and the rest of it becomes free gas directly. It is apparent that given sufficient time, the dispersed gas will disengage from the viscous oil to become free gas. Experimentally measured rates at which the dispersed gas separates from the oil to become free gas have not been reported in the literature. However, as discussed and proposed earlier in Section 5.2.3, this rate could be described by an exponential function of time.

If one defines α_{dg} as

$$\alpha_{dg} = \frac{amount\ of\ gas\ dispersed\ at\ t_{dg}}{amount\ of\ gas\ dispersed\ at\ t_{dg} = 0}, \tag{5-21}$$

then

$$\alpha_{dg} = \exp(-\lambda_{dg} t_{dg}), \tag{5-22}$$

where λ_{dg} is the decay coefficient of dispersed gas and t_{dg} is the age of the dispersed gas. Note that α_{dg} is one when t_{dg} equals zero and zero when t_{dg} is infinite.

It would be more reasonable that the rate of disengagement is higher if the volume of a certain amount of gas bubble is higher. For the same moles of gas bubbles, the gas volume is inversely proportional to the pressure. Therefore, the decay coefficient λ_{dg} may be modified to

$$\lambda_{dg} = \lambda_{sc}\left[\frac{p_{sc}}{p}\right], \tag{5-23}$$

where λ_{sc} is the decay coefficient at p_{sc}, atmospheric pressure, chosen for comparison of different tests. This modification is supported by the argument that the coalescence rate coefficient in aqueous foams is proportional to the local gas volumetric fraction in the foam (Kovscek and Radke, 1994).

For the moles of gas $\Delta n_{dg}^{i,j}$, evolved from t^{j-1} to t^{j}, the effective age (t_{dg}^{j}) by the time of interest (t^{n+1}) may be approximated as

$$t_{dg}^{j} = t^{n+1} - \frac{t^{j-1}+t^{j}}{2}. \tag{5-24}$$

Then the dispersed gas due to the pressure drop from p^{j-1} to p^{j} at time t^{n+1} is

$$\Delta n_{dg}^{i}(t^{n+1}) = \sum_{j=i}^{n+1} \Delta n_{eg}^{i,j} \cdot \alpha_{dg}^{j}. \tag{5-25}$$

The total number of moles of dispersed gas at the time of interest, t^{n+1}, is

$$n_{dg}^{n+1} = \sum_{i=1}^{n+1} \Delta n_{dg}^{i}(t^{n+1}) = \sum_{i=1}^{n+1} \sum_{j=i}^{n+1} \Delta n_{eg}^{i,j} \cdot \alpha_{dg}^{j}. \tag{5-26}$$

The rates of bubble nucleation, growth and coalescence could be dependent on the pressure decline rate, pressure drop, nucleation site distribution, etc. Therefore, a correction factor is needed to account for such effects. The amount of the dispersed gas may be modified by a correction factor, F, which represents the deviation of the effect of a specific pressure drop from the average reservoir performance. Thus, the amount of the dispersed gas may be modified as

$$\Delta n_{dg}^{i}(t^{n+1}) = \sum_{j=i}^{n+1} \Delta n_{eg}^{i,j} \cdot \alpha_{dg}^{j} \cdot F^{i}. \tag{5-27}$$

It has been suggested that there may be an upper limit to the volume fraction of gas that can be dispersed. This fraction of gas may be described by a parameter, say, the maximum dispersed gas quality, f_{max}. The quality in the foamy oil phase, f_{dg}, is defined as

$$f_{dg} = \frac{V_{dg}}{V_{fo}} = \frac{n_{dg} \nu_{dg}}{n_{fo} \nu_{fo}}, \tag{5-28}$$

where υ_{dg} and υ_{fo} are the molar specific volumes. They may be estimated from

$$\nu_{dg} = \frac{zRT}{p}, \tag{5-29}$$

and

$$\nu_{fo} = \nu_{do}X_{do} + \nu_{sg}X_{sg} + \nu_{dg}X_{dg}, \tag{5-30}$$

respectively.

Also, there is probably a minimum dispersed gas quality, f_{min}, below which the gas bubbles will remain perpetually dispersed in the liquid phase, because these microbubbles are so far separated that they cannot coalesce. Obviously, f_{max} and f_{min} are related to the oil viscosity, the distribution of nucleation sites, etc., and would be system specific.

When the calculated f_{dg}^{n+1} is greater than f_{max}, n_{dg}^{n+1} is adjusted so that the following condition is satisfied:

$$n_{dg}^{n+1}\nu_{dg}^{n+1} = f_{max}\,(n_{dg}^{n+1}\nu_{dg}^{n+1} + n_{sg}^{n+1}\nu_{sg}^{n+1} + n_{do}^{n+1}\nu_{do}^{n+1}), \tag{5-31}$$

that is,

$$n_{dg}^{n+1} = \frac{f_{max}\,(n_{sg}^{n+1}\nu_{sg}^{n+1} + n_{do}^{n+1}\nu_{do}^{n+1})}{\nu_{dg}^{n+1}\,(1 - f_{max})}. \tag{5-32}$$

When the calculated f_{dg}^{n+1} is less than f_{min}, n_{dg}^{n+1} should be

$$n_{dg}^{n+1} = \frac{f_{min}\,(n_{sg}^{n+1}\nu_{sg}^{n+1} + n_{do}^{n+1}\nu_{do}^{n+1})}{\nu_{dg}^{n+1}\,(1 - f_{min})}, \tag{5-33}$$

or

$$n_{dg}^{n+1} = n_{dg}^{n} + \sum_{i=1}^{n+1} \Delta n_{eg}^{i,n+1} = n_{dg}^{n} + \sum_{i=1}^{n+1} \Delta n_{eq}^{i} (\alpha_{eg}^{i,n+1} - \alpha_{eg}^{i,n}), \tag{5-34}$$

whichever is smaller.

5.3.5 Estimation of the Moles of Other Components and the Mole Fractions of Foamy Oil Phase

The total number of moles of dead oil at the time of interest, t^{n+1}, is

$$n_{do}^{n+1} = 1 - \frac{1}{K'(p_n)} = \left[1 - n_{eq}^{n+1}(p^{n+1})\right] \cdot \left[1 - \frac{1}{K'(p^{n+1})}\right]. \tag{5-35}$$

Since the evolved gas is composed of free gas and dispersed gas, according to Eq. 5-26, the total number of moles of free gas at t^{n+1} is

$$n_{fg}^{n+1} = \sum_{i=1}^{n+1} \sum_{j=i}^{n+1} \Delta n_{eg}^{i,j} (1 - \alpha_{dg}^{j}), \tag{5-36}$$

or more generally,

$$n_{fg}^{n+1} = \sum_{i=1}^{n+1} n_{eg}^{i,n+1} - n_{dg}^{n+1}. \tag{5-37}$$

The total number of moles of solution gas at t^{n+1} is

$$n_{sg}^{n+1} = \frac{[1 - n_{eq}^{n+1}(p^{n+1})]}{K'(p^{n+1})} + \sum_{i=1}^{n+1} \left[\Delta n_{eq}^{i} - n_{eg}^{i,n+1}\right]. \tag{5-38}$$

Note that the solution gas component comprises two parts. The first part is from thermodynamic equilibrium, and the second part is from non-equilibrium which may be either positive or negative. Thus the free gas is allowed to be redissolved into the oil phase when the reservoir pressure goes up.

The total number of moles of the foamy oil phase is

$$n_{fo}^{n+1} = n_{do}^{n+1} + n_{sg}^{n+1} + n_{dg}^{n+1} = \left(1-n_{eq}^{n+1}\right) + \sum_{i=1}^{n+1}\left(\Delta n_{eq}^{i} - n_{eg}^{i,n+1}\right) + n_{dg}^{n+1}. \qquad (5\text{-}39)$$

Then the normalized molar fractions are

$$x_{do}^{n+1} = \frac{1 - 1/K'(p_n)}{\left(1-n_{eq}^{n+1}\right) + \sum_{i=1}^{n+1}\left(\Delta n_{eq}^{i} - n_{eg}^{i,n+1}\right) + n_{dg}^{n+1}}, \qquad (5\text{-}40)$$

$$x_{sg}^{n+1} = \frac{(1-n_{eq}^{n+1})/K'(p^{n+1}) + \sum_{i=1}^{n+1}\left(\Delta n_{eq}^{i} - n_{eg}^{i,n+1}\right)}{\left(1-n_{eq}^{n+1}\right) + \sum_{i=1}^{n+1}\left(\Delta n_{eq}^{i} - n_{eg}^{i,n+1}\right) + n_{dg}^{n+1}}; \qquad (5\text{-}41)$$

$$x_{dg}^{n+1} = \frac{n_{dg}^{n+1}}{\left(1-n_{eq}^{n+1}\right) + \sum_{i=1}^{n+1}\left(\Delta n_{eq}^{i} - n_{eg}^{i,n+1}\right) + n_{dg}^{n+1}}. \qquad (5\text{-}42)$$

5.3.6 Formulation of the Model by Volumetric Quantities

The proposed model has been formulated using molar quantities. In some circumstances, it is difficult to obtain these quantities. Alternatively, the model may also be formulated using volumetric quantities which can be obtained more conveniently from standard PVT measurements.

5.3.6.1 Modification of Gas Solubility

Similar to the K value, the solution gas/oil ratio, R_s, obtained from standard PVT data is modified to R_s' as follows:

$$R_s'(p) = R_s(p) \qquad (p > p_b), \tag{5-43}$$

$$R_s'(p) = R_s(p_b) \qquad (p_n \leq p \leq p_b), \tag{5-44}$$

$$R_s'(p) = R_s(p) + \frac{R_s(p_b) - R_s(p_n)}{p_n - p_{sc}} \cdot \left[p - p_{sc}\right] \quad (p_{sc} \leq p < p_n). \tag{5-45}$$

5.3.6.2 Estimation of Evolved Gas Volume

For *one unit volume of dead oil* at standard conditions, the volume of gas flashed at standard conditions, ΔV_{eq}^i, due to a step drop in pressure from p^{i-1} to p^i, at thermodynamic equilibrium is

$$\Delta V_{eq}^i = \left[R_s'(p^i) - R_s'(p^{i-1})\right]. \tag{5-46}$$

For the gas ΔV_{eq}^i flashed due to this pressure change, the evolved gas volume $V_{eg}^{i,j}$ at standard conditions and by time t^j $(j \geq i)$ is

$$V_{eg}^{i,j} = \Delta V_{eq}^i \, \alpha_{eg}^{i,j}, \tag{5-47}$$

where $\alpha_{eg}^{i,j}$ was defined in Eq. 5-15.

From t^{j-1} to t^j, the volume increase of evolved gas is

$$\Delta V_{eg}^{i,j} = V_{eg}^{i,j} - V_{eg}^{i,j-1} = \Delta V_{eq}^{i} \, (\alpha_{eg}^{i,j} - \alpha_{eg}^{i,j-1}). \tag{5-48}$$

From the pressure drop step from p^{i-1} to p^{i}, the volume of evolved gas at standard conditions until t^{n+1} is

$$V_{eg}^{i,n+1} = \sum_{j=i}^{n+1} \Delta V_{eg}^{i,j}. \tag{5-49}$$

The total volume of evolved gas at t^{n+1} is

$$V_{eg}^{n+1} = \left[\sum_{i=1}^{n+1} V_{eg}^{i,n+1} \right] B_g(p^{n+1}), \tag{5-50}$$

where B_g is the gas volume factor.

5.3.6.3 Estimation of the Volume of Dispersed Gas

The dispersed gas volume from the gas volume $\Delta V_{eg}^{i,j}$ evolved between t^{j-1} and t^{j}, at standard conditions, is $\Delta V_{eg}^{i,j} \cdot \alpha_{dg}^{j}$. Then the dispersed gas volume ΔV_{dg}^{i} resulting from the pressure drop $\Delta p^{i} = p^{i} - p^{i-1}$ is

$$\Delta V_{dg}^{i}(p^{n+1}, t^{n+1}) = \left[\sum_{j=i}^{n+1} \Delta V_{eg}^{i,j} \cdot \alpha_{dg}^{j} \right] \cdot B_g(p^{n+1}), \tag{5-51}$$

where α_{dg}^{j} was defined in Eq. 5-22.

The total volume of dispersed gas by the time of interest, t^{n+1}, is

$$V_{dg}^{n+1}(p^{n+1}, t^{n+1}) = \left[\sum_{i=1}^{n+1} \sum_{j=i}^{n+1} \Delta V_{eg}^{i,j} \cdot \alpha_{dg}^{j} \right] \cdot B_g(p^{n+1}). \tag{5-52}$$

When the calculated f_{dg}^{n+1} is greater than f_{max}, V_{dg}^{n+1} is adjusted so that the following condition is satisfied:

$$V_{dg}^{n+1} = f_{max}\,(V_{dg}^{n+1} + V_{sg}^{n+1} + V_{do}^{n+1}), \tag{5-53}$$

that is,

$$V_{dg}^{n+1} = \frac{f_{max}\,(V_{sg}^{n+1} + V_{do}^{n+1})}{(1 - f_{max})}. \tag{5-54}$$

When the calculated $f_{dg}{}^{n+1}$ is less than f_{min}, $V_{dg}{}^{n+1}$ should be

$$V_{dg}^{n+1} = \frac{f_{min}(V_{sg}^{n+1} + V_{do}^{n+1})}{(1 - f_{min})}. \tag{5-55}$$

or

$$\begin{aligned} V_{dg}^{n+1} &= \left[V_{dg}^{n}/B_g(p^{n}) + \sum_{i=1}^{n+1} \Delta V_{eg}^{i,n+1} \right] B_g(p^{n+1}) \\ &= \left[V_{dg}^{n}/B_g(p^{n}) + \sum_{i=1}^{n+1} \Delta V_{eq}^{i}(\alpha_{eg}^{i,n+1} - \alpha_{eg}^{i,n}) \right] B_g(p^{n+1}), \end{aligned} \tag{5-56}$$

whichever is smaller.

5.3.6.4 *Estimation of the Volumes of Free Gas, Solution Gas and Dead Oil*

The total volume of free gas at the time of interest, t^{n+1}, is

$$V_{fg}^{n+1}(p^{n+1}, t^{n+1}) = \left[\sum_{i=1}^{n+1} \sum_{j=i}^{n+1} \Delta V_{eg}^{i,j}(1 - \alpha_{dg}{}^{j}) \right] \cdot B_g(p^{n+1}), \tag{5-57}$$

or more generally,

$$V_{fg}^{n+1}(p^{n+1}, t^{n+1}) = \left[\sum_{i=1}^{n+1} V_{sg}^{i,\, n+1}\right] \cdot B_g(p^{n+1}) - V_{dg}^{n+1}. \tag{5-58}$$

The total volume of solution gas at time t^{n+1} is

$$V_{sg}^{n+1}(p^{n+1}, t^{n+1}, T) = \left[R_s'(p^{n+1}) + \sum_{i=1}^{n+1}(\Delta V_{sg}^{i} - V_{sg}^{i,\, n+1})\right] \times$$
$$(\rho_{g,sc}/\rho_{sg,sc}) \times [1 - c_{sg}(p^{n+1} - p_{sc})] \times [(1 + \beta_{sg}(T - T_{sc})], \tag{5-59}$$

where $\rho_{g,sc}$ and $\rho_{sg,sc}$ are the densities of the free gas component and the liquid solution gas component at standard conditions, respectively.

The volume of dead oil at t^{n+1} is

$$V_{do}^{n+1}(p^{n+1}, T) = [1 - c_{do}(p^{n+1} - p_{sc})]\ [1 + \beta_{do}(T - T_{sc})]. \tag{5-60}$$

5.4 Verification of the Basic Model

Before presenting a comparison between the calculated results and the experimental data, a justification of the assumed functional forms for the growth of evolved gas and the decay of dispersed gas by experimental data is presented in the following.

5.4.1 Justification of Power-Law Bubble Growth

The bubble growth in porous media at isothermal conditions under solution gas drive is believed to be controlled mainly by diffusion (Firoozabadi and Kashchiev, 1993).

As noted earlier, for a constant supersaturation, ΔC_s, if the bubble growth is controlled by diffusion, the bubble radius, r_b, is proportional to the square root of time, t. However, because of the complexity of real reservoirs, the relationship between $r_b(t)$ and t for diffusion controlled bubble growth may not be applied directly. Kashchiev and Firoozabadi (1993) stated that different regimes of growth result in different $r_b(t)$ dependencies which, in general, are rather complicated. However, at constant supersaturation many of these dependencies show exact or approximate proportionality of r_b to some power of t. They stated that this finding was supported also by available experimental $r_b(t)$ data.

According to Li and Yortsos's (1993) study, for a single bubble cluster, the radius of the bubble increases according to a power function of t. For multiple clusters, gas saturation and t have a more complex power function.

Therefore, for a constant pressure drop, as an approximation, it appears reasonable to suppose that the total amount of gas formed, $n_{eg}(t)$, is proportional to some power of t:

$$n_{eg}(t) = at^{b}, \tag{5-61}$$

where the coefficient, a, and bubble growth index, b, can be found by fitting the experimental data or by history matching the field production data. For diffusion-controlled bubble growth, b is 3/2 for constant supersaturation and 3 when the supersaturation increases linearly and slowly. If bubble growth is controlled only by the inertia of the liquid, b will be 3 for constant supersaturation and 9/2 for linearly increasing supersaturation (Kashchiev and Firoozabadi, 1993).

The mass-transfer flux stops when equilibrium is established between the bulk fluid and the interface, so it is reasonable to employ a potential which is proportional to the distance from equilibrium (Sherwood *et al.*, 1975). If equilibrium is assumed at the gas/oil interface, the amount of supersaturated solution gas is chosen for that potential. Although, theoretically, the approach to equilibrium may be asymptotic, for all practical purposes the equilibrium is reached in a finite time. If it takes t_{eq} time for the supersaturated solution gas, n_{eq}, to evolve from the supersaturated oil, at time $t \leq t_{eq}$, the amount of evolved gas can be estimated by Eq. 5-5:

$$n_{eg}(t) = n_{eq}\left[\frac{t}{t_{eq}}\right]^{b}. \qquad (5\text{-}5)$$

By adjusting t_{eq} and b to history match the field performance, one may be able to account for non-equilibrium phenomena under a heavy oil solution gas drive.

To verify the proposed power function relationship, Kortekaas and van Poelgeest's (1991) experimental data were used. Their experiments were carried out on a 550-md core saturated with connate water and C_1-C_3 mixtures. The gas saturation in the core was measured. Since the pressure declines linearly, the variable t can be replaced by the pressure p. After some manipulation, the final form is

$$S_g = a'\left(1-\frac{p}{p_b}\right)^{b}. \qquad (5\text{-}62)$$

Figure 5.3 shows their experimental data and the fitted curves. The point where the gas saturation data start to deviate from the curves is explained by the flow of gas out of the core. Beyond this point, it is not known how much gas was actually produced.

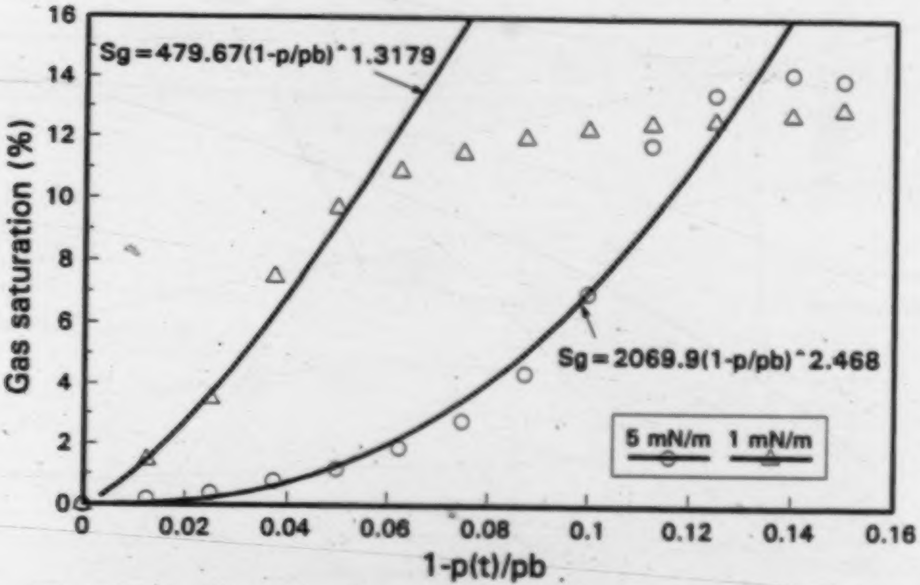

Fig. 5.3 - Measured non-equilibrium gas saturation.

Before the gas begins to flow out of the core, Figure 5.3 indicates that the gas saturations, and hence the amount of evolved gas, do follow a power function model.

5.4.2 Justification of Exponential Decay

It has been proposed in Section 5.3.4 that the amount of dispersed gas due to the pressure drop from p^{i-1} to p^{i} at time t^{n+1} is

$$\Delta n_{dg}^{i}(t^{n+1}) = \sum_{j=i}^{n+1} \Delta n_{dg}^{i,j} \cdot \alpha_{dg}^{j}. \tag{5-25}$$

By substituting the previously defined terms, the above equation can be expressed as

$$\begin{aligned}\Delta n_{dg}^{i}(t^{n+1}) = {} & \Delta n_{dg}^{i}(t^{n})\exp\left(-\lambda_{dg}(t^{n+1}-t^{n})\right) + \\ & \left(n_{eg}^{i,\,n+1}-n_{eg}^{i,\,n}\right)\exp\left[-\lambda_{dg}\left(\frac{t^{n+1}-t^{n}}{2}\right)\right]\end{aligned} \tag{5-63}$$

This equation shows that the total amount of dispersed gas decays exponentially. Such an exponential decay can be justified by analogy to aqueous foams and other areas as discussed earlier in Section 5.2.3.

Figure 5.4 presents a set of experimental data for a typical foamy oil test. The schematic diagram for the equipment used in the test is shown in Figure 4.1 of Chapter 4. The foamy oil volumes at different times were measured after the pressure was reduced suddenly from 700 psig (4927 kPa) to 350 psig (2415 kPa), the pressure was then maintained at 350 psig by a back pressure regulator. Lindbergh crude oil was used in the experiment. The initial live oil volume was 20 cm^3. Figure 5.4 shows that after the gas evolution has subsided (corresponding to the maximum volume point), the estimated volumes of dispersed gas bubbles at different times fall on the same straight line on the semilog plot which is an exponential function. Since the pressure during this part of the test is constant at 350 psig, volume is equivalent to mass or the number of moles. Therefore, the proposed exponential function may be appropriate to describe the decay of dispersed gas.

Since it is very difficult to measure the gas volume dispersed in the liquid oil phase within a porous medium, the exponential decay is justified using the experimental data from a bulk vessel. Although these data were obtained from the bulk liquid, the exponential function may be appropriate to describe the decay of dispersed gas in flow through porous media according to the literature. From their observed relationship

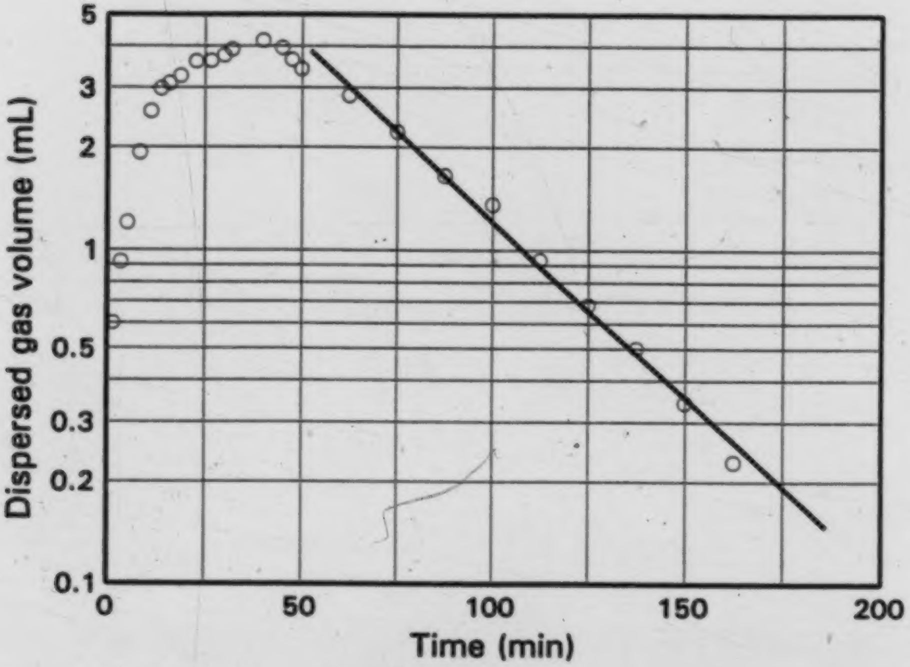

Fig. 5.4 - Lab data for the volume of dispersed bubbles.

between stability and mobility reduction factor, Maini and Ma (Sept. 1984) suggested that the same types of surface forces control the rheological properties of foam in a porous medium and the foam stability characteristics outside the porous medium. Therefore, it is believed that the exponential decay may also be applied to porous media. However, the decay coefficient in porous media could be different from that in the bulk vessel.

5.4.3 Matching the Experimental Results

The proposed basic model to calculate foamy oil properties is to be verified by comparing the calculated foamy oil volumes with the experimental data. Medicine Hat crude oil was used in the experiment. The crude oil was saturated with methane at a pressure of 700 psig (4927 kPa), and transferred to a high pressure cell equipped with a glass window and height graduations. The pressure was reduced linearly to 350 psig (2515 kPa) within 16 min (960 s), and this lower pressure was maintained afterwards. The initial live oil volume was 20 cm^3. By reading the heights of foamy oil at different times, the foamy oil volumes were recorded. The experimental apparatus is the same as shown in Figure 4.1. The conventional PVT data and the molar properties of the oil are shown in Table 5.2. The *K* values were calculated from the solution GOR, molar masses and densities of the oil and methane components, using the method described by Sheng and Zhou (1995). The resulting formula to calculate the K values for this system is

$$K = \left(\frac{3.5\times10^5}{p} + 6\times10^{-3}\cdot p \right) \cdot \exp\left(\frac{-879.84}{T-7.16} \right), \qquad (5\text{-}64)$$

where the units for *p* and *T* are Pa and K, respectively.

To match the experimental volume data, the equilibrium time, t_{eq}, the gas bubble growth index, *b*, and the decay coefficient for dispersed gas decay, λ_{sc}, were adjusted. Their adjusted values are 25 min (1500 s), 1.0 and 0.02375 s^{-1}, respectively. The nucleation threshold pressure was assumed to be 681.6 psig (4800 kPa), or, the critical supersaturation was about 18.4 psi (127 kPa). The other parameters used in matching the experimental data of foamy oil volume are shown in Table 5.2. The calculated volumes and the experimental data are compared in Figure 5.5, which shows that they are well matched.

Table 5.2 - Data Used in Matching Experimental Data

Gas bubble growth index, dimensionless	1.0
Decay coefficient λ_{se}, s^{-1}	0.02375
Initial pressure, kPa	4927.0
Nucleation threshold pressure, kPa	4800.0
Room temperature, °C	22.0
Equilibrium time, s	1500.0
Solution GOR at 4927 kPa, m^3/m^3	16.94
Oil density at standard conditions, kg/m^3	948.0
Oil molecular mass, kg/kmole	395.0
Dead oil compressibility, Pa^{-1}	1.0×10^{-9}
Solution gas liquid compressibility, Pa^{-1}	7.0×10^{-9}
Dead oil thermal expansion coefficient, $°C^{-1}$	8.89×10^{-4}
Solution gas thermal expansion coefficient, $°C^{-1}$	8.89×10^{-4}
Molar specific volume of dead oil, $m^3/(kmole)$	0.417
Molar specific volume of solution gas, $m^3/(kmole)$	0.0535
Initial live oil volume, m^3	20.0×10^{-6}
Time step size, s	60.0

5.5 Calculation Results and Sensitivity Study

Calculated results of the mole fractions, using the adjusted parameters listed above and the data of the oil sample, are shown in Figure 5.6. Figure 5.6 shows the fractions of the dead oil component, the solution gas component and the dispersed gas component in the foamy oil phase. Before the equilibrium time, as more gas is evolved from the

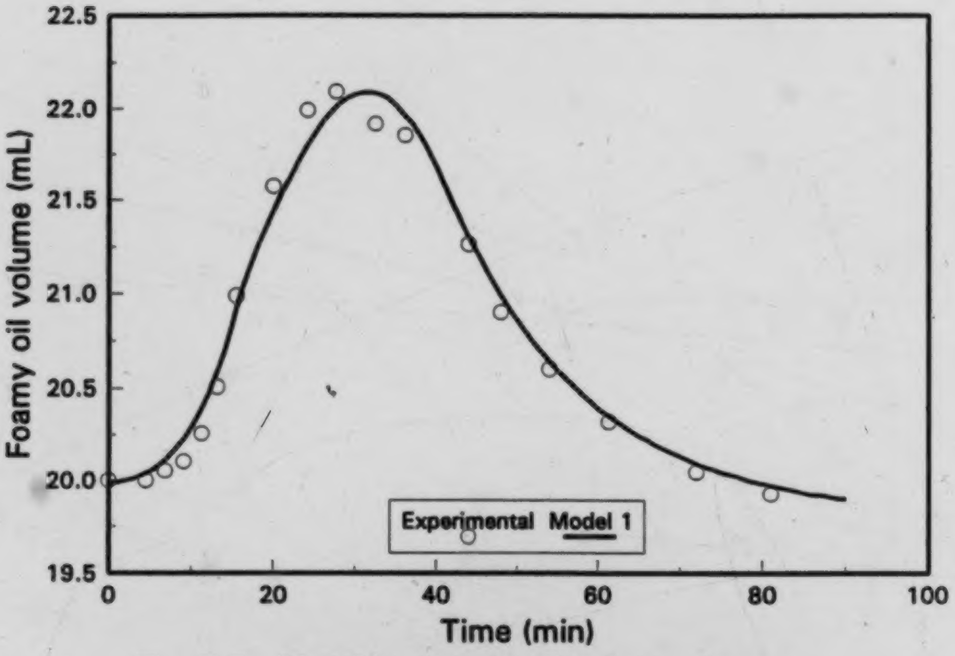

Fig. 5.5 - Matching foamy oil volume change.

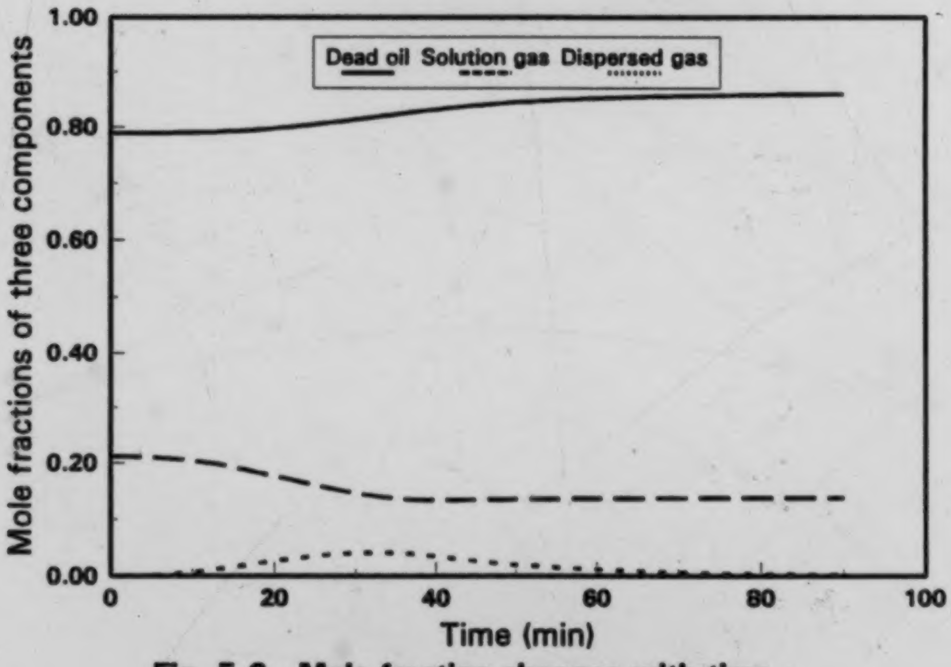

Fig. 5.6 - Mole fraction changes with time.

solution state, more gas is dispersed in the foamy oil, and thus the molar fraction of the dispersed gas component increases with time. In the later period, the dispersed gas fraction decreases as it disengages from the foamy oil to become free gas. The fraction of solution gas component decreases as more gas is evolved from the solution. Correspondingly, the fraction of the dead oil component increases in the beginning and stabilizes later on.

In the model the main parameters to be adjusted are the equilibrium time, t_{eq}, bubble growth index, b, and decay coefficient for dispersed gas decay, λ_{sc}. The data set matching the experimental data is the base case. By increasing or decreasing the individual parameters by a factor of 2, their effects on the foamy oil volume changes are investigated. Figure 5.7 shows the effect of equilibrium time. It shows that the curves for the foamy oil volume shift to the right, and the maximum volume becomes less, as t_{eq} increases. It seems that the effect of b, another parameter to control bubble growth, is less sensitive than t_{eq}, as shown in Figure 5.8. Figure 5.9 shows the effect of the decay coefficient. It shows that the curve of foamy oil volume with lower λ_{sc} stands above that with larger λ_{sc}. It also shows that initially the rate of growth is much faster than the rate of decay, and the effect of decay is not important in this period of time which is consistent with Firoozabadi and Kashchiev's (1993) argument (Section 5.2.3). Figures 5.7 to 5.9 suggest that the most sensitive parameter which affects the foamy oil behaviour is the decay coefficient for dispersed gas decay, λ_{sc}.

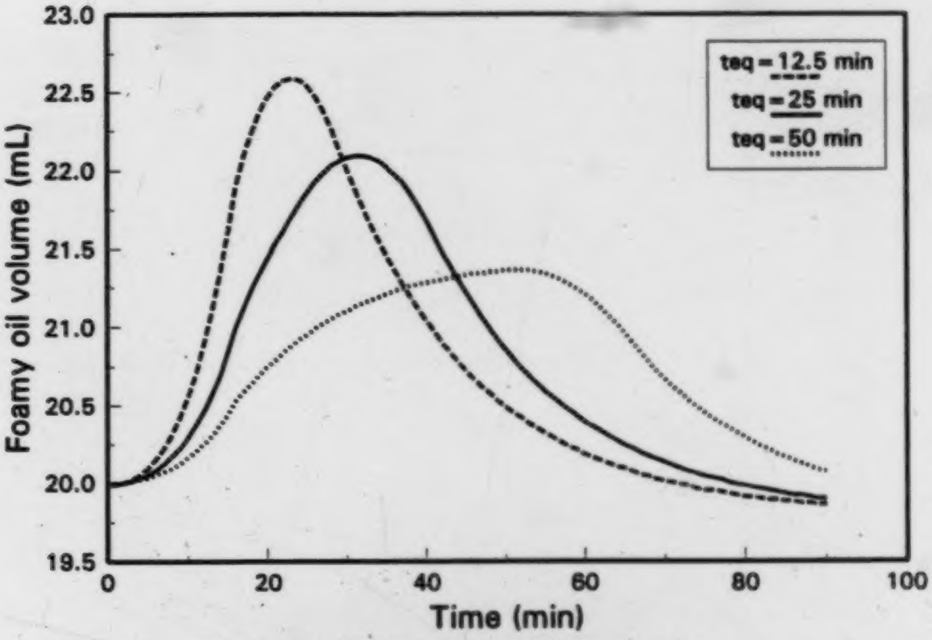

Fig. 5.7 - Effect of equilibrium time.

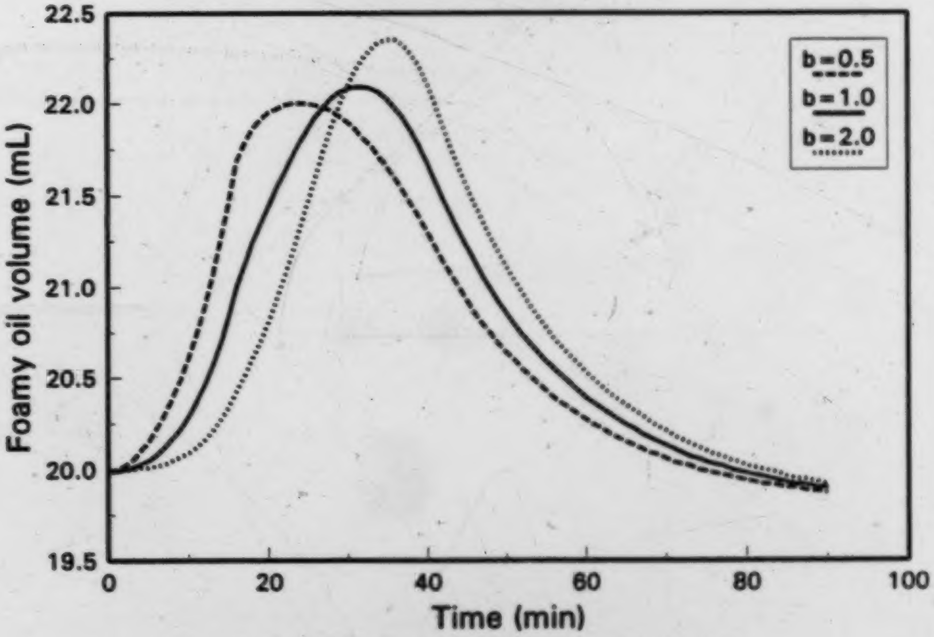

Fig. 5.8 - Effect of bubble growth index.

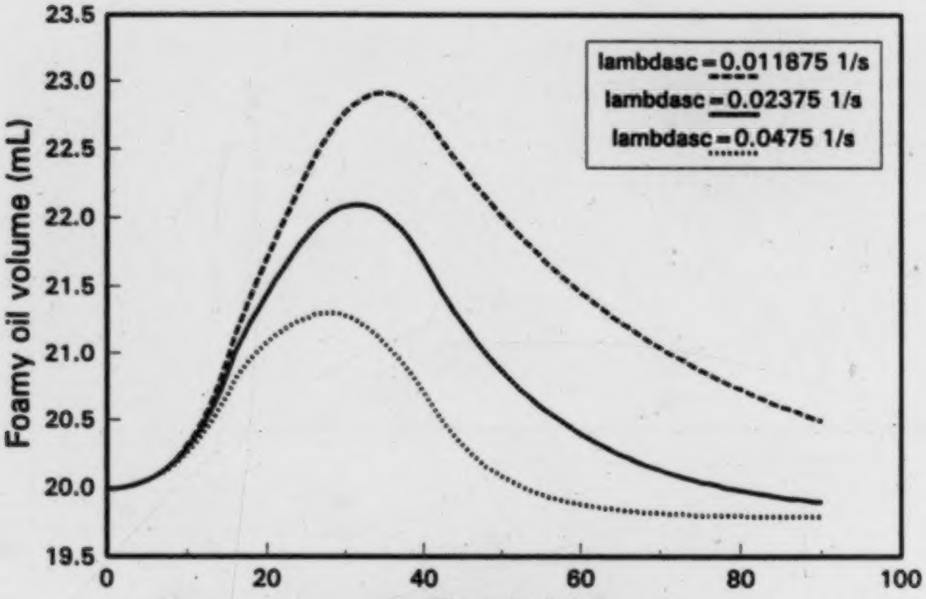

Fig. 5.9 - Effect of decay coefficient.

5.6 Other Models

One characteristic of a bubble is the bubble age or bubble history which is the period of time from the time of its formation to the time of interest. Because of the dynamic behaviour, the rates of bubble growth and decay vary with age. The proposed model (Model 1) is theoretically sound in that it takes bubble history into account. In that model, a static oil sample is considered. For one pressure drop, each element of the whole sample has the same time of nucleation or bubble age. It is straightforward to consider the property change of the whole sample caused by this pressure drop. And the principle of superposition is used to include the effects of many pressure drop steps. It is possible, at least in principle, to apply directly the methodology into a flow model. However, due to the movement of supersaturated oils through blocks in a numerical simulation model, each block consists of different oils coming from the rest of the blocks. These oils have different ages and different degrees of supersaturation. To include these time-dependent properties of the different oils in a flow model, a great amount of history data for these oils has to be stored. It also causes formulation difficulty in a simulation model. Therefore, the methodology presented in Model 1 needs to be modified. It is desirable that the information at the last time step instead of history data is used to estimate the fluid properties at the present time step. The following two models are proposed accordingly.

5.6.1 Power-Law Bubble Growth (Model 2)

The mechanism of bubble growth is that the solution gas component in the supersaturated oil diffuses into the activated nuclei (embryos) causing them to grow. As a result, the supersaturation is reduced. Model 1 suggests that the amount of solution gas transferred to the evolved gas is proportional to the amount of supersaturated solution gas and to some power of the growth time or bubble age. Based on this concept, it was proposed (Sheng *et al.*, 1996) that the mass of gas evolved from solution from t^n to t^n+1 is

$$\Delta n_{sg \to eg}^{n+1} = \Delta n_s \left[\frac{\Delta t/2}{t_{eq}} \right]^b, \tag{5-65}$$

where Δn_s is the supersaturation expressed in moles of supersaturated solution gas in the oil phase at time t^n referred to the equilibrium state at t^{n+1}. Here a power-law bubble growth is assumed. Then at t^{n+1}, the remaining solution gas in the oil is

$$n_{sg}^{n+1} = n_{sg}^{n} - \Delta n_{sg \to eg}^{n+1}. \tag{5-66}$$

The evolved gas is initially entrained in the oil phase as dispersed gas bubbles. The dispersed gas coalesces to become free gas. Similar to Model 1, exponential decay is assumed. Then the dispersed gas at t^{n+1} is

$$n_{dg}^{n+1} = n_{dg}^{n} \exp(-\lambda_{dg}\Delta t) + \Delta n_{sg \to eg}^{n+1} \exp(-\lambda_{dg}\Delta t/2). \tag{5-67}$$

The evolved gas in the free gas state is

$$n_{fg}^{n+1} = n_{fg}^{n} + n_{dg}^{n} \left[1 - \exp(-\lambda_{dg}\Delta t)\right] + \Delta n_{sg \to eg}^{n+1} \left[1 - \exp(-\lambda_{dg}\Delta t/2)\right]. \tag{5-68}$$

The amount of dead oil remains unchanged during pressure decline. If the initial saturated oil is one kmole, the amount of dead oil is always

$$n_{do} = 1 - \frac{1}{K'(p_n)}. \tag{5-69}$$

5.6.2 Exponential Bubble Growth (Model 3)

If supersaturation is assumed to decay exponentially, the mass of gas evolved from solution from t^n to t^{n+1} could also be an exponential function as follows:

$$\Delta n_{sg \to eg}^{n+1} = \Delta n_s \left[1 - \exp(-\lambda_s \Delta t/2\right], \tag{5-70}$$

where λ_s is the rate coefficient for the decay of supersaturation. The rest of the formulation follows Model 2.

5.6.3 Justification of Model 2 and Model 3

For bubble growth controlled by diffusion, the radius of a bubble can be predicted from (Moulu,1989):

$$r_b = \left[\frac{2DRT[\Delta C_s]t}{p} \right]^{1/2}, \qquad (5\text{-}71)$$

where ΔC_s is the supersaturation expressed as a difference in concentration. In Model 1, the effect of each pressure drop is considered independently. For one small pressure drop $\Delta p = p(t^n) - p(t^{n+1})$, p and ΔC_s could be considered to be constant in the above expression. Then the radius is proportional to the square root of growth time or bubble age, t. Then the volume or amount of evolved gas could also be described by a power-law function of time, which was proposed in Model 1.

However, as mentioned earlier, it is difficult to consider the effect of each pressure drop independently. It is desirable to estimate the properties of a lumped fluid at a grid block at t^{n+1} from its overall properties at t^n. To do that, let us consider the increase of evolved gas from t^n to t^{n+1}. The differential form of the above equation is

$$\frac{dr_b}{dt} = \frac{DRT[\Delta C_s(t)]}{p r_b(t)}. \qquad (5\text{-}72)$$

The volume increase of evolved gas from t^n to t^{n+1} is

$$\frac{dV_{eg}(t)}{dt} = \frac{4\pi r_b^2 dr_b}{dt} = \frac{4\pi DRT[\Delta C_s(t)]r_b(t^n)}{p}, \tag{5-73}$$

where $t^n < t < t^{n+1}$. The corresponding mass increase is

$$\frac{dn_{eg}(t)}{dt} = \frac{dV_{eg}(t)}{dt}\left[\frac{p}{RT}\right] = 4\pi Dr_b(t^n)[\Delta C_s(t)], \tag{5-74}$$

and the supersaturation decreases according to

$$\frac{d[\Delta n_s(t)]}{dt} = -\frac{dn_{eg}(t)}{dt} = -4\pi Dr_b(t^n)[\Delta C_s(t)] \propto -\Delta n_s(t). \tag{5-75}$$

The above relationship shows that the decreasing rate of supersaturation is proportional to the supersaturation. In other words, the supersaturation decays exponentially, which justifies Model 3.

If one further makes an approximation that the supersaturation remains unchanged from t^n to t^{n+1}, then from Eq. 5-74 one has

$$\Delta n_{eg} = 4\pi Dr_b[\Delta C_s][\Delta t] \propto [\Delta n_s][\Delta t]. \tag{5-76}$$

More generally, one has

$$\Delta n_{eg} \propto [\Delta n_s][\Delta t]^a, \tag{5-77}$$

which shows that gas evolves according to a power-law function of time. Therefore Model 2 is justified. Note that the supersaturation would be suddenly reduced to Δn_s-Δn_{eg} by the end of this time step, t^{n+1}.

5.6.4 Discussion of the Models

The above proposed three models can be divided into two categories. One category which is Model 1 takes bubble history into account. The other category including Model 2 and Model 3 uses the information at t^n to predict the foamy oil properties at t^{n+1}. For comparison, Model 2 and Model 3 were used to match the experiment which was well matched by Model 1 as presented in Section 5.4.3. The matching results are compared in Figure 5.10, which shows that the three models provided reasonably good matches with the experimental data. It also shows that Model 1 provided the best match. The adjusted values of parameters in Model 2 are: λ_{sc} = 0.022 s^{-1}, b = 0.9, and t_{eq} = 400 s. In Model 3, the adjusted λ_{sc} is the same as that in Model 2. The adjusted λ_s is 0.00341 s^{-1} which satisfies the following relation between Model 2 and Model 3:

$$\left[\frac{\Delta t/2}{t_{eq}}\right]^{b}_{Model\ 2} = \left[1 - \exp(-\lambda_s \Delta t/2)\right]_{Model\ 3} , \tag{5-78}$$

since the evolved gas estimated from the two models should be same.

In all the three models, a discretisation in time has to be employed. It is of interest to investigate the model performance by studying the effect of time step size. Figures 5.11 through 5.13 show the effect of the time step on the calculated foamy oil volume in Model 1, Model 2 and Model 3, respectively. The data of the base case for each model are from the data set used to match the experiment, in which the time step size was 60 s. Then time step sizes of 12 s and 300 s were tested in each model. The comparison of these results shows that Model 1 is the most stable one; and Model

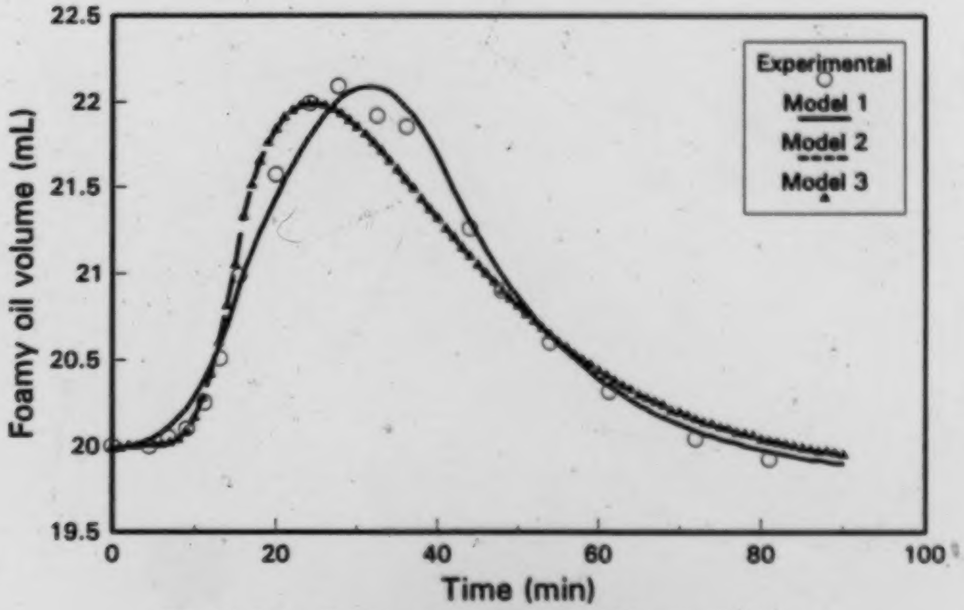

Fig. 5.10 - Comparing the matching results from three models.

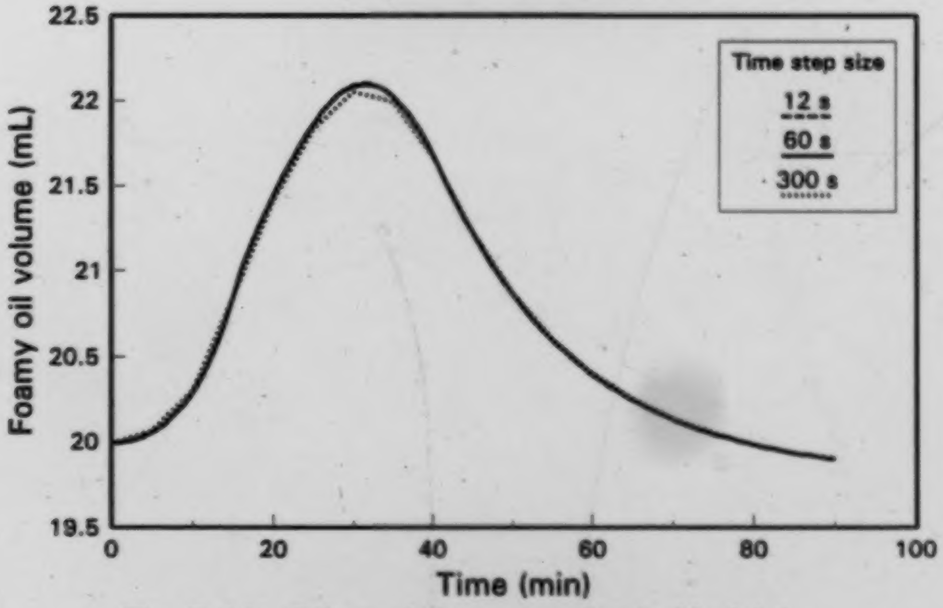

Fig. 5.11 - Effect of time step size in Model 1.

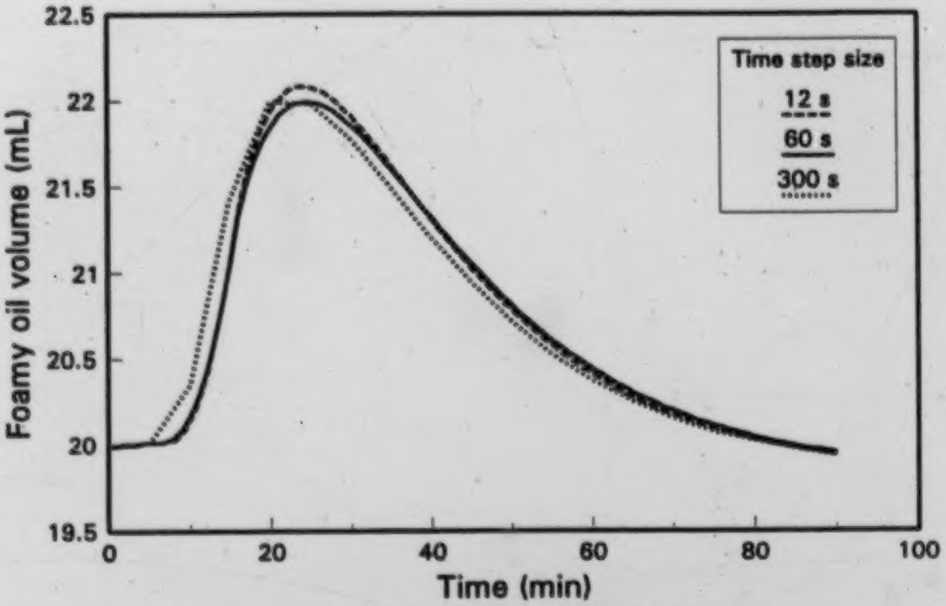

Fig. 5.12 - Effect of time step size in Model 2.

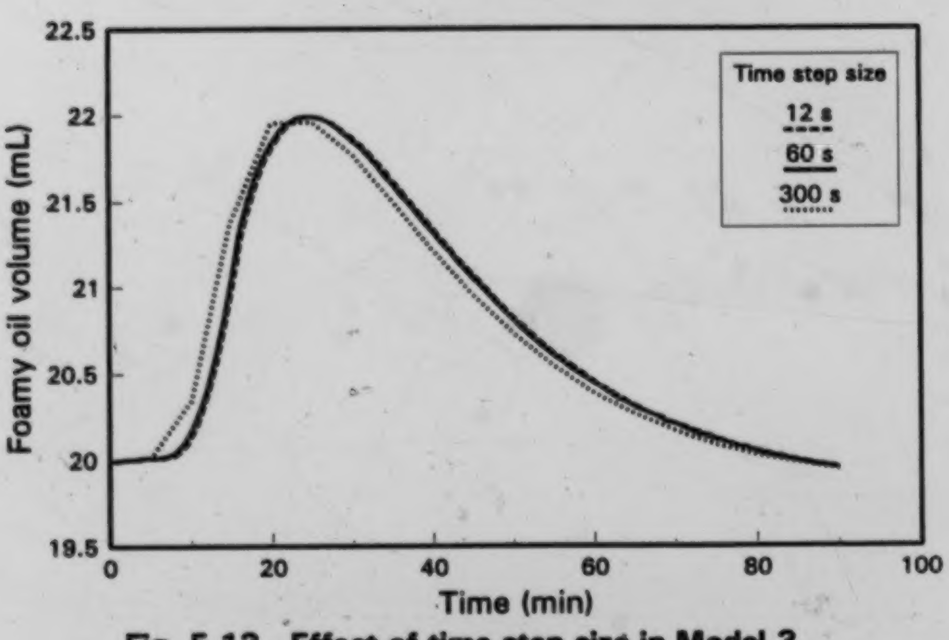

Fig. 5.13 - Effect of time step size in Model 3.

3 is more stable than Model 2.

5.7 Concluding Remarks

The main objective of this chapter was to develop a methodology to describe the dynamic processes of foamy oils when the pressure is reduced below the saturation pressure. It is believed that the rate processes involved in nucleation, growth and coalescence of gas bubbles and also in the dispersion and separation of gas bubbles from the liquid phase play important roles in the cold production of foamy heavy oils. However, perhaps due to the limitations of available reservoir simulation programs, most of the previous studies have neglected the role of dynamic processes and assigned time independent properties to foamy oils. It has been attempted to include the time effects in calculations of foamy oil properties in the models presented in this chapter.

The mechanisms of solution gas drive in heavy oil reservoirs are complex, and foamy heavy oil flow through porous media is far from fully understood. As our understanding improves, it may be necessary to consider the effects of compositions of heavy oils. Therefore, the foamy oil properties are formulated using molar quantities in Model 1. However, in some cases, the molar quantities may not be easily obtained. Formulation based on volumetric quantities is also provided.

Model 1 has taken the bubble history into account. Theoretically, it has properly considered the features of the dynamic processes. It has been shown that Model 1 is the most stable model by comparing its results with those of Model 2 and Model 3 which do not include bubble history. However, due to the difficulty met in including bubble history in a flow model, it may not be practical to implement Model 1 into a flow model. Therefore, Model 2 and Model 3 were also proposed.

Model 2 and Model 3 are the same in principle. By justifying and comparing the stability of the two models, it seems that Model 3 is the best model to be implemented into a practical reservoir simulator.

The models have been tested against experimental data obtained with bulk samples of foamy oil, i.e. under conditions not involving two-phase flow through porous media. From the discussions earlier, it was expected that these models could be applied *mutatis mutandis* to foamy oil performance in reservoirs. Model 2 was used in a foamy oil flow model to successfully history match the primary depletion tests in the laboratory (Sheng *et al.*, 1996). Similarly, Model 3 is included in the flow model to match the same depletion tests in the next chapter. Therefore, it can be concluded that these models, especially Model 1, provide the fundamentals for calculating foamy oil properties.

5.8 References

Abgrall, E. and Iffly, R.: "Physical Study of Flow by Expansion of Dissolved Gas," *Revue de L'Institut Français du Pétrole* (Sept. - Oct. 1973) **28**, No. 5, 667-92 (French).

Aldea, Gh.: "Mechanism of Heavy Oil Recovery by Dissolved Gas Expansion," *Revue de L'Institut Français du Pétrole* (Dec. 1970) **25**, No. 12, 1403-17 (French).

Atchley, A.A. and Prosperetti, A.: "The Crevice Model of Bubble Nucleation," *Journal of Acoustical Society of America* (*J. Acoust. Soc. Am.*) (Sept. 1989) **86**, No. 3, 1065-84.

Bernath, L: "Theory of bubble Formation in Liquids," *Ind. Eng. Chem.*) (June 1952) 1310-13.

Bikerman, J.J.: *Foams*, Springer-Verlag New York Inc., New York (1973) 90, 94, 232.

Brady, A.P. and Ross, S.: "The Measurement of Foam Stability," *J. Am. Chem. Soc.* (1944) **66**, 1348-56.

Callaghan, I.C. and Neustadter, E.L.: "Foaming of Crude Oils: a Study of Non-Aqueous Foam Stability," *Chemistry and Industry* (Jan. 1981) **17**, 53-57.

Chatnever, A., Indra, M.K. and Kyte, J.R.: "Microscopic Observations of Solution Gas Drive Behavior," *JPT* (June 1959) 13-15.

Claridge, E.L. and Prats, M.: "A Proposed Model and Mechanism for Anomalous Foamy Heavy Oil Behaviour," paper SPE 29243 presented at the International Heavy Oil Symposium, Calgary, AB, June 19-21, 1995; *Proc.*, 9-20; also paper SPE 29243 (USMS, 1994).

Clark, N.O.: "A Study of Mechanically Produced Foam for Combating Petro Fires," D.S.I.R., Chemistry Research, Special Report No. 6, H.M.S.C. London, 1947.

Cole, R.: "Boiling Nucleation," *Advances in Heat Transfer*, Hartnett, J.P. and Irvine, Jr., T.F., Ed., Academic Press, New York (1974) **10**, 86-166.

Cooper, M.G., Mori, K. and Stone,C.R.: "Behaviour of Vapour Bubbles Growing at a Wall with Forced Flow," *International Journal of Heat and Mass Transfer* (*Int. J. Heat Mass Transfer*) (1983) **26**, No. 10, 1489-1507.

Coskuner,G.: *Oil Field Emulsions*, PRI Report 1988-18 (Nov. 1988) 4-5.

Crum, L.A.: "Nucleation and Stabilization of Microbubbles in Liquids," *Applied Science Research* (*Appl. Sci. Res.*) (1982) **38**, 101-15.

Danesh, A., Peden, J.M., Krinis, D. and Henderson, G.D.: "Pore Level Visual Investigation of Oil Recovery by Solution Gas Drive and Gas Injection," paper SPE 16956 presented at the 62nd SPE Annual Technical Conference and Exhibition, Dallas, TX, Sept. 27-30, 1987.

de Vries, A.J.: "Foam Stability, Part I. Structure and Stability of Foams," *Rec. Trav. Chim.* (1958) **77**, 81-91 (English).

Dumore, J.M.: "Development of Gas Saturations During Solution-Gas-Drive in an Oil Layer Below a Gas Gap," *SPEJ* (Sept. 1970) 211-18.

El Yousfi, A., Zarcone, C., Bories, S. and Lenorman, R.: "Mechanisms of Solution Gas Liberation during Pressure Depletion in Porous Media," *Comptes Rendus deL' Académie des Sciences* (*C. R. Acad. Sci. Paris, t.*) **313,** Série II (1991), 1093-98 (French).

Epstein, P.S. and Plesset, M.S.: "On the Stability of Gas Bubbles in Liquid-Gas Solutions," *J. Chem. Phys.* (Nov. 1950) **18,** No. 11, 1505-09.

Ettinger, R.A. and Radke, C.: "Influence of Texture on Steady Foam Flow in Berea Sandstone," *SPERE* (Feb. 1992) 83-90.

Firoozabadi, A. and Kashchiev, D.: "Pressure and Volume Evolution During Gas Phase Formation in Solution Gas Drive Process," paper SPE 26286 (USMS, 1993).

Firoozabadi A., Mikkelson, M. and Ottesen, B.: "Reply to Discussion of Measurements of Supersaturation and Critical Gas Saturation," *SPEFE* (June 1994) 159-60.

Firoozabadi A., Ottesen, B. and Mikkelson, M.: "Measurements of Supersaturation and Critical Gas Saturation," *SPEFE* (Dec. 1992) 337-43.

Fisch, J.C., Hollomon, J.H., and Turnbull, D.: "Nucleation," *J. Appl. Phys.* (1948) **19,** 775-84.

Govier, G.W. and Aziz, K.: *The Flow of Complex Mixtures in Pipes,* Robert E. Krieger Publishing Company, Inc., Florida (1982) 3, 556.

Handy, L.L.: "A Laboratory Study of Oil Recovery by Solution Gas Drive," *Trans.* (1958), AIME, **213,** 310-15.

Hoyos, M., Moulu, J.C., Deflandre, F. and Lenormand, R.: "Untrasonic Measurements of the Bubble Nucleation Rate During Depletion Experiments in a Rock Sample," paper SPE 20525 presented at the 65th Annual Technical Conference and Exhibition of SPE of AIME, New Orleans, LA, Sept. 23-26, 1990.

Hunt Jr., E.B. and Berry Jr., V.J.: "Evolution of Gas from Liquid Flowing through Porous Media," *A.I.Ch.E Journal* (Dec. 1956) **2,** No. 4, 560-67.

Islam, M.R. and Chakma, A.: "Mechanics of Bubble Flow in Heavy Oil Reservoirs," paper SPE 20070 presented at the 60th California Regional Meeting, Ventura, CA, April 4-6, 1990.

Kamath, J. and Boyer, R.E.: "Critical Gas Saturation and Supersaturation in Low-Permeability rocks," paper SPE 26663 presented at the 68th Annual Technical Conference and Exhibition, Houston, TX, Oct. 3-6, 1993; also *SPEFE* (Dec. 1995) 10, No. 4, 247-53.

Kashchiev, D. and Firoozabadi, A.: "Kinetics of the Initial Stage of Isothermal Gas Phase Formation," *J. Chem. Phys.* (March 15, 1993) **98**, No. 6, 4690-99.

Kennedy, H.T. and Olson, R.: "Bubble Formation in Supersaturated Hydrocarbon Mixtures," *Trans.* (1952), AIME, **195**, 271-78.

Kortekaas, T.F.M. and van Poelgeest, F.: "Liberation of Solution Gas During Pressure Depletion of Virgin Watered-Out Oil Reservoirs," *SPERE* (Aug. 1991) 329-35.

Kovscek, A.R. and Radke, C.J.: "Fundamentals of Foam Transport in Porous Media," *Foams: Fundamentals and Applications in the Petroleum Industry, Advances in Chemistry Series* **242**, Schramm, L.L., Ed., American Chemical Society, Washington, DC (1994) 143.

Kraus, W.P., McCaffrey, W.J. and Boyd, G.W.: "Pseudo-Bubble Point Model for Foamy Oils," paper CIM 93-45 presented at the 44th Annual Technical Conference of the Petroleum Society of CIM, Calgary, AB, May 9-12, 1993.

Li, X.: *Bubble Growth During Pressure Depletion in Porous Media*, Ph.D dissertation, University of Southern California, Los Angeles, CA (May 1993) 106, 113-114.

Li, X. and Yortsos, Y.C.: "Visualization and Numerical Studies of Bubble Growth During Pressure Depletion," paper SPE 22589 presented at the 66th SPE Annual Technical Conference and Exhibition, Dallas, TX, Oct. 6-9, 1991.

Li, X. and Yortsos, Y.C.: "Critical Gas Saturation: Modeling and Sensitivity Studies," paper SPE 26662 presented at the 68th SPE Annual Technical Conference and Exhibition, Houston, TX, Oct. 3-6, 1993.

Madaoui, K.: "Critical Gas Saturation in Depletion Drive," *reports* of International Symposium on Hydrocarbon Exploration, Drilling and Production Techniques (Dec. 10-12, 1975) 203-20 (French).

Maini, B.B. and Ma, V.: "Laboratory Evaluation of Foaming Agents for High Temperature Applications - I. Measurements of Foam Stability at Elevated Temperatures and Pressures," paper 35-07 presented at the 35th Annual Technical Meeting of the Petroleum Society of CIM and the Canadian Association of Drilling Engineers, Calgary, AB, June 10-13, 1984.

Maini, B.B. and Ma, V.: "Relationship Between Foam Stability Measured in Static Tests and Flow Behaviour of Foams in Porous Media," paper SPE 13073 presented at the 59th Annual Technical Conference and Exhibition, Houston, TX, Sept. 16-19, 1984.

Maini, B.B., Sarma, H.K. and George, A.E.: "Significance of Foamy-Oil Behaviour in Primary Production of Heavy Oils," *JCPT* (Nov. 1993) **32**, No. 9, 50-54.

McBain, J.W. and Robinson, J.V.: "Surface Properties of Oils," *Natl. Advis. Comm. Aeronaut.*, Technical Note No. 1844 (1949).

Moulu, J.C.: "Solution Gas Drive: Experiments and Simulation," *Journal of Petroleum Science and Engineering* (*J. Pet. Sci. & Eng.*) (1989) **2**, 379-86.

Plesset, M.S. and Prosperetti, A.: "Bubble Dynamics and Cavitation," *Annual Review of Fluid Mechanics* (*Ann. Rev. Fluid Mech.*) (1977) **9**, 145-85.

Ross, S.: "Mechanisms of Foam Stabilization and Antifoaming Action," *Chem. Eng. Progr.* (Sept. 1967) **63**, 41-47.

Ross, S.: "Bubbles and Foams," *Ind. Eng. Chem.* (Oct. 1969) **61**, No. 10, 48-57.

Schramm, L.L. and Wassmuth, F.: "Foams: Basic Principles," *Foams: Fundamentals and Applications in the Petroleum Industry*, Schramm, L.L., Ed., *Advances in Chemistry Series* **242**, American Chemical Society, Washington, DC (1994) 3-46.

Scriven, L.E.: "On the Dynamics of Phase Growth," *Chemical Engineering Science* (*Chem. Eng. Sci.*) (1959) **10**, 1-13.

Sheng, J.J., Hayes, R.E., Maini, B.B. and Tortike, W.S.: "A Dynamic Model to Simulate Foamy Oil Flow in Porous Media," paper SPE 36750 presented at the 1996 Annual Technical Conference and Exhibition, Denver, CO, Oct. 6-9.

Sheng, J.J. and Zhou, X.: "Computing and Selecting Parameters in Numerical Modelling of Oil Field Thermal Recovery," *Special Oil & Gas Reservoirs* (1995) **2**, No. 3, 15-22 (Chinese).

Sherwood, T.K., Pigford, R.L. and Wilke, C.R.: *Mass Transfer*, McGraw-Hill Book Company, New York (1975) 150.

Smith, G.E.: "Fluid Flow and Sand Production in Heavy Oil Reservoirs Under Solution Gas Drive," *SPEPE* (May 1988) 169-80.

Stewart, C.R., Craig, F.F. and Morse, R.A.: "Determination of Limestone Performance Characteristics by Model Flow Tests," *Trans.* (1953), AIME, **198**, 93-102.

Stewart, C.R., Hunt, E.B., Jr., Schneider, F.N., Geffen, T.M. and Berry, V.J., Jr.: "The Role of Bubble Formation in Oil Recovery by Solution Gas Drive in Limestones," *Trans.* (1954), AIME, **201**, 294-301.

Szekely, J. and Fang, S.D.: "Non-Equilibrium Effects in the Growth of Spherical Gas

Bubbles due to Solute Diffusion -II The combined effects of viscosity, liquid inertia, surface tension and surface kinetics," *Chem. Eng. Sci.* (1973) **28,** 2127-40.

Szekely, J. and Martins, G.P.: "Non-Equilibrium Effects in the Growth of Spherical Gas Bubbles due to Solute Diffusion," *Chem. Eng. Sci.* (1971) **26,** 147-59.

Theofanous, T., Biasi, L., Isbin, H.S. and Fauske, H.: "A Theoretical Study on Bubble Growth in Constant and Time-Dependent Pressure Fields," *Chem. Eng. Sci.* (1969) **24,** 885-97.

Wall, C.G. and Khurana, A.K.: "Saturation: Permeability Relationships at Low Gas Saturations," *J. Inst. Pet.* (Sept. 1971) **57,** No. 557, 261-69.

Wall, C.G. and Khurana, A.K.: "The Effect of Rate Pressure Decline and Liquid Viscosity on Low-Pressure Gas Saturations in Porous Media," *J. Inst. Pet.* (Nov. 1972) **58,** No. 564, 335-45.

Ward, C.A., Johnson, W.R., Venter, R.D. and Ho, S.: "Heterogeneous Bubble Nucleation and Conditions for Growth in a Liquid-Gas System of Constant Mass and Volume," *J. Appl. Phys.* (April 1983) **54,** No. 4, 1833-1943.

Ward, C.A. and Levart, E.: "Conditions for Stability of Bubble Nuclei in Solid Surfaces Contacting a Liquid-Gas Solution," *J. Appl. Phys.* (1984) **56,** No. 2, 491-500.

Ward, C.A., Tikuisis, P. and Venter, R.D.: "Stability Analysis in a Closed Volume of Liquid of Liquid-Gas Solution," *J. Appl. Phys.* (1982) **53,** No. 9, 6076-84.

Wieland, D.R., and Kennedy, H.T.: "Measurements of Bubble Frequency in Cores," *Trans.* (1957), AIME, **210,** 122-25.

Wit, K.: "Solution Gas Drive in Heavy Oil Reservoirs," paper presented at the Symposium on Heavy Oil recovery, Maracaibo, July 1-3, 1974.

Wood, J.W. Jr.: "Bubble Formation in Rangely Field, Colorado," MS thesis, Texas A&M U., College Station (1953).

Yortsos, Y.C. and Parlar, M.: "Phase Change in Binary Systems in Porous Media: Application to Solution Gas Drive," paper SPE 19697 presented at the 64th Annual Technical Conference and Exhibition of SPE of AIME, San Antonio, TX, Oct. 8-11, 1989.

Chapter 6

Simulation Study of Foamy Oil Flow in Porous Media

6.1 Introduction

Foamy oil flow involves a complex interplay of several rate processes related to the nucleation, growth and coalescence of gas bubbles with the fluid mechanics of multiphase flow through porous media. However, simulation of primary depletion in foamy oil reservoirs is still based primarily on empirical adjustments to conventional solution gas drive models. These models are reviewed in this chapter first. A flow model including these rate processes is then presented. The detailed formulation is presented in Appendix A. The proposed dynamic model is used to match some primary depletion tests in a laboratory scale sand pack. The simulation results of non-equilibrium phenomenon of gas evolution and unstable phenomenon of dispersed gas bubbles are discussed.

6.2 Discussion of Published Models

A model for the flow of oil/gas mixtures in porous media including dynamic processes has not been developed. The published models include a conventional model, a pseudo-bubble point model, a modified fractional flow model and a reduced oil viscosity model. These models have been used to history match heavy oil production. They are reviewed and discussed in the following.

6.2.1 Conventional Models

The most commonly used approach to simulate reservoir performance involves adjustment of the key process parameters in conventional solution gas drive models. an effort has been made to history match reservoir performance using existing conventional simulators, by adjusting the parameters to account for the contributions of foamy oil to oil recovery. The key parameters adjusted are the critical gas saturation, the oil/gas relative permeability, the fluid and/or rock compressibility, the pressure dependent oil viscosity and the absolute permeability.

Obviously, conventional models can not be expected to capture important features of foamy oils, especially the dynamic processes. Obtaining a reasonable history match with such models often requires using unrealistic parameters. Moreover, although it may be possible to get a good history match, the predictions from these models are likely to be unreliable.

6.2.2 Pseudo-Bubble-Point Model

Kraus *et al.* (1993) proposed the concept of "pseudo-bubble-point pressure" in their model for the simulation of primary depletion in foamy oil reservoirs. The pseudo-bubble-point pressure is an adjustable parameter in their fluid property description. All of the solution gas remains dispersed in the oil phase until the reservoir pressure drops to the pseudo-bubble-point pressure. Below this pseudo-bubble-point pressure, only a fraction of the released gas remains dispersed; and this fraction decreases linearly to zero with declining pressure. They reported a methodology that could be used to calculate foamy oil fluid properties from conventional laboratory PVT data. The dispersed gas is treated as a part of the oil phase but its molar volume and compressibility are evaluated with those of the free gas. According to the amount of the gas dispersed in the oil phase, the compressibility of foamy oil is calculated as a function of pressure. This enhanced compressibility is then substituted for that of the dead oil component in a conventional simulator.

The pseudo-bubble-point model captures some of the features of foamy oil flow. It provides a mechanism to account for the high apparent compressibility of the flowing fluid. However, this model does not simulate the effects of non-equilibrium rate processes. Therefore, time dependent changes in the foamy oil flow behaviour would be difficult to simulate with this type of model.

6.2.3 Modified Fractional Flow Model

Lebel (1994) used a modified fractional flow model during the simulation various reservoir access geometries. As the gas saturation increases from zero, the fractional flow of gas increases linearly with gas saturation until a limiting dispersed gas saturation is reached. Beyond the limiting volume fraction of gas in the foamy oil, any further increase in gas saturation results in free gas. The gas begins to collect and flows as its saturation increases. The effective viscosity of the foamy oil decreases slightly from that of the oil as the volume fraction of gas increases. The density of the foamy oil is a volume weighted average of the densities of the oil and gas components. An equilibrium gas-oil PVT relationship was used in this model. He justified this model by stating that the fractional flow relationship had been calibrated to match laboratory measurements of foamy oil and gas flow during the blowdown of live oil in cores.

This model is similar to the conventional solution gas drive model. Both require the modification of relative permeability and component properties. A limiting dispersed gas saturation is adjusted in the former model, while a critical gas saturation is often adjusted in the latter model.

The modified fractional flow model captures a feature of foamy oil flow in that some fraction of the evolved gas is entrained in the oil phase, and requires only modified relative permeability and component properties to be implemented in a reservoir simulator. Like other published models, time dependent changes in foamy oil can not be simulated. Finding the right fractional flow curve may require trial and error. In his model, the foamy oil viscosity was lower than the single-phase oil viscosity. However, how the effective viscosity of the foamy oil decreases with the volume fraction of gas was not reported.

6.2.4 Reduced Oil Viscosity Model

Claridge and Prats (1995) proposed a new model for simulating anomalous foamy heavy oil behaviour. They suggested that the asphaltenes present in the crude oil adhere to the gas bubbles while the latter are still very tiny. This coating of asphaltenes on a bubble surface stabilizes the bubbles at a small size. The bubbles continue to flow through the rock pores with the oil. The key element which differentiates this model from the others discussed above lies in the net effect of asphaltene adsorption onto the bubble surfaces on the viscosity of the crude oil. They suggested that the oil viscosity decreases dramatically due to the removal of the dispersed asphaltenes. The decrease in viscosity is responsible for the higher than expected rate of production.

The concept of asphaltene adsorption proposed in this model needs to be verified experimentally. As discussed in Section 3.3.3, the proposed mechanism does not seem to be plausible. Moreover, the important features of dynamic processes are not included in this model.

6.3 Description of the Proposed Flow Model

The common weakness of the preceding models is that they do not properly describe the dynamic processes. In the model proposed herewith, efforts were made to consider these processes. This proposed model incorporates two dynamic processes: i) the process which controls the rate of transfer from the solution gas to the evolved gas which is the sum of the dispersed gas and the free gas, and ii) the process which controls the rate of transfer from evolved gas to free gas. The description of these two rate processes is based on the dynamic models proposed in Chapter 5. Bubble nucleation is assumed to be instantaneous. Two-phase flow of foamy oil and gas is modelled using the normal two-phase relative permeability-saturation relationship. The dispersed gas is assumed to flow with the oil as if it were a part of the liquid phase.

6.3.1 Model Assumptions:

1. The description of the dynamic processes of bubble nucleation, bubble growth and bubble decay is based on Model 3 presented in Chapter 5.
2. The foamy oil is assumed to have three components: (1) dead oil; (2) solution gas which has the viscosity, compressibility and molar density of normal solution gas; and (3) dispersed gas which has the compressibility and density of the gas phase but a viscosity equal to the liquid oil viscosity. In other words, the dispersed gas bubbles are assumed to move at the same velocity as the liquid oil.
3. In foamy oils microbubbles are dispersed in the liquid oil phase. The capillary pressure at the surface of a bubble is related to the bubble size. Since the bubble size is not considered, the capillary pressure could not be described in the present model. In addition, the capillary pressure between the continuous oil/gas phases is also ignored.
4. Darcy's law is assumed to be valid for the foamy oil and gas movement.
5. It was found that diffusion does not influence dispersion significantly in the case of large scales (Arya *et al.*, 1988); and numerical dispersion is usually greater

than physical dispersion (Laxity-Briceno, 1985). Therefore, the diffusion of a gas or oil component from one block to another which is caused by their respective phase concentration difference is not included in this model. The diffusion of gas molecules in the oil phase into nucleated gas embryos caused by supersaturation is considered in the rate of bubble growth.

6.3.2 Mathematical Equations

6.3.2.1 Mass Balances

The mass conservation equations for each component are as follows:

For the dead oil component in the foamy oil phase,

$$\frac{\partial(\phi S_{fo}\rho_{fo}X_{do})}{\partial t} = -\nabla\cdot(\rho_{fo}v_{fo}X_{do}) - q_{fo}X_{do}; \tag{6-1}$$

for the solution gas component in the foamy oil phase,

$$\frac{\partial(\phi S_{fo}\rho_{fo}X_{sg})}{\partial t} = -\nabla\cdot(\rho_{fo}v_{fo}X_{sg}) - q_{fo}X_{sg} - R_{sg\rightarrow eg}; \tag{6-2}$$

for the free gas component in the gas phase,

$$\frac{\partial(\phi S_{g}\rho_{g})}{\partial t} = -\nabla\cdot(\rho_{g}v_{g}) - q_{fg} + R_{eg\rightarrow fg} + R_{dg\rightarrow fg}; \tag{6-3}$$

and for the dispersed gas component in the foamy oil phase,

$$\frac{\partial(\phi S_{fo}\rho_{fo}X_{dg})}{\partial t} = -\nabla\cdot(\rho_{fo}v_{fo}X_{dg}) - q_{fo}X_{dg} + R_{eg\rightarrow dg} - R_{dg\rightarrow fg}. \tag{6-4}$$

The term q means mass production rate. The parameters $R_{sg\rightarrow eg}$, $R_{eg\rightarrow dg}$ and $R_{eg\rightarrow fg}$

are the transfer rates from solution gas to evolved gas, from evolved gas to dispersed gas and from evolved gas to free gas, respectively. The gas bubbles evolved from solution remain partly dispersed in the liquid oil phase, and the rest become free gas. At any time, these rates satisfy the condition:

$$R_{sg \to eg} = R_{eg \to dg} + R_{eg \to fg}. \tag{6-5}$$

Also, the produced gas comes from the solution gas and the dispersed gas in the oil phase and the free gas in the gas phase:

$$q_g = q_{fo} x_{sg} + q_{fo} x_{dg} + q_{fg}. \tag{6-6}$$

The mass conservation equations in this model are expressed in moles. If the densities are evaluated in mass densities instead of in molar densities, similar equations can be formulated in terms of mass.

6.3.2.2 Kinetic Equations

Darcy's law is assumed to be valid for the flow of foamy oil and free gas. Then the relationships between the flow rate and the potential gradient for oil and gas phases are

$$v_{fo} = - \frac{kk_{ro}}{\mu_{fo}} \nabla \Phi_o, \tag{6-7}$$

$$v_g = - \frac{kk_{rg}}{\mu_g} \nabla \Phi_g, \tag{6-8}$$

respectively, where

$$\Phi_f = p - \rho_f M_f g Z. \qquad (6\text{-}9)$$

with *f* being *fo* or *g*.

6.3.2.3 *Saturation Constraint*

Two phases, foamy oil and free gas, exist in the porous medium. Their saturations, S_{fo} and S_g, should satisfy the following constraint:

$$S_{fo} + S_g = 1. \qquad (6\text{-}10)$$

6.3.2.4 *Liquid Mole Fraction Constraint*

There are three components in the liquid foamy oil phase: dead oil, solution gas and dispersed gas. Their mole fractions are related as follows:

$$x_{do} + x_{sg} + x_{eg} = 1. \qquad (6\text{-}11)$$

6.3.2.5 *Boundary Conditions*

In a one-dimensional problem, there is no flow across the boundary at one end (inlet). At the other end (outlet), the pressure is reduced at a controlled rate. Then the boundary conditions are

$$\left[\frac{\partial p}{\partial X}\right]_{X=0} = 0, \qquad (6\text{-}12)$$

and

$$p(X=L) = p(t), \qquad (6\text{-}13)$$

where the values of $p(t)$ depend on the controlled pressure decline rate.

6.3.2.6 *Initial Condition*

The initial pressure is the same everywhere:

$$p(t=0) = p^0. \tag{6-14}$$

Thus Eqs. 6-1 to 6-14 complete the mathematical description of foamy oil flow. The unknowns are summarized as follows.

Pressure term: p.

Saturation terms: S_{fo}, S_g. According to the saturation constraint Eq. 6-10, only one saturation, say S_{fo}, is an independent unknown.

Mole fraction terms: x_{do}, x_{sg}, x_{dg}. Due to the constraint of Eq. 6-11, only two of three, say x_{sg} and x_{dg}, are independent.

Mass transfer terms: $R_{sg\to cg}$, $R_{cg\to dg}$, $R_{cg\to fg}$. These terms may be estimated from other independent variables and will be described in Section 6.3.5.

As a result, there are four independent unknowns: p, S_{fo}, x_{sg}, x_{dg}. The four mass conservation equations (Eqs. 6-1 to 6-4) constitute the governing equations of foamy oil flow.

Gravity cannot be included in the present one-dimensional model. Then the above mass conservation equations for the four components in finite difference form will be the following.

For the dead oil component in the foamy oil phase,

$$\frac{V}{\Delta t}\delta(\phi S_{fo}\rho_{fo}x_{do}) = \Delta(T_{fo}x_{do}\Delta p) - q_{fo}x_{do}. \tag{6-15}$$

For the solution gas component in the foamy oil phase,

$$\frac{V}{\Delta t}\delta(\phi S_{fo}\rho_{fo}x_{sg}) = \Delta(T_{fo}x_{sg}\Delta p) - q_{fo}x_{sg} - R_{sg\rightarrow eg}. \tag{6-16}$$

For the free gas component in the gas phase,

$$\frac{V}{\Delta t}\delta(\phi S_g\rho_g) = \Delta(T_{fg}\Delta p) - q_{fg} + R_{eg\rightarrow fg} + R_{dg\rightarrow fg}. \tag{6-17}$$

For the dispersed gas component in the foamy oil phase,

$$\frac{V}{\Delta t}\delta(\phi S_{fo}\rho_{fo}x_{dg}) = \Delta(T_{fo}x_{dg}\Delta p) - q_{fo}x_{dg} + R_{eg\rightarrow dg} - R_{dg\rightarrow fg}. \tag{6-18}$$

In the above equations, δ represents time difference, while Δ represents space difference. The term $\Delta(T\Delta p)$ denotes the net mass flow into the grid block due to interblock flow. For block i in a one-dimensional problem,

$$\Delta(T\Delta p) = T_{i+1/2}(p_{i+1}-p_i) - T_{i-1/2}(p_i-p_{i-1}), \tag{6-19}$$

where

$$T_{i\pm 1/2} = \left[\frac{Akk_r\,\rho}{(\Delta X)\mu}\right]_{i\pm 1/2}, \tag{6-20}$$

and A is the cross sectional area perpendicular to flow. V is the volume of one block.

6.3.3 Method of Solution

For the above finite difference equations, combining the left-hand side expansions, the explicit interblock flow term expansions and the implicit production rate representations gives

$$\sum_{j=1}^{4} C_{ij} u_j = \Delta(T_i \Delta \delta p) + R_i, \; i=1,\ldots,4, \tag{6-21}$$

where C_{ij} and R_i are the resulting coefficients; T_i is the transmissibility for component i. The parameter u_i is defined as

$$[u_1,\, u_2,\, u_3,\, u_4]^T = [\delta x_{dg},\, \delta x_{sg},\, \delta S_{fo},\, \delta p]^T. \tag{6-22}$$

Application of Gaussian elimination to the system of four equations (Eq. 6-21) results in a pressure equation for block i:

$$\alpha_i \delta p_{i-1} + \beta_i \delta p_i + \gamma_i \delta p_{i+1} = e_i, \tag{6-23}$$

where α_i, β_i, γ_i, and e_i are generated by the Gaussian elimination process (see Appendix A).

In a one-dimensional case with *NX* blocks, a system of *NX* equations in the form of Eq. 6-23 will be generated. This system of equations is solved by Thomas' algorithm for the δp_i ($i=1,2,\ldots,NX$). Once the δp_i are obtained, δS_{foi}, δx_{sgi} and δx_{dgi} are obtained explicitly.

For a detailed formulation of this section, see Appendix A.

6.3.4 Grid System and Time Step Size

There are two methods of grid construction: point-distributed grid and block-centered grid (Aziz and Setarri, 1979). In this model, the block-centered grid method was chosen for its simplicity. Seven blocks for the two-metre long sand pack were used. A uniform grid block size of 0.2857 metres was employed. A constant time step size of 60 seconds was used.

6.3.5 Estimation of the Mass Transfer Rates

6.3.5.1 Estimation of $R_{sg \to eg}$

As discussed in Section 5.6, it is desirable that the information at the last time step be used to estimate the fluid properties at the present time step in a practical simulator. And it was proposed in Model 3 described in Section 5.6.2 that the amount of gas evolved from solution state from t^n to t^{n+1} is an exponential function of time:

$$\Delta n_{sg \to eg}^{n+1} = \Delta n_s^{n+1} \left[1 - \exp(-\lambda_s \Delta t/2)\right], \tag{6-24}$$

where Δn_s^{n+1} is the supersaturation expressed in moles of supersaturated solution gas in the oil phase at time t^n referred to the equilibrium state at t^{n+1}. Then the mass transfer rate within this time interval Δt is equal to

$$R_{sg \to eg}^{n+1} = \frac{\Delta n_s^{n+1} \left[1 - \exp(-\lambda_s \Delta t/2)\right]}{\Delta t}. \tag{6-25}$$

The calculation of Δn_s^{n+1} is described in Appendix A.3.1. As an example, for n_o^n supersaturated oil with solution gas mole fraction $(x_{sg}^n)'$, when the pressure is reduced from p^n to p^{n+1}, Δn_s^{n+1} can be estimated from

$$\Delta n_s^{n+1} = \frac{n_o^n \left[(x_{sg}^n)'/K^{n+1} - 1\right]}{K^{n+1} - 1}, \tag{6-26}$$

where $(x_{sg}^n)'$ will be defined in Eq. 6-35.

It was found that the stability of the numerical solution is very sensitive to the mass transfer terms, especially $R_{sg\rightarrow eg}$.

6.3.5.2 Estimation of $R_{eg\rightarrow dg}$

The gas bubbles which evolve from solution gas initially remain dispersed in the liquid oil phase; and later these bubbles disengage from the oil to become free gas. It was proposed previously in Chapter 5 that the rate of this disengagement is proportional to the amount of the dispersed gas. The proportionality coefficient is called the decay coefficient of dispersed gas, λ_{dg}. Thus the amount of dispersed gas remaining will be an exponential function of time. Therefore, $R_{eg\rightarrow dg}$ may be calculated as

$$R_{eg\rightarrow dg} = R_{sg\rightarrow eg} \exp(-\lambda_{dg} \Delta t/2). \tag{6-27}$$

In this model, the rate is expressed in mole/s. As discussed in Section 5.3.4, the decay coefficient in the above rate expression should be modified. It is modified according to Eq. 5-23. The following modifications to λ_{dg} have also been tested and it was observed that they were not as successful as Eq. 5-23 in the history matching experiments:

$$\lambda_{dg} = \lambda_{sc} \left(\frac{p_{sc}}{p} \right)^{\alpha}, \tag{6-28}$$

$$\lambda_{dg} = \lambda_c f_{dg}^{\alpha}, \tag{6-29}$$

where λ_c is a constant value, and α is a positive number other than one for Eq. 6-28.

6.3.5.3 *Estimation of $R_{eg\to fg}$*

Since

$$R_{sg\to eg} = R_{eg\to dg} + R_{eg\to fg}, \tag{6-30}$$

the rate of evolved gas transferred to free gas is

$$R_{eg\to fg} = R_{sg\to eg}\left[1 - \exp(-\lambda_{dg}\Delta t/2)\right]. \tag{6-31}$$

6.3.5.4 *Estimation of $R_{dg\to fg}$*

Generally, the dispersed gas in a block at time t^{n+1} is composed of three parts: the existing dispersed gas at time t^{n}, the net dispersed gas flowing-in and the newly formed bubbles during the present time step. All of the dispersed gas eventually becomes free gas. Thus, the rate of dispersed gas transferred to free gas may be calculated as

$$\begin{aligned} &R_{dg\to fg}^{n+1} \\ &= n_{dg}^{n}\left[1 - \exp(-\lambda_{dg}\Delta t)\right]/\Delta t \\ &+ \left[\Delta(T_{dg}^{n+1}\Delta p^{n+1}) - q_{dg}^{n+1}\right]\left[1 - \exp(-\lambda_{dg}\Delta t/2)\right] \\ &+ R_{eg\to dg}^{n+1}\left[1 - \exp(-\lambda_{dg}\Delta t/2)\right]. \end{aligned} \tag{6-32}$$

In the above rate expression, the first part, the transfer rate from the existing dispersed gas to free gas, is the average rate during Δt. Since this rate is proportional to the existing dispersed gas, it may also be formulated by $\lambda_{dg}n_{dg}{}^{n}$ or $\lambda_{dg}n_{dg}{}^{n+1}$. This choice was observed not to improve the stability of the numerical solution. For simplicity, the second and third parts may be excluded in the above rate expression. However, it was observed that the stability of the numerical solution would be reduced slightly by doing so.

6.3.6 Fluid Properties

6.3.6.1 Viscosities

According to the discussion presented in Section 3.3, the proposed models of foamy oil viscosity do not seem to be plausible. These models may not be implemented into the flow model. The simple foamy oil viscosity model presented in Section 3.4 can not be implemented, because the bubble size distribution which is required in the viscosity model has not been considered in the proposed flow model.

If the theory of dispersion viscosity can be applied to the foamy oil viscosity, the foamy oil viscosity would be close to the live oil viscosity, because the volume fractions of the dispersed gas bubbles in foamy oils are low (see Section 4.4.7). As mentioned earlier in Section 2.2.2.2, there has been no verified method to measure foamy oil viscosity in porous media. Therefore, the foamy oil viscosity is evaluated at the value of the live oil in the present model. If the live oil viscosity data at different saturation pressures are not available, the foamy oil viscosity is obtained by a logarithmic mixing rule:

$$\ln(\mu_{fo}) = x'_{do} \ln(\mu_{do}) + x'_{sg} \ln(\mu_{sg}), \tag{6-33}$$

where

$$x'_{do} = \frac{x_{do}}{x_{do} + x_{sg}}, \tag{6-34}$$

$$x'_{sg} = \frac{x_{sg}}{x_{do} + x_{sg}}. \tag{6-35}$$

For the dead oil, μ_{do} is measured directly or obtained from other references. However, for a solution gas like methane, a measured value for the liquid phase is difficult to find. In this case, the solution gas viscosity is estimated using Eq. 6-33, provided that the dead oil viscosity and the live oil viscosity at one pressure point are known. The estimated viscosity is a hypothetical liquid viscosity composed of 100% solution gas. This estimated viscosity of solution gas is then used to calculate the oil viscosities at other pressures.

Gas viscosity changes within normal pressure and temperature ranges are relatively small, so that a constant value may be used. In this model, 0.014 mPa·s is chosen for the gas viscosity, which is within the range of experimental data of methane (Reid *et al.*, 1987).

6.3.6.2 Oil/Gas Relative Permeabilities

The relative permeability curve measured from an external gas drive test is likely to be different from that for a solution gas drive (Maini, 1995). However, directly measured solution-gas-drive relative permeability information was not available. Therefore, the conventional relative permeability curves had to be used. The oil/gas relative permeabilities measured by Muqeem (1994) are employed in the simulator, since the same Ottawa sand was used in his relative permeability measurements and in the simulated primary depletion tests. This is based on the assumption that the two-phase relative permeabilities depend on the saturation, wettability and pore structure but not on the fluid viscosity, density or flow rate (Maini, 1995). The equations used to describe the relative permeability curves are (Muqeem, 1994)

$$k_{ro} = 0.76(S_o^*)^{1.988}, \tag{6-36}$$

$$k_{rg} = 0.61(1-S_o^*)^{2.782}, \tag{6-37}$$

where the normalized oil saturation is

$$S_o^* = \frac{S_o-S_{or}}{1-S_{wi}-S_{or}-S_{gc}}. \tag{6-38}$$

An important issue in oil/gas relative permeability, in the context of primary depletion, is the critical gas saturation and how it should be measured (Maini, 1995). The literature (Stewart *et al.*, 1954; Kortekaas and van Poelgeest, 1991; Firoozabadi *et al.*, 1992; Kamath and Boyer, 1993; Hawes, *et al.*, 1994) also strongly suggests that the critical gas saturation for a solution gas drive may be different from the value measured by external gas drive tests. However, because of a lack of information, the critical gas saturation from the external gas drive test was also used in this model.

6.3.6.3 Gas Solubility

The gas solubility is formulated by the gas/oil equilibrium ratio (*K* value) in this model. The solution gas/oil ratios for different oils were obtained experimentally or from other references. In the cases where the solution gas/oil ratios were only reported at the initial pressures, a linear interpolation was used to obtain the gas/oil ratios at other lower pressures. Such an approximation is accurate enough over a considerable range of pressures (Craft *et al.*, 1991). The *K* values were calculated from these gas/oil ratio data, together with molar weights and densities of oil and gas components, using the method described by Sheng and Zhou (1995).

6.4 Validation of Model

The proposed dynamic model may be validated by comparing the results from the model with an analytical solution, or with those from a previously validated model. Unfortunately, such validation is impossible, because an analytical solution or a dynamic model of oil/gas flow does not exist. Therefore, this model has to be validated in other ways.

The proposed model is a non-equilibrium model. This non-equilibrium model may be first validated in its limiting case of equilibrium (very fast rates) which should give the same results as any of the conventional equilibrium models. To do this, the commercial simulator STARS developed by Computer Modelling Group (1995) was used. Figure 6.1 compares the average pressure in the sand pack versus cumulative oil produced from the equilibrium model version of the dynamic model and STARS, which shows that the results are quite close. The data are same as those of the primary depletion test, Boscan 3, which will be discussed later.

Comparing the model results with experimental or process data is always the best test of any model (Riggs, 1988). Therefore, the proposed dynamic model including the non-equilibrium effect can be validated based on the following two facts:

1. The model was used to simulate other depletion tests in addition to those presented in this dissertation. The results matched the experimental data and no

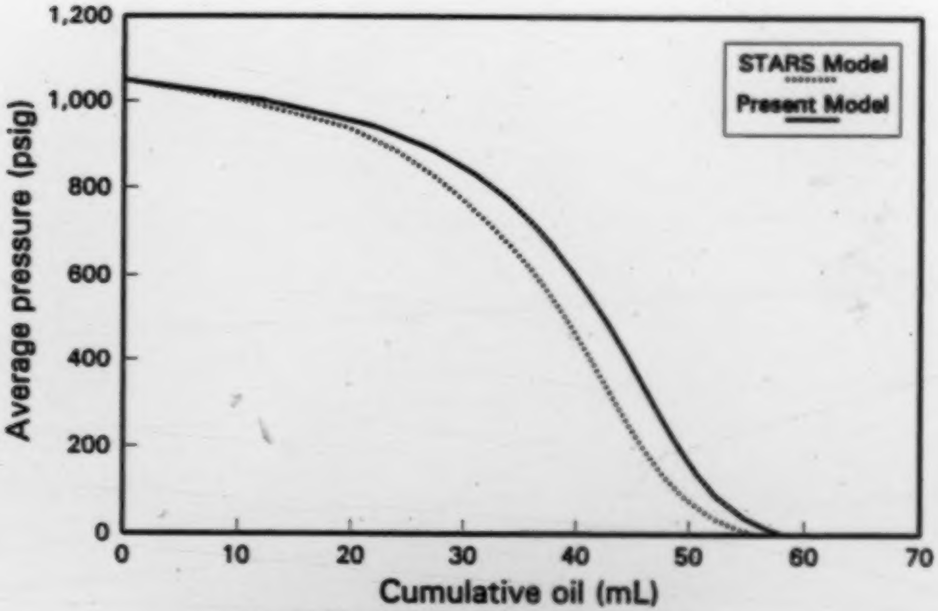

Fig. 6.1 - Comparison of results from STARS model and the present model.

unreasonable results were observed.

2. It is expected that the performance at a very slow pressure test would be similar to that predicted by a conventional equilibrium model. The dynamic model was used to match a very slow test as will be presented later. In other words, this model could function as an equilibrium model by adjusting the rate process parameters.

Also, it was tested and observed that the grid block size and the time step size did not significantly affect the simulation results. These results are presented in Figures 6.2 and 6.3. For the two-metre long sand pack, numbers of blocks of 3, 7, 35 and 85 were tested. The difference in results in Figure 6.2 is hardly noticeable. When the number of

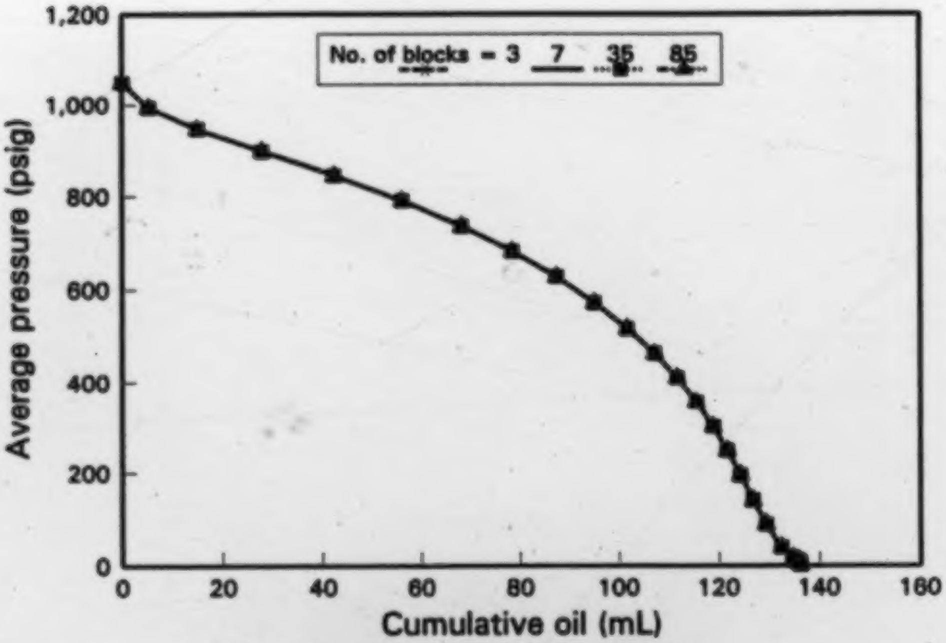

Fig. 6.2 - Effect of grid block size.

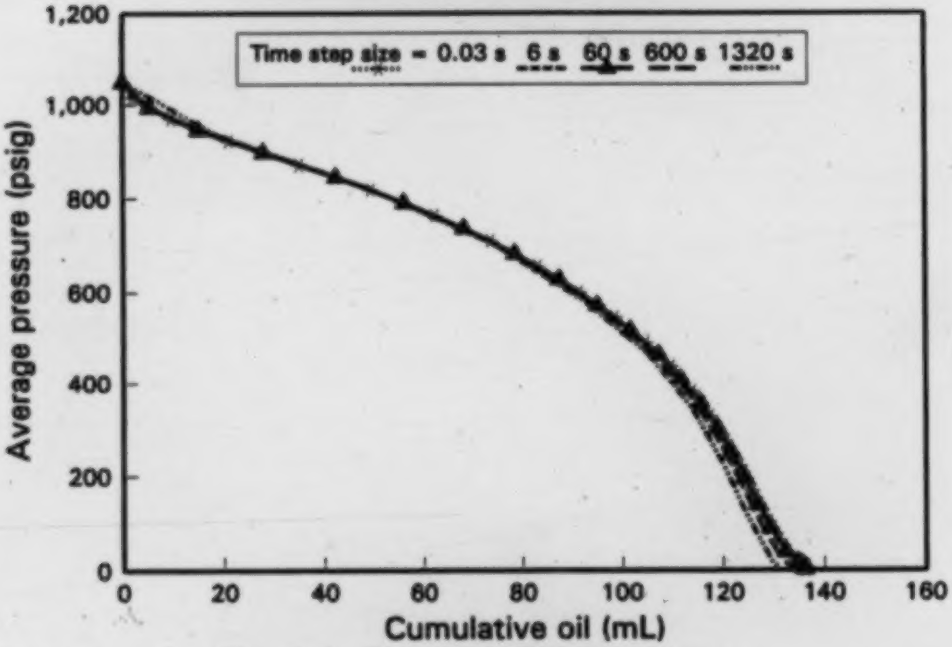

Fig. 6.3 - Effect of time step size.

blocks was increased to 91 blocks, the solution of pressure was only convergent until the 514th time step, when the time step size was 60 s. When the time step size was reduced (e.g., 30 s), the solution was convergent. In Figure 6.3, the results for the time step sizes of 0.03 s, 6 s, 60 s, 600 s and 1320 s are very close. It was tested and found that if the time step size was more than 1320 s, the solution of pressure would not be convergent. Since it took a long time (5.5 hours) to complete the simulation run when the time step size was 0.03 s, time step sizes less than 0.03 s were not tested.

6.5 Simulation of Primary Depletion Tests

The proposed model was used to simulate the primary depletion tests in a sand pack. In this model, the adjustable parameters to describe the rate processes are the supersaturation decay coefficient, λ_s, and the dispersed gas decay coefficient, λ_{gc}. Before presenting the simulation results, the experiment is briefly described.

6.5.1 Description of the Experiment

The equipment for the solution-gas-drive experiments is shown schematically in Figure 6.4. A two-metre long coreholder with six intermediate pressure taps was used to confine the sand pack. These pressure taps (spaced 33 centimetres apart) were used for dynamic monitoring of the pressure distribution during the primary depletion tests.

Recombined oil (also referred to as "live oil") was prepared by saturating the oil with gas in the recombination equipment connected to the inlet end of the coreholder. A

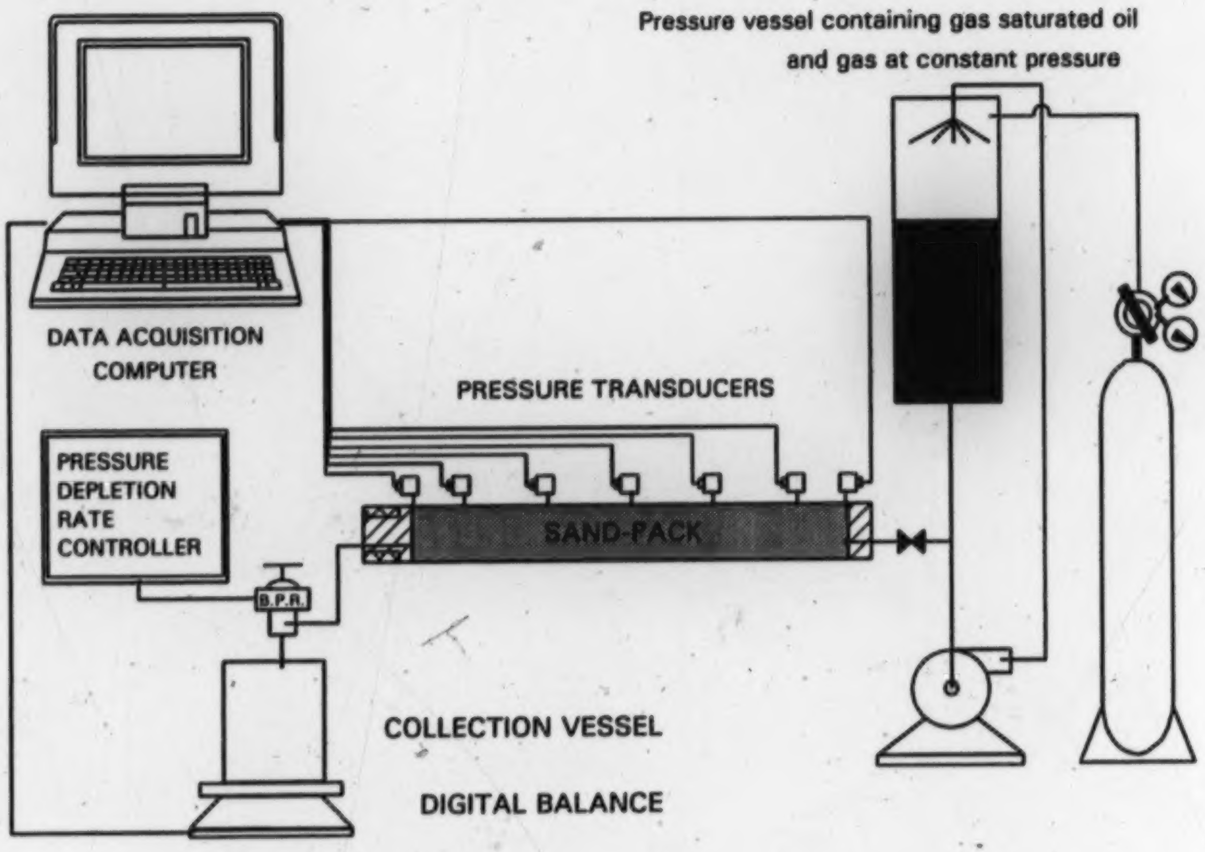
Pressure vessel containing gas saturated oil
and gas at constant pressure
DATA ACQUISITION
COMPUTER
PRESSURE TRANSDUCERS
PRESSURE
DEPLETION
RATE
CONTROLLER
SAND-PACK
B.P.R.
COLLECTION VESSEL
DIGITAL BALANCE

Fig. 6.4 - Schematic diagram of primary depletion tests.

schematic of the recombination equipment is also shown in Figure 6.4.

A back pressure regulator was used for controlling the pressure at the outlet end (production port) of the sand pack. A mass flow controller connected to the gas dome of the back pressure regulator was used to decrease continuously the pressure at the production port of the sand pack.

Produced oil flowed into a small pressure vessel placed on an electronic balance for monitoring of the oil produced. The produced gas was collected in a large pressure vessel connected to the oil collection vessel. The gas produced was monitored by measuring the increase in pressure of the gas collection vessel.

An automated data acquisition system was employed for reliable and dynamic recording of the oil production, gas production and the pressures at seven different points along the length of the sand pack. The depletion test was continued until the pressure within the sand pack declined to a low (near atmospheric) value and the production of oil and gas stopped.

Table 6.1 lists the properties of the sand-pack and fluids.

6.5.2 Simulation of the Depletion Tests with Boscan Oil

Three depletion tests (Boscan 1 to Boscan 3) with the same Boscan oil at different pressure decline rates were simulated. The tests were conducted at a temperature of 77 °C. At this test temperature, the gas-free oil viscosity is 555 mPa·s, and the density is 973 kg/m^3. The oil was saturated at 1000 psig. The solution GOR and the saturated oil viscosity at this pressure are 20 m^3/m^3 and 295 mPa·s, respectively. The oil viscosities

Table 6.1 - Properties of the Sand Pack and Fluids Used in the Tests

Sand pack length, m	2.0
Cross-section area, m^2	1.61×10^{-3}
Porosity, fraction	0.33
Permeability, m^2	3.33×10^{-12}
Sand-pack compressibility, Pa^{-1}	4.6×10^{-10}
Dead oil compressibility, Pa^{-1}	1.0×10^{-9}
Solution gas liquid compressibility, Pa^{-1}	7.0×10^{-9}
Dead oil thermal expansion coefficient, $°C^{-1}$	4.54×10^{-4}
Solution gas thermal expansion coefficient, $°C^{-1}$	4.54×10^{-4}
Molar specific volume of dead oil, m^3/kmole	0.5
Molar specific volume of solution gas, m^3/kmole	0.05875

at other pressures were calculated by a logarithmic mixing rule using the solution gas viscosity of 72 mPa·s. The gas used was a mixed gas containing 87.5% methane, 0.8% nitrogen, 3.9% ethane, 1.2% CO_2, 4.7% propane and 1.9% butane. The properties of this mixed gas were calculated based on these percentages. The molar specific volume of solution gas at standard conditions is 0.05875 m^3/kmole. The oil molecular weight is 500 kg/kmole.

During the process of history matching, the simulation results of cumulative oil produced, cumulative gas produced and the mid-point pressure at different times were compared with the experimental data. The relationship between the average pressure and cumulative oil was also compared; it was found that when this relationship is matched, the other simulation results are also well matched to experimental data. Also, this relationship has similar axis scales for different tests with the same oil system, so it is convenient for comparison. Therefore, only the comparison of this relationship is presented.

6.5.2.1 Slow Pressure Decline Test (Boscan 1)

It was assumed that the performance at a very slow pressure decline test would be similar to that from a conventional equilibrium model of a solution gas drive. Thus, the simulation results from a thermodynamic equilibrium model should be close to the experimental data of a very slow test. Therefore, the simulation results from the equilibrium version of the dynamic model were first compared with the slow pressure depletion test to demonstrate that the input data, especially the relative permeability curves, were correct. Then the dynamic model was used to history match the depletion test by adjusting the rate process parameters.

In the slow pressure decline test (Boscan 1), the outlet pressure declined from an initial pressure of 1000 psig to near atmospheric pressure over a period of 8 days. The pressure decline rate was 0.091 psi/min. Figure 6.5 shows the relationship between the average pressure and the cumulative oil produced. The simulation results from both the dynamic model and the equilibrium model are compared with the experimental data. They show that the predicted oil produced will be lower than the experiment value if the equilibrium model is assumed, even for the slow pressure decline test. The dynamic model provided a better match to the experimental results. The adjusted value of λ_g is 7.18×10^{-5} s^{-1} and that of λ_{sc} is 0.006 s^{-1}.

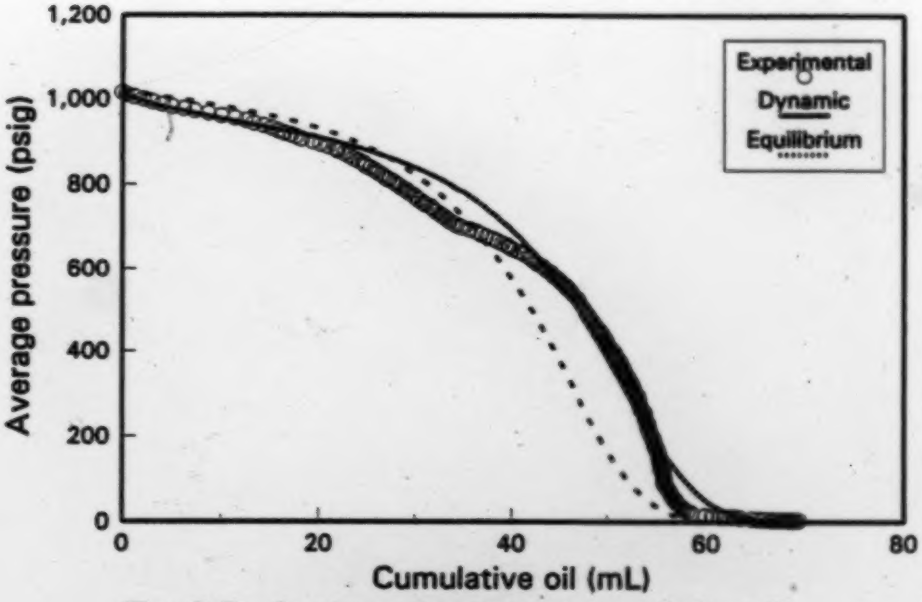

Fig. 6.5 - Average pressure vs. cumulative oil for Boscan 1.

6.5.2.2 Fast Pressure Decline Tests (Boscan 2 and Boscan 3)

In these fast pressure decline tests, the outlet pressure declined from an initial pressure of about 1000 psig to near atmospheric pressure over a period of 2.5 and 1.3 days for Boscan 2 and Boscan 3, respectively. Their corresponding pressure decline rates were 0.2758 psi/min and 0.5308 psi/min. The relationships between average pressure and cumulative oil are shown in Figures 6.6 and 6.7 for Boscan 2 and Boscan 3, respectively. These figures demonstrate that the simulation results and the experimental data are well matched. The adjusted values of λ_s are 1.32×10^{-4} s^{-1} and 2.0348×10^{-4} s^{-1} and those of λ_{sc} are 0.0027 s^{-1} and 0.0025 s^{-1} for Boscan 2 and Boscan 3, respectively. The results from the equilibrium model are also plotted in these figures. These figures show that the predicted ultimate oil recovery is much lower than that obtained in the laboratory, while

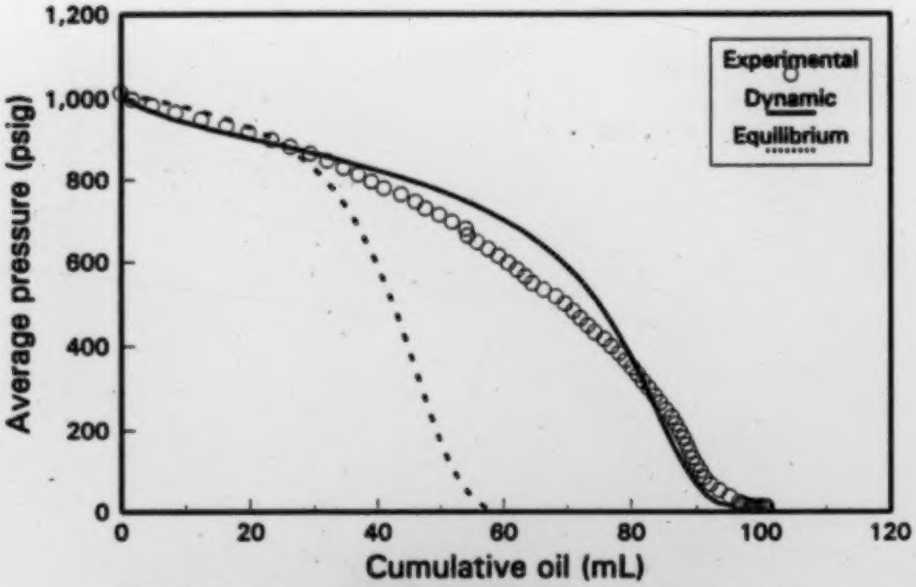

Fig. 6.6 - Average pressure vs. cumulative oil for Boscan 2.

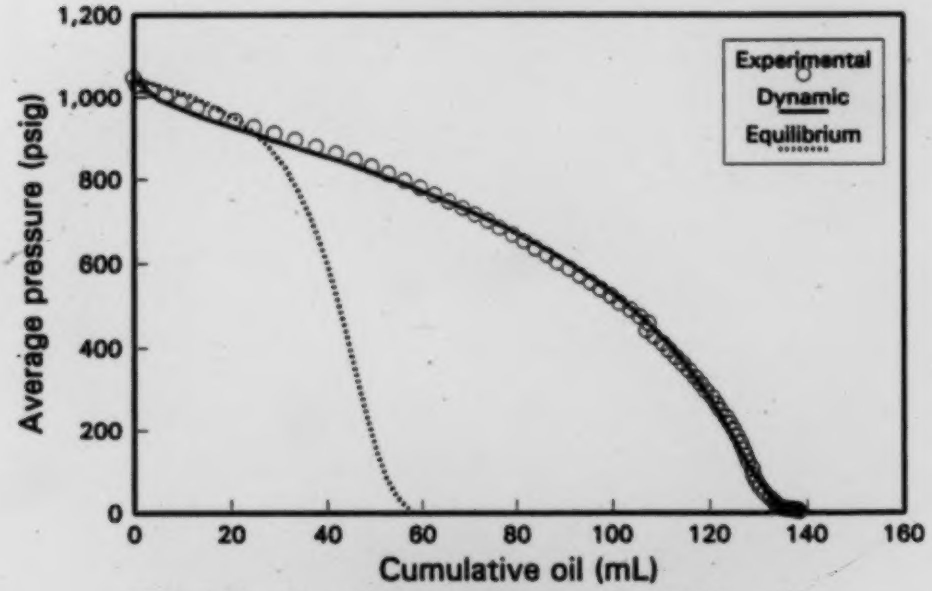

Fig. 6.7 - Average pressure vs. cumulative oil for Boscan 3.

the ultimate gas production is almost the same (see Figures 6.8 for Boscan 3 as an example). Figure 6.8 also show that the gas production in the experiment is always lower than that predicted from the equilibrium model at any time. The difference between the dynamic model and the equilibrium model is whether the dynamic processes are included or not. The comparison of the results from the equilibrium model with those from the dynamic model shows that the dynamic behaviour is important in foamy oil flow when the pressure declines fast.

Also, the predicted pressure at the mid-point of the sand pack for Boscan 3 is compared with the experimental data in Figure 6.9. It shows that the mid-point pressures predicted from both the dynamic model and the equilibrium model match the experimental data. In the two models the outlet pressure is controlled to be the same as in the experiment, and the oil and gas production is predicted. Therefore, it will be easier to match pressure than to match oil and gas production.

6.5.3 Discussion of λ_s and λ_{sc}

In the proposed dynamic model, the rate coefficient of supersaturation decay, λ_s, and the rate coefficient for dispersed gas decay at p_{sc}, λ_{sc}, are adjusted to describe the rate processes. From the adjusted values required to match the experimental results with Boscan oil presented earlier and with other oils not shown here, it seems that the values of λ_s and λ_{sc} vary with the pressure decline rate. Most likely, the faster the outlet pressure declines, the higher the values of λ_s and the lower the values of λ_{sc} that have to be used, which means that the rate of supersaturation decay is faster, and the rate of

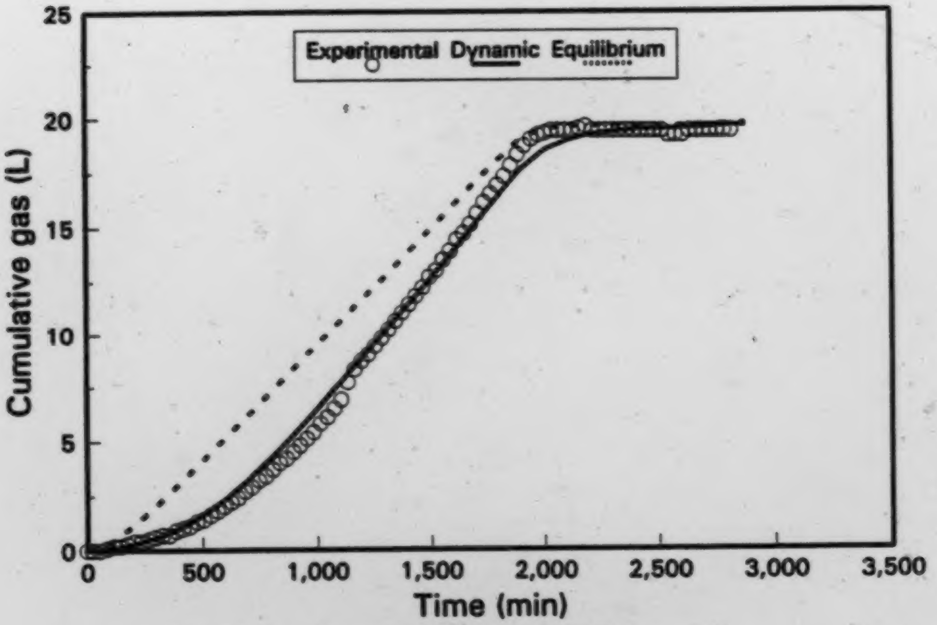

Fig. 6.8 - Cumulative gas for Boscan 3.

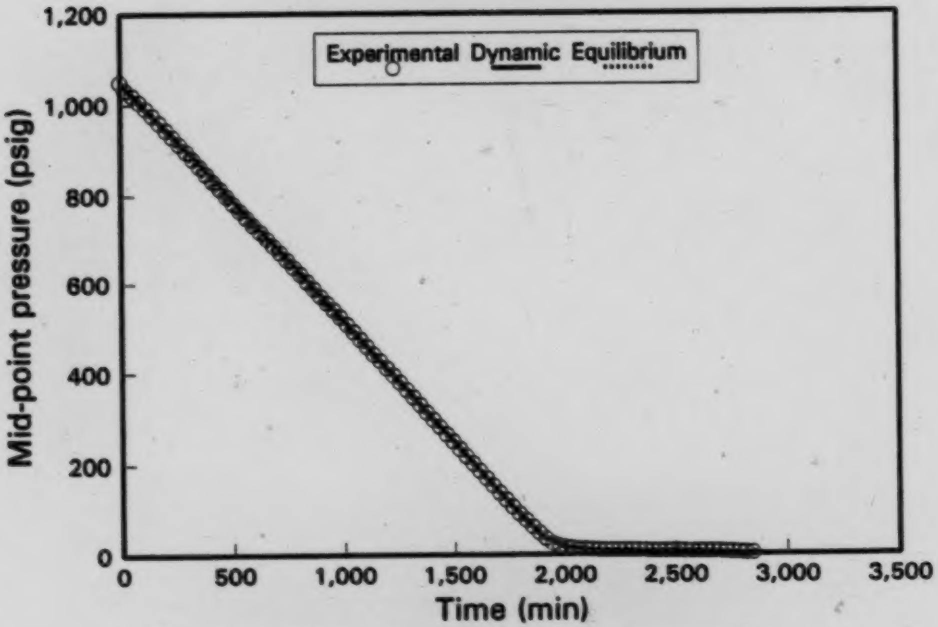

Fig. 6.9 - Mid-point pressure for Boscan 3.

disengagement of dispersed gas from the oil is slower. This is probably because, when the pressure declines faster, more nucleation sites become active and smaller gas bubbles are generated. When more nucleation sites are activated, the distance for solution gas to diffuse to the gas embryos at these sites will be shorter. Thus the supersaturation will decay faster. When more and smaller bubbles are formed, it would be easier for these bubbles to remain in the liquid oil phase. Thus the foamy oil system would be more stable. Note that for an exponential decay, the half-life is inversely proportional to the decay coefficient. Unfortunately, insufficient data were available to generate relationships that can be used to predict these two parameters when only the pressure decline rate is known.

The history-matched data of Boscan 3 were used as a base case to investigate the effect of λ_s. The average pressure versus oil produced is compared for λ_s equal to 1.0174×10^{-4} s^{-1}, 2.0348×10^{-4} s^{-1}, and 4.0696×10^{-4} s^{-1}. These results are shown in Figure 6.10. Figure 6.10 shows that the curve is shifted upwards slightly as λ_s increases. However, the ultimate recovery is not significantly affected by the value of λ_s. Similarly, the effect of the dispersed gas decay coefficient, λ_{se}, is investigated by increasing and decreasing its value in the base case by a factor of 2. The results are shown in Figure 6.11. Figure 6.11 shows that the decay coefficient significantly affects the oil recovery in the middle and late stages of depletion. In other words, the oil recovery is very sensitive to the value of λ_{se}. In the early stages, a small amount of gas is dispersed in the oil. Hence, the effect of dispersed gas on oil recovery is not significant.

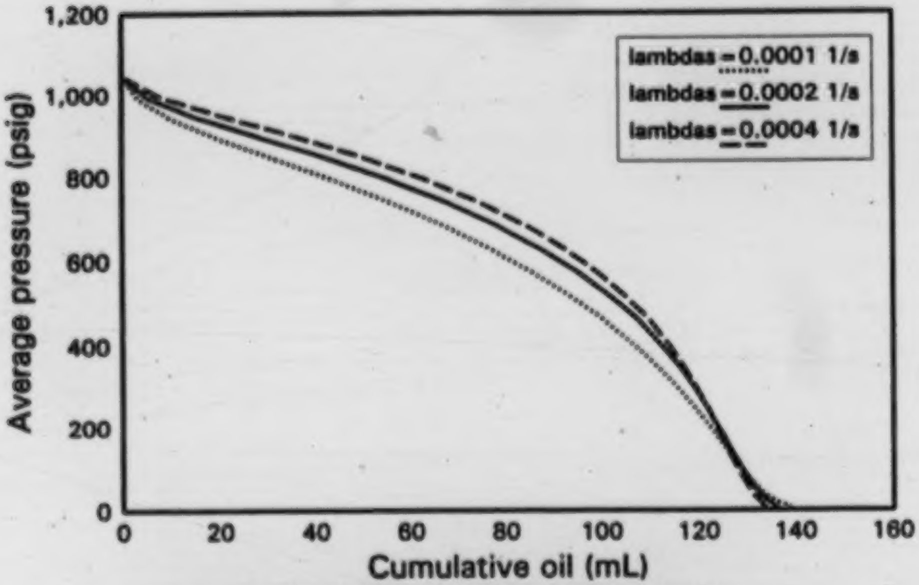

Fig. 6.10 - Effect of the supersaturation decay coefficient for a fast depletion test.

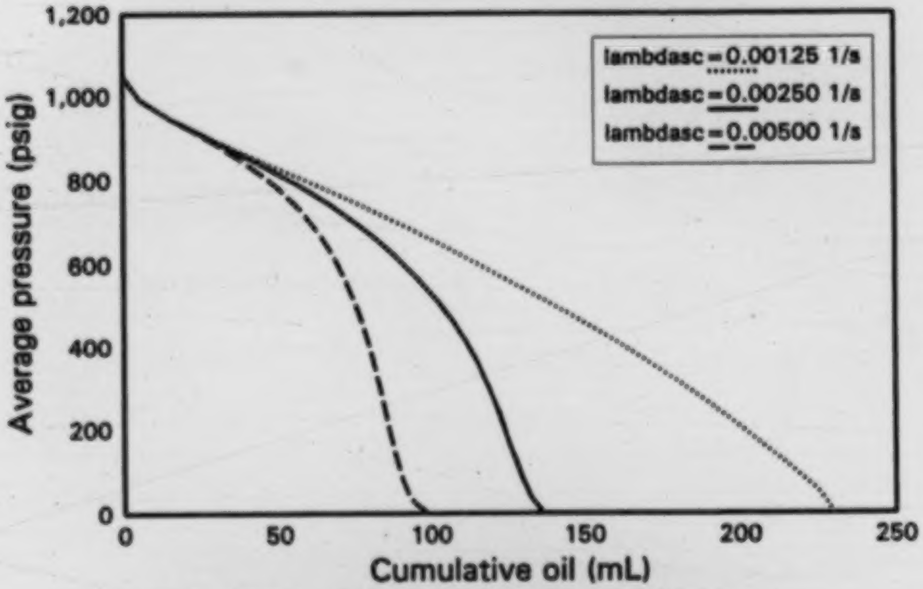

Fig. 6.11 - Effect of the dispersed gas decay coefficient for a fast depletion test.

However, oil recovery will be less sensitive to the decay coefficient in slow pressure decline cases. This can be observed from Figure 6.12 in which the data of Boscan 1 is used. The parameter λ_{sc} was also increased and decreased by a factor of 2, but the oil recoveries are not much different. Similarly, as shown in Figure 6.13, oil recovery is not very sensitive to λ_s in slow pressure decline cases. Therefore, λ_s and λ_{sc} obtained from history matching a very slow test should not be used to predict the performance of a fast test. In a very slow test close to the equilibrium state, the adjusted value of λ_s is likely to be small; and the adjusted value of λ_{sc} is likely to be large. These values could be misleading.

The adjusted values of λ_{sc} for the two fast depletion tests, Boscan 2 and Boscan 3, are 0.0025 s^{-1} and 0.0027 s^{-1}, respectively. These two values are very close. It seems that the same λ_{sc} may be used for prediction, if no other information can be used to determine λ_{sc}. This can be justified by the results of the sensitivity study of pressure decline rates. Figure 6.14 presents the calculated oil recoveries at different pressure decline rates. It shows that the higher oil recovery was predicted for the higher pressure decline rate, even if the same value of λ_s (2.0348×10^{-4} s^{-1}) and the same value of λ_{sc} (0.0025 s^{-1}) were used. These predictions are consistent with experimental observation in the sense that more oil is recovered at a higher pressure decline rate (Maini *et al.*, May and Sept., 1995).

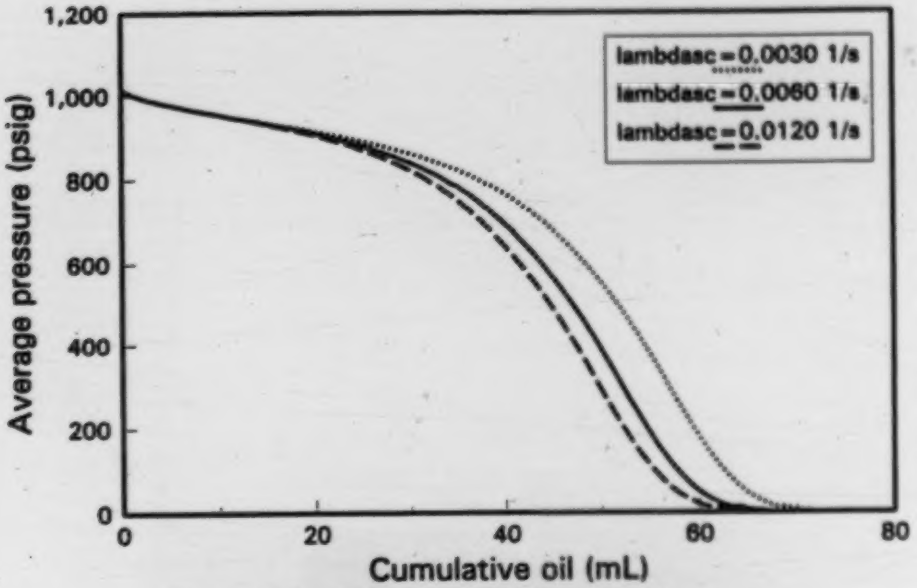

Fig. 6.12 - Effect of the dispersed gas decay coefficient for a slow depletion test.

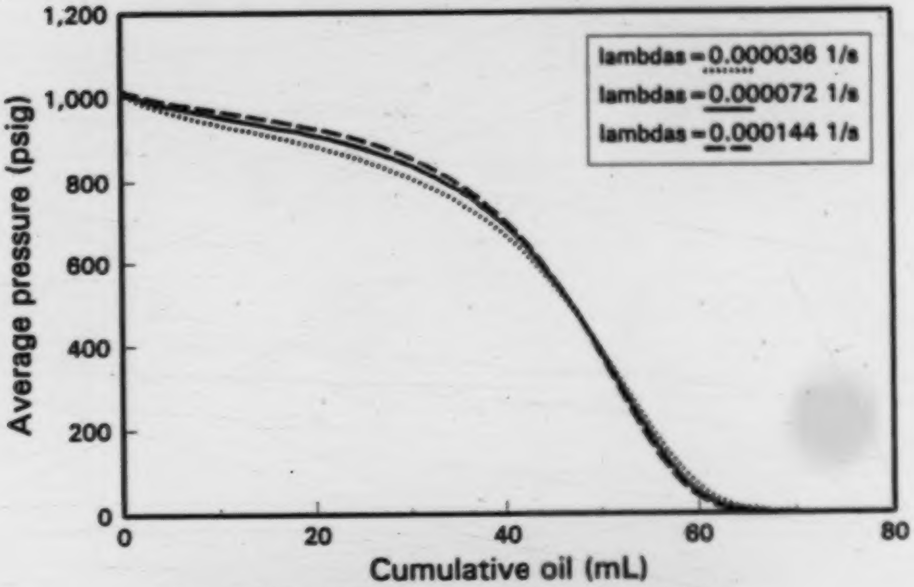

Fig. 6.13 - Effect of the supersaturation decay coefficient for a slow depletion test.

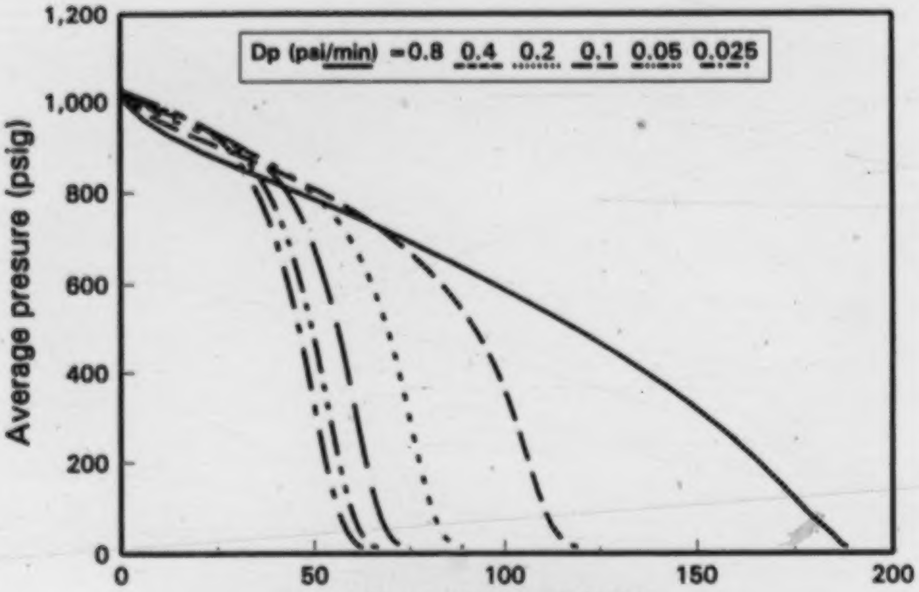

Fig. 6.14 - Effect of pressure decline rate.

6.6 Discussion of the Proposed Model

People have used existing simulators to history match and predict reservoir performance by adjusting the equilibrium properties of the rock-fluid system, such as the PVT characteristics, relative permeability, and often the critical gas saturation and absolute permeability. Figure 6.15 presents an example where the critical gas saturation has been adjusted. The depletion test, Boscan 3, was simulated with the equilibrium model by adjusting the critical gas saturation to 9%. Although the ultimate oil recovery was matched, the relationship between average pressure and cumulative oil did not follow the curve of the experimental data. For comparison, the simulated results from the dynamic model are also shown in this figure, which shows that the results well matched the experimental data. In some tests, if the equilibrium model is used, the adjusted critical gas saturations were over 20% or 30% which are likely unrealistic values. Therefore, the proposed model has improved the simulation of foamy oil flow over existing models.

Figure 6.16 presents an attempt to history match the Boscan 3 test by adjusting the absolute permeability using the equilibrium model. The absolute permeability was increased from 3.33 d to 3330 d, a 1000 fold increase. Figure 6.16 shows that the oil recovery is almost independent of the absolute permeability. Therefore, it is impossible to match the performance by adjusting the permeability in this case. Obviously, the mechanism causing the permeability increase does not contribute to the high recovery.

In addition, it was shown earlier in Section 6.5.3 that the higher oil recovery was predicted from the proposed model for the higher pressure decline rate, which is consistent with experimental observation. Therefore, the proposed model has captured some of the physics of foamy oil flow. By history matching the experiments and field performance under various operating conditions, this model can provide a tool to evaluate the significance of the dynamic processes under these conditions. However, although it provides a more reliable simulation of field performance, a short production history is needed to adjust λ_g and λ_{gc} before predicting the performance of a foamy oil reservoir, because the theory to determine these parameters has not been developed. Fortunately, these two parameters have different effects on the simulation results as discussed earlier in Section 6.5.3, and it is therefore relatively straightforward to adjust their values.

It has been observed that the values of the parameters, λ_g and λ_{gc}, vary with the

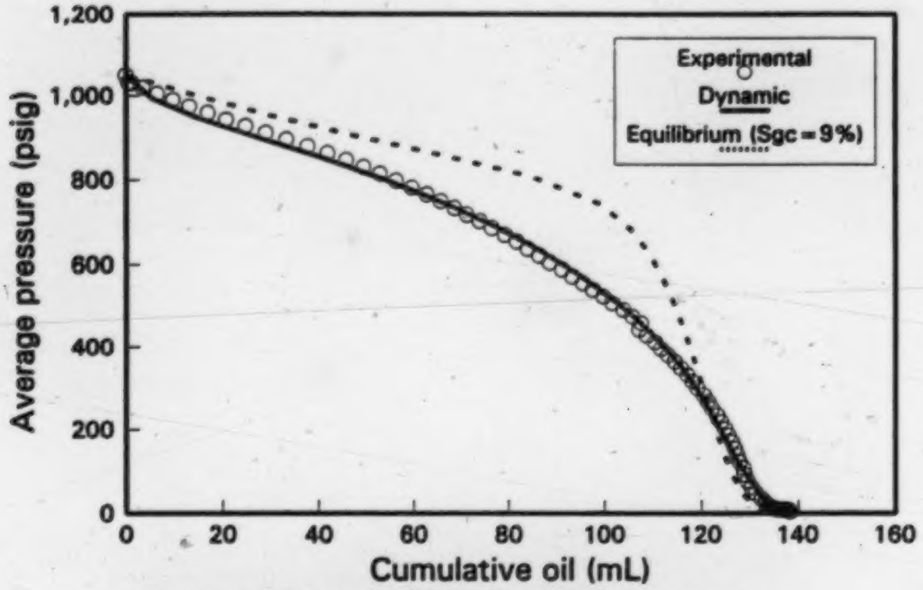

Fig. 6.15 - Comparison of the results from the dynamic model and the equilibrium model.

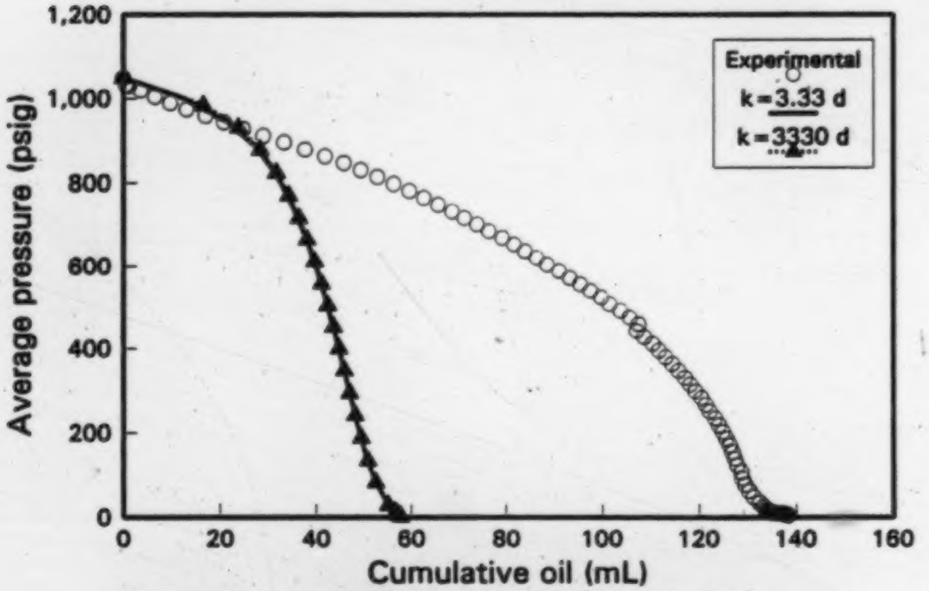

Fig. 6.16 - An attempt to match Boscan 3 by adjusting k using the equilibrium model.

pressure decline rate. Thus, it can inferred that their values may vary with the fluid velocity or the pressure gradient. An effort was made to modify these parameters to include the effect of the pressure gradient. Unfortunately, this effort was not successful because of a lack of experimental data.

6.7 Discussion of Simulation Results

In this flow model, two phenomena are included. One is the non-equilibrium phenomenon which is described by the process of bubble growth. The supersaturation decays exponentially and thus the amount of evolved gas increases according to the corresponding exponential function of time. Another is the unstable phenomenon which is described by the process of bubble decay. The dispersed gas bubbles gradually separate from the liquid oil phase to form a free phase. The amount of dispersed gas remaining in the oil phase decreases exponentially with time. The decay coefficient of supersaturation, λ_s, and the decay coefficient of dispersed gas, λ_{sc}, have been adjusted to history match the primary depletion tests. These two parameters may be used to evaluate the significance of these phenomena. The halflife, $t_{1/2}$, may be used to describe an exponential decay which is estimated from

$$t_{1/2} = \frac{0.693}{\lambda}. \tag{6-39}$$

The estimated halflives of the decays of supersaturation and dispersed gas are shown in Table 6.2. In Table 6.2, because λ_{dg} varies with pressure, an arbitrary pressure of 500 psia was chosen. The results for the three depletion tests in Table 6.2 show that the halflives of either supersaturation or dispersed gas are not more than 3 hours. Although these halflives are very short compared to the test period, they do not represent the degree of the non-equilibrium phenomenon and the unstable phenomenon in the tests, as will be discussed in the following.

Table 6.2 - Halflives of the Decays of Supersaturation and Dispersed Gas

Test	Supersaturation		Dispersed gas	
	λ_s (s^{-1})	Halflife (min)	λ_{dg} at 500 psia (s^{-1})	Halflife (min)
Boscan 1	7.18×10^{-5}	160.9	1.764×10^{-4}	65.5
Boscan 2	1.32×10^{-4}	87.5	7.938×10^{-5}	145.5
Boscan 3	2.0348×10^{-4}	56.8	7.35×10^{-5}	157.1

For a specific pressure drop, the solution gas evolves and thermodynamic equilibrium is reached within a short period of time. However, before this equilibrium is reached, more supersaturation is created because the pressure in the sand pack continues to decline. Therefore, the non-equilibrium phenomenon would exist during the whole period of a test, which can be seen in Figure 6.17. Figure 6.17 shows the supersaturation in the sand pack for the three depletion tests (Boscan 1 to Boscan 3). The calculation formula of the supersaturation in pressure is shown in Appendix B. The average supersaturations in Boscan 1, Boscan 2 and Boscan 3 are about 20 psia, 140 psia and 90 psia, respectively. The argument that the higher pressure decline rate would

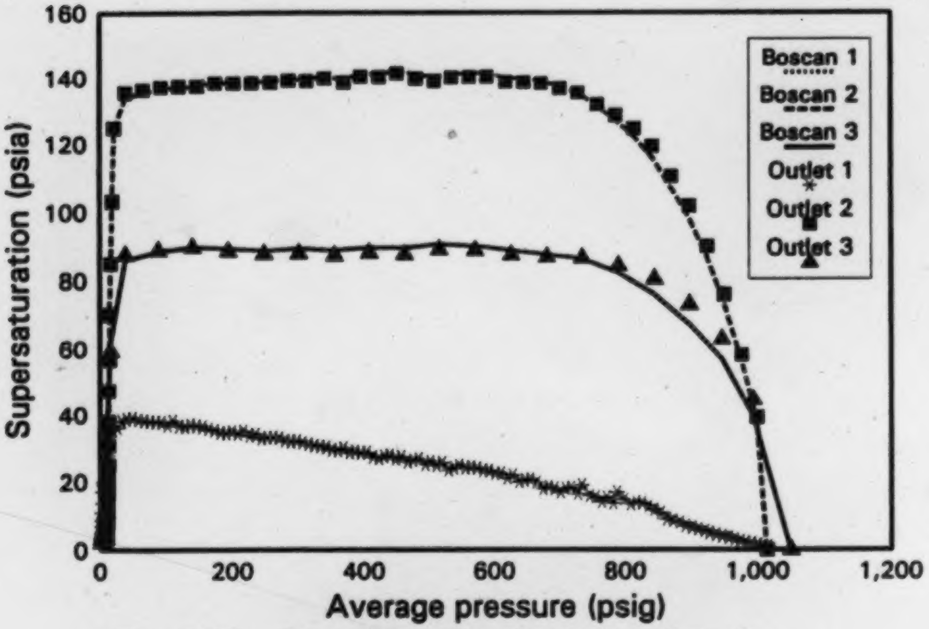

Fig. 6.17 - Supersaturation in the sand pack.

create higher supersaturation was not confirmed by these data. The supersaturation in Boscan 2 is higher than that in Boscan 3, while the pressure decline rate in Boscan 2 is lower than that in Boscan 3. Also, the final oil recovery in Boscan 2 is lower than that in Boscan 3. It seems that there is no direct relationship between supersaturation and oil recovery. This observation is not a surprise, because the optimum conditions for higher oil recovery should be fast gas evolution and slow gas disengagement from the liquid oil phase. Interestingly, it can seen from Figure 6.17 that the supersaturation at the outlet block (e.g., Outlet 1 for Boscan 1 in Figure 6.17) is very close to the average supersaturation in the whole sand pack.

Similarly, for a specific pressure drop, the dispersed gas bubbles separate from the liquid oil phase within a short period of time. However, before these bubbles totally separate from oil, new bubbles are dispersed in the oil because of the continuing pressure decline in the sand pack. Therefore, it is likely that there are always gas bubbles dispersed in the oil phase during the whole period of a test, which is shown in Figure 6.18. Figure 6.18 shows the volumetric fraction of dispersed gas in the sand pack for the three depletion tests. The maximum fractions in Boscan 1, Boscan 2 and Boscan 3 are about 0.5%, 4% and 9.5%, respectively. Figure 6.18 clearly shows that the higher the pressure decline rate is, the higher the volumetric fraction of dispersed gas would be. Since the higher pressure decline rate would result in a higher oil recovery, there is a direct relation between the fraction of dispersed gas in the oil and the oil recovery. In other words, the amount of gas dispersed in the oil phase is important to oil recovery. Also, the volumetric fraction at the outlet block (e.g., Outlet 1 for Boscan 1 in Figure 6.18) is very close to the average fraction in the whole sand pack.

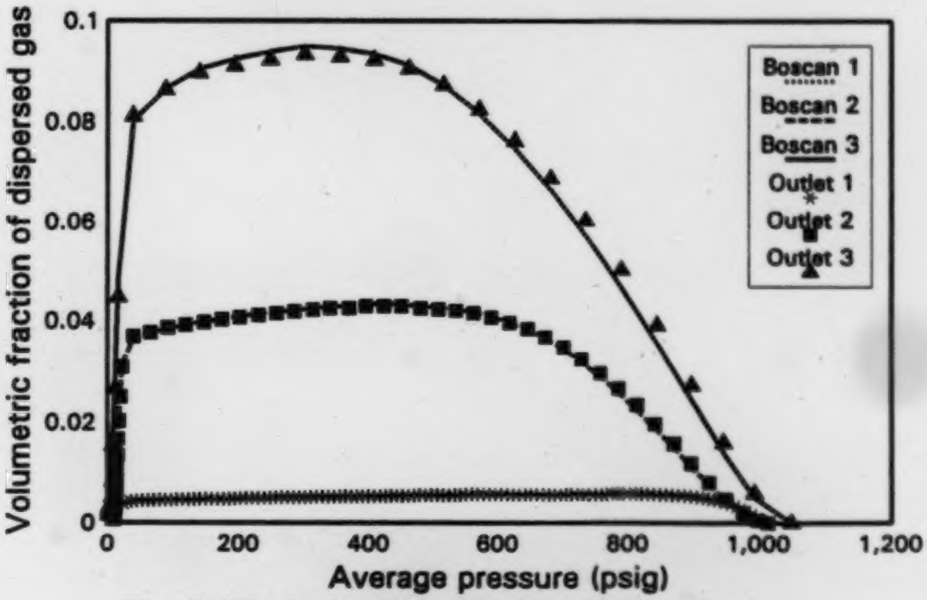

Fig. 6.18 - Volumetric fraction of dispersed gas in the sand pack.

6.8 Conclusions

Based on the simulation study, the following conclusions were drawn:

1. The proposed model captures the important features of foamy oil flow, especially dynamic processes. Therefore, it can be used to simulate foamy oil flow in porous media.
2. The model improves the simulation of foamy oil flow over existing models.
3. The model can provide a tool to evaluate the significance of dynamic processes under various operation conditions. It may be extended to investigate the effects of various process parameters on oil recovery and it may provide more reliable predictions of field performance.
4. The adjustable parameters, λ_s and λ_{sc}, in the model are likely to vary with the pressure decline rate.
5. The oil recovery is more sensitive to λ_{sc} than to λ_s; and the final oil recovery mainly depends on how many gas bubbles are dispersed in the oil.
6. Although the lifetimes of supersaturation and dispersed gas bubbles are short, supersaturation is likely to exist, and some gas bubbles are likely to be dispersed in the oil phase during the whole period of production, if the system pressure continues to decline.

6.9 References

Arya, A., Hewett, T.A., Larson, R.G. and Lake, L.W.: "Dispersion and Reservoir Heterogeneity," *SPERE* (Feb. 1988) 139-48.

Aziz, K. and Setarri, A.: *Petroleum Reservoir Simulation*, Applied Science Publishers Ltd., London (1979) 69.

Claridge, E.L. and Prats, M.: "A Proposed Model and Mechanism for Anomalous Foamy Heavy Oil Behaviour," paper SPE 29243 presented at the International Heavy Oil Symposium, Calgary, AB, June 19-21, 1995; *Proc.*, 9-20; also paper SPE 29243 (USMS, 1994).

Computer Modelling Group: *STARS 96.00, User's Guide*, Computer Modelling Group, Calgary, AB (1996).

Craft, B.C. and Hawkins, M.F.: *Applied Petroleum Reservoir Engineering*, 2nd edition, revised by R.E. Terry, Prentice-Hall, Inc., Englewood Cliffs, NJ (1991) 32.

Firoozabadi A., Ottesen, B. and Mikkelson, M.: "Measurements of Supersaturation and Critical Gas Saturation," *SPEFE* (Dec. 1992) 337-43.

Hawes, R.L., Dawe, R.A. and Evans, R.N.: "Depressurisation of Waterflooded Reservoirs: The Critical Gas Saturation," paper SPE/DOE 27753 presented at the SPE/DOE 9th Symposium on Improved Oil Recovery, Tulsa, OK, April 17-20, 1994.

Kamath, J. and Boyer, R.E.: "Critical Gas Saturation and Supersaturation in Low-Permeability rocks," paper SPE 26663 presented at the 68th Annual Technical Conference and Exhibition, Houston, TX, Oct. 3-6, 1993; also *SPEFE* (Dec. 1995) 10, No. 4, 247-53.

Kortekaas, T.F.M. and van Poelgeest, F.: "Liberation of Solution Gas During Pressure Depletion of Virgin Watered-Out Oil Reservoirs," *SPERE* (Aug. 1991) 329-35.

Kraus, W.P., McCaffrey, W.J. and Boyd, G.W.: "Pseudo-Bubble Point Model for Foamy Oils," paper CIM 93-45 presented at the 44th Annual Technical Conference of the Petroleum Society of CIM, Calgary, AB, May 9-12, 1993.

Laxity-Briceno, D.: *Simulation of High Pressure Gas Drive - A Compositional Approach*, M.Sc. thesis, University of Alberta, Edmonton, AB (1985).

Lebel, J.P.: "Performance Implications of Various Reservoir Access Geometries," paper presented at the 11th Annual Heavy Oil & Oil Sands Technical Symposium, March 2, 1994.

Maini, B.B.: "Is it Futile to Measure Relative Permeability for Heavy Oil Reservoirs?" paper 95-97 presented at the 46th Annual Technical Meeting of the Petroleum Society of CIM, Banff, AB, May 14-17, 1995.

Maini, B.B., Sheng, J.J. and Nicola, F.: "Foamy Oil Flow - Improved Primary Heavy Oil Recovery," paper presented at the Annual Conference and Exhibit of the Petroleum Recovery Institute, Calgary, AB, May 25, 1995.

Maini, B.B., Sheng, J.J. and Nicola, F.: "Laboratory Investigation of Foamy Oil Flow for Improved Primary Production," Final Report to CANMET (Sept. 1995).

Muqeem, M.: "*Effect of Temperature on Three-Phase Relative Permeability,*" Ph.D. dissertation, University of Alberta (1994).

Reid, R.C., Prausnitz, J.M. and Poling B.E.: *The properties of Gases and Liquids*, 4th Edition, McGraw-Hill Book Company (1987), 399.

Riggs, J.B.: "A Systematic Approach to Modeling," *Chemical Engineering Education* (Winter 1988) 26-29.

Sheng, J.J. and Zhou, X.: "Computing and Selecting Parameters in Numerical Modelling of Oil Field Thermal Recovery," *Special Oil & Gas Reservoirs* (1995) **2**, No. 3, 15-22 (Chinese).

Stewart, C.R., Hunt, E.B., Jr., Schneider, F.N., Geffen, T.M. and Berry, V.J., Jr.: "The Role of Bubble Formation in Oil Recovery by Solution Gas Drive in Limestones," *Trans.* (1954), AIME, **201**, 294-301.

Chapter 7

Conclusions and Recommendations

7.1 Conclusions

Based on this study, the conclusions which can be drawn are summarized in the following issues.

7.1.1 Definition of Foamy Oil

Generally, a dispersion of gas-liquid is called foam when the volume concentration is very high (from 50% to > 90%) (de Vries, 1958). However, the results of the foamy oil stability tests presented in Chapter 4 show that the maximum volume fractions of dispersed gas bubbles are less than 20% in any of the tests. For the pressure depletion tests in the sand pack, the history-matched results using the dynamic flow model described in Chapter 6 show that the maximum volume fraction of dispersed gas is only 9.5% (see Figure 6.18). According to the volume fraction, it seems that the name foamy oil may not be the most appropriate name to describe such a dispersion of gas bubbles in the oil.

7.1.2 Foamy Oil Stability

The experimental results presented in Chapter 4 show that foamy oil stability increases with higher oil viscosity, higher oil column, higher dissolved gas content and higher pressure decline rate. It is also shown that, although the asphaltene content improves foamy oil stability, this improvement was not observed to be significant. Foamy oil could be more stable in porous media than in a bulk vessel.

7.1.3 Foamy Oil Properties

Since foamy oil is related to the dynamic processes of bubble nucleation, bubble growth and bubble disengagement from the liquid oil, the properties are not only pressure-dependent, but also time-dependent. The discussion in Section 2.2.2.1 shows that the foamy oil compressibility is mainly dependent upon the amount of gas dispersed in the oil. It is also shown that the time-dependent effect is very important to foamy oil properties.

According to the discussion and understanding presented in Chapter 3, the proposed oil viscosity reduction models (Smith, 1988; Poon and Kisman, 1992; Claridge and Prats, 1995; Shen and Batycky, 1996) do not seem to be plausible. Based on the theory of dispersion viscosity and the simple derivation of the foamy oil viscosity presented in Section 3.4, it is most likely that the oil viscosity would be increased if gas bubbles are dispersed in the oil phase.

7.1.4 Description of Dynamic Processes

7.1.4.1 Bubble Nucleation

Based on the discussion of the literature on bubble nucleation in Section 5.2.1, it is reasonable to assume that the nucleation in porous media is instantaneous and heterogeneous nucleation.

7.1.4.2 Bubble Growth

For a constant pressure drop, the amount of the evolved gas could be estimated by a power-law function of time as an approximation:

$$n_{eg}(t) = n_{eq}\left[\frac{t_{eg}}{t_{eq}}\right]^{b}. \tag{7-1}$$

When the effects of all factors controlling bubble growth are incorporated, especially the effect of porous media which has not been formulated quantitatively, the relationship between the amount of evolved gas and time could be very complex. By adjusting b and t_{eq} to match a set of experimental data or field data, one may incorporate these effects into a simple relationship which can be easily implemented into a flow model. Because of the effect of the porous medium, the values of b and t_{eq} in porous media could be different from those in a bulk vessel.

7.1.4.3 Bubble Disengagement

The mechanisms of bubble disengagement are far from fully understood. Empirically, an exponential decay could be used to describe the disengagement of dispersed gas from the liquid oil:

$$n_{dg}(t) = n_{dg}(0)\exp\left(-\lambda_{dg}t_{dg}\right). \tag{7-2}$$

The value of the decay coefficient, λ_{dg}, in porous media could be different from that in a bulk vessel because of the effect of the porous medium.

7.1.4.4 Dynamic Models to Describe the Dynamic Processes

The preceding Sections 7.1.4.1 to 7.1.4.3 summarize the description of the dynamic processes for a constant pressure drop. When the system pressure is declining gradually, the total pressure drawdown can be modelled as a series of small step drops in pressure. The dynamic processes are considered for each step. The effect of the total pressure change is the sum of effects of these small step changes. Model 1 described in Chapter 5 is based on this concept.

Model 1 is theoretically sound in that it takes bubble age into account. However, it is difficult to include the bubble ages of different oils in a numerical flow model. Therefore, Model 2 and Model 3 are proposed to avoid this fault. In Model 2, supersaturation is assumed to decay by a power-law function of time, while in Model 3, an exponential decay is assumed. Consequently, the bubble growth is described by a power-law function and an exponential function of time in Model 2 and Model 3, respectively. In both models, the decay of dispersed gas is assumed to be exponential. It was observed that the results from Model 3 are less sensitive to the time step size than are those from Model 2.

7.1.5 Dynamic Flow Model

Based on the studies in other chapters, especially the dynamic processes in Chapter 5, a dynamic model for foamy oil flow in porous media was proposed in Chapter 6. This flow model has considered the dynamic processes and thus has captured the important features of foamy oil flow. Therefore, it can be used to simulate foamy oil flow in porous media. It has improved the simulation of foamy oil flow over other existing models. It also provides a tool to evaluate the significance of the dynamic processes under various operation conditions. Although it can be used to provide a more reliable simulation of field performance, a short production history is needed to adjust λ_g and λ_{gr} before predicting the performance of a foamy oil reservoir, because the theory to determine these parameters has not been developed. It seems that the values of λ_g and λ_{gr} are pressure-decline-rate dependent, which limits the model's capacity for prediction.

7.1.6 Recovery Mechanisms Involved in Foamy Oil Reservoirs

The reported theoretical and experimental studies of the recovery mechanisms involved in solution-gas-drive foamy oil reservoirs are very limited. The mechanisms related to the reduced oil viscosity have not been verified by experimental studies. One obviously important mechanism involved in heavy oil recovery is the more effective utilization of expansion energy from the foamy oil system. Because of the low gas diffusivity in heavy oils, it takes time for the solution gas to be evolved. Also, because of the high viscosity of the oil and/or other factors, gas cannot separate from the oil rapidly. Expanding gradually, gas provides the energy that drives the crude oil through the formation. As discussed in Section 6.7, although the lifetimes of supersaturation and dispersed gas bubbles are short, supersaturation is likely to exist, and some gas bubbles are likely to be dispersed in the oil phase during production when the pressure continues to decline fast (see Figures 6.17 and 6.18). The discussions in Sections 2.2.2.1, 5.5 and 6.5.3 show that the amount of gas dispersed in the oil or the process of bubble disengagement most significantly affects foamy oil properties and foamy oil flow behaviour.

From the discussion in Section 2.5, it seems that one of the mechanisms of unusually high oil recovery in solution gas drive reservoirs is related to high permeability channels such as fractures, fissures and wormholes, etc. High permeability channels probably provide a condition to generate high pressure gradients. As discussed in Section 2.3.4.3, the high pressure gradient enhances foamy oil behaviour.

7.1.7 Effects of Pressure Decline Rate

The pressure decline rate is an important parameter in foamy oil flow. Its effects on foamy oil flow are discussed in the following.

(1) The literature reviewed in Section 5.2.1.1 shows that the degree of supersaturation most likely increases as the pressure decline rate increases. As a result, more bubbles are formed for higher pressure decline rates. Subsequently, the pressure decline rate affects the rate of bubble growth and the rate of bubble decay or the stability of foamy oils. Higher volumetric fractions of dispersed gas were observed for higher pressure decline rates (Figure 6.18); and foamy oil stability increased with the higher

pressure decline rates (Section 4.4.5).

(2) From Table 2.1, it can be accepted generally that S_{gc} increases with an increase in pressure decline rate. Consequently, the pressure decline rate also affects the relative permeabilities.

(3) Higher oil recoveries can be obtained when the pressure decline rate is higher. This conclusion was directly supported by experimental studies (Handy, 1958; Maini *et al.*, May and Sept., 1995), the discussion presented in Section 2.3.4.3, and the simulation results (Section 6.5.3 or Figure 6.14). It can also be indirectly inferred from the effect of the pressure decline rate on S_{gc}.

7.2 Recommendations for Future Work

Based on the understanding gained from this study, it is recommended that future work focus on the following issues.

(1) The low production GOR in foamy oil reservoirs suggests that, for future investigations into foamy oil recovery mechanisms, attention should be paid to the factors that cause low gas relative permeability. The viscous coupling effect in foamy oil flow should be investigated.

(2) Foamy oil mobility remains unexplored which includes the issues of oil/gas relative permeabilities and foamy oil viscosity. It presents several challenges. It is

recommended that future work focus on the effects of gas bubbles of different sizes on oil viscosity and relative permeabilities.

(2) Foamy oil flow is associated with bubble formation, bubble growth and the eventual disengagement of gas bubbles from the liquid oil. In the flow model proposed in Chapter 6, the foamy oil phase containing dispersed gas bubbles is treated as a pseudo-single phase; and these bubbles flow with the oil. For further work, it should be considered at what size and at what conditions the relative phase velocity would become non-zero. Also, it should be explored how dispersed gas bubbles whose sizes are larger than the pore sizes would affect oil flow in porous media. The effect of bubble size can be included in the present model by adding additional gas components representing different sizes of gas bubbles.

(4) The adjustable parameters, λ_g and λ_{gc}, used to describe the dynamic processes in the flow model are likely to vary with the pressure decline rate. Thus they would vary with the pressure gradient or the flow velocity of the fluids. For future work, these parameters should be modified to include the effect of flow velocity for the simulation of practical field performance. Such work is recommended to be conducted in one of the following ways:

(i) Conduct a number of primary depletion tests with the same oil using a linear sand pack as described in Figure 6.4. In these tests, only the pressure decline rate is changed. The flow model is used to history match these tests by adjusting λ_g and λ_{gc}. By analyzing the values of λ_g and λ_{gc} for different tests, a correlation between λ_g or λ_{gc} and the pressure decline rate (or the flow velocity) may be obtained. This correlation may be extrapolated to field cases.

(ii) Conduct several primary depletion tests in a radial geometry sand pack. The linear flow model presented in Chapter 6 is converted into a radial model. The radial model is used to history match these tests. By modifying λ_s and λ_{sc} to include the effect of flow velocity so that the tests are history matched, we may find how λ_s and λ_{sc} are related to the flow velocity or the pressure gradient.

(5) It has been observed in the laboratory that when the pressure decline rate is very low (e.g., Boscan 1 discussed in Chapter 6), the production performance can be estimated using conventional solution gas drive theory. If the effect of the pressure decline rate is extrapolated to field conditions, the unusually high primary production should not be observed. However, some heavy oil reservoirs do show unusually high performance. This puzzle needs to be explored. It is recommended that a reservoir which is observed to show obvious foamy oil behaviour should be investigated in detail.

(6) It is recommended that the mechanisms of foam formation and decay for conventional foams, such as snap-off and lamella division, should be investigated for their roles in foamy oil flow, when the effect of flow velocity or the pressure gradient is studied.

7.3 References

Claridge, E.L. and Prats, M.: "A Proposed Model and Mechanism for Anomalous Foamy Heavy Oil Behaviour," paper SPE 29243 presented at the International Heavy Oil Symposium, Calgary, AB, June 19-21, 1995; *Proc.*, 9-20; also paper

SPE 29243 (USMS, 1994).

de Vries, A.J.: "Foam Stability, Part I. Structure and Stability of Foams," *Rec. Trav. Chim.* (1958) **77**, 81-91 (English).

Handy, L.L.: "A Laboratory Study of Oil Recovery by Solution Gas Drive," *Trans.* (1958), AIME, **213**, 310-15.

Maini, B.B., Sheng, J.J. and Nicola, F.: "Foamy Oil Flow - Improved Primary Heavy Oil Recovery," paper presented at the Annual Conference and Exhibit of the Petroleum Recovery Institute, Calgary, AB, May 25, 1995.

Maini, B.B., Sheng, J.J. and Nicola, F.: "Laboratory Investigation of Foamy Oil Flow for Improved Primary Production," Final Report to CANMET (Sept. 1995).

Poon, D.C. and Kisman, K.: "Non-Newtonian Effects on the Primary Production of Heavy Oil Reservoirs," *JCPT* (Sept. 1992) **31**, No.7, 55-59; also paper CIM/AOSTRA 91-33 presented at the CIM/AOSTRA Technical Conference, Banff, AB, April 21-24, 1991.

Shen, C. and Batycky, J.P.: "Some Observations of Mobility Enhancement of Heavy Oils Flowing through Sand Pack under Solution Gas Drive," paper 96-27 presented at the 47th Annual Technical Conference of the Petroleum Society of CIM, Calgary, AB, June 10-12, 1996.

Smith, G.E.: "Fluid Flow and Sand Production in Heavy Oil Reservoirs Under Solution Gas Drive," *SPEPE* (May 1988) 169-80.

Appendix A

Mathematical Formulation of the Numerical Flow Model

A.1 Basic Finite-Difference Formulation

The following identities are employed in this formulation:

$$\delta u \equiv u^{n+1} - u^{n}, \tag{A-1}$$

$$\begin{aligned}\delta(u_1 u_2) &\equiv (u_1 u_2)^{n+1} - (u_1 u_2)^{n} \\ &\equiv u_1^{n+1}\delta u_2 + u_2^{n}\delta u_1 \equiv u_2^{n+1}\delta u_1 + u_1^{n}\delta u_2,\end{aligned} \tag{A-2}$$

$$\Delta(\Delta u) = [u_{i+1} - u_i] - [u_i - u_{i-1}]. \tag{A-3}$$

Here u represents an unknown variable which is x_{dg}, x_{sg}, S_{fo} or p. The formulation involves variables dated at the new time level $n+1$. Since these new time level values are unknown until convergence, all such $n+1$ level variables are approximated in the calculation by their latest (l) iterative values. When an interblock property is calculated, the values of the parameters at the upstream block are used. The upstream block is determined at the start of each iteration $l+1$ by the values of pressure.

The four mass conservation equations for the four components in finite difference form are repeated as follows.

The dead oil component in the foamy oil phase:

$$\frac{V}{\Delta t}\delta(\phi S_{fo}\rho_{fo}x_{do}) = \Delta(T_{fo}x_{do}\Delta p) - q_{fo}x_{do}. \tag{6-15}$$

The solution gas component in the foamy oil phase:

$$\frac{V}{\Delta t}\delta(\phi S_{fo}\rho_{fo}x_{sg}) = \Delta(T_{fo}x_{sg}\Delta p) - q_{fo}x_{sg} - R_{sg\to eg}. \tag{6-16}$$

The free gas component in the gas phase:

$$\frac{V}{\Delta t}\delta(\phi S_{g}\rho_{g}) = \Delta(T_{fg}\Delta p) - q_{fg} + R_{eg\to fg} + R_{dg\to fg}. \tag{6-17}$$

The dispersed gas component in the foamy oil phase:

$$\frac{V}{\Delta t}\delta(\phi S_{fo}\rho_{fo}x_{dg}) = \Delta(T_{fo}x_{dg}\Delta p) - q_{fo}x_{dg} + R_{eg\to dg} - R_{dg\to fg}. \tag{6-18}$$

In the above equations, δ represents the time difference, while Δ represents the space difference. The term $\Delta(T\Delta p)$ denotes the net mass flow into the grid block due to interblock flow. For block i in a 1D problem,

$$\Delta(T\Delta p) = T_{i+1/2}(p_{i+1}-p_i) - T_{i-1/2}(p_i-p_{i-1}), \tag{6-19}$$

where

$$T_{i\pm1/2} = \left[\frac{Akk_r\rho}{(\Delta X)\mu}\right]_{i\pm1/2}. \tag{6-20}$$

For the left-hand side (LHS) of Eq. 6-15,

$$\begin{aligned} LHS & \\ &= \frac{V}{\Delta t}\{x_{do}^{n+1}\,\delta(\phi\rho_{fo}S_{fo}) + (\phi\rho_{fo}S_{fo})^{n}\,\delta x_{do}\} \\ &= \frac{V}{\Delta t}\{x_{do}^{n+1}\,[S_{fo}^{n}\,\delta(\phi\rho_{fo}) + (\phi\rho_{fo})^{n+1}\,\delta S_{fo}] + (\phi\rho_{fo}S_{fo})^{n}\,\delta x_{do}\} \\ &= \frac{V}{\Delta t}\{x_{do}^{n+1}\,[S_{fo}^{n}\,(\phi^{n+1}\delta\rho_{fo} + \rho_{fo}^{n}\delta\phi) + (\phi\rho_{fo})^{n+1}\,\delta S_{fo}] + (\phi\rho_{fo}S_{fo})^{n}\,\delta x_{do}\}. \end{aligned} \tag{A-4}$$

One has

$$\frac{1}{\rho_{fo}} = \frac{x_{do}}{\rho_{do}} + \frac{x_{sg}}{\rho_{sg}} + \frac{x_{dg}}{\rho_{dg}}, \tag{A-5}$$

where

$$\rho_{do}^{-1} = \nu_{do} = \nu_{do,sc}\,[1-c_{do}(p-p_{sc})]\,[1+\beta_{do}(T-T_{sc})], \tag{A-6}$$

$$\rho_{sg}^{-1} = \nu_{sg} = \nu_{sg,sc}\,[1-c_{sg}(p-p_{sc})]\,[1+\beta_{sg}(T-T_{sc})], \tag{A-7}$$

$$\rho_{dg} = \frac{p}{zRT}. \tag{A-8}$$

At isothermal conditions, these densities are a function of pressure only; that is

$$\rho_c = \rho_c(p), \quad c = do,\ sg,\ or\ dg. \tag{A-9}$$

Also

$$x_{do} = 1 - x_{sg} - x_{dg}. \tag{A-10}$$

Then

$$\begin{aligned} &\delta\rho_{fo} \\ &\equiv \delta\rho_{fo}(x_{dg},\ x_{sg},\ p) \\ &= \rho_{fo,\,x_{dg}}\delta x_{dg} + \rho_{fo,\,x_{sg}}\delta x_{sg} + \rho_{fo,p}\delta p, \end{aligned} \tag{A-11}$$

where

$$\rho_{fo,\,x_{dg}} = \frac{\rho_{fo}(x_{dg}^{n+1},\ x_{sg}^{n},\ p^{n+1}) - \rho_{fo}(x_{dg}^{n},\ x_{sg}^{n},\ p^{n+1})}{x_{dg}^{n+1} - x_{dg}^{n}}, \tag{A-12}$$

$$\rho_{fo,\,x_{sg}} = \frac{\rho_{fo}(x_{dg}^{n+1},\ x_{sg}^{n+1},\ p^{n+1}) - \rho_{fo}(x_{dg}^{n+1},\ x_{sg}^{n},\ p^{n+1})}{x_{sg}^{n+1} - x_{sg}^{n}}, \tag{A-13}$$

$$\rho_{fo,p} = \frac{\rho_{fo}(x_{dg}^{n},\ x_{sg}^{n},\ p^{n+1}) - \rho_{fo}(x_{dg}^{n},\ x_{sg}^{n},\ p^{n})}{p^{n+1} - p^{n}}. \tag{A-14}$$

The porosity is treated as a function of pressure according to

$$\phi = \phi^0[1 + c_f(p-p^0)]. \tag{A-15}$$

Thus, the left-hand side can be expanded as

$$
\begin{aligned}
&LHS \\
&= \frac{V}{\Delta t}\{x_{ao}^{n+1}[S_{fp}^{n}(\phi^{n+1}(\rho_{fp,x_{ag}}\delta x_{ag} + \rho_{fp,x_{sg}}\delta x_{sg} + \rho_{fp,p}\delta p) \\
&+ \rho_{fp}^{n}\delta\phi) + (\phi\rho_{fp})^{n+1}\delta S_{fp}] + (\phi\rho_{fp}S_{fp})^{n}\delta x_{ao}\} \\
&= \frac{V}{\Delta t}\{-(\phi\rho_{fp}S_{fp})^{n} + x_{ao}^{n+1}S_{fp}^{n}\phi^{n+1}\rho_{fp,x_{ag}}\}\ \delta x_{ag} \qquad \text{(A-16)} \\
&+ \frac{V}{\Delta t}\{-(\phi\rho_{fp}S_{fp})^{n} + x_{ao}^{n+1}S_{fp}^{n}\phi^{n+1}\rho_{fp,x_{sg}}\}\ \delta x_{sg} \\
&+ \frac{V}{\Delta t}\{(x_{ao}\phi\rho_{fp})^{n+1}\}\ \delta S_{fp} \\
&+ \frac{V}{\Delta t}\{x_{ao}^{n+1}S_{fp}^{n}\ (\phi^{n+1}\rho_{fp,p} + \rho_{fp}^{n}\phi^{0}c_{r})\}\ \delta p.
\end{aligned}
$$

For the right-hand side (RHS) of Eq. 6-15,

$$
\begin{aligned}
&RHS \\
&= \Delta[(T_{fp}x_{ao})^{n+1}(\Delta p^{n} + \Delta\delta p)] - (q_{fp}x_{ao}) \qquad \text{(A-17)} \\
&= \Delta[(T_{fp}x_{ao})^{n+1}\Delta\delta p] + \Delta[(T_{fp}x_{ao})^{n+1}\Delta p^{n}] - (q_{fp}x_{ao})^{n},
\end{aligned}
$$

where

$$
T_{fp} = \frac{Akk_{rp}}{(\Delta X)\mu_{fp}}\rho_{fp}. \qquad \text{(A-18)}
$$

Here the production term $q_{fp}x_{ao}$ is temporally formulated explicitly, i.e., evaluated at time step n. To improve the stability, it is necessary to treat the production terms implicitly as formulated later in Section A.2.

As a result, Eq. 6-15 becomes:

$$C_{11}\delta x_{dg} + C_{12}\delta x_{sg} + C_{13}\delta S_{fo} + C_{14}\delta p = Y_1 + R_1, \qquad \text{(A-19)}$$

where

$$C_{11} = \frac{V}{\Delta t}\,\{-(\phi\rho_{fo}S_{fo})^n + x_{do}^{n+1}S_{fo}^n\phi^{n+1}\rho_{fo,\,x_m}\}, \qquad \text{(A-20)}$$

$$C_{12} = \frac{V}{\Delta t}\,\{-(\phi\rho_{fo}S_{fo})^n + x_{do}^{n+1}S_{fo}^n\phi^{n+1}\rho_{fo,\,x_m}\}, \qquad \text{(A-21)}$$

$$C_{13} = \frac{V}{\Delta t}\,\{(x_{do}\phi\rho_{fo})^{n+1}\}, \qquad \text{(A-22)}$$

$$C_{14} = \frac{V}{\Delta t}\,\{x_{do}^{n+1}S_{fo}^n(\phi^{n+1}\rho_{fo,p} + \rho_{fo}^n\phi^0 c_f)\}, \qquad \text{(A-23)}$$

$$R_1 = \Delta[(T_{fo}x_{do})^{n+1}\Delta p^n] - (q_{fo}x_{do})^n, \qquad \text{(A-24)}$$

$$Y_1 = \Delta[(T_{fo}x_{do})^{n+1}\Delta\delta p]. \qquad \text{(A-25)}$$

Similarly, Eq. 6-16 is:

$$C_{21}\delta x_{dg} + C_{22}\delta x_{sg} + C_{23}\delta S_{fo} + C_{24}\delta p = Y_2 + R_2, \qquad \text{(A-26)}$$

where

$$C_{21} = \frac{V}{\Delta t}\,\{x_{sg}^{n+1}S_{fo}^n\phi^{n+1}\rho_{fo,\,x_m}\}, \qquad \text{(A-27)}$$

$$C_{22} = \frac{V}{\Delta t}\,\{(\phi\rho_{fo}S_{fo})^n + x_{sg}^{n+1}S_{fo}^n\phi^{n+1}\rho_{fo,\,x_m}\}, \qquad \text{(A-28)}$$

$$C_{23} = \frac{V}{\Delta t}\,\{(x_{sg}\phi\rho_{fo})^{n+1}\}, \qquad \text{(A-29)}$$

$$C_{24} = \frac{V}{\Delta t}\ \{x_{sg}^{n+1} S_{fr}^{n}(\phi^{n+1}\rho_{fr,p} + \rho_{fr}^{n}\phi^{0}c_{f})\}, \tag{A-30}$$

$$R_2 = \Delta[(T_{fr}x_{sg})^{n+1}\Delta p^{n}] - (q_{fr}x_{sg})^{n} - R_{sg\to eg}, \tag{A-31}$$

$$Y_2 = \Delta[(T_{fr}x_{sg})^{n+1}\Delta\delta p]. \tag{A-32}$$

Eq. 6-17 is:

$$C_{31}\delta x_{dg} + C_{32}\delta x_{sg} + C_{33}\delta S_{fr} + C_{34}\delta p = Y_3 + R_3, \tag{A-33}$$

where

$$C_{31} = 0, \tag{A-34}$$

$$C_{32} = 0, \tag{A-35}$$

$$C_{33} = \frac{V}{\Delta t}\ \{-(\phi\rho_{g})^{n+1}\}, \tag{A-36}$$

$$C_{34} = \frac{V}{\Delta t}\ \{S_{g}^{n}(\phi^{n+1}\rho_{g,p} + \rho_{g}^{n}\phi^{0}c_{f})\}, \tag{A-37}$$

$$R_3 = \Delta(T_{g}^{n+1}\Delta p^{n}) - q_{g}^{n} + R_{sg\to fg} + R_{dg\to fg}, \tag{A-38}$$

$$Y_3 = \Delta(T_{g}^{n+1}\Delta\delta p). \tag{A-39}$$

Eq. 6-18 is:

$$C_{41}\delta x_{dg} + C_{42}\delta x_{sg} + C_{43}\delta S_{fr} + C_{44}\delta p = Y_4 + R_4, \tag{A-40}$$

$$C_{41} = \frac{V}{\Delta t}\ \{(\phi \rho_{fo} S_{fo})^n + x_{dg}^{n+1} S_{fo}^n \phi^{n+1} \rho_{fo,x_{dg}}\}, \tag{A-41}$$

$$C_{42} = \frac{V}{\Delta t}\ \{x_{dg}^{n+1} S_{fo}^n \phi^{n+1} \rho_{fo,x_{dg}}\}, \tag{A-42}$$

$$C_{43} = \frac{V}{\Delta t}\ \{(x_{dg} \phi \rho_{fo})^{n+1}\}, \tag{A-43}$$

$$C_{44} = \frac{V}{\Delta t}\ \{x_{dg}^{n+1} S_{fo}^n (\phi^{n+1} \rho_{fo,p} + \rho_{fo}^n \phi^0 c_p)\}, \tag{A-44}$$

$$R_4 = \Delta[(T_{fo} x_{dg})^{n+1} \Delta p^n] - (q_{fo} x_{dg})^n + R_{eg \to dg} - R_{dg \to fg}, \tag{A-45}$$

$$Y_4 = \Delta[(T_{fo} x_{dg})^{n+1} \Delta \delta p]. \tag{A-46}$$

The above four mass balance equations can be represented by

$$\begin{bmatrix} C_{11} & C_{12} & C_{13} & C_{14} \\ C_{21} & C_{22} & C_{23} & C_{24} \\ C_{31} & C_{32} & C_{33} & C_{34} \\ C_{41} & C_{42} & C_{43} & C_{44} \end{bmatrix} \begin{bmatrix} \delta x_{dg} \\ \delta x_{sg} \\ \delta S_{fo} \\ \delta p \end{bmatrix} = \begin{bmatrix} 1 & & & \\ & 1 & & \\ & & 1 & \\ & & & 1 \end{bmatrix} \begin{bmatrix} Y_1 \\ Y_2 \\ Y_3 \\ Y_4 \end{bmatrix} + \begin{bmatrix} R_1 \\ R_2 \\ R_3 \\ R_4 \end{bmatrix}. \tag{A-47}$$

The four equations are arranged in such an order that the diagonal coefficients would be the maximum. Also, it is considered that the dispersed gas will not exist in the early and later stages of depletion; thus some coefficients of the equation for the dispersed gas will be zero.

By the Gaussian elimination process, the above matrix form can be transformed to

$$\begin{bmatrix} 1 & A_{12} & A_{13} & A_{14} \\ & 1 & A_{23} & A_{24} \\ & & 1 & A_{34} \\ & & & A_{44} \end{bmatrix} \begin{bmatrix} \delta x_{dg} \\ \delta x_{sg} \\ \delta S_{fo} \\ \delta p \end{bmatrix} = \begin{bmatrix} B_{11} & & & \\ B_{21} & B_{22} & & \\ B_{31} & B_{32} & B_{33} & \\ B_{41} & B_{42} & B_{43} & 1 \end{bmatrix} \begin{bmatrix} Y_1 \\ Y_2 \\ Y_3 \\ Y_4 \end{bmatrix} + \begin{bmatrix} E_1 \\ E_2 \\ E_3 \\ E_4 \end{bmatrix} . \tag{A-48}$$

From the fourth equation of the above matrix, we have the following equation for δp:

$$\begin{aligned} A_{44}\delta p &= B_{41}Y_1 + B_{42}Y_2 + B_{43}Y_3 + Y_4 + E_4 \\ &= B_{41}\ \Delta[(T_{fo}x_{do})\Delta\delta p] + B_{42}\ \Delta[(T_{fo}x_{sg})\Delta\delta p] \\ &\quad + B_{43}\ \Delta[T_g\Delta\delta p] + \Delta[(T_{fo}x_{dg})\Delta\delta p] + E_4. \end{aligned} \tag{A-49}$$

For block *i*:

$$\begin{aligned} &A_{44}\delta p_i \\ &= B_{41}\ [(T_{fo}x_{do})_{i+1/2}\ (\delta p_{i+1}-\delta p_i) - (T_{fo}x_{do})_{i-1/2}\ (\delta p_i-\delta p_{i-1})] \\ &+ B_{42}\ [(T_{fo}x_{sg})_{i+1/2}\ (\delta p_{i+1}-\delta p_i) - (T_{fo}x_{sg})_{i-1/2}\ (\delta p_i-\delta p_{i-1})] \\ &+ B_{43}\ [(T_g)_{i+1/2}\ (\delta p_{i+1}-\delta p_i) - (T_g)_{i-1/2}\ (\delta p_i-\delta p_{i-1})] \\ &+ [(T_{fo}x_{dg})_{i+1/2}\ (\delta p_{i+1}-\delta p_i) - (T_{fo}x_{dg})_{i-1/2}\ (\delta p_i-\delta p_{i-1})] + E_4, \end{aligned} \tag{A-50}$$

which can be written as

$$\alpha_i\delta p_{i-1} + \beta_i\delta p_i + \gamma_i\delta p_{i+1} = e_i, \tag{A-51}$$

where

$$\begin{aligned} \alpha_i &= B_{41}(T_{fo}x_{do})_{i-1/2} + B_{42}(T_{fo}x_{sg})_{i-1/2} \\ &\quad + B_{43}(T_g)_{i-1/2} + (T_{fo}x_{dg})_{i-1/2}, \end{aligned} \tag{A-52}$$

$$e_i = -E_4. \tag{A-53}$$

$$\begin{aligned}\beta_i = &- B_{41}\ [(T_{fo}x_{do})_{i-1/2} + (T_{fo}x_{do})_{i+1/2}] \\ &- B_{42}\ [(T_{fo}x_{sg})_{i-1/2} + (T_{fo}x_{sg})_{i+1/2}] \\ &- B_{43}\ [(T_g)_{i-1/2} + (T_g)_{i+1/2}] \\ &- [(T_{fo}x_{dg})_{i-1/2} + (T_{fo}x_{dg})_{i+1/2}] - A_{44},\end{aligned} \tag{A-54}$$

$$\begin{aligned}\gamma_i = &\ B_{41}(T_{fo}x_{do})_{i+1/2} + B_{42}(T_{fo}x_{sg})_{i+1/2} \\ &+ B_{43}(T_g)_{i+1/2} + (T_{fo}x_{dg})_{i+1/2},\end{aligned} \tag{A-55}$$

For a one-dimensional problem with *NX* blocks, a system of *NX* equations in the form of Eq. A-51 will be generated. This system may be solved by Thomas' algorithm for the δp_i (i = 1,...,NX). Once the δp_i are obtained, δS_{foi}, δx_{sgi} and δx_{dgi} may be obtained explicitly from

$$\begin{aligned}&\delta S_{foi} \\ &= B_{31}Y_1 + B_{32}Y_2 + B_{33}Y_3 + E_3 - A_{34}\delta p_i \\ &= B_{31}\ [(T_{fo}x_{do})_{i+1/2}\ (\delta p_{i+1} - \delta p_i) - (T_{fo}x_{do})_{i-1/2}\ (\delta p_i - \delta p_{i-1})] \\ &+ B_{32}\ [(T_{fo}x_{sg})_{i+1/2}\ (\delta p_{i+1} - \delta p_i) - (T_{fo}x_{sg})_{i-1/2}\ (\delta p_i - \delta p_{i-1})] \\ &+ B_{33}\ [(T_g)_{i+1/2}\ (\delta p_{i+1} - \delta p_i) - (T_g)_{i-1/2}\ (\delta p_i - \delta p_{i-1})] + E_3 - A_{34}\delta p_i,\end{aligned} \tag{A-56}$$

$$\begin{aligned}&\delta x_{sgi} \\ &= B_{21}Y_1 + B_{22}Y_2 + E_2 - A_{23}\delta S_{foi} - A_{24}\delta p_i \\ &= B_{21}\ [(T_{fo}x_{do})_{i+1/2}\ (\delta p_{i+1} - \delta p_i) - (T_{fo}x_{do})_{i-1/2}\ (\delta p_i - \delta p_{i-1})] \\ &+ B_{22}\ [(T_{fo}x_{sg})_{i+1/2}\ (\delta p_{i+1} - \delta p_i) - (T_{fo}x_{sg})_{i-1/2}\ (\delta p_i - \delta p_{i-1})] \\ &+ E_2 - A_{23}\delta S_{foi} - A_{24}\delta p_i,\end{aligned} \tag{A-57}$$

$$
\begin{aligned}
&\delta x_{dgi} \\
&= B_{11} Y_1 + E_1 - A_{12}\delta x_{sgi} - A_{13}\delta S_{foi} - A_{14}\delta p_i \\
&= B_{11} \left[(T_{fo} x_{do})_{i+1/2} (\delta p_{i+1} - \delta p_i) - (T_{fo} x_{do})_{i-1/2} (\delta p_i - \delta p_{i-1}) \right] \\
&+ E_1 - A_{12}\delta x_{sgi} - A_{13}\delta S_{foi} - A_{14}\delta p_i .
\end{aligned}
\tag{A-58}
$$

This constitutes the first iteration. In the second iteration, the coefficients C_{ij}, R_i are updated with the results from the first iteration. The iterations are continued until the following tolerances are met:

$$|\delta p^{l+1} - \delta p^{l}| \le \varepsilon_p , \tag{A-59}$$

$$|\delta S_{fo}^{l+1} - \delta S_{fo}^{l}| \le \varepsilon_{S_p} , \tag{A-60}$$

$$|\delta x_{sg}^{l+1} - \delta x_{sg}^{l}| \le \varepsilon_{x_{sg}} , \tag{A-61}$$

$$|\delta x_{dg}^{l+1} - \delta x_{dg}^{l}| \le \varepsilon_{x_{dg}} , \tag{A-62}$$

where l and $l+1$ represent the latest and present iterations, respectively. Tolerances of $\varepsilon_p = 5.0$ Pa, $\varepsilon_{Sfo} = 10^{-4}$, $\varepsilon_{xsg} = 10^{-5}$, and $\varepsilon_{xdg} = 10^{-5}$ have been used. At each time step, the material balances for each component and the total oil and total gas are checked. For these checks of convergence, the pressure check was found to be the controlling one.

A.2 Implicit Treatment of Production Rates

The formulation in the previous section is based on an explicit treatment of production rates. It has been found that an implicit treatment of production rates significantly improves the stability of the model. Therefore, the production rates are implicitly treated in this section.

The volumetric production rate of foamy oil is

$$q_{fov} = \frac{Akk_{ro}(S_{fo})}{(\Delta X/2)\mu_{fo}} \left[p - p_{out}\right]. \qquad \text{(A-63)}$$

In the above equation, the foamy oil viscosity could be a function of pressure, saturation and mole fractions. For simplicity, the viscosity is evaluated at time step *n*. In this way, q_{fov} is a function of pressure and saturation only. Then,

$$q_{fov}^{n+1} = q_{fov}^{n} + q_{fov,p}\delta p + q_{fov,S_{fo}}\delta S_{fo}, \qquad \text{(A-64)}$$

where

$$q_{fov,p} = \frac{q_{fov}(p^{n+1},\ S_{fo}^{n+1}) - q_{fov}(p^{n},\ S_{fo}^{n+1})}{p^{n+1} - p^{n}}, \qquad \text{(A-65)}$$

$$q_{fov,S_{fo}} = \frac{q_{fov}(p^{n},\ S_{fo}^{n+1}) - q_{fov}(p^{n},\ S_{fo}^{n})}{S_{fo}^{n+1} - S_{fo}^{n}}. \qquad \text{(A-66)}$$

Since

$$q_{do} \equiv q_{fo}x_{do} \equiv q_{fov}\,\rho_{fo}x_{do}, \tag{A-67}$$

one has

$$\begin{aligned} \delta q_{do} &\equiv q_{do}^{n+1} - q_{do}^{n} \\ &= q_{fov}^{n}\delta(\rho_{fo}x_{do}) + (\rho_{fo}x_{do})^{n+1}\delta q_{fov} \\ &= q_{fov}^{n}\,[x_{do}^{n+1}\delta\rho_{fo} + \rho_{fo}^{n}\delta x_{do}] + (\rho_{fo}x_{do})^{n+1}\delta q_{fov}. \end{aligned} \tag{A-68}$$

Substitute

$$\delta\rho_{fo} = \rho_{fo,\,x_{dg}}\delta x_{dg} + \rho_{fo,\,x_{sg}}\delta x_{sg} + \rho_{fo,p}\delta p, \tag{A-69}$$

and

$$\delta q_{fov} = q_{fov,p}\delta p + q_{fov,S_{fo}}\delta S_{fo}, \tag{A-70}$$

into δq_{do}:

$$\begin{aligned} &\delta q_{do} \\ &= q_{fov}^{n}\,(x_{do}^{n+1}\rho_{fo,\,x_{dg}} - \rho_{fo}^{n})\delta x_{dg} + q_{fov}^{n}\,(x_{do}^{n+1}\rho_{fo,\,x_{sg}} - \rho_{fo}^{n})\delta x_{sg} \\ &+ \rho_{fo}^{n+1}x_{do}^{n+1}q_{fov,S_{fo}}\delta S_{fo} + (q_{fov}^{n}x_{do}^{n+1}\rho_{fo,p} + \rho_{fo}^{n+1}x_{do}^{n+1}q_{fov,p})\delta p. \end{aligned} \tag{A-71}$$

This equation can be written as

$$\delta q_{do} = C_{11q}\delta x_{dg} + C_{12q}\delta x_{sg} + C_{13q}\delta S_{fo} + C_{14q}\delta p. \tag{A-72}$$

Here the coefficients C_{1jq} (j = 1,...,4) are obviously defined by comparing Eqs. A-72 with A-71.

Similarly,

$$\delta q_{sg} = C_{21q}\delta x_{dg} + C_{22q}\delta x_{sg} + C_{23q}\delta S_{fo} + C_{24q}\delta p, \tag{A-73}$$

and

$$\delta q_{dg} = C_{41q}\delta x_{dg} + C_{42q}\delta x_{sg} + C_{43q}\delta S_{fo} + C_{44q}\delta p, \tag{A-74}$$

where

$$C_{21q} = q_{fov}^{n} x_{sg}^{n+1} \rho_{fo,\, x_{dg}}, \tag{A-75}$$

$$C_{22q} = q_{fov}^{n}(x_{sg}^{n+1} \rho_{fo,\, x_{sg}} + \rho_{fo}^{n}), \tag{A-76}$$

$$C_{23q} = \rho_{fo}^{n+1} x_{sg}^{n+1} q_{fov,S_{fo}}, \tag{A-77}$$

$$C_{24q} = q_{fov}^{n} x_{sg}^{n+1} \rho_{fo,p} + \rho_{fo}^{n+1} x_{sg}^{n+1} q_{fov,p}, \tag{A-78}$$

$$C_{41q} = q_{fov}^{n}(x_{dg}^{n+1} \rho_{fo,x_{dg}} + \rho_{fo}^{n}), \tag{A-79}$$

$$C_{42q} = q_{fov}^{n} x_{dg}^{n+1} \rho_{fo,\, x_{sg}}, \tag{A-80}$$

$$C_{43q} = \rho_{fo}^{n+1} x_{dg}^{n+1} q_{fov,S_{fo}}, \tag{A-81}$$

$$C_{44q} = q_{fov}^{n} x_{dg}^{n+1} \rho_{fo,p} + \rho_{fo}^{n+1} x_{dg}^{n+1} q_{fov,p}. \tag{A-82}$$

For the free gas component, the volumetric production rate is

$$q_{fgv} = \frac{Akk_{rg}(S_{fo})}{(\Delta X/2)\mu_g}\left[p-p_{out}\right] \equiv q_{fgv}(p,\ S_{fo}), \tag{A-83}$$

$$q_{fgv}^{n+1} = q_{fgv}^{n} + q_{fgv,p}\delta p + q_{fgv,S_{fo}}\delta S_{fo}, \tag{A-84}$$

where

$$q_{fgv,p} = \frac{q_{fgv}(p^{n+1},\ S_{fo}^{n+1}) - q_{fgv}(p^{n},\ S_{fo}^{n+1})}{p^{n+1} - p^{n}}, \tag{A-85}$$

$$q_{fgv,S_{fo}} = \frac{q_{fgv}(p^{n},\ S_{fo}^{n+1}) - q_{fgv}(p^{n},\ S_{fo}^{n})}{S_{fo}^{n+1} - S_{fo}^{n}}. \tag{A-86}$$

Since

$$q_{fg} \equiv q_{fgv}\rho_g, \tag{A-87}$$

one has

$$\delta q_{fg} \equiv q_{fg}^{n+1} - q_{fg}^{n} = q_{fgv}^{n}\delta\rho_g + \rho_g^{n+1}\delta q_{fgv}. \tag{A-88}$$

Substitute

$$\delta\rho_g = \rho_{g,p}\delta p, \tag{A-89}$$

$$\delta q_{fgv} = q_{fgv,p}\delta p + q_{fgv,S_{fo}}\delta S_{fo}, \tag{A-90}$$

into δq_{fg}:

$$\delta q_{fg} = \rho_g^{n+1} q_{fgv,S_{fo}}\delta S_{fo} + (q_{fgv}^{n}\rho_{g,p} + \rho_g^{n+1} q_{fgv,p})\delta p. \tag{A-91}$$

The above equation can be written as

$$\delta q_{fg} = C_{31q}\delta x_{dg} + C_{32q}\delta x_{sg} + C_{33q}\delta S_{fo} + C_{34q}\delta p. \qquad \text{(A-92)}$$

Here the coefficients C_{3jq} (j = 3, 4) are obviously defined by comparing Eqs. A-92 with A-91, with $C_{31q} = C_{32q} = 0$.

As a result, if the production rates are treated implicitly, the coefficients C_{ijq} should be added to C_{ij} (i,j = 1,...,4).

A.3 Calculation of Mass Transfer Rates

A.3.1 Calculation of $R_{sg\to eg}$

To calculate $R_{sg\to eg}$, first calculate the moles of supersaturated gas component n_s. For a live oil saturated or supersaturated with $n_{sg}{}^{n}$ moles of solution gas at time step n, the supersaturation expressed in moles at time step $n+1$, $\Delta n_s{}^{n+1}$, is

$$\Delta n_s^{n+1} = n_{sg}^{n} - n_{sg,eq}^{n+1} = n_o^{n}(x_{sg}^{n})' - n_{o,eq}^{n+1}(x_{sg,eq}^{n+1})'. \qquad \text{(A-93)}$$

Here the prime means the live oil system of dead oil and solution gas components without taking the dispersed gas component into account. For example, $(x_{sg}{}^{n})'$ is defined in Eq. 6-35. The subscript *eq* means thermodynamic equilibrium.
At thermodynamic equilibrium,

$$n_{o,eq}^{n+1} = n_o^{n} - \Delta n_s^{n+1}, \qquad \text{(A-94)}$$

and

$$x_{sg,eq}^{n+1} = \frac{1}{K^{n+1}}. \tag{A-95}$$

By substituting these conditions into Eq. A-93, the supersaturation is

$$\Delta n_s^{n+1} = \frac{n_o^n[(x_{sg}^n)/K^{n+1} - 1]}{K^{n+1} - 1}. \tag{A-96}$$

For block i during the time interval Δt from t^n to t^{n+1}, there are three kinds of live oil to be considered: stationary oil in block i ($n_{o,i}$), flowing-in oil from the upstream block u ($n_{o,in}$), and flowing-out oil to the downstream block d ($n_{o,out}$). The supersaturation of these oils can be estimated differently depending on the ways to treat their changes of state during the time interval from t^n to t^{n+1}. In this model, the state of the stationary oil in block i, $n_{o,i}$, is treated to change from S_i^n to S_i^{n+1} within the time interval. Here S means the state of oil. For example, S_i^n means that the properties of oil are evaluated with the variables at block i and at time step n. According to Eq. A-96, the supersaturation of $n_{o,i}$ is then calculated as

$$\Delta n_{s,st}^{n+1} = \frac{n_{o,i}^n[(x_{sg,i}^n)/K_i^{n+1} - 1]}{K_i^{n+1} - 1}. \tag{A-97}$$

The flowing-in oil, $n_{o,in}$, is considered from state S_u^{n+1} to state S_i^{n+1}. Then its supersaturation is estimated from

$$\Delta n_{s,in}^{n+1} = \frac{n_{o,in}^{n+1}[(x_{sg,u}^{n+1})/K_i^{n+1} - 1]}{K_i^{n+1} - 1}. \tag{A-98}$$

The flowing-out oil, $n_{o,out}$, is considered from state S_i^{n+1} to state S_d^{n+1}. No supersaturation is contributed to this block. Therefore, the total supersaturation for block i is

$$\Delta n_{s,i}^{n+1} = \Delta n_{s,st}^{n+1} + \Delta n_{s,in}^{n+1}. \tag{A-99}$$

Alternatively, the total supersaturation may be calculated as follows.

The flowing-in oil, $n_{o,in}$, is considered from state S_u^n to state S_i^{n+1}. Then the supersaturation is

$$\Delta n_{s,in}^{n+1} = \frac{n_{o,in}^{n+1}[(x_{sg,u}^{n})/K_i^{n+1}-1]}{K_i^{n+1}-1}. \tag{A-100}$$

The flowing-out oil, $n_{o,out}$, is considered from state S_i^n to state S_d^{n+1}. No supersaturation is contributed to this block, but rather the stationary oil in block i is reduced by $n_{o,out}$. Thus the supersaturation of the stationary oil in this block is

$$\Delta n_{s,st}^{n+1} = \frac{[n_{o,i}^{n}-n_{o,out}^{n}][(x_{sg,i}^{n})/K_i^{n+1}-1]}{K_i^{n+1}-1}. \tag{A-101}$$

The total supersaturation is also calculated by Eq. A-99.

Once the supersaturation is obtained, the rate of solution gas transferred to evolved gas for block i is

$$R_{sg\to eg,i}^{n+1} = \frac{\Delta n_{s,i}^{n+1}[1 - \exp(-\lambda_s \Delta t/2)]}{\Delta t}, \tag{A-102}$$

with the condition:

$$|R_{sg\to eg,i}^{n+1}| \le \frac{|\Delta n_{s,i}^{n+1}|}{\Delta t}. \tag{A-103}$$

If the pressure builds up, the oil may be undersaturated. In this case, $\Delta n_{s,i}^{n+1}$ is less than zero. There are two cases to be considered: 1) there exist dispersed gas and/or free gas at the end of time step, t^{n+1}; 2) there is no gas present at the end of time step, t^{n+1}. In the first case, Eqs. A-102 and A-103 can also be used with a negative transfer rate representing gas dissolved into oil. In the second case, $x_{dg}^{n+1} = 0$ and $s_g^{n+1} = 0$. The gas (dispersed gas and free gas) available for dissolution in block i is

$$n_{g,i}^{n+1} = n_{g,i}^{n} + n_{g,in}^{n+1} - n_{g,out}^{n+1} - q_g^{n+1}\Delta t. \tag{A-104}$$

Thus,

$$R_{sg\to eg,i}^{n+1} = -\frac{n_{g,i}^{n+1}}{\Delta t}. \tag{A-105}$$

A.3.2 Calculation of $R_{eg\to dg}$ and $R_{eg\to fg}$

Part of the gas evolved from solution remains in the oil to become dispersed gas, while the rest of it becomes free gas. The corresponding transfer rates are

$$R_{eg\to dg}^{n+1} = R_{sg\to eg}^{n+1}\exp(-\lambda_{dg}\Delta t/2), \tag{A-106}$$

and

$$R_{eg\to fg}^{n+1} = R_{sg\to eg}^{n+1}[1 - \exp(-\lambda_{dg}\Delta t/2)]. \tag{A-107}$$

A.3.3 Calculation of $R_{dg\to fg}$

The dispersed gas in block is composed of that initially existing, newly-formed from evolved gas and net flowing-in from neighbouring blocks. These dispersed gases will decay exponentially to become free gas. Mathematically, the rate of dispersed gas transferred to free gas is

$$\begin{aligned} R_{dg\to fg}^{n+1} = n_{dg}^{n}[1 - \exp(-\lambda_{dg}\Delta t)]/\Delta t + R_{eg\to dg}^{n+1}[1 - \exp(-\lambda_{dg}\Delta t/2)] \\ + [\Delta(T_{dg}^{n+1}\Delta p^{n+1}) - q_{dg}^{n+1}][1 - \exp(-\lambda_{dg}\Delta t/2)]. \end{aligned} \tag{A-108}$$

It has been suggested that there may be maximum and minimum limits for the dispersed gas in the oil phase (Section 5.3.4). When the dispersed gas in block is greater than the maximum value $n_{dg,max}$, the coalescence process speeds up. $R_{dg\to fg}$ has to be adjusted according to

$$\{R_{dg\to fg}^{n+1}\}_{adjusted} = R_{dg\to fg}^{n+1} + \frac{n_{dg}^{n+1} - n_{dg,max}}{\Delta t}. \tag{A-109}$$

Here $R_{dg\to fg}{}^{n+1}$ and $n_{dg}{}^{n+1}$ are the values before adjustment. After the adjustment, the dispersed gas will equal the maximum value $n_{dg,max}$.

When the dispersed gas in block is less than the minimum value $n_{dg,min}$, the coalescence process slows down or even stops. In this case, the amount of dispersed gas possibly available in this block has to be first estimated from

$$\{n_{dg}^{n+1}\}_{available} = n_{dg}^{n} + [\Delta(T_{fo}^{n+1}x_{dg}^{n+1}\Delta p^{n+1}) - q_{dg}^{n+1}]\Delta t + R_{eg\to dg}^{n+1}\Delta t. \tag{A-110}$$

If $\{n_{dg}{}^{n+1}\}_{available}$ is greater than $n_{dg,min}$, $R_{dg\to fg}{}^{n+1}$ has to be adjusted to

$$\{R_{dg\to fg}^{n+1}\}_{adjusted} = R_{dg\to fg}^{n+1} + \frac{n_{dg}^{n+1} - n_{dg,min}}{\Delta t}. \tag{A-111}$$

After adjustment, the dispersed gas equals the minimum value $n_{dg,min}$.

If $\{n_{dg}^{n+1}\}_{available}$ is less than $n_{dg,min}$, $R_{cg\to dg}^{n+1}$, $R_{cg\to fg}^{n+1}$ and $R_{dg\to fg}^{n+1}$ have to be adjusted according to

$$\{R_{cg\to dg}^{n+1}\}_{adjusted} = R_{fg\to cg}^{n+1}, \tag{A-112}$$

$$\{R_{cg\to fg}^{n+1}\}_{adjusted} = 0, \tag{A-113}$$

and

$$\{R_{dg\to fg}^{n+1}\}_{adjusted} = 0. \tag{A-114}$$

After adjustment, the amount of dispersed gas will be less than the minimum value $n_{dg,min}$.

Appendix B

Calculation of Supersaturation

Supersaturation here is defined as the difference between the saturation pressure, p_s, corresponding to the amount of gas dissolved and the system pressure, p. The system pressure is a measurable parameter. Therefore, to calculate supersaturation, one must derive an expression to calculate the saturation pressure.

The gas solubility is formulated using the gas/oil equilibrium ratio (K value) in this model. For the oil/gas two-phase flow model, the mole fraction of gas is 1.0. Then values of K can be calculated from

$$K = \frac{1}{x_{sg}'}, \tag{B-1}$$

where x_{sg}' is defined in Eq. 6-35.

In this model the expression for K is

$$K = \left[\frac{C_{K1}}{p_s} + C_{K2}p_s\right] \cdot \exp\left[\frac{C_{K3}}{T+C_{K4}}\right]. \tag{B-2}$$

Then the saturation pressure corresponding to this x_{sg}' can be estimated from

$$p_s = \frac{K\cdot\exp[-C_{K3}/(T+C_{K4})] - \sqrt{K^2\cdot\exp[-2C_{K3}/(T+C_{K4})] - 4C_{K1}C_{K2}}}{2C_{K2}}. \quad \text{(B-3)}$$

According to the definition, the supersaturation Δp_s is

$$\Delta p_s = p_s - p. \quad \text{(B-4)}$$